INVESTIGATION OF THE BIOLOGICAL AND PHYSICOCHEMICAL PROPERTIES OF *BACILLUS ANTHRACIS* SPORES DURING GERMINATION, VIRULENCE, AND KILLING

A Dissertation

Submitted to the Faculty of

WORCESTER POLYTECHNIC INSTITUTE

in partial fulfillment of the requirements for the

Degree of

Doctor of Philosophy in

Biomolecular Engineering

January 2012

by

_____

Paola A. Pinzón-Arango

_____

Terri A. Camesano, Ph.D.
Professor, Research Advisor
Department of Chemical Engineering
Worcester Polytechnic Institute

_____

Nancy A. Burnham, Ph.D.
Associate Professor of Physics
Worcester Polytechnic Institute

_____

George D. Pins, Ph.D.
Associate Professor of Biomedical Engineering
Worcester Polytechnic Institute

_____

Maria M. Santore, Ph.D.
Professor of Polymer Science and Engineering
University of Massachusetts Amherst

_____

Robert W. Thompson, Ph.D.
Professor of Chemical Engineering
Worcester Polytechnic Institute

This thesis is dedicated to my parents,

Alberto Pinzón and Luz Arango de Pinzón,

for giving up everything they had in Colombia

so we could have a better education.

Table of Contents

Abstract

Bacillus anthracis has been classified as one of the most dangerous bioterrorism agents causing high mortality rates in short periods of time. Anthrax spores are extremely resistant to chemical and environmental factors, and have the ability to return into a vegetative (virulent) state during the process of germination. Previous research has suggested that spores can be eradicated with common disinfectants after germination and release of spore coats. During germination, the spore coat is degraded, making the spore susceptible to penetration of chemicals into the spore core. While previous research has focused on a qualitative understanding of germination of spores by obtaining high-resolutions images of spore coats to understand how protein coat layers change during germination, very few studies have evaluated changes in mechanical properties of spores during germination, and how germination affects virulence of macrophages. In this study, we performed a series of *in vitro* experiments to do an in-depth analysis of germination and virulence of *B. anthracis.*

Atomic force microscopy (AFM) was used to investigate changes in spore surface properties during germination including morphology, roughness, elasticity, and spring constant. AFM results suggested that germination mechanisms depend on germinants used to trigger germination and roughness of *Bacillus* species increase during germination. In addition, the elasticity and spring cell constant of *B. anthracis* spores are affected during germination since the elastic moduli and cell spring constant values decreased with time as the spore was germinating, making the cells more susceptible. Spore killing was also tested both in sporulated and vegetative *B. anthracis* using the antimicrobial peptide chrysophsin-3 and the surfactant dodecylamine (DDA). Both killing agents were capable of eradicating *B. anthracis* spores, but more killing was observed for spores that were germinating or had become vegetative.

The presence of germinant receptors from the Ger operon and its role on germination kinetics of *B. anthracis* was also investigated. The germination of mutant spores that carried one receptor or lacked all germinant receptors was compared to the germination kinetics of wild-type *B. anthracis*. Our results suggest that germination of spores is modified by the presence or absence of germinant receptors. Furthermore, the mutant *B. anthracis* strain lacking all receptors germinated suggesting that other receptor independent pathways may exist in *B. anthracis*.

Finally the ability of *B. anthracis* to adhere, grow, and invade macrophages was investigated. Invasion of macrophages by *B. anthracis* was dependent on germinant receptors and the ability of spores to germinate and multiply. Our results suggest that macrophages were not capable of killing infecting spores, and on the contrary, germination of spores inside macrophages caused the lysis of macrophages. An uncontrolled release of cytokines by macrophages was elicited by spores and germinated *B. anthracis*.

Our study helps understand the process of germination of *B. anthracis* spores at a nanomolecular level. Our investigation may be a valuable tool in the design and development of antisporal compounds.

Authorship

The contents of this thesis are a representation of the work done by the main author. Contributions to this project were made by Geoffrey Scholl, a molecular research biologist that worked at the US Army Natick Research and Development Center. Geoffrey was of great assistance on spore killing experiments using dodecylamine and in measuring the concentrations of dipicolinic acid released from *Bacillus atrophaeus* during germination.

Charlene M. Mello is an adjunct professor at the University of Massachusetts Dartmouth and a research chemist at the US Army Natick Research and Development Center. Dr. Mello contributed to helpful discussions when preparing the manuscript presented in Chapter 3 before publication.

Ramanathan Nagarajan is a research engineer at the US Army Natick Research and Development Center. Dr. Nagarajan has been of great assistance in developing experiments and during discussions before submission of all papers in this thesis.

Acknowledgments

First and foremost, I would like to thank God for giving me strength and patience and guiding me through this journey. It was my faith in Him that allowed me to face all the challenges that I encountered during the past few years.

My thanks go to my research advisor, Dr. Terri A. Camesano, who believed in me. There are no words to express my gratitude. You continually supported me and saw me grow as a person and as a researcher. I thank you for your guidance and encouragement, which enabled me to overcome numerous challenges in order to complete this thesis. I hope that I didn't drive you too crazy during the past...XX…years. I am very lucky to have you as a friend as well. You have been with me during good and bad times, and I will be eternally grateful for that.

Thanks to my committee members Dr. Pins, Dr. Santore, Dr. Burnham, and Dr. Thompson for their support during this project. Your observations and insights were valuable for the completion of this project. Thank you for always being available for discussion. It has been truly an honor working with you.

Thanks to Dr. Nagarajan who was always supportive. Nagu, you are like an open encyclopedia and you came in handy many times during this project. Thank you for that!

To my lab mates over the past few years: Kathleen, Kellie, Yatao, Josh, Arzu, Laila, Ray, Ivan, Kerrie, Lupe, Yuxian, Angela, Sophia, and Sena. Working in the lab with you was really fun and you made the lab environment the best. I would especially like to thank Yatao for encouraging me to write so many papers. At some point I really wanted to hit you for pushing me to go into the PhD program. But now I understand why you did it and I'm thankful for that. You are a valuable friend and I'm lucky to have you in my life. Kathleen, I know I drove you

crazy many times but I really cherish the times we were in the cubicles together making sure we didn't die of boredom when we were writing. Thanks for helping me with my spelling and proofreading my stuff, including this section ;) Thank you for being in my life.

My friends at WPI: Harita, Prachi, Charu, Shilpa, Felicia and Tiffany. I want to thank you for supporting me and for helping me during my experiments. Your friendship is very valuable to me and I hope that after we leave WPI we will still be in touch. You guys better come to my wedding. I love you guys!

Finally, my greatest thanks go to my family. Especially my parents who gave up everything they had in Colombia so we could move here and so we could have a better life and education. The sacrifice that you have made was tremendous and I hope to make you proud and make sure that your decision of leaving all your loved ones in Colombia was worthwhile. To my sister, Claudia (marisca), for her support all these years, I know being in grad school took me away from spending time with you, but I cherish all the few moments I had with you. To my brothers Eduardo and Hernan for supporting me all these years. At least I had my brother Hernan working in the same building with me so we could sometimes chat.

And don't think I'm forgetting you, Joe! My love and best friend. Your love and patience have encouraged me to keep going and not give up. I love you!! I'm sorry when sometimes I couldn't see you because I had to be in lab. Thank you for being there whenever I had to complain about my experiments. You supported me every step of the way and you always believed in me. I am truly blessed to have you in my life and I am very much looking forward to our future together.

Publications

This thesis is a compilation of the following manuscripts:

Chapter 3: Pinzón-Arango PA, Sholl G, Nagarajan R, Mello CM, Camesano TA. *Atomic force microscopy study of germination and killing of* Bacillus atrophaeus *spores.* Journal of Molecular Recognition 2009, 22, 373-379.

Chapter 4: Pinzón-Arango PA, Nagarajan R, Camesano TA. *Effects of L-alanine and inosine germinants on the elasticity of* Bacillus anthracis *spores.* Langmuir 2010, 26 (9), 6535-6541.

Chapter 5: Pinzón-Arango PA, Nagarajan R, Camesano TA. *Changes in mechanical properties and killing of* Bacillus anthracis *34F2 after exposure to the antimicrobial peptide chrysophsin-3.* (submitted manuscript to Biotechnology and Bioengineering)

Chapter 6: Pinzón-Arango PA, Nagarajan R, Camesano TA. *Role of the Ger receptor in germination of* Bacillus anthracis. (In Preparation).

Chapter 7: Pinzón-Arango PA, Nagarajan R, Camesano TA. *Role of germinant receptors of* Bacillus anthracis *on invasion and cytokine response.* (In Preparation).

Chapter 8: Pinzón-Arango PA, Nagarajan R, Camesano TA. *Thermodynamic model to predict macrophage*-Bacillus anthracis *spore interactions.* (In preparation)

Conference Abstracts

P.A. Pinzón-Arango, T.A. Camesano, and R. Nagarajan. "Anti-sporal activity of antimicrobial peptides against Bacillus anthracis". ACS National Meeting, Boston, MA. August 2010 (Oral Presentation).

P.A. Pinzón-Arango, T.A. Camesano, and R. Nagarajan. "Changes in the Mechanical Properties of *Bacillus anthracis* by Germinants and Antimicrobial Peptide Chrysophsin-3". International Meeting on AFM in Life Sciences and Medicine, Red Island, Croatia. May 2010 (Oral Presentation)

P.A. Pinzón-Arango, R. Nagarajan, and T.A. Camesano. "Changes in the elasticity of *Bacillus anthracis* during germination" ACS National Meeting, San Francisco, CA, March 2010 (Oral Presentation)

P.A. Pinzón-Arango, R. Nagarajan, and T.A. Camesano. "Characterizing the mechanical properties of *Bacillus anthracis* spores using atomic force microscopy. ACS National Meeting, San Francisco, CA, March 2010 (Oral Presentation)

P.A. Pinzón-Arango, T.A. Camesano, and R. Nagarajan. "Quantifying the Nanomechanical Properties of Bacillus anthracis and Implications for Spore Killing". First Global Congress on NanoEngineering for Medicine and Biology. Houston, TX, February 2010. (Oral Presentation)

P.A. Pinzón-Arango, G. Scholl, R. Nagarajan, C.M. Meelo, and T.A. Camesano. "Atomic force microscopy study of germination and killing of *Bacillus atrophaeus* spores". International Meeting of AFM in Life Sciences and Medicine, Monterrey, CA, October 2008 (Oral Presentation)

P.A. Pinzón-Arango, G. Scholl, T.A. Camesano, C.M. Mello and R. Nagarajan. "Nanoscopic study of bacterial spores from dormancy to death" National Meeting of the American Chemical Society, Boston, MA, August 19-22, 2007.

Glossary of Abbreviations

AAID-1	amino acid and inosine-dependent-1 pathway
AAID-2	amino acid and inosine-dependent-2 pathway
AEP	aromatic amino acid-enhanced pathway
AFM	atomic force microcopy
Ala	alanine germination pathway
AMP	antimicrobial peptide
ANOVA	analysis of variance
AP	alanine and proline pathway
ATCC	American type culture collection
ATP	adenosine triphosphate
BclA	*Bacillus* collagen-like protein A
BslA	*Bacillus* S-layer protein A
BWC	biological and toxin weapons convention
Ca^{2+}	calcium
cAMP	cyclic AMP
CDC	centers for disease control and prevention

CFU	colony forming unit
CLE	cortex lytic enzymes
COS	chitooligosaccharides
d	deflection of cantilever
d_0	deflection offset
Da	Dalton
DDA	dodecylamine
DNA	deoxyribonucleic acid
DPA	dipicolinic acid or pyridine-2,6-dicarboxylic acid
E	Young's modulus or elastic modulus
EdTx	edema toxin
EF	edema factor
ELISA	enzyme-linked immunosorbent assay
EM	electron microscopy
F	force or load
FBS	fetal bovine serum
g	grams

g/L	grams per liter
HCl	hydrochloric acid
HPLC	high-perfomance liquid chromatography
hrs	hours
Hz	Hertz
IL	interleukin
IL-12	interleukin 12
IL-1β	interleukin 1-beta
IL-6	interleukin 6
k_c	spring constant of cantilever
kg	kilogram
kHz	kilohertz
LeTx	lethal toxin
LF	lethal factor
LPS	lipopolysaccharide
M	molar
MAP	mitogen-activated protein

MAPKK	mitogen-activated protein kinase kinases
mg	milligrams
min	minute
mJ	milliJoules
mm	millimeter
mM	millimolar
$MnCL_2 \cdot 4H_2O$	manganese (II) chloride tetrahydride
MPa	mega Pascals
mRNA	messenger RNA
ms	millisecond
N/m	Newton per meter
nm	nanometer
OD	optical density
PA	protective antigen
PCR	polymerase chain reaction
RNA	ribonucleic acid
RPM	revolutions per minute

R_{rms}	root-mean-squared roughness
Sp.	species
$(Tb(DPA)_3)^{3-}$	terbium dipicolinate
$TbCl_3$	terbium chloride
TNF-α	tumor necrosis factor- alpha
TSB	tryptic soy broth
U	units
UV	ultraviolet
W	Watt
wk	week
WMD	weapon of mass destruction
wt	weight
WWI	World War I
yr	year
z	tip-sample separation distance
z_0	separation distance offset
Zn^{2+}	zinc

α	half opening angle of conical AFM tip
γ_{AB}	acid-base interactions
γ_{LW}	Lifshitz-van der Waals interactions
$\gamma_{mac\text{-}L}$	interfacial tension between macrophages and liquid media
$\gamma_{S\text{-}L}$	interfacial tension between spores and liquid media
$\gamma_{S\text{-}mac}$	interfacial tension between spores and macrophages
γ_{TOTAL}	interfacial tension
δ	indentation depth
ΔG_{adh}	Gibbs free energy of adhesion change
ν	Poisson ratio
π	pi
σ^{H}	sigma factor
µL	microliter
µm	micrometer
µM	micromolar
µm/s	micrometer per second

Chapter One

Overview

1.1 Research Motivation

The U.S. Centers for Disease Control and Prevention (CDC) have placed *B. anthracis* in the highest rank of bioterrorism agents, along with the ebola virus, since it can cause infections with high mortality rates, with a major impact in public health[1]. Terrorism events throughout history have shown that *B. anthracis*, the etiologic agent that causes anthrax, can be easily manipulated and used as a bioweapon[2, 3]. It is believed that at least 17 nations around the world have weaponized *B. anthracis* spores and the intentional release of spores in the 2001 terrorist attacks have demonstrated the lethal potential of *B. anthracis* and the ease of pathogen dissemination[4-6].

B. anthracis is one of the few members of prokaryotic cells that are able to sporulate under conditions of nutrient deprivation[7]. During sporulation, *B. anthracis* synthesizes thick protein coats that surround and encase the bacterial genetic material protecting it against harsh chemical and environmental conditions[8]. Extreme heat, UV radiation, desiccation, pH extremes, and toxic chemicals are ineffective in killing spores, making them one of the most resistant life forms known[9]. *B. anthracis* can remain in a dormant state for years and only in the presence of nutrients the bacterium germinates and regains metabolic activity.

Germination is triggered in response to nutrients including amino acids, sugars, and purine nucleosides, which cause the release dipicolinic acid (DPA) from the spore and the re-entry of water into the spore core[10]. After the spore has been rehydrated, metabolism recommences and macromolecular synthesis converts the spore into a fully virulent bacterium capable of releasing toxins and causing infections[2, 11]. While the process of germination is well understood, no studies have investigated the mechanical changes that occur during germination and how these changes relate to virulence and killing of *B. anthracis.* Furthermore, while it is known that germination

occurs when small molecules specifically bind to germinant receptors located on the inner membrane of the spore[10, 12], no studies have investigated the role of these germinant receptors on virulence and the physico-chemical properties of spores. A clear understanding on the role of each receptor on spore germination is needed in order to diminish or prevent infections caused by *B. anthracis.*

Pulmonary anthrax, the most lethal form of infection caused by *B. anthracis,* is caused by the accidental inhalation of pathogenic *B. anthracis* spores that get deposited in alveolar spaces[13]. Once in the pulmonary system, the spores get transported to lymphatic nodules by alveolar macrophages where spores germinate into virulent bacteria and start releasing toxins[14]. Septic shock and bacterial invasion of bloodstream quickly develops, followed by death[2]. Survival of patients with pulmonary anthrax ranges from 15 to 60%[6]. Successful eradication of the infection and therapy is only achieved with early administration of antibiotics and aggressive supporting care[15]. Unfortunately, the disease is often difficult to diagnose causing a delay in treatment, which is often fatal[13, 16]. Infections caused by *B. anthracis* are currently treated with high doses of antibiotics[15, 17]. While *B. anthracis* are sensitive to some antibiotics, the use of these compounds as the primary course of treatment is often ineffective due to the development of antibiotic resistance[2, 18].

Due to difficulties in diagnosis and treatment, alternative therapies for treatments are needed. Antimicrobial peptides (AMPs) are short peptides found in the immune system of animals and plants and have shown antibacterial activity against Gram-negative and Gram-positive organisms[19]. While the majority of studies focuses on the ability of AMPs to penetrate and kill microorganisms[20-23], no studies have investigated how AMPs change the mechanical properties of *B. anthracis* spores.

Chrysophsin-3, an AMP isolated from the gills of the red sea bream *Chrysophrys major*, has been found to have antimicrobial properties at low concentrations[24]. There has been limited evidence suggesting that chrysophsin-3 kills *B. subtilis*[24]. However, no studies have tested the ability of chrysophsin-3 to kill *B. anthracis* in its sporulated form or how the peptide affects the physical properties of the cell.

The research described in this document is based on the following principles:

a) The development of pulmonary anthrax cannot occur unless there is proper germination of the spore inside macrophages (specific receptor-ligand interaction).
b) Killing of *B. anthracis* is only achieved if small enough molecules are able to penetrate the thick spore coat that protects all genetic material.
c) Germination of spores is necessary to kill *B. anthracis.*

The following sections of this document will focus primarily on a basic understanding of spore germination with amino acids, purine nucleosides or surfactants, and the role of germinant receptors on the physico-chemical properties and virulence of *B. anthracis.* Furthermore, a basic understanding of how the AMP chrysophsin-3 may be used as a deactivation agent against *B. anthracis* spores is presented.

1.2 Research Summary

Chapter 2 comprises of an extended literature review on the use of *B. anthracis* as a biological weapon, and the development of anthrax infections. Basic understanding of germination inside macrophages and release of toxins during pulmonary anthrax is summarized. An extended background on the germination and sporulation of *Bacillus* sp. spores is presented,

as is the role of germinant receptors on the inner membrane of *B. anthracis*. The use of antimicrobial peptides as an alternative for antibiotic treatments for infections is reviewed and the use of cationic peptides to kill microorganisms is presented.

Chapter 3 is based upon a research project performed in collaboration with Geoffrey Scholl, Ramanathan Nagarajan, and Charlene Mello, members of the molecular sciences and engineering team of the Natick Soldier Research, Development, and Engineering Center in Natick, MA. We specifically investigated the germination and killing of *B. atrophaeus* spores. Special attention was paid to the use of surfactants to germinate spores and how germination takes place and differs from germinating spores with amino acids. An in-depth study of morphological changes of spores during germination was performed using atomic force microscopy (AFM). The kinetics of germination of spores with various concentrations of amino acids and surfactants are presented by measuring the amount of dipicolinic acid (DPA) released from the spore core. The germination mechanisms of *B. atrophaeus* after exposure to different germinants are proposed. Finally, we also investigated how surfactants can also be used as a deactivation method against spores.

Chapter 4 describes a project completed in collaboration with Ramanathan Nagarajan from the molecular sciences and engineering team of the Natick Soldier Research, Development, and Engineering Center in Natick, MA. The focus of this project was to study the elastic properties of *B. anthracis* spores during germination by using mathematical models that can be used to describe data obtained with the atomic force microscope (AFM). The Hertz model of continuum mechanics is explained in detail. Furthermore, the effects of different germinants and germinant concentrations on the elastic properties of the spores were investigated.

Chapter 5 describes a complete study done in collaboration with Ramanathan Nagarajan from the molecular sciences and engineering team of the Natick Soldier Research, Development, and Engineering Center in Natick, MA. The work focused on evaluating the use of the antimicrobial peptide (AMP) chrysophsin-3 against *B. anthracis* spores. Changes in the mechanical properties of the spore after exposure to the peptide were investigated by using the AFM. Special attention was paid to calculating the elastic modulus and the spring constant of *B. anthracis.* Furthermore, the use of the peptide in conjunction with germinants to kill spores was investigated. The benefits of using AMPs as a deactivation method against spores are explained.

Chapter 6 focuses on a research project where the role of germinant receptors of the *ger* operon on germination and killing of *B. anthracis* spores are investigated. Special attention was paid to the $gerH^{+}$, $gerS^{+}$, and ger_{null} mutants and how these behave differently compared to the wild type *B. anthracis* 34F2 strain. Phase microscopy was used to observe differences in germination, and viability tests after exposure to dodecylamine were performed.

Chapter 7 expands the results from chapter 6 and is a project that focuses on the role of germinant receptors on the virulence and invasion of spores in murine macrophages. Optimized ELISA and microscopy techniques are presented and the release of chemical signals from macrophages is studied.

Chapter 8 describes and attempt to understanding macrophage-*B. anthracis* spore interactions through a thermodynamic model that predicts the favorability of adhesion based on the calculations of interfacial free energies from measuring contact angles on *B. anthracis* and macrophages, following the van Oss-Chaudhury-Good (VCG) approach[25, 26].

Chapter 9 is a compilation of short investigations and tests done on *B. anthracis* spores that have not been submitted for publication in scientific journals. Kinetic studies of the release of dipicolinic acid from the spore core during germination as a function of germinant concentration are presented.

Chapter 10 describes the overall conclusions of this project and experiments that are currently under investigation. Recommendations are made in this section for future examination of *B. anthracis* spore properties as well as the use of antimicrobial peptides as a deactivation method.

REFERENCES

1. CDC *Biological and chemical terrorism: strategic plan for preparedness and response*; Morbidity and Mortality Weekly Report (MMWR): 2000; pp 49(no. RR-4).

2. Oncu, S.; Oncu, S.; Sakarya, S., Anthrax--an overview. *Med Sci Monit* **2003,** 9, (11), RA276-83.

3. Bush, L. M.; Abrams, B. H.; Beall, A.; Johnson, C. C., Index case of fatal inhalational anthrax due to bioterrorism in the United States. *N Engl J Med* **2001,** 345, (22), 1607-10.

4. Christopher, G. W.; Cieslak, T. J.; Pavlin, J. A.; Eitzen, E. M., Jr., Biological warfare. A historical perspective. *Jama* **1997,** 278, (5), 412-7.

5. Inglesby, T. V.; Henderson, D. A.; Bartlett, J. G.; Ascher, M. S.; Eitzen, E.; Friedlander, A. M.; Hauer, J.; McDade, J.; Osterholm, M. T.; O'Toole, T.; Parker, G.; Perl, T. M.; Russell, P. K.; Tonat, K., Anthrax as a biological weapon: medical and public health management. Working Group on Civilian Biodefense. *JAMA* **1999,** 281, (18), 1735-45.

6. Jernigan, J. A.; Stephens, D. S.; Ashford, D. A.; Omenaca, C.; Topiel, M. S.; Galbraith, M.; Tapper, M.; Fisk, T. L.; Zaki, S.; Popovic, T.; Meyer, R. F.; Quinn, C. P.; Harper, S. A.; Fridkin, S. K.; Sejvar, J. J.; Shepard, C. W.; McConnell, M.; Guarner, J.; Shieh, W. J.; Malecki, J. M.; Gerberding, J. L.; Hughes, J. M.; Perkins, B. A., Bioterrorism-related inhalational anthrax: the first 10 cases reported in the United States. *Emerg Infect Dis* **2001,** 7, (6), 933-44.

7. Giorno, R.; Bozue, J.; Cote, C.; Wenzel, T.; Moody, K. S.; Mallozzi, M.; Ryan, M.; Wang, R.; Zielke, R.; Maddock, J. R.; Friedlander, A.; Welkos, S.; Driks, A., Morphogenesis of the *Bacillus anthracis* spore. *J Bacteriol* **2007,** 189, (3), 691-705.

8. Atrih, A.; Foster, S. J., Bacterial endospores the ultimate survivors. *Int. Dairy J.* **2002,** 12, (2-3), 217-223.

9. Nagarajan, R.; Muller, W. S.; Ashley, R.; Mello, C. M. In *Decontamination Of Bacterial Spores by a Peptide-Mimic*, 25th Army Science Conference, Orlando, FL, December, 2006, 2006; Orlando, FL, 2006.

10. Setlow, P., Spore germination. *Curr Opin Microbiol* **2003,** 6, (6), 550-6.

11. Indest, K. J.; Buchholz, W. G.; Faeder, J. R.; Setlow, P., Workshop report: modeling the molecular mechanism of bacterial spore germination and elucidating reasons for germination heterogeneity. *J Food Sci* **2009,** 74, (6), R73-8.

12. Ireland, J. A.; Hanna, P. C., Macrophage-enhanced germination of *Bacillus anthracis* endospores requires gerS. *Infect Immun* **2002,** 70, (10), 5870-2.

13. Dixon, T. C.; Meselson, M.; Guillemin, J.; Hanna, P. C., Anthrax. *N Engl J Med* **1999,** 341, (11), 815-26.

14. Banks, D. J.; Barnajian, M.; Maldonado-Arocho, F. J.; Sanchez, A. M.; Bradley, K. A., Anthrax toxin receptor 2 mediates *Bacillus anthracis* killing of macrophages following spore challenge. *Cell Microbiol* **2005,** 7, (8), 1173-85.

15. Bell, D. M.; Kozarsky, P. E.; Stephens, D. S., Clinical issues in the prophylaxis, diagnosis, and treatment of anthrax. *Emerg Infect Dis* **2002,** 8, (2), 222-5.

16. Goldenberg, A.; Shmueli, G.; Caruana, R. A.; Fienberg, S. E., Early statistical detection of anthrax outbreaks by tracking over-the-counter medication sales. *Proc Natl Acad Sci U S A* **2002,** 99, (8), 5237-40.

17. Pile, J. C.; Malone, J. D.; Eitzen, E. M.; Friedlander, A. M., Anthrax as a potential biological warfare agent. *Arch Intern Med* **1998,** 158, (5), 429-34.

18. Chen, Y.; Tenover, F. C.; Koehler, T. M., Beta-lactamase gene expression in a penicillin-resistant *Bacillus anthracis* strain. *Antimicrob Agents Chemother* **2004,** 48, (12), 4873-7.

19. Rajanbabu, V.; Chen, J. Y., Applications of antimicrobial peptides from fish and perspectives for the future. *Peptides* **2011,** 32, (2), 415-20.

20. Brogden, K. A.; Ackermann, M.; McCray, P. B., Jr.; Tack, B. F., Antimicrobial peptides in animals and their role in host defences. *Int J Antimicrob Agents* **2003,** 22, (5), 465-78.

21. Cole, A. M.; Weis, P.; Diamond, G., Isolation and characterization of pleurocidin, an antimicrobial peptide in the skin secretions of winter flounder. *J Biol Chem* **1997,** 272, (18), 12008-13.

22. Hancock, R. E.; Scott, M. G., The role of antimicrobial peptides in animal defenses. *Proc Natl Acad Sci U S A* **2000,** 97, (16), 8856-61.

23. Wang, Q.; Bao, B.; Wang, Y.; Peatman, E.; Liu, Z., Characterization of a NK-lysin antimicrobial peptide gene from channel catfish. *Fish Shellfish Immunol* **2006,** 20, (3), 419-26.

24. Iijima, N.; Tanimoto, N.; Emoto, Y.; Morita, Y.; Uematsu, K.; Murakami, T.; Nakai, T., Purification and characterization of three isoforms of chrysophsin, a novel antimicrobial peptide in the gills of the red sea bream, *Chrysophrys major*. *Eur J Biochem* **2003,** 270, (4), 675-86.

25. van der Mei, H. C.; Bos, R.; Busscher, H. J., A reference guide to microbial cell surface hydrophobicity based on contact angles. *Colloids Surf B Biointerfaces`* **1998,** 11, 213-221.

26. van Oss, C. J.; Good, R. J.; Chaudhury, M. K., Additive and Nonadditive Surface Tension Components and the Interpretation of Contact Angles. *Langmuir* **1988,** 4, 884-891.

Chapter Two

Literature Review

The development of new deactivation methods against biological weapons requires a comprehensive understanding of the biology of microorganisms and how these interact with the host. Special attention has been paid to the bacterium *Bacillus anthracis*, causative agent of anthrax infections, in an effort to find alternative methods to deactivate spores and diminish the use of them for bioterrorism attacks. Current understanding of spore deactivation relies in the transformation of spores into vegetative bacteria, which are more susceptible to killing agents. However, vegetative *B. anthracis* are highly virulent and incorrect manipulation of the microorganism could result in death. Before sporicidal compounds can be developed, a basic understanding of spore formation, germination, and virulence of *B. anthracis* is needed.

2.1 Anthrax and Bioterrorism

Anthrax is a zoonosis or infection that can be transmitted from animals to humans, which is naturally found in pastures[1]. *B. anthracis* spores can persist in the environment for many years, especially in settings that are rich in soil nitrogen and organic content[2]. After livestock becomes infected with anthrax spores, human infection can easily occur through contact with the infected animal[1]. West Africa is the most affected area of the world and epidemics of anthrax have resulted in thousands of humans getting infected and hundreds of deaths[2]. Anthrax has also been a significant problem in other parts of Africa, Central America, Spain, Greece, Turkey, Albania, Romania, Central Asia, and the Middle East[3].

Currently, after being considered as just the cause of a zoonotic disease, anthrax is now one of the few biological agents identified by the Centers for Disease Control and Prevention (CDC) as a Category A bioterrorism agent[4]. Biological agents under this category are high priority microorganisms that can be easily disseminated, cause high mortality, social disruption,

and requires special action for public-health preparedness[5]. Some microorganisms in this category also include *Yersinia pestis* (plague), filoviruses (ebola), *Clostridium botulinum* (botulism), and *Francisella tularensis* (tularemia)[4].

Bacillus anthracis is of special importance because this microorganism is highly toxic and can sporulate and remain viable for years without the need for nutrients. *B. anthracis* has been researched for more than 80 years for their potential use as a bioweapon and nations around the world have weaponized the spore[6, 7]. Several outbreaks of anthrax, whether or not they were intentional, have taken place in several countries and have caused social disruption:

- 1941-1942, testing of anthrax aerial bombs and cannon shells for biological warfare over Gruinard Island in Scotland[8]. As a result of the Gruinard test, the island is so badly contaminated that it has been sealed off to visitors[3].
- 1979, accidental release of *B. anthracis* spores from a military microbiology facility in Sverdlovsk (now Yekaterinburg, Russia), which resulted in the killing of 86% of the people exposed to the pathogen. Death occurred in less than 4 days and cases were also reported in animals located more than 50 km from the site of the accident[9, 10].
- 1990-1995, the Japanese terrorist group known as Aum Shinrikyo attempted to disseminate anthrax spores in the subway system of Tokyo, Japan[7].
- 1998, Larry Wayne Harris, a microbiologist linked to white-supremacist groups, was arrested after he threatened to release "military-grade anthrax" in Las Vegas, USA[11].
- 2001, after the terrorist attacks of September 11, letters contaminated with anthrax spores were mailed to several news media offices and Democratic U.S. Senators[8]. Five people were killed and at least 17 more were hospitalized[9, 12]. Eleven cases of inhalational

anthrax and 11 cases of cutaneous anthrax were reported and more than 10,000 persons potentially exposed to anthrax in Connecticut, Florida, New Jersey, New York City, and Washington, DC were recommended to take post-exposure antibiotic prophylaxis[13].

With the successful attacks of 2001, there was a realization of the potential dangers of *B. anthracis* for bioterrorism. Research has indicated that 10 grams of inhaled spores could produce as many casualties as a ton (one million grams) of nerve agents[14]. The U.S. Congressional Office of Technology Assessment has estimated that an aircraft release of 100 kg of *B. anthracis* spores upwind of a city the size of Washington DC could result in up to three million deaths[14]. According to the CDC, the associated costs of a *B. anthracis* bioterror attack would be more than $26 billion per 100,000 of persons exposed[13, 15].

2.2 Anthrax Infections

Anthrax infections are initiated by endospores of the Gram-positive soil organism *B. anthracis.* These endospores do not have measurable metabolism, do not divide, and are resistant to harsh chemical and environmental settings[16]. After entry into the host, spores germinate to become virulent vegetative bacteria and multiply releasing toxins within the body. The course of infection is depicted in Figure 1.

In humans, three types of anthrax infections can occur: Inhalational or pulmonary, cutaneous, and gastrointestinal anthrax. After *B. anthracis* have been introduced into the body by inhalation, abrasion, or ingestion, the spores are captured by local macrophages and carried to regional lymph nodes[17]. Within macrophages, *B. anthracis* begins the process of germination where spores become virulent vegetative bacteria that multiply and release toxins[3]. Lysis of macrophages follows, which results in the release of vegetative *B. anthracis* into the blood

stream where up to 10^7 or 10^8 cells/mL of blood can be found[17]. This concentration of *B. anthracis* in the blood stream causes massive septicemia, which is followed by death of the host. Death can occur one to seven days after exposure to the pathogen unless prompt diagnosis and early administration of antibiotics takes place[17, 18].

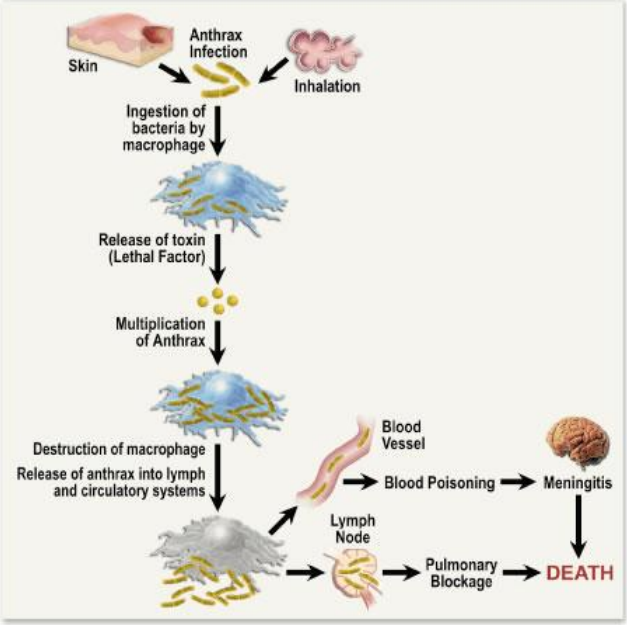

Figure 1. Pathophysiology of anthrax infections. Adapted from Dixon et al.[17]

2.2.1 Cutaneus Anthrax

Cutaneous anthrax is the most common form of infection, accounting for 95% of anthrax cases in the United States[2]. Cutaneous anthrax remains endemic in many parts of the world including Asia, Africa, South America, and Australia, and up to 200,000 cases occur annually[19]. The disease predominantly occurs in people working with livestock after exposure to anthrax-infected animals or products[7]. However, during the bioterrorist attacks of 2001 in the U.S., more than 50% of the infected individuals developed cutaneous anthrax[13].

The infection begins after *B. anthracis* spores are introduced subcutaneously through a cut or abrasion[7]. The incubation period ranges from 1 to 12 days. The infection begins with spore germination and production of toxins resulting in a skin lesion that is usually a nondescript, painless, pruritic papule that appears three to five days after inoculation of *B. anthracis* spores (Figure 2)[7, 17]. Development of edema around the lesion with a number of purplish vesicles is a major diagnosis characteristic of cutaneous anthrax[3]. Patients can experience systemic symptoms including high fever, toxemia, regional painful lymphadenopathy (gland enlargement), and extensive or severe edema[3]. Antibiotic treatment is recommended to prevent or decrease the development of edema and systemic symptoms; however, lesions can self-heal after the eschar dries, loosens, and falls off in the next 1 to 2 weeks[7, 17]. Mortality rates only reach 20% without, and less than 1% with antibiotic treatment[2, 3].

2.2.2 Gastrointestinal Anthrax

Gastrointestinal anthrax, an extremely rare type of anthrax infection in developed countries, has an extremely high mortality rate of 25% to 60%[3]. The infection begins 2 to 5 days following consumption of contaminated meat or drink[2]. Oropharyngeal anthrax occurs when *B. anthracis* spores germinate in the upper gastrointestinal tract, and is characterized by the development of an oral of esophageal ulcer (Figure 2)[7]. The symptoms include severe sore throat, fever, dysphagia (difficulty swallowing), and respiratory distress[20]. Regional lymphadenopathy can be seen and can be accompanied by massive edema and sepsis[3, 7].

Another form of anthrax infection presents itself in the lower gastrointestinal tract after an incubation period of 1 to 7 days following ingestion of contaminated meat[3]. It is believed that the inoculation of bacteria takes place at a breach in the mucosal lining; however, the exact location where spores germinate is unknown. Symptoms accompanying this infection include

fainting spells, asthenia, low fever, abdominal pain, nausea, vomiting, diarrhea, accumulation of fluid in the peritoneal cavity and headache[21]. Aggressive medical intervention may reduce mortality rates; although, given the difficulty of early diagnosis, mortality is usually high[3, 7]. Morbidity is due to blood loss, fluid, electrolyte imbalances, and subsequent shock[17]. Death usually results from intestinal perforation or anthrax toxemia[17].

2.2.3 Pulmonary Anthrax

Pulmonary anthrax, also known as inhalational anthrax, is the most lethal form of anthrax infections and is caused by inhalation of pathogenic *B. anthracis* spores that get deposited in alveolar spaces[17]. As a defense mechanism against infection, alveolar macrophages ingest the spores and transport the microorganisms to mediastinal lymph nodes. Within macrophages, spores germinate and become virulent vegetative bacteria that start replicating, and producing and releasing toxins, causing the lysis of macrophages and the subsequent release of bacteria into the lymphatic system[22]. Septicimia or invasion of bloodstream by bacteria quickly develops, followed by death[3, 23].

Pulmonary anthrax is a two-stage disease. The first stage develops 1 to 6 days after exposure to *B. anthracis* spores and is characterized by low fever, nonproductive cough, myalgias (muscular pain), malaise, dyspnea (labored breathing), chills, and chest pain[2, 7]. The initial "flu-like" symptoms make the disease difficult to diagnose unless there is a high level of suspicion, and may delay the infected people from seeking medical tretmenat[9, 17]. Early in the course of the disease, chest x-rays show a widened mediastinum (Figure 2), which is evidence of hemorrhagic mediastinitis, and mark pleural effusions[17]. The fulminant stage of the disease appears abruptly and is characterized by respiratory failure, acute dyspnea, circulatory collapse, cyanosis, pleural effusion, and fever[3]. Death follows within 24 hours of the onset of the second

stage due to toxemia and suffocation, making mortality rates extremely high, despite the use of appropriate antibiotics[2, 3]. Prompt diagnosis and treatment must occur within the first stage of infection to achieve full recovery, which often fails to take place.

Figure 2. Common types of anthrax infections. A) Seven-month old infant infected with *B. anthracis* after the terrorist attacks of 2001[24]; B) 27-year old man, 5 days after the onset of symptoms of oropharyngeal anthrax; C) mediastinal widening with pulmonary anthrax[7].

2.2.3.1 Incidence of Pulmonary Anthrax

The intentional release of aerosolized *B. anthracis* spores following the September 11, 2001 terrorist attacks showed a weakness in the U.S. medical response to bioterrorism[25]. Between September and October of 2001, the first 22 cases of bioterrorism-related anthrax were identified in the United States resulting in 11 cases of pulmonary anthrax and five deaths[13]. Despite the heroic efforts, physicians were unprepared to recognize the early symptoms of the rapidly progressive infection, and 4 out of the 11 patients with pulmonary anthrax were sent home after a diagnosis of a "viral syndrome", bronchitis or gastroenteritis was given[12]. The past few incidents have confirmed that airborne delivery of spores has to be the focus of biological weapon programs in order to prevent attacks that may result in mass casualties.

2.2.3.2 Diagnosis and Treatment

Successful eradication of an anthrax infection and therapy is only achieved with early administration of antibiotics and aggressive supportive care[18]. Unfortunately, due to the

remarkable similarity of initial symptoms observed during an influenza-like illness and pulmonary anthrax, the disease is difficult to diagnose causing a delay in treatment and increasing mortality rates[9, 17]. Rapid diagnostic tests such as enzyme-linked immunosorbent assays (ELISA) and polymerase chain reaction (PCR) to identify specific markers of *B. anthracis* and specific virulence plasmid markers are available but only at national reference laboratories[3].

While diagnosis of pulmonary anthrax is difficult, the sudden appearance of a large number of patients in a region with acute flu-like symptoms and death occurring within 24 to 48 hours is an indication of an anthrax or pneumonic plague[7]. Early administration of antibiotics and aggressive supportive care are needed to treat anthrax. Table 1 summarizes pharmacologic therapy for anthrax infections.

Table 1 Pharmacologic Therapy for Pulmonary Anthrax. Adapted from Dixon et al.[17]

Therapy	**Dosage for Adults**	**Dosage for Children**
Penicillin G	8 million-12 million U total, intravenously in divided doses every 4-6 hrs	100,000-150,000 U/kg/day in divided doses every 4-6 hrs
Streptomycin	30 mg/kg intramuscularly or intravenously per day-gentamicin can also be used (in conjunction with penicillin)	

Table 1. Continued…

Tetracycline	250-500 mg intravenously 4 times/day	Not approved for children
Doxycycline	200 mg intravenously as a loading dose, then 50-100 mg every 12 hrs	Not approved for children < 9 yr old
Erythromycin lactobionate	15-20 mg/kg (maximum 4 g) intravenously per day	20-40 mg/kg/day intravenously in divided doses every 6 hours (1-2 hr infusion)
Chloramphenicol	50-100 mg/kg/day intravenously in divided doses every 6 hrs	50-75 mg/kg/day in divided doses every 6 hrs
Ciprofloxacin	200-400 mg intravenously every 12 hrs	20-30 mg/kg/day in divided doses every 12 hours. Not approved for patients <18 yr old

While research has proved that *B. anthracis* in their vegetative state are susceptible to several families of antibiotics, other studies have observed natural resistance of *B. anthracis* strains to existing antibiotics[7].

2.3 *Bacillus anthracis*

B. anthracis is a member of the *Bacillus* species, which also include *B. cereus, B. mycoides, B. thuringiensis, B. megaterium, and B. subtilis. B. anthracis*, the etiologic agent of anthrax, is a Gram-positive, aerobic, or optionally anaerobic, nonmotile, rod-shaped bacterium (1 µm by 5-8 µm) with a centrally located ellipsoidal to cylindrical spore[3]. The bacterium has the ability to synthesize anthrax toxin proteins and the poly-D-glutamic acid capsule that can be easily observed microscopically using India Ink exclusion[26].

The sporulated state of *B. anthracis* is considered the predominant form of the bacterium[26]. Upon infection inside the host, spores germinate becoming vegetative cells that can replicate in high numbers in just a few hours[3]. The vegetative cells are frequently found in long chains of 4 or 5 cells, giving the appearance of bamboo[3]. *B. anthracis* produces colonies that are opaque, white or gray in color, flat and irregular, 4 to 5 mm in diameter, with an undulate margin[3, 26]. In their vegetative state, *B. anthracis* produces two exotoxins known as lethal factor (LF) and edema factor (EF) that depend on a third protein called protective antigen (PA) for their biological activity[27]. Vegetative *B. anthracis* have poor survival and can be killed with common antibacterial agents.

In the absence of nutrients *B. anthracis* can develop into dormant spores that can remain viable for decades[7]. In its sporulated state, *B. anthracis* do not divide, have no measurable metabolism, and are extremely resistant to drying, heat, ultraviolet light, gamma radiation, and many disinfectants[17]. The genetic material of *B. anthracis* is protected by a series of protein coats that are synthesized during the process of sporulation. The inner cell membrane surrounds and protects the core of the spore, which contains its chromosome and other cellular contents (Figure

3). This membrane is protected from external environmental factors by a ~130 nm barrier that consists of a polymer layer and protein coat[28].The protein coat, which is composed of as many as 25 highly cross-linked polypeptide species, plays a role as a permeability barrier against chemical and enzymatic assaults[29]. Beneath the spore coat is a thick layer of peptidoglycan (cortex) that consists of two layers, the thin inner primordial cell wall and the outer cortex[30]. These two layers maintain the spore's dormancy and heat resistance[28]. The primordial cell wall prevents the loss of cellular integrity after germination and serves as a template for peptidoglycan biosynthesis during outgrowth[30].

The spore core contains all metabolic components of the cell as well as genetic material. In dormant spores, the core is highly mineralized and is dehydrated, allowing its contents to be heat and UV resistant[30].

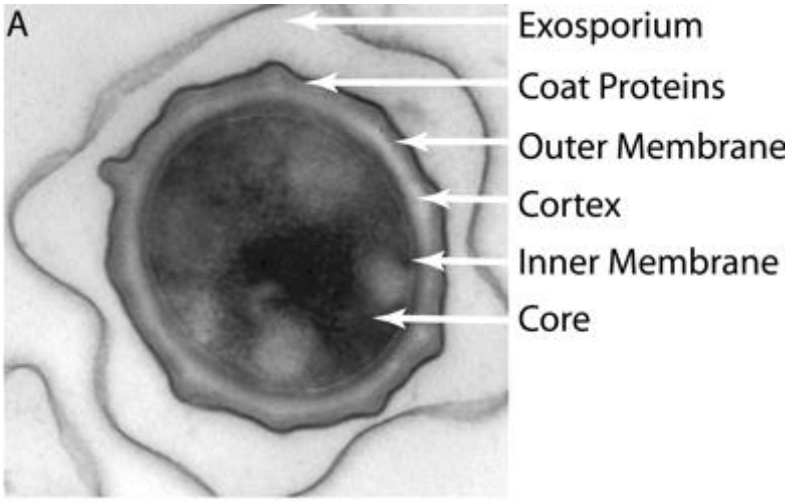

Figure 3. Electron micrograph of a cross section of a *Bacillus anthracis* spore. Adapted from Liu et al.[31]

A distinguishing characteristic of *B. anthracis* spores is the presence of an outermost layer called exosporium[26]. The exosporium is a loosely fitting shell that surrounds the coat. The space between the exosporium and the coat consists of proteins that have not been well studied,

but are likely to have intimate interactions with the environment and may be potential candidates for the development of vaccines[32]. The overall function of the exosporium is unknown as well as its role in pathogenesis of *B. anthracis*[33].

2.3.1 Sporulation of *Bacillus anthracis*

One of the unique characteristics of *Bacillus* species is that under conditions of nutrient deprivation bacteria are capable of undergoing the process of sporulation (Figure 4)[34]. During sporulation, vegetative metabolism is minimized, and a series of alternative sigma factors are sequentially expressed and activated to coordinate the expression of mRNAs responsible for the development of spores[31].

The main stimulus for sporulation is starvation and high cell density[35]. Starvation of vegetative *B. anthracis* results in the activation of a master transcription regulator, Spo0A, which controls several hundreds of genes, and the sigma factor, σ^H, which interacts with core RNA polymerase and directs it to initiate transcription[35, 36]. With the activation of Spo0A and σ^H, asymmetric cellular division takes place and the *spoIIA*, *spoIIE*, and *spoIIG* loci are transcribed[36]. This asymmetric cellular division results in two distinct cells, the smaller prespore (also known as forespore), which develops into the mature spore, and the mother cell, which initiates the sporulation process but enters programmed cell death[35].

After replication of DNA, a portion of cytoplasm and DNA are isolated by the formation of a spore septum that sets apart the prespore during polar division[37]. Plasma membrane starts to surround DNA, cytoplasm, and the membrane that was previously isolated. A double membrane is formed and peptidoglycan layers are synthesized between the membranes to form the spore coat and cortex, which protect the spore from environmental stress factors[38]. The interior of the

spore undergoes marked changes in physicochemical properties as it develops into a mature spore. Low molecular weight proteins are synthesized in large amounts to coat the DNA, providing protection against several kinds of DNA damage[35]. The mother cell also synthesizes large amounts of dipicolinic acid (DPA), which is taken by the prespore along with divalent cations[35]. The DPA and minerals stored in the core allow the spore to dehydrate and mineralized the spore.

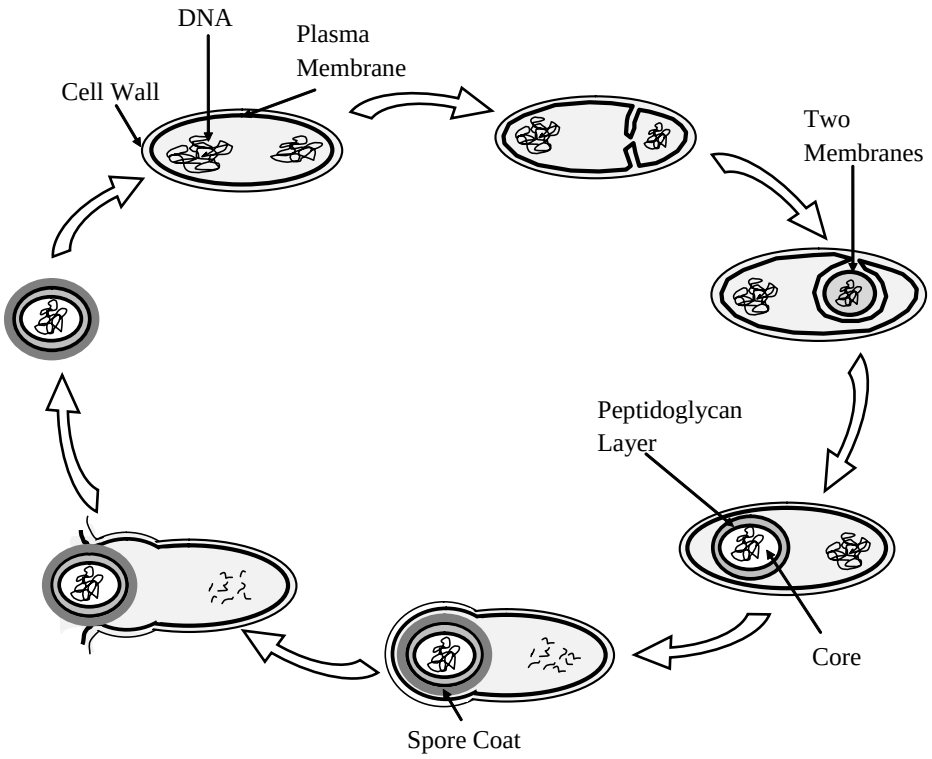

Figure 4. The sporulation cycle of *Bacillus anthracis*

After formation of coats is completed, the mother cell lyses releasing the newly formed spore[37]. The sporulation process takes 8 to 10 hours to complete after its onset[28].

Bacillus spores can remain in a dormant state with no metabolic activity and no production of ATP for decades or even hundreds of years[39]. However, the spores possess a

sensing mechanism that is capable of responding promptly to changes in their environment, such as the engulfment of spores by macrophages, where nutrients are available, and germination into a fully virulent bacterium can take place.

2.3.2 Germination and Outgrowth of *Bacillus anthracis*

Phagocytosis of *B. anthracis* by macrophages results in a change in environmental conditions that promote the germination of spores into fully virulent bacteria. Within macrophages, nutrients including carbon sources can be accessible to pathogens, resulting in the activation of germination processes[40]. Germination is also triggered in response to nutrients, such as amino acids, sugars, and purine nucleosides, or by non-nutrient factors, such as lysozyme, Ca^{2+}-DPA, cationic surfactants, high pressures, and salts[41].

The mechanism of germination triggered by nutrients involves the presence of spore-germination receptors on the surface of the inner membrane of the spore, which stimulate the cell to germinate and achieve vegetative growth[42]. L-alanine is an amino acid that interacts with receptors on the inner membrane of the spore and is a well studied molecule for the germination of several *Bacillus* species including *B. anthracis*, *B. subtilis*, *B. cereus,* and *B. atrophaeus*[43-46]. Inosine is a purine ribonucleoside that has been shown to be a strong germinant for *B. cereus* spores[47]. L-alanine or inosine alone can trigger the germination of *B. cereus,* but for *B. anthracis* spores, the use of both germinants together has shown to be more effective[42, 43].

Dodecylamine (DDA) is a cationic surfactant that has been used as a trigger to stimulate spore germination[48, 49]. Studies have suggested that DDA does not interact with any germinant receptors but instead acts against and compromises the spore's inner membrane[49]. DDA both initiates germination and deactivates *Bacillus* species at low molar concentrations[48]. Non-

nutrient germination stimuli are not generally encountered by spores in nature, and this trigger is usually used only in laboratories[50]. However, understanding how such agents trigger germination may provide insight into the mechanisms of spore germination and aid in the development of decontamination strategies for spores of *B. anthracis.*

Germination can be separated into three stages (Figure 5). The first stage of germination begins with the release of monovalent cations and Zn^{2+}, causing an elevation of pH in the spore core[41, 51]. The release of Ca^{2+} and pyridine-2,6-dicarboxyl acid (dipicolinic acid (DPA)) from the core follows, which accounts for approximately 10% of the spores dry weight[41]. As DPA is released from the spore core, water molecules enter and hydrate the core[52]. Rehydration of the core results in loss of heat resistance of the spore[41]. During the second stage, further water intake results in hydrolysis of the spore peptidoglycan cortex by cortex lytic enzymes (CLEs) and swelling of the core and germ cell wall occurs[50]. CLEs specifically recognize muramic acid-δ-lactam, which is only present in the peptidoglycan cortex, to ensure that only cortex petidoglycan and not germ cell wall peptidoglycan is degraded during germination[50]. Once the spore cortex has expanded the last stage of germination starts where metabolism recommences and macromolecular synthesis converts the spore into fully virulent germinated cells by breaking the spore coat and releasing the vegetative bacterium.

The current theory of spore inactivation assumes that in most deactivation technologies germination must occur before spores can be killed by anti-sporal agents[30]. The physical changes that *B. anthracis* undergo during germination need to be understood to investigate the possibility of deactivating *B. anthracis* spores without the need to initiate or complete germination.

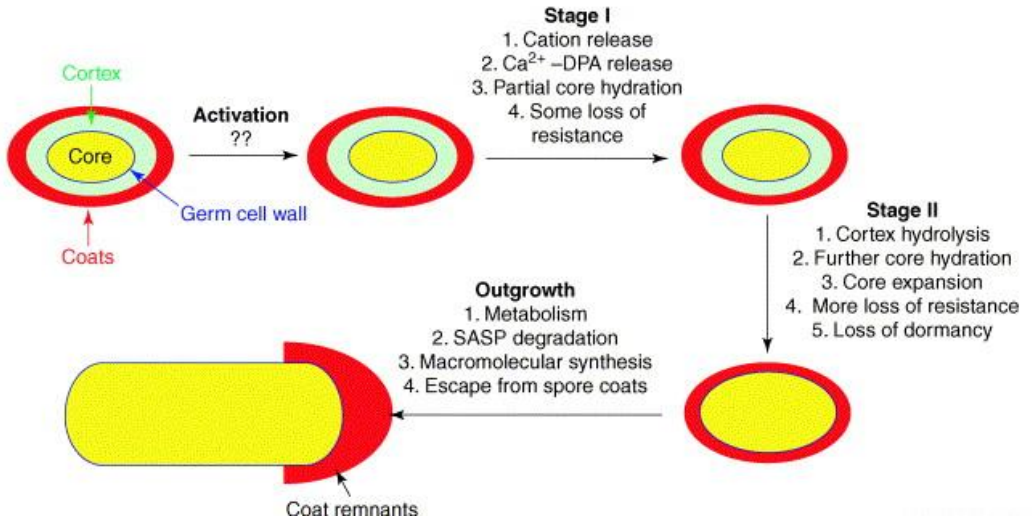

Figure 5. Process of spore germination. Adapted from Setlow[41].

2.3.3 Role of the *ger* Gene in Spore Germination

Small molecules from the environment, such as amino acids, specifically bind to germinant receptors located on the inner membrane of the spore[41, 53]. Activation of these germinant receptors initiates a series of complex biophysical processes, where intracellular proteases and extracellular hydrolases are activated to facilitate the cellular differentiation from spore to the vegetative form[54].

When a nutrient ligand binds to germinant receptors, some of these receptors alone can trigger germination, while other receptors may cooperate in responding to mixtures of nutrient germinants[50]. The number of germinant receptors in the membrane of the spore are low, averaging tens of molecules per spore[55]. However, germinant receptors can interact directly with other receptors or with additional components, such as proteins, needed for spore germination, to initiate DPA and cation movement within the core[41].

In *B. anthracis,* five distinct germination pathways have been recognized[54]:

- The alanine germination pathway (Ala): Requires the presence of L-alanine in concentrations above 30 mM, which are higher than concentrations of L-alanine available in the host.
- Alanine and proline pathway (AP): At lower, physiologically relevant concentrations (< 1 mM), L-alanine can work together with L-proline to initiate germination.
- Aromatic amino acid-enhanced pathway (AEP): L-alanine can cooperate with L-histidine, L-tyrosine, or L-tryptophan.
- Amino acid and inosine-dependent 1 pathway (AAID-1): The purine ribonucleoside inosine works in combination with a second cogerminant (L-alanine, L-serine, L-valine, L-methionine, or L-proline) to trigger germinantion.
- Amino acid and inosine-dependent 2 pathway (AAID-2): Inosine pairs with L-histidine, L-tyrosine, L-tryptophan, or L-phenylalanine to trigger germination.

Germinant receptors are composed of three different subunits that are essential to establish receptor function (Figure 6)[56]. Spores of the *Bacillus* species have 3 to 7 different germinant receptors each having an exquisite nutrient specificity[50]. In *B. anthracis,* germinant receptors are encoded by the tricistronic operons *gerH, gerK, gerL, gerS, gerX, gerA,* and *gerY* [57]. The *gerX* operon is located on the pXO1 virulence plasmid of the bacterium, while the other six operons are found on the chromosome of the spore[54].

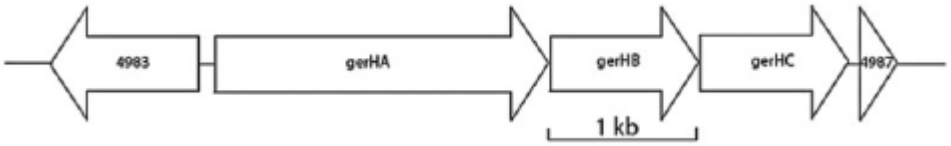

Figure 6. Gene map of the *gerH* operon. Adapted from Carr et al.[57]

Only few studies have investigated the roles of germinant receptors on spore germination[53, 57, 58]. The presence of the GerS receptor has been shown to be sufficient for germination in rich media; however, when *gerS*$^{+}$ strains were exposed to only L-alanine without inosine, only ~50% of the spores germinated as observed by the loss of heat resistance and loss of optical density[57]. In another study, mutant strains lacking the GerS receptor were unable to germinate in murine macrophages[53]. Weiner and Hanna concluded that the GerH receptor is necessary to induce germination of spores in macrophages[58]. There results suggest that GerH and GerS are not the only receptors necessary to initiate germination of spores in macrophages, and the presence of other receptors may be needed for the spore to have full virulence and germination capabilities within macrophages. The *gerX* operon has been shown to play a role in germination *in vivo* and in virulence in an animal model of infection[54]. However, the *gerA* and *gerY* operons do not contribute to germination of spores and their specific functions are not known.

From *in vivo* experiments, data suggests that the route of infection dictates which of the five germinant receptors is stimulated[57]. The presence of one of the receptors is sufficient to initiate disease via an intratracheal route of infection, and the GerH receptor is the primary receptor required for the germination and establishment of disease in a subcutaneous route of infection[57].

The effects of germination receptors on mechanical properties and virulence of spores have not been well studied; however, it is known that germination needs to take place for *B. anthracis* to produce toxins and affect the host. An in depth analysis of how each germinant receptors affects germination and the physico-chemical properties of *B. anthracis* spores is needed to the development of deactivation technologies against anthrax.

2.4 *Bacillus anthracis*-Macrophage Interactions

After deposition of spores in alveolar spaces, macrophages interact with *B. anthracis* spores and entrap them with the intent to eradicate the infection. After phagocytosis, spores within the phagosomal compartment of bronchoalveolar macrophages germinate *en route* to regional lymph nodes[17, 59]. After germination vegetative *B. anthacis* must survive the hostile intracellular environment of the macrophage phagosome and lastly be released from the phagocyte for infection to spread into the lymphatic system[60].

The macrophage is a highly specialized cell type with multiple functions that are specific to tissue location and activation status. In the lung alveoli, macrophages play a central role in cell-mediated immune response and act as guard cells, clearing invading bacteria from the lungs[59]. *B. anthracis* spores take advantage of the location of alveolar macrophages and adapt to their environment to use these cells as a sanctuary during the early phase of infection both to get started and to cross the host permeability barriers (Figure 7).

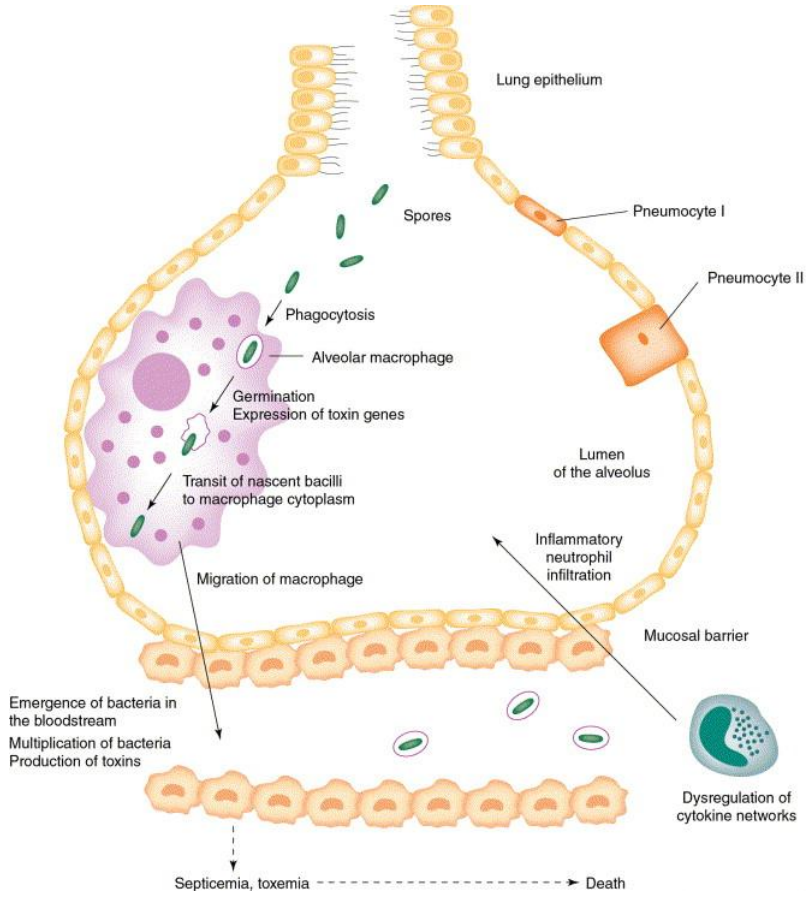

Figure 7. Cellular mechanism involved in the early phase of pulmonary anthrax. Adapted from Guidi-Rontani[59].

In the early phase of an anthrax infection, macrophages are key cells in *B. anthracis* pathogenesis. After encountering *B. anthracis* spores, macrophages are stimulated, resulting in sequestration of the invading spores into an enclosed vacuole, known as the phagosome, where oxygen is secreted and protein and proteases are released following fusion of lysosomes to form the phagolysosome[61]. Within the phagolysosome, *B. anthracis* spores germinate and produce toxins (edema factor and lethal factor), which promote the disruption of the phagolysosome membrane[60]. Disruption of the membrane results in nascent bacilli to move from the phagolysosome into the macrophage cytoplasm. Within the cytoplasm, vegetative *B. anthracis*

continue replicating and accumulate in the macrophage cytoplasm until lysis of the macrophage occurs[60].

While replication of nascent bacilli is taking place within the macrophage, bacteria are carried from the primary site of infection (lung alveoli) by migrating macrophages to the blood stream[59]. Bacteria continue spreading through the blood and lymph causing bacillemia and toxemia, which are fatal in an anthrax infection[17, 59].

2.4.1 Release of Lethal and Edema Factor into the Host

The virulence of anthrax depends on the presence of two major plasmids, pXO1 and pXO2[17]. The pXO1 plasmid (184.5 kb) carries genes whose function is to produce anthrax toxins. The pXO2 plasmid (95.3 kb) carries the genes involved in the synthesis of a poly-D-glutamyl antiphagocytic capsule[17].

After the resumption of metabolic activity during germination within macrophages, vegetative *B. anthracis* produce and release two toxins, lethal toxin (LeTx) and edema toxin (EdTx)[2]. These toxins are composed of three entities, which act in concert and are responsible for some of the clinical manifestations of the disease: the lethal factor (90 kDa; LF), the edema factor (89 kDa; EF), and the protective antigen (83 kDa; PA)[62, 63]. The protective antigen (PA) on vegetative bacteria specifically binds to the anthrax toxin receptors located on the surface of a variety of cell types including neural, cardiac, pulmonary cells, and lymphocytes (Figure 8)[22, 63]. These receptors are expressed at high levels on cells surfaces (3×10^4 receptors/cell), and represent the major uptake routes of *B. anthracis* spores[62, 63].

After binding to the receptor, PA is activated by a furin-like-cell-surface membrane protease resulting in cleavage and dissociation of a small 20 kDa fragment (PA_{20}) in the

medium[63]. The loss of the PA_{20} fragment causes the cleaved C-terminal PA_{63} fragment to self-associate into symmetric, ring-shaped, membrane-inserting heptamers (prepore)[64]. LF and EF toxin enzymes bind to the heptamer where endocytosis of toxins occurs[65]. Low pH induces the complexes to undergo a conformation transition from a prepore to a pore, leading to the formation of a membrane spanning cation-selective channel that allows passage and release of the EF and LF into the cytosol[63, 66].

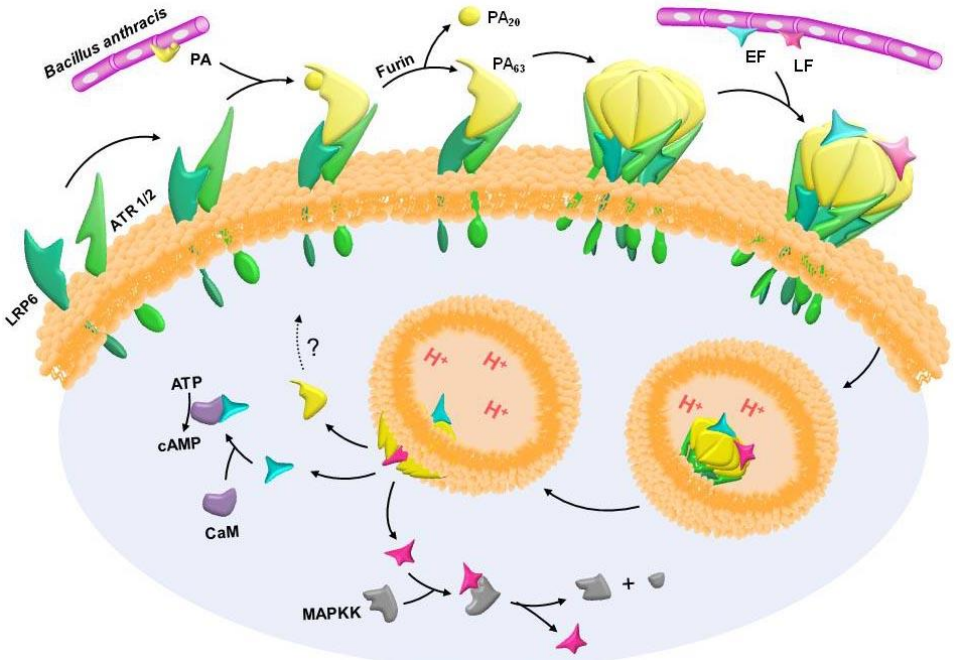

Figure 8. Internalization of anthrax toxins. Adapted from Golden et al.[63]

EF and LF can distrupt the normal physiology of the cell by modifying cytosolic substrates. LF cleaves members of the mitogen-activated protein kinase kinases (MAPKK), thus inhibiting signaling pathways and causing cell death in macrophages[63]. MAP kinases protect against pathogens by inducing inflammatory changes in macrophages, leading to the production of proinflammatory cytokines, activation of the oxidative burst pathway, and the release of oxygen intermediates[63]. By inducing apoptosis of activated macrophages, LF could prevent the

proper release of chemokines and cytokines that alert the immune system to the presence of infecting *B. anthracis* and facilitate the systemic spread of the infection[65].

EF within the host protects bacteria from phagocytic destruction, and increases intracellular levels of cyclic AMP (cAMP) leading to swelling of tissues (edema), and death[67].

2.4.2 Immunological Response to Anthrax Infections

With the inhalation and accumulation of *B. anthracis* spores in the lung alveoli, alveolar macrophages are rapidly recruited to the site of infection to initiate an immune response and clear invading bacteria[59]. As the spores are being transported to regional lymph nodes, macrophages start to produce pro-inflammatory cytokines including interleukin (IL)-10, IL-6, IL-12, IL-8, IL-1β, and tumor necrosis factor (TNF)–α[68, 69]. The EdTx induces IL-6 production in human monocytes and significantly decreases lipopolysaccharide-induced monocyte TNF-α production[63]. However, research has suggested that with the release of *B. anthracis* toxins within macrophages, there is a down regulation of TNF-α and IL-1β[59]. In another study, expression of Il-1β and TNF-α was induced by sub-lytic concentrations of *B. anthracis* toxins[70]. These studies suggest that there may be a dysregulation of cytokine networks that could be linked to the number of germinating *B. anthracis* cells present and the amount of toxins produced and released.

2.5 Antimicrobial Peptides

The increase of antibiotic resistance of several microorganisms has become a medical concern for the treatment of bacterial infections in developed and developing countries[71]. *B. anthracis* not only poses a threat for their ability to sporulate and remain viable in harsh

environmental conditions, but their increased levels of antibiotic resistance during treatment of anthrax infections is a concern that needs to be immediately addressed.

Long term treatment of anthrax infections may induce antibiotic resistance in *B. anthracis* as it has been observed with antibiotics, such as ciprofloxacin, tetracycline, vancomycin, and erythromycin[72]. Natural resistance of *B. anhtracis* to other antibiotics including sulfamethoxasole, trimethoprim, cefuroxime, cefotaxime, sodium, aztreonam, and celfazidime has also been observed[7]. Development of antibiotic resistance of *B. anthracis* to antibiotics can also be easily achieved in laboratories with technologies that do not require expensive equipment or difficult techniques[73]. Intentional development of antibiotic resistance in microorganisms such as *B. anthracis* is a serious concern since these microbes can be used for bioterrorism where common antibiotic treatments may be ineffective.

Alternative therapies for eradication of infections are being sought and special attention is being paid to antimicrobial peptides (AMPs). The antimicrobial properties of secretions, blood, leukocytes, and lymphatic tissues have been recognized for decades and early investigators suggested that antimicrobial basic proteins and polypeptides combine with cell nucleoproteins or other negatively charged surface constituents of bacteria, thus disrupting important cell function[74].

AMPs are short polypeptides that are associated with the innate immune system of the host organism, and are widely distributed in the animal and plant kingdoms[75]. More than 880 different AMPs have been identified including peptides that are produced in many tissues and cell types of a variety of plant and animal species[76]. These peptides have been classified according to their amino acid composition and structure, size, sequence, charge, hydrophobicity,

and amphipathicity. Classes of AMPs include anionic peptides, linear cationic α-helical peptides, cationic peptides enriched for specific amino acids, anionic and cationic peptides that contain cysteine and form disulphide bonds, and anionic and cationic peptide fragments of larger proteins[77].

Specific steps need to occur to induce bacterial killing by AMPs, First, AMPs need to be attracted to the bacterial surface and bonding between anionic or cationic peptides and structures on the bacterial surface occur through electrostatic interactions[75]. The membrane of bacteria is organized in such a way that the outermost leaflet of the lipid bilayer is populated with negatively charged phospholipids[75]. AMPs are then attracted to the net negative charges that exist in the bacterial envelope, to the anionic phospholipids and phosphate groups on lipopolysaccharides of Gram-negative bacteria, and to teichoic acids on the surface of Gram-positive bacteria[77]. Once the AMP has been attracted through electrostatic interactions, peptides must attach and traverse capsular polysaccharides before they can interact with the outer membrane of Gram-negative and Gram-positive bacteria[77]. After attachment of the peptide on the cell membrane, peptide insertion and membrane permeability take place. Three main models have been proposed to explain membrane permeabilization.

In the *barrel-stave model* (Figure 9A), the attached peptides aggregate and insert into the lipid bilayer, forming a transmembrane channel/pore by bundles of amphipathic α-helices. The hydrophobic peptide regions align with the lipid core region of the bilayer and the hydrophilic peptide regions form the interior of the pore[78]. For this model to occur, the monomers that bind to the membrane need to be in a α-helical structure and recognize each other. Recruitment of additional monomers may occur to increase the size of the pore[78].

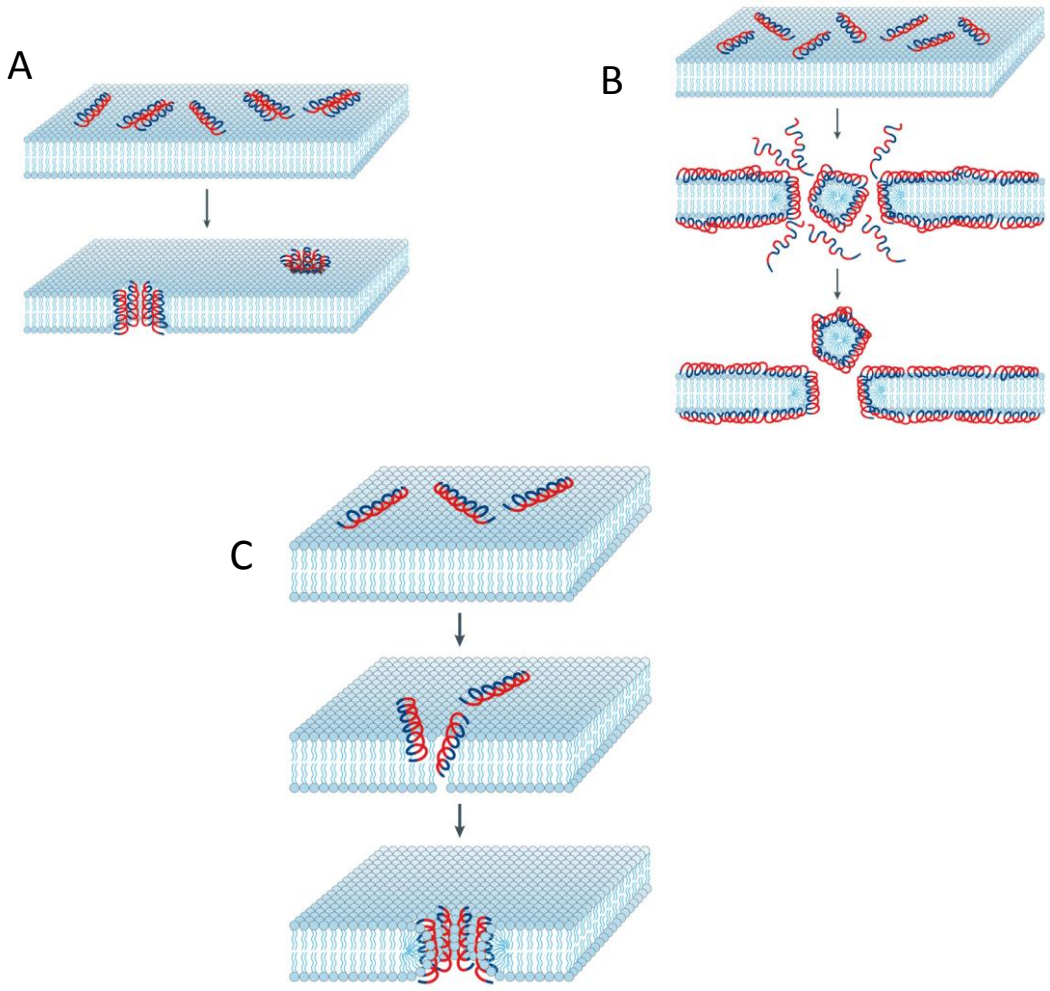

Figure 9. Mechanisms of peptide insertion and membrane permeability for A) the barrel-stave model; B) the carpet model; and C) the toroidal model. Hydrophilic regions are shown in red and hydrophobic regions are shown in blue. Adapted from Brogden[77].

In the *carpet model* (Figure 9B), peptides accumulate on the surface of the lipic bilayer, which orient parallel to the membrane surface[77]. Though electrostatic interactions, the peptides are attracted to the surfaces and attach to the membrane in a carpet-like manner. In this model, AMPs are in contact with the phospholipid head group throughout the entire process of membrane permeation were at critical peptide concentrations, the peptide form toroidal transient holes in the membrane that eventually form micelles after the disruption of the bilayer curvature[77, 78].

In the *toroidal-pore model* (Figure 9C), AMPs helices insert into the membrane and induce the lipid monolayers to bend continuously through the pore so the water core is lined by both the inserted peptides and the lipid head groups[79]. This model differs from the carpet-stave model since the AMPs are always associated with the lipid head groups even when they are in a perpendicular position while they are forming pores[77].

Once pores or micelles have been formed in the membrane of bacteria, lysis rapidly occurs due to a destabilization of the bacterial membrane. It is remarkable that most animals including insects rely heavily on antimicrobial peptides for defense against microbes, and do so effectively without the help of antibodies of lymphocytes[75]. Studies on AMPs show promising results and provide an alternative mechanism for the development of antimicrobial compounds where antibiotic resistance is not a major concern.

2.5.1 Chrysophsin-3

AMPs from fish are of particular interest since they have shown antibacterial, antifungal, antiviral, antiparasitic, immunomodulatory, and antitumor functions[80]. Chrysophsin-1, -2, and -3 are a family of peptides that have been isolated from the eosinophilic granule cell-like cells of the gills of the red sea bream *Chrysophrys major*[81]. The AMPs are all bactericidal to pathogenic bacteria at low micromolecular concentrations[82]. Chrysophsin-3 is an amphipathic, cationic α-helical peptide that is rich in histidine residues and has a 20 amino acid sequence (FIGLLISAGKAIHDLIRRRH) and a molecular mass of 2287 Da (Figure 10)[81]. Hydrophobic and charged residues are segregated into a separate section of the primary sequence.

The peptide has an unusual RRRH motif that makes the molecule positively charged causing secondary amphipathicity and a change in hydrophobicity between the N and C termini.

The C-terminal RHHH has been shown to have a large effect on the insertion of the peptide into the lipid membranes and was found crucial for pore formation and toxicity to fibroblasts[82]. Toxicity of chrysophsin to eukaryotic fibroblasts may suggest a role of the AMP in defense against predation[82].

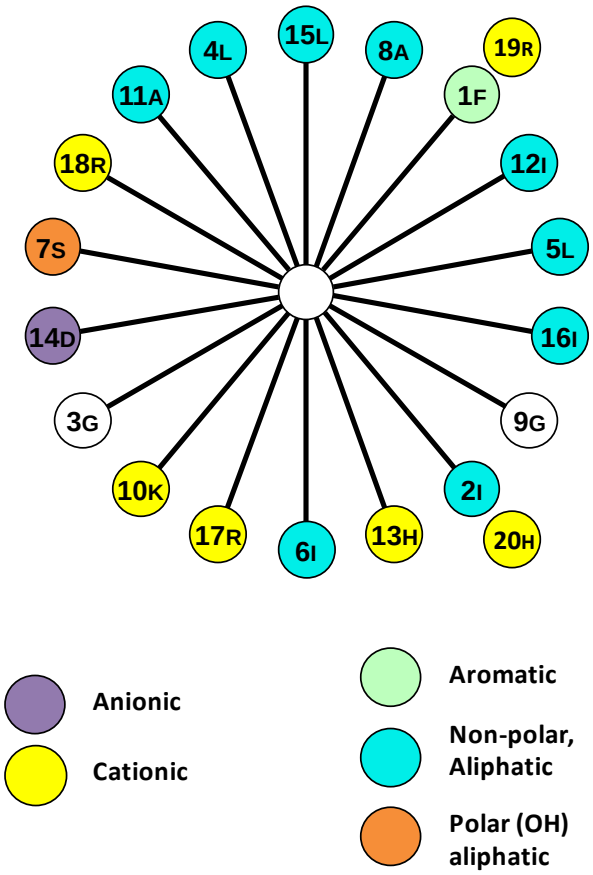

Figure 10. Helical wheel diagram of chrysophsin-3. Shaded gray indicates hydrophobic amino acids. Residue numbers starting from the N-terminus are shown. Adapted from Wang et al.[83]

There are numerous types of AMPs that have shown antibacterial activity against Gram-positive and Gram-negative bacteria[76, 84-86]. However, only one study has evaluated the effect that chrysophsin-3 on vegetative bacteria[81]. Chrysophsin-3 has been effective in the killing of several organisms at concentrations lower than 40 µM, including vegetative *B. subtilis*[81]. Although these studies are encouraging, no prior study has investigated the effects of

chrysophsin-3 on bacterial spores. A clear understanding of how AMPs may affect spore surfaces may be essential in the development of alternative strategies to eradicate *B. anthracis.*

REFERENCES

1. Schmid, G.; Kaufmann, A., Anthrax in Europe: its epidemiology, clinical characteristics, and role in bioterrorism. *Clin Microbiol Infect* **2002,** 8, (8), 479-88.

2. Pile, J. C.; Malone, J. D.; Eitzen, E. M.; Friedlander, A. M., Anthrax as a potential biological warfare agent. *Arch Intern Med* **1998,** 158, (5), 429-34.

3. Oncu, S.; Oncu, S.; Sakarya, S., Anthrax--an overview. *Med Sci Monit* **2003,** 9, (11), RA276-83.

4. Khan, A. S.; Morse, S.; Lillibridge, S., Public-health preparedness for biological terrorism in the USA. *Lancet* **2000,** 356, (9236), 1179-82.

5. Darling, R. G.; Catlett, C. L.; Huebner, K. D.; Jarrett, D. G., Threats in bioterrorism. I: CDC category A agents. *Emerg Med Clin North Am* **2002,** 20, (2), 273-309.

6. Christopher, G. W.; Cieslak, T. J.; Pavlin, J. A.; Eitzen, E. M., Jr., Biological warfare. A historical perspective. *Jama* **1997,** 278, (5), 412-7.

7. Inglesby, T. V.; Henderson, D. A.; Bartlett, J. G.; Ascher, M. S.; Eitzen, E.; Friedlander, A. M.; Hauer, J.; McDade, J.; Osterholm, M. T.; O'Toole, T.; Parker, G.; Perl, T. M.; Russell, P. K.; Tonat, K., Anthrax as a biological weapon: medical and public health management. Working Group on Civilian Biodefense. *Jama* **1999,** 281, (18), 1735-45.

8. Szinicz, L., History of chemical and biological warfare agents. *Toxicology* **2005,** 214, (3), 167-81.

9. Goldenberg, A.; Shmueli, G.; Caruana, R. A.; Fienberg, S. E., Early statistical detection of anthrax outbreaks by tracking over-the-counter medication sales. *Proc Natl Acad Sci U S A* **2002,** 99, (8), 5237-40.

10. Sidell, F.; Takafuji, E.; Franz, D., *Medical Aspects of Chemical and Biological Warfare*. Office of the Surgeon General at TMM Publications: Washington, DC, 2008.

11. Tucker, J. B., Historical trends related to bioterrorism: An empirical analysis. *Emerg Infect Dis* **1999,** 5, (4), 498-504.

12. Jernigan, J. A.; Stephens, D. S.; Ashford, D. A.; Omenaca, C.; Topiel, M. S.; Galbraith, M.; Tapper, M.; Fisk, T. L.; Zaki, S.; Popovic, T.; Meyer, R. F.; Quinn, C. P.; Harper, S. A.; Fridkin, S. K.; Sejvar, J. J.; Shepard, C. W.; McConnell, M.; Guarner, J.; Shieh, W. J.; Malecki, J. M.; Gerberding, J. L.; Hughes, J. M.; Perkins, B. A., Bioterrorism-related

inhalational anthrax: the first 10 cases reported in the United States. *Emerg Infect Dis* **2001,** 7, (6), 933-44.

13. Fowler, R. A.; Sanders, G. D.; Bravata, D. M.; Nouri, B.; Gastwirth, J. M.; Peterson, D.; Broker, A. G.; Garber, A. M.; Owens, D. K., Cost-effectiveness of defending against bioterrorism: a comparison of vaccination and antibiotic prophylaxis against anthrax. *Ann Intern Med* **2005,** 142, (8), 601-10.

14. U.S.Congress, O. o. T. A. *Proliferation of Weapons of Mass Destruction: Assessing the Risk.*; Report no. OTA-ISC-559; U.S. Government Printing Office: Washington, DC, 1993.

15. Kaufmann, A. F.; Meltzer, M. I.; Schmid, G. P., The economic impact of a bioterrorist attack: are prevention and postattack intervention programs justifiable? *Emerg Infect Dis* **1997,** 3, (2), 83-94.

16. Kohout, E.; Sehat, A.; Ashraf, M., Anthrax: a Continous Problem in Southwest Iran. *Am J Med Sci* **1964,** 247, 565-75.

17. Dixon, T. C.; Meselson, M.; Guillemin, J.; Hanna, P. C., Anthrax. *N Engl J Med* **1999,** 341, (11), 815-26.

18. Bell, D. M.; Kozarsky, P. E.; Stephens, D. S., Clinical issues in the prophylaxis, diagnosis, and treatment of anthrax. *Emerg Infect Dis* **2002,** 8, (2), 222-5.

19. Freedman, A.; Afonja, O.; Chang, M. W.; Mostashari, F.; Blaser, M.; Perez-Perez, G.; Lazarus, H.; Schacht, R.; Guttenberg, J.; Traister, M.; Borkowsky, W., Cutaneous anthrax associated with microangiopathic hemolytic anemia and coagulopathy in a 7-month-old infant. *Jama* **2002,** 287, (7), 869-74.

20. Swartz, M. N., Recognition and management of anthrax--an update. *N Engl J Med* **2001,** 345, (22), 1621-6.

21. Kanafani, Z. A.; Ghossain, A.; Sharara, A. I.; Hatem, J. M.; Kanj, S. S., Endemic gastrointestinal anthrax in 1960s Lebanon: clinical manifestations and surgical findings. *Emerg Infect Dis* **2003,** 9, (5), 520-5.

22. Banks, D. J.; Barnajian, M.; Maldonado-Arocho, F. J.; Sanchez, A. M.; Bradley, K. A., Anthrax toxin receptor 2 mediates *Bacillus anthracis* killing of macrophages following spore challenge. *Cell Microbiol* **2005,** 7, (8), 1173-85.

23. Bush, L. M.; Abrams, B. H.; Beall, A.; Johnson, C. C., Index case of fatal inhalational anthrax due to bioterrorism in the United States. *N Engl J Med* **2001,** 345, (22), 1607-10.

24. Roche, K. J.; Chang, M. W.; Lazarus, H., Images in clinical medicine. Cutaneous anthrax infection. *N Engl J Med* **2001,** 345, (22), 1611.

25. Hupert, N.; Bearman, G. M.; Mushlin, A. I.; Callahan, M. A., Accuracy of screening for inhalational anthrax after a bioterrorist attack. *Ann Intern Med* **2003,** 139, (5 Pt 1), 337-45.

26. Koehler, T. M., *Bacillus anthracis* physiology and genetics. *Mol Aspects Med* **2009,** 30, (6), 386-96.

27. Brossier, F.; Mock, M., Toxins of *Bacillus anthracis*. *Toxicon* **2001,** 39, (11), 1747-55.

28. Henriques, A. O.; Moran, C. P., Jr., Structure and assembly of the bacterial endospore coat. *Methods* **2000,** 20, (1), 95-110.

29. Pinzón-Arango, P. A.; Scholl, G.; Nagarajan, R.; Mello, C. M.; Camesano, T. A., Atomic force microscopy study of germination and killing of *Bacillus atrophaeus* spores. *J Mol Recognit* **2009,** 22, (5), 373-379.

30. Atrih, A.; Foster, S. J., Bacterial endospores the ultimate survivors. *Int. Dairy J.* **2002,** 12, (2-3), 217-223.

31. Liu, H.; Bergman, N. H.; Thomason, B.; Shallom, S.; Hazen, A.; Crossno, J.; Rasko, D. A.; Ravel, J.; Read, T. D.; Peterson, S. N.; Yates, J., 3rd; Hanna, P. C., Formation and composition of the *Bacillus anthracis* endospore. *J Bacteriol* **2004,** 186, (1), 164-78.

32. Kailas, L.; Terry, C.; Abbott, N.; Taylor, R.; Mullin, N.; Tzokov, S. B.; Todd, S. J.; Wallace, B. A.; Hobbs, J. K.; Moir, A.; Bullough, P. A., Surface architecture of endospores of the *Bacillus cereus/anthracis/thuringiensis* family at the subnanometer scale. *Proc Natl Acad Sci U S A* **2011,** 108, (38), 16014-9.

33. Sylvestre, P.; Couture-Tosi, E.; Mock, M., A collagen-like surface glycoprotein is a structural component of the Bacillus anthracis exosporium. *Mol Microbiol* **2002,** 45, (1), 169-78.

34. Ghosh, S.; Setlow, P., Isolation and characterization of superdormant spores of *Bacillus* species. *J Bacteriol* **2009,** 191, (6), 1787-97.

35. Errington, J., Regulation of endospore formation in *Bacillus subtilis*. *Nat Rev Microbiol* **2003,** 1, (2), 117-26.

36. Piggot, P. J.; Hilbert, D. W., Sporulation of *Bacillus subtilis*. *Curr Opin Microbiol* **2004,** 7, (6), 579-86.

37. Piggot, P. J.; Coote, J. G., Genetic aspects of bacterial endospore formation. *Bacteriol Rev* **1976,** 40, (4), 908-62.

38. Mallozzi, M.; Bozue, J.; Giorno, R.; Moody, K. S.; Slack, A.; Cote, C.; Qiu, D.; Wang, R.; McKenney, P.; Lai, E. M.; Maddock, J. R.; Friedlander, A.; Welkos, S.; Eichenberger, P.; Driks, A., Characterization of a *Bacillus anthracis* spore coat-surface protein that influences coat-surface morphology. *FEMS Microbiol Lett* **2008,** 289, (1), 110-7.

39. Nagarajan, R.; Muller, W. S.; Ashley, R.; Mello, C. M. In *Decontamination Of Bacterial Spores by a Peptide-Mimic*, 25th Army Science Conference, Orlando, FL, December, 2006, 2006; Orlando, FL, 2006.

40. Lorenz, M. C.; Fink, G. R., Life and death in a macrophage: role of the glyoxylate cycle in virulence. *Eukaryot Cell* **2002,** 1, (5), 657-62.

41. Setlow, P., Spore germination. *Curr Opin Microbiol* **2003,** 6, (6), 550-6.

42. Barlass, P. J.; Houston, C. W.; Clements, M. O.; Moir, A., Germination of *Bacillus cereus* spores in response to L-alanine and to inosine: the roles of *gerL* and *gerQ* operons. *Microbiology* **2002,** 148, (Pt 7), 2089-95.

43. Ireland, J. A.; Hanna, P. C., Amino acid- and purine ribonucleoside-induced germination of *Bacillus anthracis* ΔSterne endospores: *gerS* mediates responses to aromatic ring structures. *J Bacteriol* **2002,** 184, (5), 1296-303.

44. Akoachere, M.; Squires, R. C.; Nour, A. M.; Angelov, L.; Brojatsch, J.; Abel-Santos, E., Identification of an in vivo inhibitor of *Bacillus anthracis* spore germination. *J Biol Chem* **2007,** 282, (16), 12112-8.

45. Gounina-Allouane, R.; Broussolle, V.; Carlin, F., Influence of the sporulation temperature on the impact of the nutrients inosine and l-alanine on *Bacillus cereus* spore germination. *Food Microbiol* **2008,** 25, (1), 202-6.

46. Titball, R. W.; Manchee, R. J., Factors affecting the germination of spores of *Bacillus anthracis*. *J Appl Bacteriol* **1987,** 62, (3), 269-73.

47. Clements, M. O.; Moir, A., Role of the gerI operon of *Bacillus cereus* 569 in the response of spores to germinants. *J Bacteriol* **1998,** 180, (24), 6729-35.

48. Rode, L. J.; Foster, J. W., Germination of bacterial spores with alkyl primary amines. *J Bacteriol* **1961,** 81, 768-79.

49. Setlow, B.; Cowan, A. E.; Setlow, P., Germination of spores of *Bacillus subtilis* with dodecylamine. *J Appl Microbiol* **2003,** 95, (3), 637-48.

50. Indest, K. J.; Buchholz, W. G.; Faeder, J. R.; Setlow, P., Workshop report: modeling the molecular mechanism of bacterial spore germination and elucidating reasons for germination heterogeneity. *J Food Sci* **2009,** 74, (6), R73-8.

51. Jedrzejas, M. J.; Setlow, P., Comparison of the binuclear metalloenzymes diphosphoglycerate-independent phosphoglycerate mutase and alkaline phosphatase: their mechanism of catalysis via a phosphoserine intermediate. *Chem Rev* **2001,** 101, (3), 607-18.

52. Slieman, T. A.; Nicholson, W. L., Role of dipicolinic acid in survival of *Bacillus subtilis* spores exposed to artificial and solar UV radiation. *Appl Environ Microbiol* **2001,** 67, (3), 1274-9.

53. Ireland, J. A.; Hanna, P. C., Macrophage-enhanced germination of *Bacillus anthracis* endospores requires gerS. *Infect Immun* **2002,** 70, (10), 5870-2.

54. Fisher, N.; Hanna, P., Characterization of *Bacillus anthracis* germinant receptors in vitro. *J Bacteriol* **2005,** 187, (23), 8055-62.

55. Paidhungat, M.; Setlow, P., Localization of a germinant receptor protein (GerBA) to the inner membrane of *Bacillus subtilis* spores. *J Bacteriol* **2001,** 183, (13), 3982-90.

56. Ross, C.; Abel-Santos, E., The Ger receptor family from sporulating bacteria. *Curr Issues Mol Biol* **2010,** 12, (3), 147-58.

57. Carr, K. A.; Lybarger, S. R.; Anderson, E. C.; Janes, B. K.; Hanna, P. C., The role of *Bacillus anthracis* germinant receptors in germination and virulence. *Mol Microbiol* **2010,** 75, (2), 365-75.

58. Weiner, M. A.; Hanna, P. C., Macrophage-mediated germination of *Bacillus anthracis* endospores requires the gerH operon. *Infect Immun* **2003,** 71, (7), 3954-9.

59. Guidi-Rontani, C., The alveolar macrophage: the Trojan horse of *Bacillus anthracis*. *Trends Microbiol* **2002,** 10, (9), 405-9.

60. Dixon, T. C.; Fadl, A. A.; Koehler, T. M.; Swanson, J. A.; Hanna, P. C., Early *Bacillus anthracis*-macrophage interactions: intracellular survival survival and escape. *Cell Microbiol* **2000,** 2, (6), 453-63.

61. Baillie, L.; Hibbs, S.; Tsai, P.; Cao, G. L.; Rosen, G. M., Role of superoxide in the germination of *Bacillus anthracis* endospores. *FEMS Microbiol Lett* **2005,** 245, (1), 33-8.

62. Bradley, K. A.; Mogridge, J.; Mourez, M.; Collier, R. J.; Young, J. A., Identification of the cellular receptor for anthrax toxin. *Nature* **2001,** 414, (6860), 225-9.

63. Golden, H. B.; Watson, L. E.; Lal, H.; Verma, S. K.; Foster, D. M.; Kuo, S. R.; Sharma, A.; Frankel, A.; Dostal, D. E., Anthrax toxin: pathologic effects on the cardiovascular system. *Front Biosci* **2009,** 14, 2335-57.

64. Little, S. F.; Ivins, B. E., Molecular pathogenesis of *Bacillus anthracis* infection. *Microbes Infect* **1999,** 1, (2), 131-9.

65. Ascenzi, P.; Visca, P.; Ippolito, G.; Spallarossa, A.; Bolognesi, M.; Montecucco, C., Anthrax toxin: a tripartite lethal combination. *FEBS Lett* **2002,** 531, (3), 384-8.

66. Sellman, B. R.; Mourez, M.; Collier, R. J., Dominant-negative mutants of a toxin subunit: an approach to therapy of anthrax. *Science* **2001,** 292, (5517), 695-7.

67. Leppla, S. H., Anthrax toxin edema factor: a bacterial adenylate cyclase that increases cyclic AMP concentrations of eukaryotic cells. *Proc Natl Acad Sci U S A* **1982,** 79, (10), 3162-6.

68. Pickering, A. K.; Merkel, T. J., Macrophages release tumor necrosis factor alpha and interleukin-12 in response to intracellular Bacillus anthracis spores. *Infect Immun* **2004,** 72, (5), 3069-72.

69. Pickering, A. K.; Osorio, M.; Lee, G. M.; Grippe, V. K.; Bray, M.; Merkel, T. J., Cytokine response to infection with *Bacillus anthracis* spores. *Infect Immun* **2004,** 72, (11), 6382-9.

70. Hanna, P. C.; Acosta, D.; Collier, R. J., On the role of macrophages in anthrax. *Proc Natl Acad Sci U S A* **1993,** 90, (21), 10198-201.

71. Neu, H. C., The crisis in antibiotic resistance. *Science* **1992,** 257, (5073), 1064-73.

72. Athamna, A.; Athamna, M.; Abu-Rashed, N.; Medlej, B.; Bast, D. J.; Rubinstein, E., Selection of *Bacillus anthracis* isolates resistant to antibiotics. *J Antimicrob Chemother* **2004,** 54, (2), 424-8.

73. Choe, C. H.; Bouhaouala, S. S.; Brook, I.; Elliot, T. B.; Knudson, G. B., In vitro development of resistance to ofloxacin and doxycycline in *Bacillus anthracis* Sterne. *Antimicrob Agents Chemother* **2000,** 44, (6), 1766.

74. Skarnes, R. C.; Watson, D. W., Antimicrobial factors of normal tissues and fluids. *Bacteriol Rev* **1957,** 21, (4), 273-94.

75. Zasloff, M., Antimicrobial peptides of multicellular organisms. *Nature* **2002,** 415, (6870), 389-95.

76. Brogden, K. A.; Ackermann, M.; McCray, P. B., Jr.; Tack, B. F., Antimicrobial peptides in animals and their role in host defences. *Int J Antimicrob Agents* **2003,** 22, (5), 465-78.

77. Brogden, K. A., Antimicrobial peptides: pore formers or metabolic inhibitors in bacteria? *Nat Rev Microbiol* **2005,** 3, (3), 238-50.

78. Shai, Y., Mechanism of the binding, insertion and destabilization of phospholipid bilayer membranes by alpha-helical antimicrobial and cell non-selective membrane-lytic peptides. *Biochim Biophys Acta* **1999,** 1462, (1-2), 55-70.

79. Park, S. C.; Kim, J. Y.; Shin, S. O.; Jeong, C. Y.; Kim, M. H.; Shin, S. Y.; Cheong, G. W.; Park, Y.; Hahm, K. S., Investigation of toroidal pore and oligomerization by melittin using transmission electron microscopy. *Biochem Biophys Res Commun* **2006,** 343, (1), 222-8.

80. Rajanbabu, V.; Chen, J. Y., Applications of antimicrobial peptides from fish and perspectives for the future. *Peptides* **2011,** 32, (2), 415-20.

81. Iijima, N.; Tanimoto, N.; Emoto, Y.; Morita, Y.; Uematsu, K.; Murakami, T.; Nakai, T., Purification and characterization of three isoforms of chrysophsin, a novel antimicrobial peptide in the gills of the red sea bream, *Chrysophrys major*. *Eur J Biochem* **2003,** 270, (4), 675-86.

82. Mason, A. J.; Bertani, P.; Moulay, G.; Marquette, A.; Perrone, B.; Drake, A. F.; Kichler, A.; Bechinger, B., Membrane interaction of chrysophsin-1, a histidine-rich antimicrobial peptide from red sea bream. *Biochemistry* **2007,** 46, (51), 15175-87.

83. Wang, K.; Nagarajan, R.; Mello, C. M.; Camesano, T. A., Characterization of Supported Lipid Bilayer Disruption by Chrysophsin-3 using QCM-D. *J Phys Chem B* **In press**.

84. Cole, A. M.; Weis, P.; Diamond, G., Isolation and characterization of pleurocidin, an antimicrobial peptide in the skin secretions of winter flounder. *J Biol Chem* **1997,** 272, (18), 12008-13.

85. Hancock, R. E.; Scott, M. G., The role of antimicrobial peptides in animal defenses. *Proc Natl Acad Sci U S A* **2000,** 97, (16), 8856-61.

86. Lauth, X.; Shike, H.; Burns, J. C.; Westerman, M. E.; Ostland, V. E.; Carlberg, J. M.; Van Olst, J. C.; Nizet, V.; Taylor, S. W.; Shimizu, C.; Bulet, P., Discovery and characterization of two isoforms of moronecidin, a novel antimicrobial peptide from hybrid striped bass. *J Biol Chem* **2002,** 277, (7), 5030-9.

Chapter 3

Atomic force microscopy study of germination and killing of *Bacillus atrophaeus* spores

Journal of Molecular Recognition, 2009. **22:** 373-379

3.1 Abstract

Bacterial spores such as *Bacillus atrophaeus* are one of the most resistant life forms known, and are extremely resistant to chemical and environmental factors in the dormant state. During germination, as bacterial spores progress towards the vegetative state, they become susceptible to anti-sporal agents. *B. atrophaeus* spores were exposed to the non-nutritive germinant dodecylamine (DDA), a cationic surfactant that can also be used as a killing agent, for up to 60 min, or to the nutrient germinant L-alanine. In kinetic studies, 99% of the spores were killed within 5 min of exposure to DDA. Atomic force microscopy (AFM) can be used as a sensitive tool to assess how the structure of the spore coat changes upon exposure to germinants or killing agents. Changes in cell height and roughness over time of exposure to DDA were examined using AFM. DDA caused the spore height to decrease by >50%, which may have been due to a partial breakdown of the spore coat. Treatment of *B. atrophaeus* with the nutrient germinant resulted in a decrease in height of spores after 2 hours of incubation, from 0.7 ± 0.1 μm to 0.3 ±0.2 μm. However, treatment with L-alanine did not change the surface roughness of the spores, indicating that the changes that occur during germination take place underneath the spore coat. We propose that exposure to DDA at high concentrations causes pores to form in the coat layer, killing *B. atrophaeus* without the need to fully germinate spores.

3.2 Introduction

Under nutrient deprivation, vegetative cells of *Bacillus* sp. and *Clostridium* sp. are able to undergo a restructuring and differentiation process known as sporulation[1-3]. Bacterial spores are metabolically dormant and are the most resistant life forms known. Their inner cell membrane surrounds and protects the core of the spore, which contains its chromosome and other cellular

contents. This membrane is protected from external environmental factors by a nearly 100 nm barrier consisting of a polymer layer and protein coat (Figure 11)[4]. Because of their unique structure and morphology, spores can overcome environmental and chemical factors such as radiation, desiccation, heat, changes in pH, and exposure to toxic chemicals[5-7]. Dormant spores are able to constantly monitor their surrounding environment so that when nutrients become available, they can return to a vegetative state, after passing through the stages of germination and outgrowth [6]. Because of their virulent pathogenic nature, *B. anthracis* and other spores are problematic since they can be used as biowarfare and bioterrorism agents causing severe and frequently lethal foodborne and airborne diseases, such as pulmonary anthrax[2, 8].

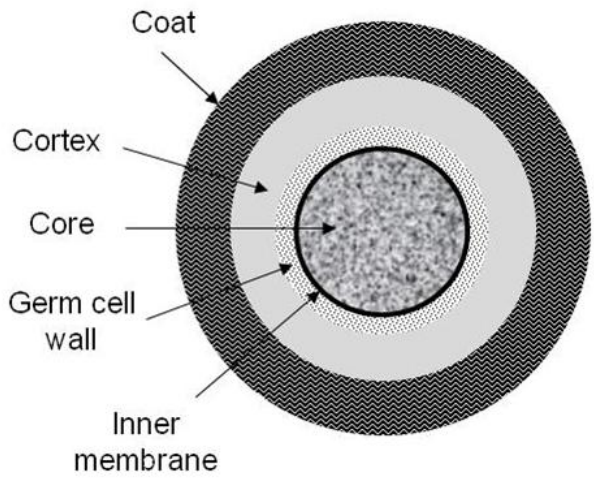

Figure 11. Schematic representation of *B. atrophaeus* spore structure. Common dimension of the different layers of spore structure are: spore coat (60 – 100 nm), spore cortex (50 - 100 nm), germ cell wall (2 - 10 nm); inner membrane (3 – 4 nm) and spore core (0.7 to 1 μm).

The current theory of spore inactivation assumes that in most deactivation technologies germination must occur before spores can be killed by anti-sporal agents[2], while some examples of spore killing, even in the absence of germination, also exist[9]. Germination can be triggered in response to nutrients, such as amino acids, sugars, and purine nucleosides, or by non-nutrient

factors such as lysozyme, Ca^{2+}-DPA, cationic surfactants, high pressures or salts[6]. During the first phase of germination, the spore releases H^+, monovalent cations, and Zn^{2+}, which causes an elevation of pH in the core[6, 10]. This is followed by the release of Ca^{2+} and pyridine-2 6-dicarboxylic acid (dipicolinic acid; DPA), accounting for ~10% of the spores dry weight[6]. As DPA is released, water molecules enter and hydrate the core, causing a loss of heat resistance[5]. During the second stage, further water uptake allows for hydrolysis of the spore cortex and swelling of the core and germ cell wall. After expansion of the core, metabolism begins and macromolecular synthesis converts the spore into a germinated cell, by breaking of the spore coat and final release of a vegetative cell (outgrowth)[2]. Bacteria from the *Bacillus* sp. remain in this vegetative state for as long as nutrients are available to sustain replication and growth of cells. As soon as nutrients start being scarce bacteria start the process of sporulation to convert back to dormant spores.

Dodecylamine (DDA) is a cationic surfactant that has been used as a chemical agent to stimulate spore germination[11, 12]. Previous work with *B. subtilis* indicated that the mechanism by which DDA triggers germination is different from how other nutrients and non-nutrient factors, such as Ca^{2+}-DPA, trigger germination[11]. Rather than binding to nutrient germinant receptors or to cortex lytic enzymes, DDA may act against and compromise the spore's inner membrane[11]. *B. megaterium* spores exposed to 6×10^{-5} M DDA for more than 3 min could be killed as germination was taking place, suggesting that DDA both germinates and deactivates *B. megaterium*[12].

Traditional methods to study spore germination rely on bulk or indirect measurements. For example, spore germination is monitored by quantifying the amount of DPA released, through optical density measurements[11]. Spore activity can also be monitored, such as

assessment of the percentage of mammalian cells killed due to germination of spores[8]. One direct method to study spore germination is to use electron microscopy to examine how the morphology of the spores changes during germination[13]. However, this technique has limitations since sample preparation dehydrates cells and can affect morphology, which would lead to misinterpretation of the images.

Atomic force microscopy (AFM) is a technique that can be used to examine individual spores with minimal sample preparation, and it has been widely used to study epithelial cells, bacteria, viruses, and fungi in their native conditions[14]. Changes in morphology and ultrastructure of several *Bacillus* species before and after exposure to different nutrient germinants were studied using AFM, such as determining how mutations in particular coat proteins affect germination [3]. Most of these studies focused on a qualitative understanding of how the spore coat changes during germination and how these changes affect spore size[7, 13, 15, 16]. To our knowledge, no study has assessed the morphological changes that spores undergo when treated with non-nutrient germinants, such as DDA, and how different treatments affect the roughness of the spore surface as it is being germinated.

In this study, AFM was used to quantify spore surface roughness as a function of incubation time in nutrient and non-nutrient germinants, and to measure changes in the heights of the spores, during the process of germination with DDA and L-alanine. Our results suggest that DDA kills *B. atrophaeus* spores before outgrowth occurs. Therefore, DDA may serve as a deactivation agent against a broad spectrum of normal and mutant *Bacillus* species, since complete germination is not required in order for deactivation to occur.

3.3 Materials and Methods

3.3.1 Bacterial Strains and Spore Preparations

Bacillus atrophaeus, previously classified as *Bacillus subtilis* var. *niger, Bacillus niger,* or *Bacillus globigii*[17], is a Gram-positive, aerobic, spore-forming bacterium that has been widely used as a nonpathogenic surrogate for *B. anthracis* and as a biological indicator for decontamination and sterilization processes, and environmental biotracers[18, 19]. *B. atrophaeus* NRRL B-4418 was purchased (American Tissue Culture Collection, ATCC 6455). *B. atrophaeus* cultures were grown on plates of sporulation media, consisting of 8 g nutrient broth, 4 g yeast extract, 0.001 g $MnCl_2.4H_2O$, 5 g peptone and 15 g agar in 1 L of ultrapure water (Milli-Q water, Millipore Corp., Bedford, MA) and maintained at a pH of 7.2.

Plates were incubated at 37˚C for 4 days. Spores were collected by centrifugation at 5000 RPM for 20 min and resuspended in ultrapure water. The cells were washed eight times to separate the spores from vegetative and partially sporulated cells and stored at 4˚C. The spores were allowed to remain in water overnight and then washed two more times to remove any remaining vegetative cells or semi-sporulated cells.

3.3.2 Kinetics Studies of Spore Killing by Dodecylamine

A solution of *B. atrophaeus* at 10^7 spores/mL was centrifuged and resuspended in 1mM dodecylamine (DDA; Sigma-Aldrich, St. Louis, MO). Spores were incubated at 37˚C for 0, 1, 5, 10, 20, 25, 30, 40, 50, and 60 min and kept in an ultrasonication bath (Bronson 1510, 40 kHz, 130 W, Branson Ultrasonics Corp., Danbury, CT) to prevent settling. The action of DDA on the spores at the end of the incubation period was terminated by immersion of spore suspension into an ice bath.

To determine the effects of DDA on spore viability, the treated spore solution was serially diluted and aliquots of spore solution were inoculated onto sporulation agar plates and cultured in an incubator at 37˚C. The number of surviving spores or colony forming units (cfu) that became vegetative cells on the agar plates was determined after 18 hours.

3.3.3 Monitoring the Germination of *B. atrophaeus* Spores

Germination of *B. atrophaeus* was monitored by determining the amount of dipicolinic acid (DPA) released from the core of the spore, using time resolved fluorescence intensity measurements. A spore solution of approximately 10^7 cfu/mL was incubated at 37˚C in the presence of L-alanine or DDA at various concentrations, for 0, 2, 10, 20, 30, 40, 50, 60 and 100 min. The spore solution was combined with a stock solution of terbium chloride ($TbCl_3$; Sigma-Aldrich, St. Louis, MO) to yield a 1 mM $TbCl_3$. Terbium chloride reacts with DPA and forms the chelate, terbium dipicolinate, $(Tb(DPA)_3)^{3-}$, which luminesces with UV excitation[20]. After addition of $TbCl_3$ in a microtiter 96-well plate, 200 µL of spore solution were placed in each well, and the mixed system was excited at 270 nm. Photoluminescence excitation and emission spectra were measured from each sample with a Gemini XPS microplate Spectrofluorometer (Molecular Devices, now part of MDS Analytical Technologies Inc., Toronto, Canada).

3.3.4 Imaging of *B. atrophaeus* Spores with Atomic Force Microscopy (AFM)

AFM was used to study the morphological changes of *B. atrophaeus* spores after exposure to 1 mM dodecylamine for 0, 1, 5, 15, 20, 25, 30, 40, 50, and 60 min, or after exposure to 25 mM L-alanine for 120 min. Droplets of treated *B. atrophaeus* spores (5 µL) were deposited directly onto freshly cleaved mica and allowed to air dry for imaging under ambient conditions.

Images were collected using an atomic force microscope (Digital Instruments Dimension 3100 with Nanoscope IIIa controller; Veeco Metrology; Santa Barbara, CA) that was operated in intermittent contact mode to minimize lateral forces on the sample during imaging. Rectangular cantilevers with conical silicon tips having force constants of ~40 N/m and resonance frequencies of ~300 kHz were used (Applied Nanostructures; Santa Clara, CA). Images were captured with scan areas of 0.5, 1, 5, 10, and 20 μm^2. Images of larger areas (10 and 20 μm^2) were acquired using hard tapping, where the proportional and integral gains were 1.2 – 1.5 and 0.8 – 1.0, respectively, and low amplitude setpoints. Smaller scanned areas (0.5, 1 and 5 μm^2) were probed using light tapping, where the proportional and integral gains were decreased to 0.5 – 0.8 and 0.2 – 0.4, respectively, and the amplitude setpoint was moderately increased to avoid missing important surface structures. All images were captured at a scan rate of 1 Hz and with a resolution of 512 x 512 points.

3.3.5 Off-line Image Analysis

AFM height and amplitude images were collected simultaneously. At least ten images were obtained per time period and condition. Height images were used for quantitative analysis of the root-mean-square roughness (R_{rms}), as well as height and length profiles of the spores. Amplitude images were used to obtain qualitative information. Height images were flattened using a zero order filter to remove the Z offset between scan lines before calculating R_{rms} values. The R_{rms} values were acquired on areas ranging from 0.05 to 0.5 μm^2.

Between 10 and 20 spores were analyzed per image and the calculated height and roughness values of the spores were analyzed using SigmaStat 2.03 statistical software. Statistical analysis was performed by one-way analysis of variance (ANOVA) for repeated measurements. Tukey's test was used for multiple comparisons among treatment groups, while

Dunnett and Duncan's test was used for comparisons between treatment and control groups. A difference was considered significant if $P < 0.05$.

3.4 Results

3.4.1 Anti-sporal Activity of DDA against *B. atrophaeus*

Exposure of *B. atrophaeus* to 1 mM DDA resulted in a significant decrease in surviving spores with increasing exposure time to the anti-sporal agent (Figure 12). After 1 min of treatment with DDA, the number of colony forming units (cfu) decreased from ~5 x 10^7 cfu to ~2 x 10^6 cfu, corresponding to 90% of the spores being killed. After 5 min of exposure, 99% of the spores had been killed, and only 10^3 cfu remained after exposure to DDA for 60 min.

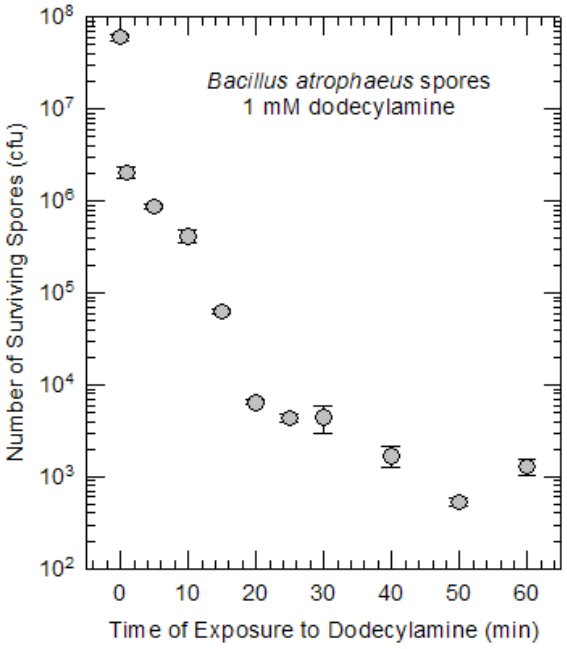

Figure 12. Kinetics of *B. atrophaeus* spore killing by DDA. Number of spore colony forming units (cfu) as a function of time of exposure to 1 mM DDA. Error bars represent the standard deviation. Original spore inoculum was at 1 x 10^7 spores/mL.

Since germinated spores are more susceptible to anti-sporal agents, the germination of *B. atrophaeus* spores was monitored in terms of DPA release from the core. Exposure of *B. atrophaeus* to different concentrations of L-alanine caused DPA to be released within 30 min (Figure 13A). The maximum concentration of DPA released from the core was obtained by exposing spores to a concentration of 12.5 mM or 25 mM L-alanine, in which the amount of DPA released from the core was greater than the amount released with lower concentrations.

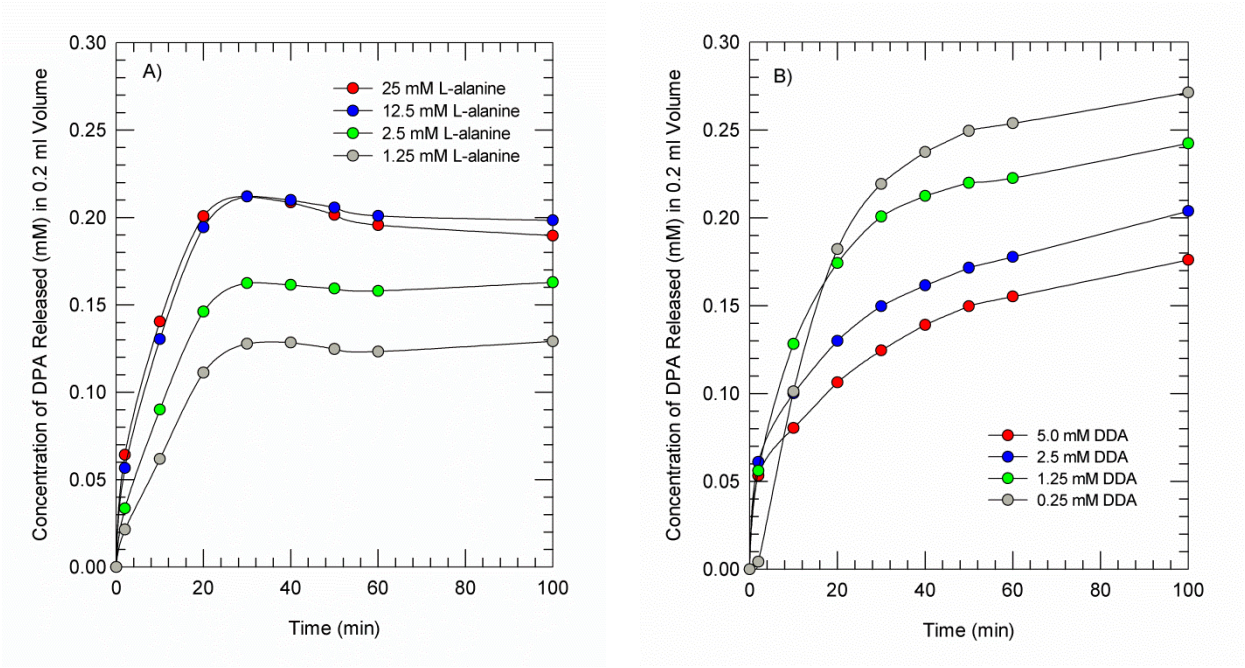

Figure 13. Germination of *B. atrophaeus* spores with various concentrations of A) L-alanine or B) DDA. The amount of DPA released from the core was measured by terbium enhanced fluorescence lifetime measurements. Original spore inoculum was at 1 x 10^7 spores/mL.

Exposure of *B. atrophaeus* to various concentrations of DDA resulted in a suppression of DPA released when compared to the effects of L-alanine. Total release of DPA took 100 min when bacteria were exposed to DDA, and lower concentrations of DDA used to germinate the spore resulted in higher amounts of DPA released from the spore core (Figure 13B). The effect of DDA concentration on germination is complex and is affected by the self-assembly behavior

of DDA in solution (the critical concentration for aggregation is between 0.5 and 1 mM) and also by the promotion of clustering of spores with increasing DDA concentration.

3.4.2 *B. atrophaeus* Size and Surface Morphology

The morphology of *B. atrophaeus* was characterized via AFM, and images showed rodlet structures typically observed for these spores (Figure 14A). Drying of the *B. atrophaeus* on mica surfaces resulted in some clumping. Even when the spore concentration was decreased, spores always aggregated during the drying process on mica, thus it was difficult to observe isolated spores. Spore morphology changed after treatment with 1 mM DDA for 15 or 30 min (Figure 14B and 14C). Spores treated for 15 min appeared dehydrated and the images showed more creases or folds on the spore surface (Figure 14B). The spores treated with DDA for 30 min did not show as much evidence of dehydration, but we noticed that no rodlets were present on the surface, compared to the control case.

R_{rms} values were measured for *B. atrophaeus* exposed to DDA for several time points. Spores that were not treated with DDA had an average R_{rms} value of 25.0 ± 2.3 nm when areas of 500 nm^2 covering the surface of the spores were analyzed (Figure 15A). After treating the spores for 1 min with DDA, the average R_{rms} value increased to 28.2 ± 4.1 nm. The average roughness of the spores continued to increase with time, reaching a local maximum R_{rms} corresponding to 1 mM DDA treatment for 15 min, which was 44.5 ± 2.9 nm. At 20 min, R_{rms} decreased to an average of 14.7 ± 3.6 nm, but began to increase again after 25 min, and continued increasing until 60 min. Statistical analysis showed that R_{rms} values from times 5, 15, 20, 25, 30, and 60 min were significantly different when compared to the control group (untreated spores; $P<0.001$).

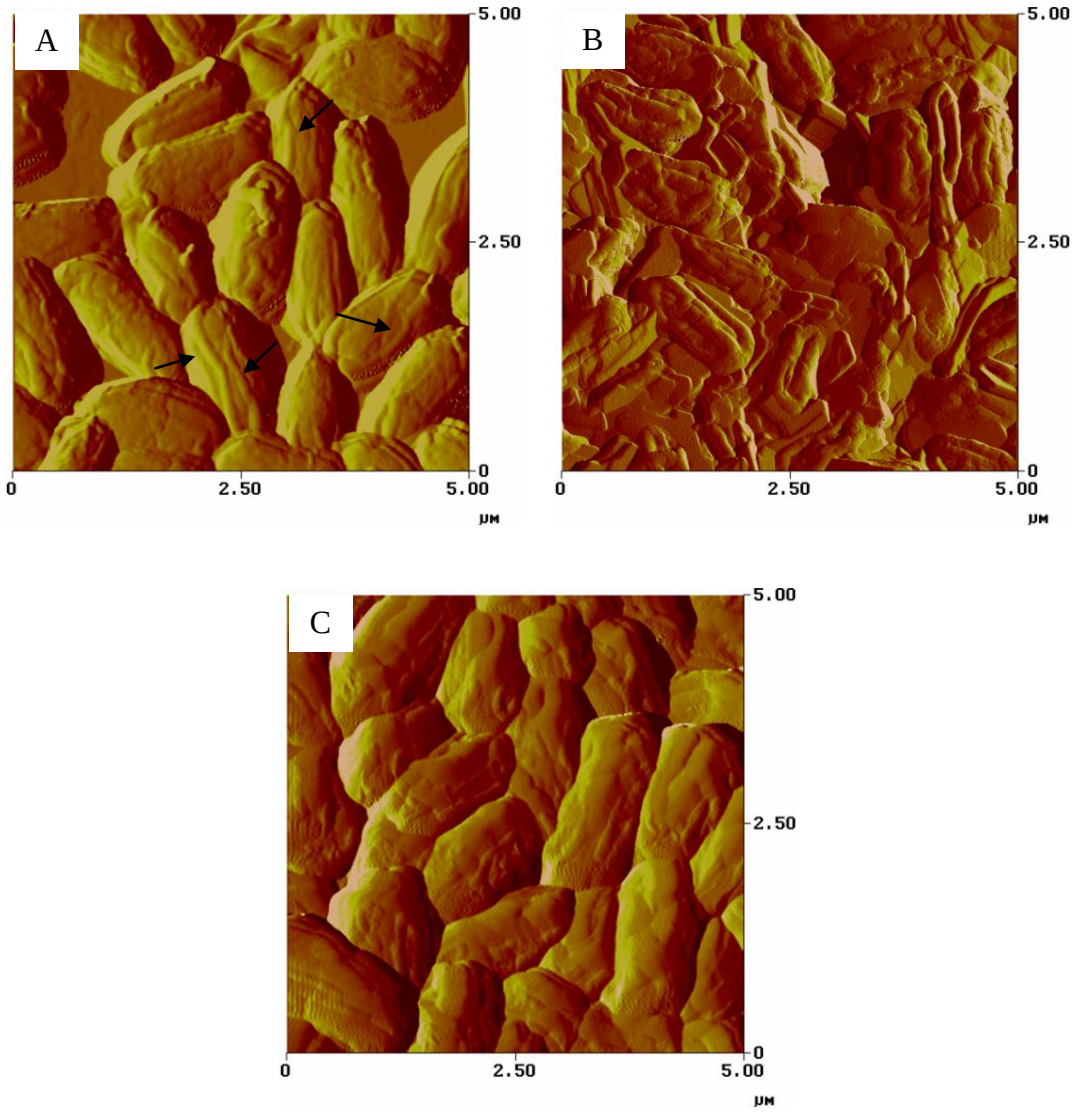

Figure 14. Representative amplitude AFM images of *B. atrophaeus* after exposure to 1 mM DDA for A) 0 min, B) 15 min and C) 30 min. Arrows depict rodlets found on the surface of untreated spores. Images collected in intermittent contact mode.

Roughness values were also obtained using smaller scan areas of 50 nm^2 on a 0.5 μm^2 image. Sampled at a different scale, the roughness values decreased compared to the 5 μm^2 scanned image (Figure 15B). The roughness measured at this scale showed the same trend we observed for the larger scale, with roughness increasing until 15 min, then dropping and increasing again. Statistical analysis showed that the R_{rms} values at times 15, 40, 50, and 60 min were significantly different compared to the control group ($P<0.001$).

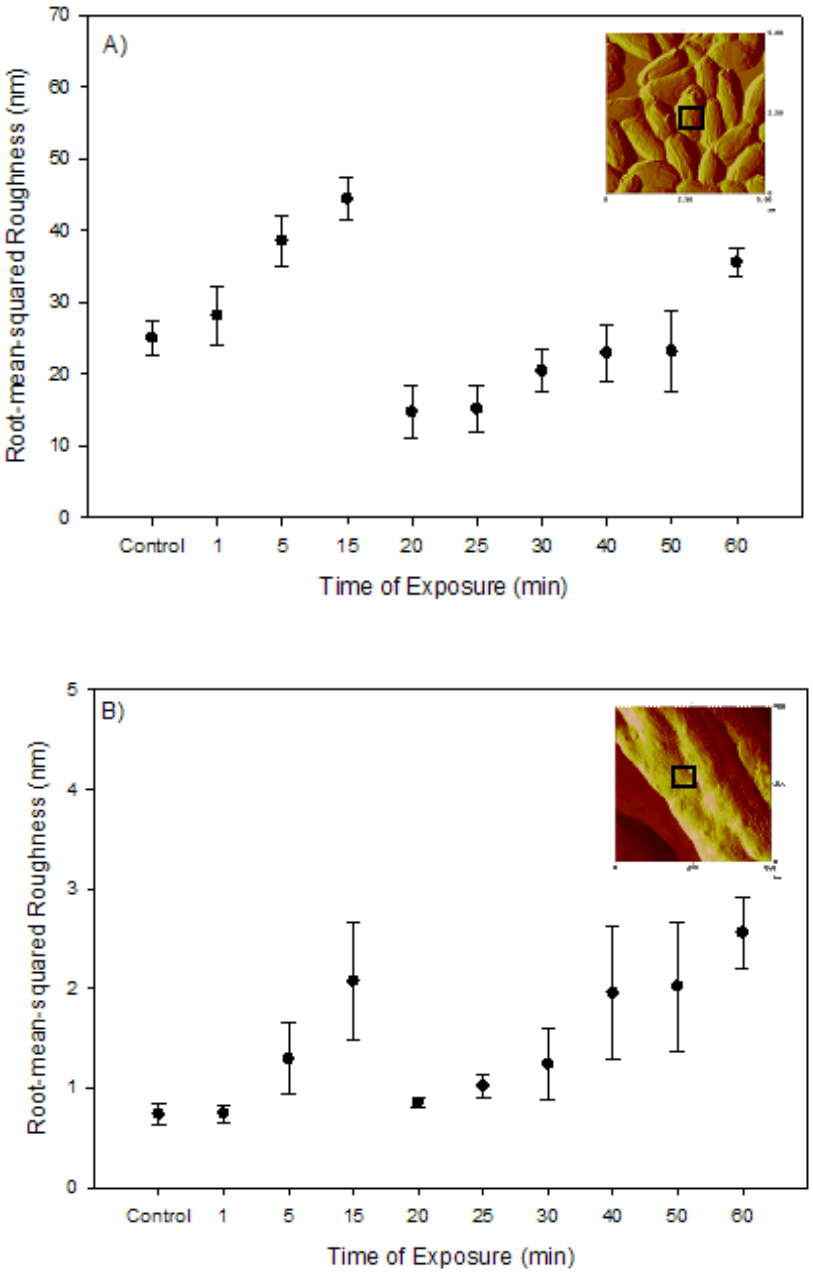

Figure 15. R_{rms} of *B. atrophaeus* as a function of exposure time to 1 mM DDA, for scan areas of A) 5 μm^2 and B) 0.5 μm^2. Data are expressed as the average R_{rms} with standard deviation. Inset AFM image represents how roughness analysis was carried out: for scan areas of 5 μm^2, a 500 nm^2 area box covering the surface of the spore was analyzed. For scan areas of 0.5 μm^2, the roughness within a 50 nm^2 area box of the spore surface was analyzed.

Morphology changes were observed for spores exposed to L-alanine, as quantified by height measurements. Chemical treatments affected spore morphology (Figure 16A and 16B),

and the height of spores decreased after treatment with DDA or L-alanine. After exposure to L-alanine, the height of the spores decreased from an average of 0.7 ± 0.1 µm to 0.3 ±0.2 µm. Treatment with DDA resulted in a similar decrease of spore height, from an average of 0.7 ± 0.1 µm to 0.26 ± 0.1 µm. The differences in height were significant against the control group (P<0.05). However, the roughness of the L-alanine treated spores did not increase (data not shown), in contrast with the spores exposed to DDA.

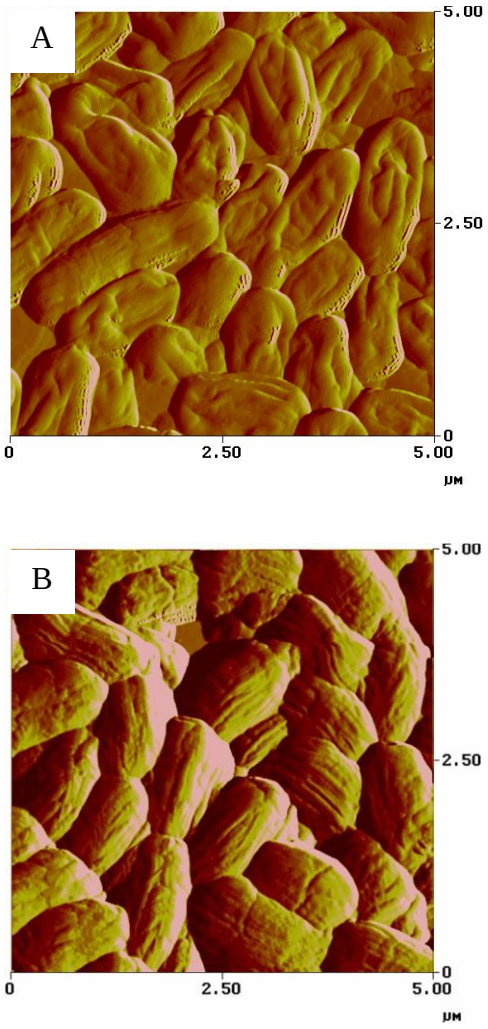

Figure 16. Representative amplitude AFM images of *B. atrophaeus* before and after exposure to L-alanine or DDA for A) dead spores after 1 mM DDA treatment, and B) germinated spores after 25 mM L-alanine treatment. Images collected in intermittent contact mode.

3.5 Discussion

Previous studies have addressed the effects that nutrient and non-nutrient germinants have on *Bacillus* and *Clostridium* cells[21, 22]. Current theory suggests that germination of spores must occur before killing, since the peptidoglycan layer of vegetative cells is easier to penetrate than the thick multilayered structure of the spore coat (Figure 11). There are several studies that examined how nutrient and non-nutrient germinants affect spores[8, 12, 23]. While most studies focused on germination of spores using nutrients, such as L-alanine and inosine[7, 13, 23], the use of non-nutrient germinants, such as DDA, have not been well studied. The mechanism of action of nutrient germinants such as L-alanine has been investigated and it is known that nutrient germinants bind to receptors located in the spore's inner membrane, which causes the opening of ion/DPA channels[6]. In this study, we exposed *B. atrophaeus* spores to the nutrient germinant L-alanine and to the non-nutrient germinant DDA. We propose the mechanism of action of DDA against bacterial spores and discuss how it is different from germination with L-alanine.

3.5.1 Germination Mechanisms of *B. atrophaeus* after Exposure to L-alanine

L-alanine has been widely used to study changes in morphology as well as biochemical alterations during germination[12, 23]. In *B. cereus* the major receptor for alanine germination was identified as GerL, from the GerA family at the inner membrane[23]. Using L-alanine as the germinant, we observed that there is a rapid release of DPA and the amount of DPA released from the core was a function of the concentration of germinant used (Figure 13A). Maximum concentrations of DPA released were observed after exposure to at least 12.5 mM L-alanine. By 30 min of incubation time, a maximum release of DPA was observed (Figure 13A).

Treatment with L-alanine caused a >50% decrease in the height of the spores after 2 hours of treatment, which is due in part to DPA release from the core. Prior work showed that the rapid release of DPA from the core due to L-alanine germination caused an estimated 32% loss of dry weight in bacterial spores[12]. A flattening of *B. subtilis* spores and collapse around spore center was observed after exposure to L-alanine for 1 hour, according to a previous optical microscopy study[24]. Although these spores were considered to be germinating, as observed qualitatively by the decrease in phase brightness, no swelling of the spore could be detected.

Although DPA release supports that germination began in our study with L-alanine, we did not observe outgrowth within the 2 hr period, as no vegetative bacteria were observed in the AFM images. This may be because a longer time would be necessary to transform the spore to the vegetative state, which could vary within *Bacillus* species. For instance, Zaman et al. found *B. anthracis* became vegetative after treatment with L-alanine for 3 hours[13], since the length of the spores increased from 0.8-0.9 to 3.4-3.8 μm. However, another study showed that approximately 30% of a *B. atrophaeus* population did not proceed to outgrowth after exposure to L-alanine for 3 to 7 hours[7]. The percentage of outgrowing cells was even lower in a different study where vegetative cells were only observed in a few cases, suggesting that L-alanine initiates the process of germination and metabolic activity but not the synthesis of macromolecules, such as cell wall peptidoglycan, for all the spore population[24].

The roughness of L-alanine-treated spores was similar to the roughness of untreated spores, suggesting that the effects of L-alanine on the spore occur underneath the coat layer. This was confirmed by the AFM images, showing similar morphology for treated and control spores (Figures 14A and 16B). These findings suggest that during the first stages of germination, the spore coat remains intact and L-alanine causes internal restructuring of the spore. Since there is

no degradation of the coat, this layer is a limiting barrier for outgrowing spores, which may explain why vegetative cells were not observed and why outgrowth did not occur consistently in previous studies. One recent study suggested that the spore coat has to crack laterally on one or both sides to allow the vegetative cell to expand[24]. L-alanine may start germination by changing the internal structure of the spore, and this effect may work its way to the outside of the spore after all internal changes, such as DPA release and hydrolysis of the cortex, have occurred.

3.5.2 Germination Mechanisms of *B. atrophaeus* after Exposure to Dodecylamine

Although some studies have investigated the process of spore germination using a non-nutrient germinant, such as DDA[11, 12, 25], the efficacy of this cationic surfactant as a sporicide has not been well studied. In the early 1960s, Rode and Foster reported that exposing *B. megaterium* spores to 10^{-5} M DDA for more than three min resulted in loss of heat resistance for 97% of the spore population and exposure to DDA for 10 min caused the killing of ~96% of the spores[12]. In our studies, we have observed that ~95% of killed spores can be obtained under 1 minute and 99% after 5 min if they are exposed to 1 mM DDA (Figure 12).

Even though spore killing occurs with exposure to 1 mM DDA, we studied the germination of spores by measuring the amount of DPA released from the core as a function of time (Figure 13B). Exposing spores to 1.25 mM DDA resulted in complete DPA release within 100 min. In a previous study, researchers using 1 mM DDA to germinate *B. subtilis* spores showed that it took ~3 hours for the DPA to be released from the core[11]. This difference in DPA release rate may be related to variability within the *Bacillus* species, growth conditions, or treatment. For instance, Selow et al. boiled spore cultures for 30 minutes to determine DPA

release, while we did not[11]. We also observed that decrease of DDA concentrations resulted in an increase in the amount of DPA released from the core. Even thought DDA can be used at low concentrations to germinate *Bacillus* spores, high concentrations of DDA may initiate the process of germination of spores by releasing low amounts of DPA, but the process may be affected during killing of spores and not all of the DPA may get released from the core.

The spore heights were significantly lower for DDA-treated spores, compared to untreated spores. We suggest that these height changes are due to decreased hydration of the core, and a breakdown of the spore coat. A previous study showed that exposure of *Bacillus* spores to DDA results in a 45 to 55% loss of dry weight, which could have contributed to the reduced height of spores[12]. In another study, it was observed that spores germinated with DDA did not rehydrate well and core water content in these spores was low, which prevented them from expanding normally[11]. From our roughness analysis we also observed that the outer coat of the spore was affected by DDA treatments since there was an initial increase in roughness values. This increase in roughness indicates that the coat of the spore is rupturing and disintegrating. The inner and outer coat of spores can be up to 130 nm thick[4], which could lead to a diameter decrease of 260 nm. When spore coat breakdown and loss of hydration simultaneously occurred, we observed a decrease in height and increase in roughness of the spores.

Based on our roughness, height, and DPA release measurements, we considered a mechanism of action of DDA against bacterial spores. DDA does not interact with any receptors in the inner membrane of spores, as reported previously [11]. From our roughness measurements we can state that DDA starts acting from the outside of the spore and works its way in by causing the coat to rupture and form pores on the surface. The drop in roughness observed after 15 min

of treatment with DDA indicates that the outer coat layer was completely removed; leaving behind another smoother coat that will be subsequently ruptured or disintegrated after prolonged treatment with DDA. In other words, DDA may germinate spores by causing the disintegration of one coat layer at the time. With prolonged DDA treatment, the protective coat layers of the spore were compromised, decreasing the overall cell height. While most of the cells were killed within one minute of exposure to DDA, this happened during the first stages of germination since there was a continuous release of DPA from the core. However, germination was interrupted and spores were killed without outgrowing. Using DDA as a germinant or sporicide may be a more effective mechanism to deactivate *B. atrophaeus* and perhaps other hazardous species such as *B. anthracis,* since DDA can act against spores that have not progressed to the fully vegetative state.

3.6 Acknowledgments

This work was supported in part by the National Science Foundation (CBET 0827229) and DTRA Project BA07PRO102.

We also thank Robert Stote for helpful discussions during the course of this research.

REFERENCES

1. Giorno, R.; Bozue, J.; Cote, C.; Wenzel, T.; Moody, K. S.; Mallozzi, M.; Ryan, M.; Wang, R.; Zielke, R.; Maddock, J. R.; Friedlander, A.; Welkos, S.; Driks, A., Morphogenesis of the *Bacillus anthracis* spore. *J Bacteriol* **2007,** 189, (3), 691-705.

2. Atrih, A.; Foster, S. J., Bacterial endospores the ultimate survivors. *Int. Dairy J.* **2002,** 12, (2-3), 217-223.

3. Chada, V. G.; Sanstad, E. A.; Wang, R.; Driks, A., Morphogenesis of *Bacillus* spore surfaces. *J Bacteriol* **2003,** 185, (21), 6255-61.

4. Henriques, A. O.; Moran, C. P., Jr., Structure and assembly of the bacterial endospore coat. *Methods* **2000,** 20, (1), 95-110.

5. Slieman, T. A.; Nicholson, W. L., Role of dipicolinic acid in survival of *Bacillus subtilis* spores exposed to artificial and solar UV radiation. *Appl Environ Microbiol* **2001,** 67, (3), 1274-9.

6. Setlow, P., Spore germination. *Curr Opin Microbiol* **2003,** 6, (6), 550-6.

7. Plomp, M.; Leighton, T. J.; Wheeler, K. E.; Hill, H. D.; Malkin, A. J., In vitro high-resolution structural dynamics of single germinating bacterial spores. *Proc Natl Acad Sci U S A* **2007,** 104, (23), 9644-9.

8. Akoachere, M.; Squires, R. C.; Nour, A. M.; Angelov, L.; Brojatsch, J.; Abel-Santos, E., Identification of an in vivo inhibitor of *Bacillus anthracis* spore germination. *J Biol Chem* **2007,** 282, (16), 12112-8.

9. Tennen, R.; Setlow, B.; Davis, K. L.; Loshon, C. A.; Setlow, P., Mechanisms of killing of spores of *Bacillus subtilis* by iodine, glutaraldehyde and nitrous acid. *J Appl Microbiol* **2000,** 89, (2), 330-8.

10. Jedrzejas, M. J.; Setlow, P., Comparison of the binuclear metalloenzymes diphosphoglycerate-independent phosphoglycerate mutase and alkaline phosphatase: their mechanism of catalysis via a phosphoserine intermediate. *Chem Rev* **2001,** 101, (3), 607-18.

11. Setlow, B.; Cowan, A. E.; Setlow, P., Germination of spores of Bacillus subtilis with dodecylamine. *J Appl Microbiol* **2003,** 95, (3), 637-48.

12. Rode, L. J.; Foster, J. W., Germination of bacterial spores with alkyl primary amines. *J Bacteriol* **1961,** 81, 768-79.

13. Zaman, M. S.; Goyal, A.; Dubey, G. P.; Gupta, P. K.; Chandra, H.; Das, T. K.; Ganguli, M.; Singh, Y., Imaging and analysis of *Bacillus anthracis* spore germination. *Microsc Res Tech* **2005,** 66, (6), 307-11.

14. Dûfrene, Y. F., Atomic force microscopy, a powerful tool in microbiology. *J Bacteriol* **2002,** 184, (19), 5205-13.

15. Plomp, M.; Leighton, T. J.; Wheeler, K. E.; Malkin, A. J., The high-resolution architecture and structural dynamics of Bacillus spores. *Biophys J* **2005a,** 88, (1), 603-8.

16. Zolock, R. A.; Li, G.; Bleckmann, C.; Burggraf, L.; Fuller, D. C., Atomic force microscopy of *Bacillus* spore surface morphology. *Micron* **2006,** 37, (4), 363-9.

17. Fritze, D.; Pukall, R., Reclassification of bioindicator strains Bacillus subtilis DSM 675 and Bacillus subtilis DSM 2277 as Bacillus atrophaeus. *Int J Syst Evol Microbiol* **2001,** 51, (Pt 1), 35-7.

18. Plomp, M.; Leighton, T. J.; Wheeler, K. E.; Pitesky, M. E.; Malkin, A. J., Bacillus atrophaeus outer spore coat assembly and ultrastructure. *Langmuir* **2005b,** 21, (23), 10710-6.

19. Burke, S. A.; Wright, J. D.; Robinson, M. K.; Bronk, B. V.; Warren, R. L., Detection of molecular diversity in *Bacillus atrophaeus* by amplified fragment length polymorphism analysis. *Appl Environ Microbiol* **2004,** 70, (5), 2786-90.

20. Rosen, D. L.; Sharpless, C.; McGown, L. B., Bacterial Spore Detection and Determination by Use of Terbium Dipicolinate Photoluminescence. *Anal. Chem.* **1997,** 69, (6), 1082-1085.

21. Powell, J. F.; Strange, R. E., Biochemical changes occurring during the germination of bacterial spores. *Biochem J* **1953,** 54, (2), 205-9.

22. Ando, Y., Mechanism of nitrite-induced germination of *Clostridium perfringens* spores. *J Appl Bacteriol* **1980,** 49, (3), 527-35.

23. Barlass, P. J.; Houston, C. W.; Clements, M. O.; Moir, A., Germination of *Bacillus cereus* spores in response to L-alanine and to inosine: the roles of *gerL* and *gerQ* operons. *Microbiology* **2002,** 148, (Pt 7), 2089-95.

24. Leuschner, R. G. K.; Ferdinando, D. P.; Lillford, P. J., Structural analysis of spores of *Bacillus subtilis* during germination and outgrowth. *Colloids Surf., B* **2003,** 19, 31-41.

25. Paredes-Sabja, D.; Torres, J. A.; Setlow, P.; Sarker, M. R., *Clostridium perfringens* spore germination: characterization of germinants and their receptors. *J Bacteriol* **2008,** 190, (4), 1190-201.

Chapter 4

Effects of L-alanine and inosine germinants on the elasticity of *Bacillus anthracis* spores

Langmuir, 2010. **26(9):** 6535-6541

4.1 Abstract

The surface of dormant *Bacillus anthracis* spores consists of a multilayer of protein coats and a thick peptidoglycan layer that allow the cells to resist chemical and environmental insults. During germination, the spore coat is degraded, making the spore susceptible to chemical inactivation by antisporal agents as well as to mechanical inactivation by high pressure or mechanical abrasion processes. While chemical changes during germination, especially the release of the germination marker, dipicolinic acid (DPA) have been extensively studied, there is yet no investigation of the corresponding changes in the mechanical properties of the spore. In this work, we used atomic force microscopy (AFM) to characterize the mechanical properties of the surface of *Bacillus anthracis* spores during germination. The Hertz model of continuum mechanics of contact was used to evaluate the Young's moduli of the spores before and after germination by applying the model to load-indentation curves. The highest modulus was observed for dormant spores, with average elasticity values of 197 ± 81 MPa. The elasticity decreased significantly after incubation of the spores with the germinants L-alanine or inosine (47.5 ± 41.7 MPa and 35.4 ± 15.8 MPa; respectively). Exposure of *B. anthracis* spores to a mixture of both germinants resulted in a synergistic effect with even lower elasticity, with a Young's modulus of 23.5 ± 14.8 MPa. The elasticity of the vegetative *B. anthracis* cells was nearly 15 times lower than that of the dormant spores (12.4 ± 6.3 MPa vs. 197.0 ± 80.5 MPa; respectively). Indeed from a mechanical strength point of view, the germinated spores were closer to the vegetative cells than to the dormant spores. Further, the decrease in the elasticity of the cells was accompanied by increasing AFM tip indentation depths on the cell surfaces. Indentation depths of up to 246.2 nm were observed for vegetative *B. anthracis* compared to 20.5 nm for the dormant spores. These results provide quantitative information on how the

mechanical properties of the cell wall change during germination, which may explain how spores become susceptible to inactivation processes based on mechanical forces during germination and outgrowth. The study of spore elasticity may be a valuable tool in the design of improved anti-sporal treatments.

4.2 Introduction

Bacillus and *Clostridium* cells are some of the most resistant life forms known, due to their ability to undergo the restructuring and differentiation process of sporulation under nutrient deprivation.[1] During this process, vegetative cells synthesize a series of polymer and protein layers that encase the cellular contents and genetic information in a ~100-200 nm barrier, which protects the cell from external environmental stressors.[2, 3] Spores are metabolically dormant, but they maintain the ability to germinate and transform into vegetative cells once nutrients are available.[4, 5] In their vegetative state, organisms such as *Bacillus anthracis* (*B. anthracis*) are highly virulent and they are considered as potent biological threat agents since they cause critical or fatal airborne diseases, such as pulmonary anthrax.[6, 7]

The first step of the process in which the spores return to a fully vegetative, pathogenic state is known as germination. Germination is usually initiated in response to availability of nutrients, such as amino acids and sugars, non-nutrient chemicals such as dodecylamine and dipicolinic acid (DPA) or by other factors such as high pressure and temperature.[5, 8] Germination involves a series of steps where the release of monovalent cations, dipicolinic acid (DPA), calcium, and the intake of water molecules result in the loss of heat resistance and initiation of metabolic activity, converting the spore into a vegetative, fully virulent bacterium.[5, 9]

The mechanism of germination triggered by nutrients involves the presence of spore-germination receptors on the surface of the inner membrane of the spore, which stimulate the cell to germinate and to achieve vegetative growth.[10] L-alanine is an amino acid that interacts with receptors on the inner membrane of the spores,[11] and is a well studied molecule for the germination of several *Bacillus* species, such as *B. subtilis*, *B. cereus*, *B. anthracis*, and *B. atrophaeus*.[6, 8, 12] Inosine is a purine ribonucleoside that has been shown to be a strong germinant of *B. cereus* spores.[13] While either germinant, L-alanine or inosine, alone can cause the germination of *B. cereus,* for *B. anthacis* spores, a binary mixture of the germinants has been shown to be more effective. [10, 11]

In contrast to the considerable attention paid to investigating the effects of nutrients on germination of spores, there are fewer studies in the literature on the effects of physical insults, such as pressure,.[14, 15] While it is widely known that the microbial cell wall has a structural role in maintaining the cellular shape and resisting turgor pressure[16], changes in the mechanical properties of the cell wall during germination remains essentially unknown. *B. subtilis* spores exposed to 100 MPa and 550 MPa resulted in the killing of <25% and <50% spores, respectively.[14] Treatment pressures at 550 MPa were able to induce the germination of spores without the need of activation of germinant receptors, as was confirmed by the number of viable colonies in Luria broth medium agar plates. However, spores treated at 100 MPa produced very few colonies on agar plates, suggesting that there may be a critical mechanical force necessary to initiate germination in the absence of nutrients[14]. Understanding the mechanical properties of *B. anthracis* spores, such as cell wall elasticity, may help us understand how germination affects the spore surface, and ultimately, how the cell resists chemical and physical insults.

Germination of spores is usually monitored by changes in optical densities that occur as DPA is released from the spore core after addition of germinants.[4] Electron microscopy (EM) has also been used to study changes in morphology of the spores during germination.[17] While EM explicitly demonstrates changes in cell structure, sample preparation necessitates dehydration and coating with a reflective material, which can cause artifacts.

Atomic force microscopy (AFM) is a technique that has proven practical for the physical characterization of individual spores, since it provides high resolution imaging of the sample, and the ability to obtain the adhesion forces present between the AFM probe and the cell surface under native conditions.[18] By studying the interaction of the AFM tip as it approaches or retracts from the spore surface, it is possible to study specific physical and chemical properties of the spore, such as elasticity, adhesion, and length of surface polymers. A few AFM studies available in the literature have addressed how nutrient germinants, such as L-alanine, affect the morphology of *Bacillus* species.[17, 19-21] AFM has been used to obtain high resolution images of the spore coat of *Bacillus* spores and understand how protein coat layers change during germination.[19, 21]

Quantitative elasticity measurement with AFM is a new way to characterize how germinants affect the mechanical properties of the spore surface. Using the AFM probe as a nanoindentation tool, AFM deflection data can be converted into load vs. indentation depth plots and analyzed using theoretical models that provide quantitative information on the elasticity of the sample (represented by the Young's modulus).[22] These models have been applied towards bacteria, such as *E. coli,* where it was suggested that the elasticity of the cells can change significantly depending on the solvent in which the cells are exposed.[23] The elasticity for *E. coli* in water was ~12.8 MPa, while the elasticity of the same bacterium in a more polar solvent, such

as formamide, decreased to ~0.8 MPa.[23] The same technique has been applied with other types of cells, such as the yeast *Saccharomyces cerevisiae,* where the Young's modulus was ~0.6 MPa at the cell wall, but ~6.1 MPa at the site of cellular division.[22] While these elasticity studies help characterize the physical properties of some bacterial strains, none of the cells studied possess the complex protein layers and coat structure that is common in sporulated *B. anthracis*.

Therefore, our objective was to use AFM to characterize how the nutrient germinants L-alanine and/or inosine affected the Young's modulus of *B. anthracis* spores. These results were compared with elasticity measurements on the dormant spores and also on the vegetative *B. anthracis* cells, these being the two limiting states of the spore subjected to germinants.

4.3 Experimental Section

4.3.1 Bacterial Strain and Preparation of Spores

Bacillus anthracis Sterne (referred to hereafter as "*B. anthracis*") was kindly provided by the U. S. Army Natick Soldier Research, Development & Engineering Center, Natick, Massachusetts. The Sterne strain is a low virulence strain that lacks the pXO2 extra chromosomal plasmid, which forms and develops the bacterial capsule; however, it contains the pXO1 extra chromosomal plasmid, which is responsible for the expression of virulent factors.[17]

Bacterial strains were grown in sporulation media as described previously.[3] A solution of sporulation media consisting of 8 g nutrient broth, 4 g yeast extract, 0.001 g $MnCl_2.4H_2O$, 5 g peptone, and 15 g agar in 1 L of ultrapure water (Milli-Q water, Millipore Corp., Bedford, MA) was maintained at a pH of 7.2 and sterilized for 60 minutes, followed by preparation in Petri dishes.

Fresh cultures of *B. anthracis* Sterne were obtained by adding 100 µL of spores from a glycerol stock solution into a flask with 25 mL of sterilized nutrient broth (Himedia; Mumbai, India). The flask was agitated at 200 RPM at 37 °C for ~20 hours. This culture was used to inoculate plates of sporulation media using 50 µL aliquots and the plates were incubated at 37 °C for 4 days to allow vegetative cells to sporulate. Harvesting of spores was done in autoclaved ultrapure water and spores were collected by centrifugation at 5000 RPM for 20 minutes and resuspended in ultrapure water. The cells were washed eight times to separate spores from vegetative and partially sporulated cells since there is a significant difference in density between these two cell types.[24] The spores were stored overnight at 4 °C. After ~18 hours, the cells were washed two more times to remove any remaining vegetative *B. anthracis* cells.

4.3.2 Spore Germination Assays and Atomic Force Microscopy (AFM)

The surface elasticity of dormant and germinated spores and of vegetative cells of *B. anthracis* was investigated. To germinate the spores, *B. anthracis* were exposed to 50 mM L-alanine (Sigma-Aldrich, St. Louis, MO), 5 mM inosine (Sigma-Aldrich), or both germinants together, in 50 mM Tris/HCl buffer (pH 8.0), and incubated at 37 °C for 2 and 4 hours. The final concentration of the spore solution was approximately 10^7 cells/mL. As a control condition, dormant *B. anthracis* spores were incubated for 4 hours in 50 mM Tris/HCl buffer at 37 °C. To study the elasticity of vegetative *B. anthracis* cells, a one mL sample of dormant spore solution was suspended in tryptic soy broth (30 g/L; Sigma-Aldrich), supplemented with 1% yeast extract, and grown for 6 hours at 37 °C with rotation at 18 RPM.

To test the effect of germinant concentration on the elasticity of the spores, additional experiments were carried out where *B. anthracis* spores were germinated with 25 mM L-alanine

and/or 2.5 mM inosine for 2 hours. The elasticity values obtained were compared with those obtained at higher concentrations of germinants (50 mM L-alanine and/or 5 mM inosine).

AFM was used to study changes in the elasticity of *B. anthracis* spores induced by exposure to different germinants. After incubation with L-alanine and/or inosine, the spore solution was centrifuged at 5000 RPM for 5 min and resuspended in ultrapure water to stop treatment. Droplets of treated *B. anthracis* spores (5 µL) were deposited onto freshly cleaved mica and dried for 18 hours.

AFM experiments were carried out with a Dimension 3100 with Nanoscope IIIa controller (Veeco Metrology; Santa Barbara, CA) that was operated in tapping mode in air to represent conditions of airborne spores. *B. anthracis* are commonly found in soil at concentrations of up to 3,000 spores per gram of soil.[25, 26] Since germination can be affected by humidity[27], AFM measurements were taken at 30-35% relative humidity in air. A single rectangular cantilever with a conical silicon tip having a spring constant of 14 N/m and a resonant frequency of 315 kHz was used (Mikromasch; San Jose, CA). Samples were scanned at a rate of 1 Hz and once a spore was located, it was centered so that force measurements could be performed on the cell away from the edges. Forces were measured on five spores, and ten force cycles were recorded per spore for a total of 50 force curves obtained for each treatment. The ten force cycles obtained within each spore were taken at the same location of the cell (center of the spore away from edges) to ensure that no deformation of the surface was taking place. The force cycle was set so the tip stayed in contact with the sample for 1 ms before retracting and the tip traveled at 2 µm/s with a loading rate of 3×10^{-5} N/s during the force cycle. Data in ASCII format were exported to a spreadsheet and converted from deflection to force.

4.3.3 Elasticity of *B. anthracis* Spores Obtained from Force-Indentation Depth Curves

The conversion of cantilever deflection data to force data allows for the assessment of the elasticity of the surface of the spores in response to exposure to germinants. AFM data were converted to force-indentation depth curves following procedures described previously[28-30]. Briefly, the deflection of the cantilever, *d*, as it approaches and retracts from the surface is plotted as a function of tip-sample separation distance, *z*. Since there was some scanner hysteresis and drift in the detection system, we often observed that the deflection of the free cantilever was not equal to zero. To correct this, a deflection offset, d_0, was subtracted from all deflection values. This deflection offset was determined from the cantilever deflection-sample separation distance plot by calculating the average cantilever deflection when the AFM probe was far away from the sample surface. This was observed as a horizontal line, where no repulsive or attractive forces were experienced by the AFM tip. The cantilever deflection was converted to force or load (*F*) using Hooke's law

$$F = k_c (d - d_0) \quad (1)$$

where k_c is the spring constant.

Similar to the deflection offset, a separation distance offset, z_0, was defined. The value of this offset was the initial point where the tip makes contact with the sample surface or more specifically, when the deflection of the cantilever begins to increase from the horizontal line that represents the zero cantilever deflection (deflection offset). The distance offset was subtracted from all distance values.

Next, the force-indentation curves were created by taking into account the compliance of the sample surface. On a hard surface, such as mica, the slope of the compliance region of the cantilever deflection-separation distance curve is equal to 1, but this slope is expected to decrease for biological samples, such as bacteria.[22, 23] The difference between the separation distance on a hard surface and the separation distance on the surface of the spore is the indentation depth of the sample, δ, and is defined by,

$$\delta = (z - z_0) - (d - d_0) \quad (2)$$

From Equations 1 and 2, the cantilever deflection-separation distance curves were converted into load, *F*, versus indentation depth, δ. Force curves were made on freshly cleaved mica free of spores before any measurements were taken on cells, in order to calibrate the sensitivity of the photodetector.

4.3.4 Young's Modulus of *B. anthracis*

The tensile elastic modulus or Young's modulus was obtained by applying the Hertz model of continuum mechanics of contact to the load-indentation depth data[22, 23]. The Hertz model can be used for samples that are elastic, isotropic, homogeneous, and semi-infinite although it does not take into account tip-surface adhesion[22, 31]. Since there were not significant adhesion forces observed during the force cycle, this model was applicable.

From Hertzian theory, the model describes the indentation (without permanent deformation) of an indenter (the silicon AFM probe) into an infinitely deformable elastic half space (spore surface). The geometry of the indenter was taken into account and it was related to the load – indentation depth curves by

$$F_{cone} = (2/\pi)\, tan\alpha\, (E / (1-\nu^2))\, \delta^2 \quad (3)$$

where α is the half opening angle of the conical tip used, taken as 40° as specified by the manufacturer, *E* is the Young's modulus or tensile elastic modulus of the spore, and ν is the Poisson ratio of the spore, taken as 0.5.[22]

A MatLab script was written to analyze all raw data obtained with the AFM and calculate the elastic modulus of the spores for all treatments (MatLab Works Inc.; Natick, MA)

4.3.5 Statistical Analysis

Young's modulus and indentation depth values were analyzed using the Kruskal-Wallis one way analysis of variance (ANOVA) on ranks for repeated measurements since the samples did not have equal variances. The null hypothesis tested was that there were no differences in the distribution of values between different groups. Tukey's test was used for multiple comparisons among treatment groups. A difference was considered significant if $P < 0.05$.

4.4 Results and Discussion

4.4.1 Rationale for Germination Conditions

Germination of *Bacillus* spores has been extensively studied over the past few decades. L-alanine has been shown to influence the germination of spores of many *Bacillus* species.[6, 8, 12] For *Bacillus anthracis*, it has been shown that L-alanine is a strong independent germinant at concentrations higher than 10 mM, and that rapid germination responses are observed at high L-alanine concentrations (100 mM).[11] In the same study, it was observed that lower L-alanine concentrations could germinate *B. anthracis* spores as long as there was another germinant present, such as inosine.[11] L-alanine at a concentration of 10 mM acting together with inosine at a concentration of 1 mM were able to germinate 73% of *B. anthracis* spores in less than 15

minutes.[11] In another study, optimal germination conditions for *B. anthracis* were observed when spores were exposed to 15 – 150 mM L-alanine and over 99% of the spore population had germinated within 24 hours.[12] Clements and Moir observed that 50 mM L-alanine and 5 mM inosine were concentrations at which the germination rates were the maximum for *B. cereus*, which is a close genetic relative of *B. anthracis*.[13] In another study, inosine concentrations that ranged from 1 to 10 mM resulted in comparable germination processes as measured by the fall in optical density.[8] While inosine has been shown to be a weak germinant while acting alone compared to L-alanine, it has been suggested that inosine as a co-germinant is able to induce strong germination responses in *B. anthracis.* Germination with L-alanine as the sole germinant has been shown to involve a single receptor while inosine as a sole germinant has been shown to require the interaction of two different receptors in *B. cereus.*[10] Based on these findings, and knowing that germinants at high enough concentrations resulted in optimal germination responses, we chose high concentrations of L-alanine and inosine for our elasticity studies. To assess whether germinant concentration had an effect on elasticity, AFM experiments were also carried out on spores that were exposed to different concentrations of L-alanine and/or inosine.

4.4.2 Rational for Application of the Hertz Model

While other mathematical models that describe the elastic response of a substrate after applying pressure with an AFM tip are available, the Hertz model is a simple and classical way of describing at a very fundamental level the contact mechanics of an elastic half space (spore) by a rigid object (AFM tip). Several assumptions need to be met when applying the Hertz model: the sample being studied needs to be elastic, isotropic, homogeneous, and semi-infinate. While at the macroscopic level, spores may be considered homogeneous and isotropic, at a microscopic and nanomolecular level the surface of spores may be completely heterogeneous having physical

properties that differ when measurements are made in different locations of the cell. The Johnson, Kendall, and Roberts (JKR) model, which is a modification of the Hertz theory, may be more appropriate when investigating the elastic properties of spores since accounts for the influence of surface energy. However, this model is more complex and difficult to use. The Hertz model, while not exact, can provide of a general idea of the properties of spores while they are undergoing the process of germination.

The shape of the AFM tip also is an important factor that needs to be considered when analyzing AFM data. Conical tips get dulled with usage and at some point may start losing its sharpness and start behaving like a spherical tip. It would be then recommended to evaluate the sharpnes of the tip and calculate the radius of curvature of the probe to determine which Hertz equation is the most appropriate Hertz to describe the data. However, since we used a brand new conical tip and the AFM was operated in intermittent contact mode, it is safe to assume that dullness of the tip did not occur during our experiments.

4.4.3 Elasticity of *B. anthracis* after Exposure to Germinants

Cantilever deflection vs. tip-sample separation curves were converted to load vs. indentation depth plots to quantify the elasticity of *B. anthracis* spores after exposure to L-alanine and/or inosine (Figure 17A). A distinct non-linear region of the curve was observed for all samples, which allowed for the detection of deflection and separation distance offsets. Once these offsets were defined, the plot was converted to loading force vs. indentation depth (Figure 17B). When we probed a hard surface, such as mica, the non-linear region of the curve was absent, so the deflection and separation offsets were defined as the point where a sudden jump to contact was observed in the approach curve.[22] The Young's modulus of the spores was obtained

by fitting the non-linear portion of the loading force vs. indentation depth curves to the Hertz model.

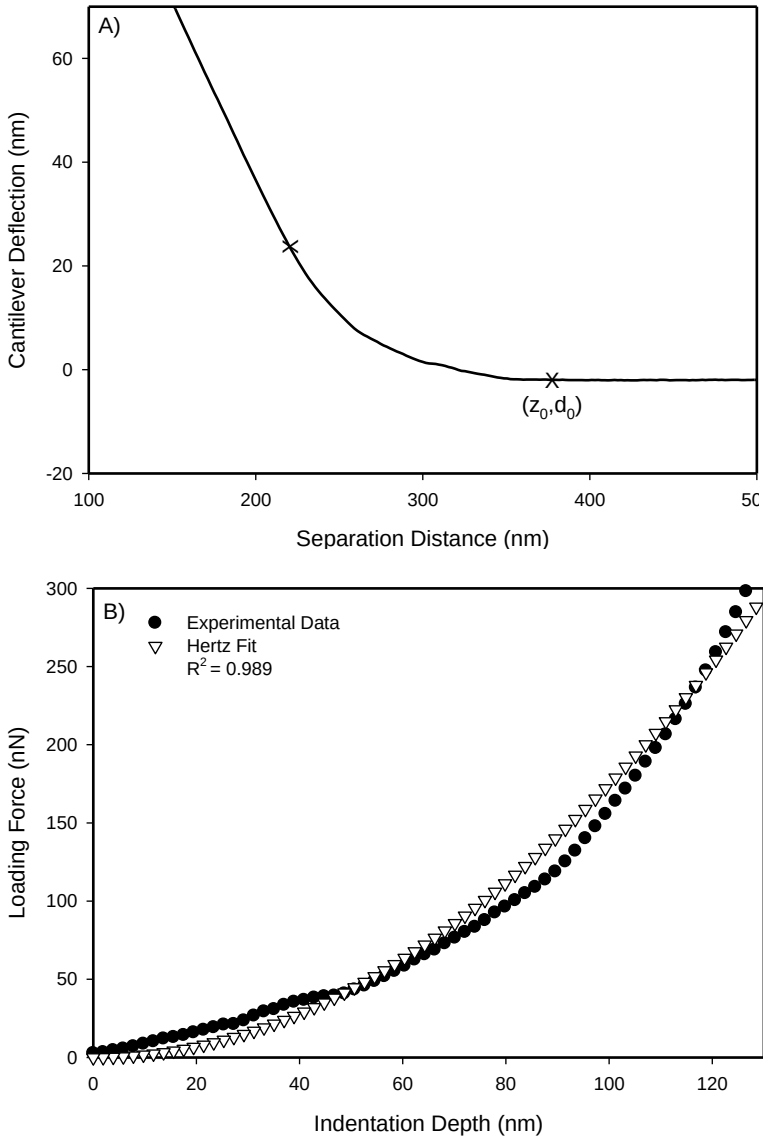

Figure 17. A) Representative AFM approach curve obtained when a silicon AFM tip approaches and indents a *B. anthracis* Sterne spore. The deflection offset d_0 and the offset in the separation distance z_0 used to calibrate the deflection vs. distance plot are shown. The non-linear portion of the curve is depicted within the two X marks. B) Loading force – indentation depth curve corresponding to the deflection-distance curve in (A). The open triangles correspond to the best fit obtained after applying the Hertz model to the non-linear portion of the approach curves (Equation 3).

A quasi-quadratic relation was observed between the loading force and the indentation depth (Figure 17B), which was predicted by the model for a conical AFM probe. There was good agreement between the Hertz model and the experimental data obtained, which suggests that this model can be used for the measurement of elasticity of cells with harder surfaces such as *Bacilllus* and *Clostridium* species. Furthermore, for all treatments, no adhesion forces were observed during approach or retraction of the AFM tip, allowing for the analysis of the data using the Hertz model. The lack of adhesive interactions during AFM force cycles has been associated with the crystalline nature of the surface of microorganisms, such as the one present in *Lactobacilli*.[32] A crystalline cell surface protein, S-layer, has been observed in the structure of *Bacillus* species,[33] which may consist of compactly folded proteins that prevent the AFM tip from experiencing adhesion during force measurements.

The slope of the load vs. indentation depth curve was higher when taking AFM measurements on the dormant *B. anthracis* spores that were not exposed to any germinants or yeast extract, and decreased significantly after incubation with either L-alanine or inosine (Figure 18). Based on the shape of the loading force vs. indentation depth curve, fewer data points were available to fit the Hertz model for the cells that showed harder surfaces (dormant, untreated spores), since the non-linear portion of the curve that describes the indentation of the AFM probe into the untreated *B. anthracis* cell was significantly smaller. This may be due to the multiple protein layers that surround the cell, making the spore surface harder than the cell wall of vegetative bacteria.

Treatment of spores with TSB supplemented with yeast extract resulted in vegetative cells with weaker surfaces since very low loads were required to substantially indent the sample with the AFM tip. The slope of the load vs. indentation depth curve for the vegetative *B.*

anthracis resulting from the TSB and yeast extract treatment was the lowest of all conditions (Figure 18). Since untreated *B. anthracis* spores are covered by multiple layers of protein coats, higher loading forces were required to cause indentation of the spore. This suggests that the protein coat layers of dormant spores strengthen the surface and resist applied pressure, such as the one created by the AFM probe during force cycles. Similar changes in the slope of the load vs. indentation plot have been observed for other microorganisms, such as *S. cerevisiae*.[22] During the division of *S. cerevisiae*, a scar is formed on the cell wall where the bud emerges, resulting in a steeper slope in the AFM data, which suggests strengthening of the surface and higher loading forces being required to indent the cell with an AFM probe.

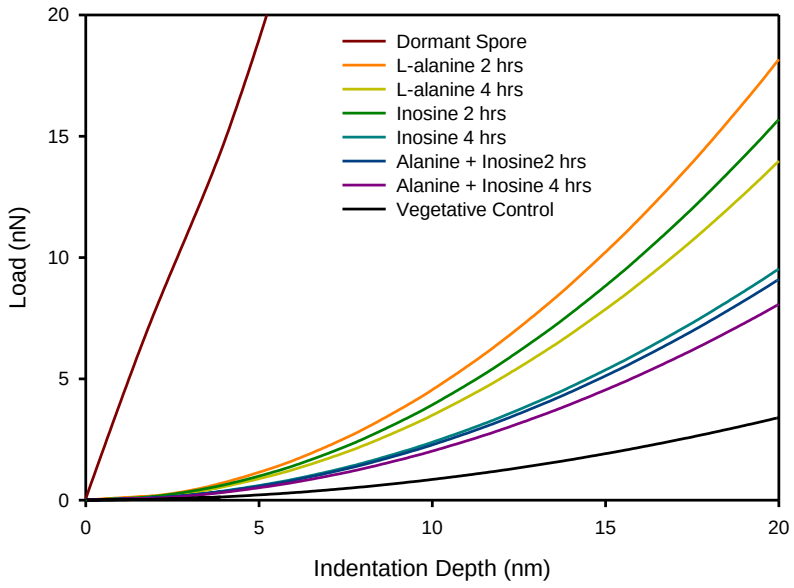

Figure 18. Representative load vs. indentation depth curves of *B. anthracis* Sterne before and after incubation with 50 mM L-alanine and/or 5 mM inosine, or tryptic soy broth supplemented with 1% yeast extract (vegetative control). Each line is the average of 50 approach curves measured between *B. anthracis* Sterne and a silicon AFM probe.

The effects of pressure on the germination of spores have been previously studied.[14, 15, 26] Exposure of spores to high pressure can initiate the process of germination.[14] Exposure of

Bacillus spores to pressures of 550 MPa resulted in initiation of germination without the involvement of any germinant receptors.[14] However, treatment at lower pressures (100 MPa) did not initiate germination, unless one of the spore's germinant receptors was activated by nutrients. Since the pressure applied by the AFM tip to the spores was much lower than 100 MPa, a pressure-induced germination of untreated spores probably did not occur in our study.

The highest Young's moduli were obtained with dormant spores that were not exposed to germinants or yeast extract (197.02 ± 80.48 MPa; Figure 19). The high elasticity value may be due to the thickness of the inner and outer coats of the sporulated cells, which can be up to 130 nm.[2] This thickness may result in a hardening of the spore surface, protecting it from environmental insults. Young's moduli of *B. anthracis* spores decreased significantly after incubation for 4 hours with L-alanine, inosine, or both germinants (47.54 ± 41.79 MPa, 35.41 ± 15.88 MPa, and 23.50 ± 14.87 MPa, respectively; $P< 0.05$). Incubation of *B. anthracis* with both germinants resulted in >90% of the spores having an elastic modulus lower than 50 MPa. There was no statistically significant difference between the Young's modulus of spores treated with L-alanine for 2 or 4 hours; in the case of inosine, the elasticity decreased from 66.42 ± 25.90 MPa after 2 hours of incubation to 35.41 ± 15.88 MPa after 4 hour incubation ($P>0.05$). The rather large standard deviation values obtained for all conditions suggest that there may be heterogeneity of the distribution of proteins on the spore surface, especially in the dormant spores. The germination of spores using only inosine as the triggering molecule has been shown to require the interaction of the germinant with two different receptors in *B. cereus* spores, GerI and GerQ, since the activation of only one of them does not provide sufficient activation of the spore to carry on with the germination process.[10] *B. cereus* is a close relative of *B. anthracis*, and the similar operons are also present in *B. anthracis* and recognize inosine as a germinant.[34] Based

on our results, germination with inosine may require longer exposure time of the cells to the ribonucleoside to allow for the interaction with both receptors. Our investigation also suggests that while other studies have shown that inosine acting alone is a weak germinant for *B. anthracis* spores as measured by the rate of optical density change, it does display a stronger impact on the mechanical properties of the cells since the surface elasticity decreases significantly compared to the dormant spore.

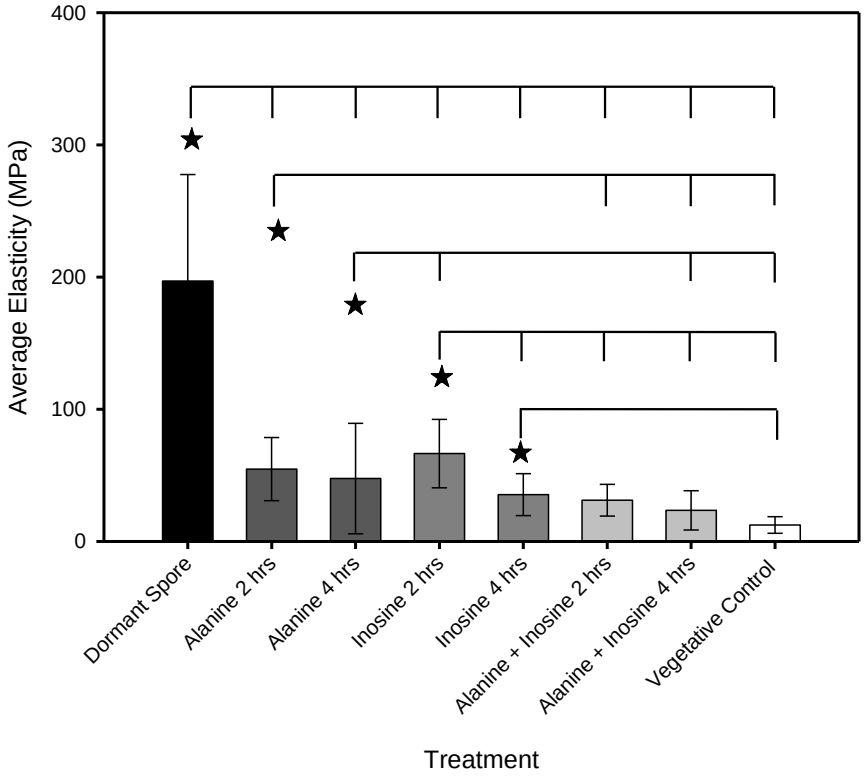

Figure 19. Elasticity of *B. anthracis* Sterne spores as a function of treatment. Spores germinated with 50 mM L-alanine and/or 5 mM inosine for 2 or 4 hours. Bars depict the average elasticity of 50 spores per condition. Error bars show the standard deviation. The top lines connect statistically distinct points ($P<0.05$) calculated by Kruskal-Wallis one-way ANOVA on ranks with Tukey's test to make pair wise comparisons The star symbol indicates the condition that is being compared to other treatments.

The elasticity values of *B. anthracis* incubated with both germinants were significantly lower compared to the spores incubated with each of the individual nutrients ($P < 0.05$). It has been suggested in the literature that *B. anthracis* may not germinate in the presence of inosine alone, but may require coupling with another germinant, such as an amino acid.[6, 11] Ireland and Hanna showed that high concentrations of inosine (up to 50 mM) did not trigger a germination response from *B. anthracis* even when incubated for up to 16 hr.[11] In the same study, it was concluded that L-alanine is a strong germinant only at high concentrations (>10mM) but the presence of a second co-germinant, such as inosine, will result in a stronger germination response.[11] Our results suggest that a weakening of the spore surface is taking place after incubation of *B. anthracis* with L-alanine and inosine, since the elasticity values decreased significantly ($P < 0.05$). The use of two germinants may not only weaken the surface of the spore but speed up the degradation of the spore coat and the peptidoglycan cortex that protects the spore core, which would change the mechanical properties of the cell.

Spores treated with lower concentrations of L-alanine and/or inosine (25 mM and/or 2.5 mM, respectively) did not show significantly different Young's moduli when compared to the values obtained with higher concentrations of L-alanine and/or inosine (50 mM and/or 5 mM, respectively; Table 2). Clements and Moir have shown that comparable germination rates of *Bacillus* spores were achieved over inosine concentrations ranging from of 1 mM to 30 mM, and over L-alanine concentrations ranging from 10 mM to 100 mM.[13] In another study, spore germination was measured by studying the decrease of optical density of spore suspensions after addition of germinants and it was determined that inosine concentrations of 1 or 10 mM, and L-alanine concentrations of 10 mM or 100 mM caused the same decrease of optical density of

spore suspensions.[8] Based on these studies, the concentrations of L-alanine and inosine chosen for our elasticity experiments fall within the range where optimal spore germination rates occur.

Table 2. Effects of germinant concentration on Young's modulus and indentation depths of *Bacillus anthracis*

Germinant Concentration	Average Young's Modulus (MPa)	*P* Value[a, b]	Average Indentation Depth[d] (nm)	*P* Value[a, c]
25 mM L-alanine	55.7 ± 31.9		137.7 ± 31.6	
		0.8		0.6
50 mM L-alanine	54.7 ± 23.9		135.0 ± 41.6	
2.5 mM inosine	69.5 ± 16.6		121.8 ± 19.7	
		0.6		0.5
5 mM inosine	66.4 ± 25.9		117.8 ± 25.1	
25 mM L-alanine + 2.5 mM inosine	32.3 ± 14.2		224.7 ± 35.1	
		0.6		0.1
50 mM L-alanine + 5 mM inosine	31.15 ± 11.9		223.9 ± 82.1	

[a]Comparisons of Young's modulus and indentation depth data between germinant concentrations were done using one way analysis of variance (ANOVA) for repeated measurements. Tukey's test was used for multiple comparisons among treatment groups. A difference was considered significant if $P < 0.05$.

[b]*P* value obtained when comparing average Young's moduli.

[c]*P* value obtained when comparing average indentation depths.

[d]All measurements were made with a loading rate of 3×10^{-5} N/s and a tip velocity of 2 μm/s

In this study we observe surface elasticity values for *B. anthracis* that are unaffected by the change in germinant concentration when the spores are exposed to high concentrations of L-

alanine (25 mM and 50 mM) or inosine (2.5 mM and 5 mM). Similarly, mixtures of both germinants at concentrations of 50 mM L-alanine and 5 mM inosine, or 25 mM L-alanine and 2.5 mM inosine yielded comparable Young's moduli. These results suggest that once the spores have been exposed to high enough concentrations of the germinants, the changes in elasticity will be the same independent of the amount of L-alanine and/or inosine in the spore suspension. The elasticity of vegetative *B. anthracis* showed the lowest Young's modulus with an average of 12.39 ± 6.32 MPa, and the values were significantly different when compared to other treatments ($P < 0.05$), except when the cells were treated with L-alanine and inosine for 4 hours ($P > 0.05$). This elasticity value is close to the elastic modulus of other vegetative bacteria. For *E. coli*, a Young's modulus of ~12.8 MPa was estimated.[23] Once a spore has completely germinated, there is an outgrowth process leading to the vegetative cell where the spore coat is lost, leaving the cell with a membrane that is much thinner and allows for the transport of nutrients and release of waste products.[5, 35]

4.4.4 Indentation Depths of *B. anthracis* as a Function of Treatment

The degradation of the spore coat resulted in a cell that could be more easily indented by the AFM probe, as was observed on vegetative bacteria and spores that were exposed to both germinants (Figure 20). Indentation depths were significantly lower for the untreated spores than for those treated with L-alanine, inosine, or TSB supplemented with yeast extract ($P < 0.05$). For the dormant spores (untreated spores), the depth indented by the AFM probe was 20.45 ± 14.88 nm. However, this indentation depth increased significantly after incubation of germinants for 2 or 4 hours. Higher indentation depth values were observed for spores treated with L-alanine compared to inosine. For the germinant-treated spores, the highest indentation depths were observed for spores treated with both L-alanine and inosine for 2 hours (223.97 ± 82.14 nm), or

with incubation of the cells in L-alanine for 4 hours (225.37 ± 98.65 nm). Lower concentrations of L- alanine and/or inosine (25 mM and 2.5 mM, respectively) showed similar indentation depth values suggesting that there is no appreciable effect of germinant concentration on surface elasticity and indentation depth, once an optimal germination condition has been achieved (Table 2).

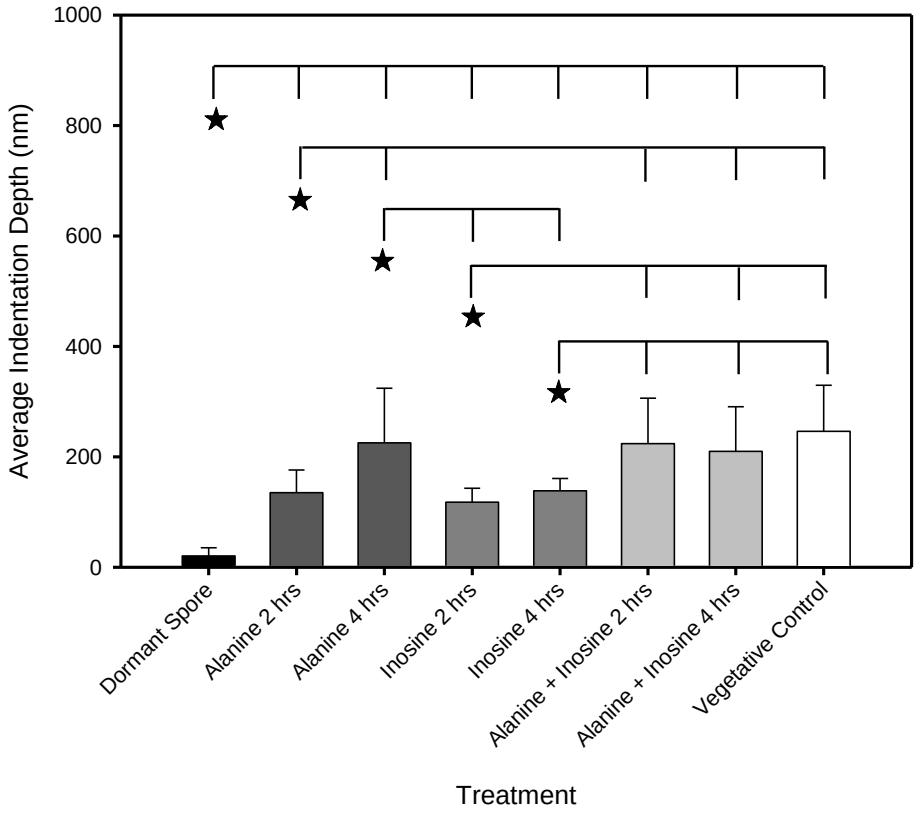

Figure 20. Average indentation depths of *B. anthracis* Sterne spores probed with a silicon AFM tip as a function of treatment. Spores germinated with 50 mM L-alanine and/or 5 mM inosine for 2 or 4 hours. Error bars show the standard deviation of 50 measurements obtained for each condition. The top lines connect statistically distinct points ($P<0.05$) calculated by Kruskal-Wallis one-way ANOVA on ranks The star symbol indicates the condition that is being compared to other treatments.

The incubation of *B. anthracis* spores in TSB supplemented with yeast extract resulted in the highest indentation depths (246.23 ± 84.31 nm). Our results suggest that the surface of

dormant (untreated) *B. anthracis* spore is harder and therefore higher loading forces are required to indent the cell. Once germination is initiated, there is a degradation of the spore coat that allows the spore to outgrow and become a vegetative cell.[5] Vegetative *B. anthracis* need to have a much thinner cell wall with more flexibility to allow the release of waste products, as well as toxins during infection and invasion of macrophages.[5, 35] Because of the more flexible and thinner surface, the AFM probe can indent the vegetative cell more than the sporulated cell. Analogous changes in the elasticity have been observed for *S. cerevisiae* at the location where the bud emerges during cell division.[22] When the cell undergoes cellular division, a chitin ring of polysaccharide of (β1-4)-linked *N*-acetylglucosamine forms to strengthen the bud scar, marking the division site.[22] The proteins that form this chitin ring are highly glycosylated peptides that are 50-95% carbohydrate by weight, which makes chitin fibers insoluble, causing stiffening of the bud scar.[36] Due to the rigidity of the chitin ring, the portion of the cell that had the bud scar had higher Young's modulus values and lower indentation depths made by the AFM probe compared to the rest of the cell surface. In another study, the spring constant of the *S. cerevisiae* cell body and the bud scar were determined from the slope of the linear portion of the force-distance curve, and the bud scar displayed higher cell spring constant due to the increased chitin content of the area.[37]

4.5 Conclusions

The rigidity of the spore coat of dormant *B. anthracis* cells is severely compromised by exposure to germinants or nutrients, such as TSB and yeast extract. During germination, the spores start losing their coat, making the cell's surface more flexible, lowering the surface elastic modulus, and allowing the AFM probe to indent the surface more during the force cycle. Vegetative *B. anthracis* showed the weakest cell surface with elasticity values that were 15 times

lower than sporulated cells. This decrease in elasticity accompanied by a decrease in the thickness of the spore coat, which we previously observed,[3] would explain why vegetative cells are sensitive to sporicidal compounds. Based on our findings, the study of elasticity of spores may be a valuable tool to predict how to weaken spores, thus making them more susceptible to spore inactivation processes based on mechanical forces, such as the high pressure, high temperature inactivation method practiced in the food industry. Indeed, based on our results we anticipate that the decrease in the elastic modulus of the spores caused by germinants such as L-alanine, inosine, dodecylamine, etc, either alone or in mixtures, would make spore inactivation possible at lower pressures compared to that in the absence of such germinators. It may also be possible to reduce the small population of "difficult to kill" or "super dormant" spores that often survive the current high pressure inactivation methods by the use of germinants in the high pressure spore inactivation process.

4.6 Acknowlegments

This work was supported in part by the National Science Foundation (CBET 0827229) and the Defence Threat Reduction Agency (DTRA) Project BA07PRO102.

We also thank Ms. Angela Tao for her assistance in the development of the MatLab script used for elasticity measurements, Mr. Robert Stote and Ms. Stephanie Marcott of NSRDEC for help with spore preparation, and Prof. Nancy Burnham for helpful discussions.

REFERENCES

1. Atrih, A.; Foster, S. J., Bacterial endospores the ultimate survivors. *Int. Dairy J.* **2002,** 12, (2-3), 217-223.

2. Henriques, A. O.; Moran, C. P., Jr., Structure and assembly of the bacterial endospore coat. *Methods* **2000,** 20, (1), 95-110.

3. Pinzón-Arango, P. A.; Scholl, G.; Nagarajan, R.; Mello, C. M.; Camesano, T. A., Atomic force microscopy study of germination and killing of *Bacillus atrophaeus* spores. *J Mol Recognit* **2009,** 22, (5), 373-379.

4. Setlow, B.; Cowan, A. E.; Setlow, P., Germination of spores of *Bacillus subtilis* with dodecylamine. *J Appl Microbiol* **2003,** 95, (3), 637-48.

5. Setlow, P., Spore germination. *Curr Opin Microbiol* **2003,** 6, (6), 550-6.

6. Akoachere, M.; Squires, R. C.; Nour, A. M.; Angelov, L.; Brojatsch, J.; Abel-Santos, E., Identification of an in vivo inhibitor of *Bacillus anthracis* spore germination. *J Biol Chem* **2007,** 282, (16), 12112-8.

7. Drysdale, M.; Heninger, S.; Hutt, J.; Chen, Y.; Lyons, C. R.; Koehler, T. M., Capsule synthesis by *Bacillus anthracis* is required for dissemination in murine inhalation anthrax. *Embo J* **2005,** 24, (1), 221-7.

8. Gounina-Allouane, R.; Broussolle, V.; Carlin, F., Influence of the sporulation temperature on the impact of the nutrients inosine and l-alanine on *Bacillus cereus* spore germination. *Food Microbiol* **2008,** 25, (1), 202-6.

9. Slieman, T. A.; Nicholson, W. L., Role of dipicolinic acid in survival of *Bacillus subtilis* spores exposed to artificial and solar UV radiation. *Appl Environ Microbiol* **2001,** 67, (3), 1274-9.

10. Barlass, P. J.; Houston, C. W.; Clements, M. O.; Moir, A., Germination of *Bacillus cereus* spores in response to L-alanine and to inosine: the roles of *gerL* and *gerQ* operons. *Microbiology* **2002,** 148, (Pt 7), 2089-95.

11. Ireland, J. A.; Hanna, P. C., Amino acid- and purine ribonucleoside-induced germination of *Bacillus anthracis* ΔSterne endospores: *gerS* mediates responses to aromatic ring structures. *J Bacteriol* **2002,** 184, (5), 1296-303.

12. Titball, R. W.; Manchee, R. J., Factors affecting the germination of spores of *Bacillus anthracis*. *J Appl Bacteriol* **1987,** 62, (3), 269-73.

13. Clements, M. O.; Moir, A., Role of the gerI operon of *Bacillus cereus* 569 in the response of spores to germinants. *J Bacteriol* **1998,** 180, (24), 6729-35.

14. Paidhungat, M.; Setlow, B.; Daniels, W. B.; Hoover, D.; Papafragkou, E.; Setlow, P., Mechanisms of induction of germination of *Bacillus subtilis* spores by high pressure. *Appl Environ Microbiol* **2002,** 68, (6), 3172-5.

15. Wuytack, E. Y.; Boven, S.; Michiels, C. W., Comparative study of pressure-induced germination of *Bacillus subtilis* spores at low and high pressures. *Appl Environ Microbiol* **1998,** 64, (9), 3220-4.

16. Vadillo-Rodriguez, V.; Beveridge, T. J.; Dutcher, J. R., Surface viscoelasticity of individual Gram-negative bacterial cells measured using atomic force microscopy. *J Bacteriol* **2008,** 190, (12), 4225-32.

17. Zaman, M. S.; Goyal, A.; Dubey, G. P.; Gupta, P. K.; Chandra, H.; Das, T. K.; Ganguli, M.; Singh, Y., Imaging and analysis of *Bacillus anthracis* spore germination. *Microsc Res Tech* **2005,** 66, (6), 307-11.

18. Dûfrene, Y. F., Atomic force microscopy, a powerful tool in microbiology. *J Bacteriol* **2002,** 184, (19), 5205-13.

19. Plomp, M.; Leighton, T. J.; Wheeler, K. E.; Hill, H. D.; Malkin, A. J., In vitro high-resolution structural dynamics of single germinating bacterial spores. *Proc Natl Acad Sci U S A* **2007,** 104, (23), 9644-9.

20. Plomp, M.; Leighton, T. J.; Wheeler, K. E.; Malkin, A. J., The high-resolution architecture and structural dynamics of *Bacillus* spores. *Biophys J* **2005a,** 88, (1), 603-8.

21. Plomp, M.; Leighton, T. J.; Wheeler, K. E.; Pitesky, M. E.; Malkin, A. J., *Bacillus atrophaeus* outer spore coat assembly and ultrastructure. *Langmuir* **2005b,** 21, (23), 10710-6.

22. Touhami, A.; Nysten, B.; Dûfrene, Y. F., Nanoscale mapping of the elasticity of microbial cells by atomic force microscopy. *Langmuir* **2003,** 19, (11), 4539-4543.

23. Abu-Lail, N. I.; Camesano, T. A., The effect of solvent polarity on the molecular surface properties and adhesion of *Escherichia coli*. *Colloids Surf B Biointerfaces* **2006,** 51, (1), 62-70.

24. Tamir, H.; Gilvarg, C., Density gradient centrifugation for the separation of sporulating forms of bacteria. *J Biol Chem* **1966,** 241, (5), 1085-90.

25. Patra, G.; Vaissaire, J.; Weber-Levy, M.; Le Doujet, C.; Mock, M., Molecular characterization of *Bacillus* strains involved in outbreaks of anthrax in France in 1997. *J Clin Microbiol* **1998,** 36, (11), 3412-4.

26. Ryu, C.; Lee, K.; Yoo, C.; Seong, W. K.; Oh, H. B., Sensitive and rapid quantitative detection of anthrax spores isolated from soil samples by real-time PCR. *Microbiol Immunol* **2003,** 47, (10), 693-9.

27. Westphal, A. J.; Price, P. B.; Leighton, T. J.; Wheeler, K. E., Kinetics of size changes of individual *Bacillus thuringiensis* spores in response to changes in relative humidity. *Proc Natl Acad Sci U S A* **2003,** 100, (6), 3461-6.

28. Burnham, N. A.; Colton, R. J., Measuring the nanomechanical properties and surface forces of materials using an atomic force microscope. *J Vac Sci Technol A* **1989,** 7, (4), 2906-13.

29. Tomasetti, E.; Legras, R.; Nysten, B., Quantitative approach towards the measurement of polypropylene/(ethylene-propylene) copolymer blends surface elastic properties by AFM. *Nanotechnology* **1998,** 9, (4), 305-315.

30. Weisenhorn, A. L.; Khorsandi, M.; Kasas, S.; Gotzos, V.; Butt, H.-J., Deformation and height anomaly of soft surfaces studied with an AFM. *Nanotechnology* **1993,** 4, (2), 106-13.

31. Murakoshi, M.; Yoshida, N.; Iida, K.; Kumano, S.; Kobayashi, T.; Wada, H., Local mechanical properties of mouse outer hair cells: atomic force microscopic study. *Auris Nasus Larynx* **2006,** 33, (2), 149-57.

32. Schaer-Zammaretti, P.; Ubbink, J., Imaging of lactic acid bacteria with AFM--elasticity and adhesion maps and their relationship to biological and structural data. *Ultramicroscopy* **2003,** 97, (1-4), 199-208.

33. Kotiranta, A.; Haapasalo, M.; Kari, K.; Kerosuo, E.; Olsen, I.; Sorsa, T.; Meurman, J. H.; Lounatmaa, K., Surface structure, hydrophobicity, phagocytosis, and adherence to matrix proteins of *Bacillus cereus* cells with and without the crystalline surface protein layer. *Infect Immun* **1998,** 66, (10), 4895-902.

34. Baillie, L.; Hibbs, S.; Tsai, P.; Cao, G. L.; Rosen, G. M., Role of superoxide in the germination of *Bacillus anthracis* endospores. *FEMS Microbiol Lett* **2005,** 245, (1), 33-8.

35. Leuschner, R. G. K.; Ferdinando, D. P.; Lillford, P. J., Structural analysis of spores of *Bacillus subtilis* during germination and outgrowth. *Colloids Surf., B* **2003,** 19, 31-41.

36. Alsteens, D.; Dupres, V.; Mc Evoy, K.; Wildling, L.; Gruber, H. J.; Dufrene, Y. F., Structure, cell wall elasticity and polysaccharide properties of living yeast cells, as probed by AFM. *Nanotechnology* **2008,** 19, (38), 384005/1-384005/9.

37. Pelling, A. E.; Sehati, S.; Gralla, E. B.; Valentine, J. S.; Gimzewski, J. K., Local nanomechanical motion of the cell wall of *Saccharomyces cerevisiae*. *Science* **2004,** 305, (5687), 1147-50.

Chapter 5

Changes in mechanical properties and killing of *Bacillus anthracis* 34F2 after exposure to the antimicrobial peptide chrysophsin-3

Biotechnology and Bioengineering (submitted December 2011)

5.1 Abstract

Bacillus anthracis spores are capable of surviving harsh chemical and environmental factors that would eradicate other microorganisms. Previous research has suggested that spores can only be eradicated with common disinfectants after germination and release of spore coats. The effects of surfactants and germinants on spore surface properties have been investigated; however, there are limited studies on the effects of antimicrobial peptides on the mechanical properties and killing of *B. anthracis*. The antimicrobial peptide (AMP) chrysophsin-3 was tested for its antisporal activities and its effects on mechanical properties of the spores. L-alanine and inosine were used as germinants and atomic force microscopy (AFM) was used to obtain the Young's modulus and spring constant of *B. anthracis* 34F2 spores after exposure to the AMP. No statistically significant change in the Young's modulus was observed for spores treated with chrysophsin-3 compared to untreated spores. However, vegetative *B. anthracis* 34F2 exposed to chrysophsin-3 exhibited a change in Young's modulus from 12 ±16 MPa without the AMP to 84 ±17 MPa with AMP. In addition, exposure to chrysophsin-3 only affected the spring constant of vegetative *B. anthracis*, but not the spring constant of spores. AFM images suggested that chrysophsin-3 caused the lysis of *B. anthracis* 34F2 due to loss of water content and cellular material from the spore. In viability studies, 0.22 mM chrysophsin-3 killed sporulated, germinated, and vegetative *B. anthracis* 34F2. Our results suggest that chrysophsin-3 may be useful for the deactivation of *B. anthracis* spores since the AMP is capable of penetrating the spore coat and kill spores without the need to initiate germination.

5.2 Introduction

B. anthracis, the microorganism responsible for development of anthrax infections, has been researched for more than 120 years in an effort to understand the physico-chemical

properties of the spore and how to prevent its use as a biological weapon[1-3]. *B. anthracis* are capable of undergoing the process of sporulation under conditions of nutrient deprivation[4]. As a spore, the genetic material of *B. anthracis* is protected and encased in a thick protein coat (~100 nm thick)[5], which cannot be penetrated by common antibiotics. Extreme heat, UV radiation, desiccation, pH extremes, and toxic chemicals are also ineffective in killing spores, making them one of the most resistant life forms known[6, 7].

Dormant spores can resume their metabolic activity during the process of germination. During germination, amino acids and purine nucleosides, such as L-alanine and inosine, trigger the process of germination by binding to receptors on the inner membrane of the spore[8, 9]. Germination causes the release of monovalent cations, Zn^{2+}, Ca^{2+}, and dipicolinic acid (DPA) from the spore core[10-12]. Rehydration of the spore core and hydrolyzation of the spore cortex occur, followed by the resumption of metabolism and macromolecular synthesis. These events cause the spore coat to break down and release a fully virulent germinated cell (Figure 21)[10, 13].

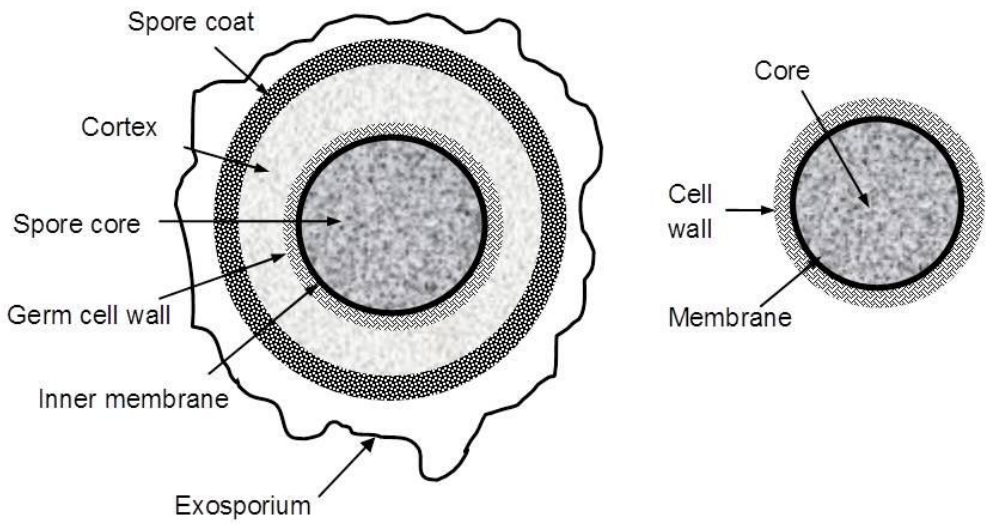

Figure 21. Schematic representation of *B. anthracis* in the spore state (left) and in their vegetative state (right). Dimensions or thickness of each layer vary among *Bacillus* species.

Anthrax infections can only be eradicated with early administration of antibiotics and aggressive supportive care[14]. Unfortunately, since the initial symptoms of pulmonary anthrax are very similar to an influenza-like illness, the infection is often difficult to diagnose causing a delay in treatment[15, 16]. Furthermore, recent studies have found that the high dosage and long therapy used to treat anthrax infections have resulted in development of antibiotic resistance in *B. anthracis*[14, 17-19].

Due to difficulties in diagnosis and treatments, alternative therapies against *B. anthracis* infections are needed. Antimicrobial peptides (AMPs) are short polypeptides that are associated with the innate immune system of host organisms, and are widely distributed in the animal and plant kingdoms[20]. AMPs from fish are of particular interest since they have shown antibacterial, antiviral, antifungal, antiparasitic, immunomodulatory, and antitumor functions[21].

Chrysophsin-1, -2, and -3 are a family of peptides that have been isolated from the eosinophilic granule cell-like cells of the gills of the red sea bream (*Chrysophrys major*)[22]. Chrysophsin-3 is an amphipathic, cationic α-helical peptide that is rich in histidine residues with a 20 amino acid sequence (FIGLLISAGKAIHDLIRRRH) and a molecular mass of 2287 Da[22]. The peptide has an unusual RRRH motif that makes the molecule positively charged, causing secondary amphipathicity and a change in hydrophobicity between the N and C termini (Figure 22)[23]. While there are numerous types of AMPs that have shown antibacterial activity, only one study has evaluated the effect of Chrysophsin-3 on Gram-positive and Gram-negative bacteria[22]. Iijima et al. observed that chysophsin-3 was effective in killing various organisms at concentrations lower than 40 μM, including vegetative *B. subtilis* [22]. Although the bactericidal activity of chrysophsin-3 is encouraging, no prior study has investigated the effects of this peptide on bacterial spores. It was previously assumed that AMPs would not be able to penetrate

the spore coat, and thus they would be ineffective against spores. Furthermore, there is not a clear understanding of how the AMP interacts with the spore coat, vegetative bacteria, or spores that are undergoing the process of germination.

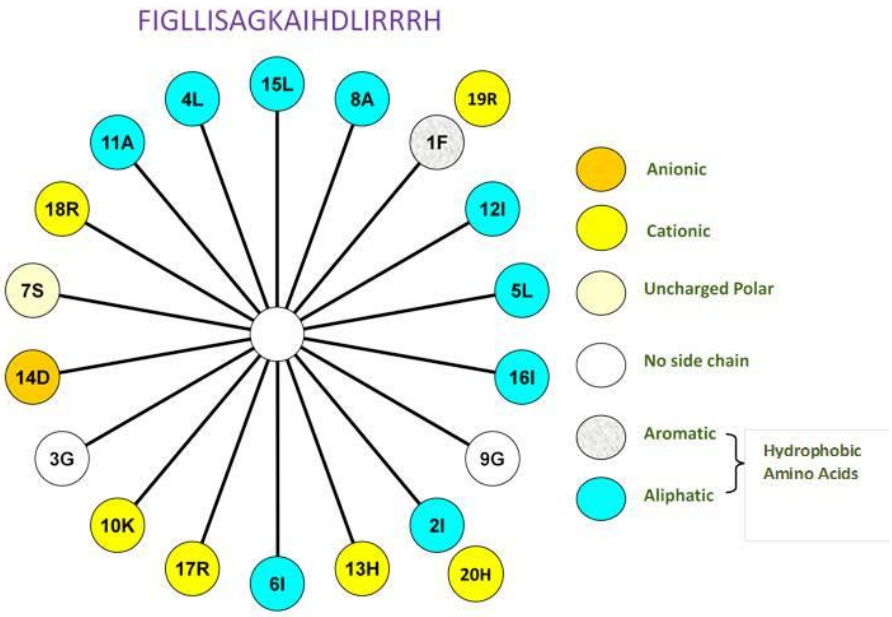

Figure 22. Helical wheel diagram demonstrating the amphipathic α-helical conformation of chrysophsin-3. The blue color indicates amino acids that are hydrophobic in nature.

In this study, we investigated the effect of chrysophsin-3 on *B. anthracis* spores at a nanomolecular level using AFM, which has been widely used to characterize the morphology and the mechanical properties of microbial cells[24, 25]. By monitoring the interaction between the AFM tip and individual cells, it is possible to study mechanical properties of bacteria, such as adhesion, elasticity, cellular spring constant, and roughness[26, 27]. Several studies have addressed how germinants, such as L-alanine, affect the morphology of *Bacillus* spores[8, 28, 29]. In a previous study, we used the AFM as a nanoindentation tool to investigate changes in spore surface elasticity during germination and found that the Young's modulus of the spore decreases as the spore is germinating[26].

In the present study, we focused on characterizing the changes in surface elasticity and spring constant of *B. anthracis* after exposure to the AMP and compared the interaction of chrysophsin-3 with *B. anthracis* in three states: spore, germinating, and vegetative. We also investigated the bactericidal activity of chrysophsin-3 on sporulated, germinated, and vegetative *B. anthracis*, to determine whether bactericidal activity and biophysical properties of the spores are correlated.

5.3 Materials and Methods

5.3.1 Antimicrobial Peptide (AMP)

The AMP chrysophsin-3 was synthetically produced with α-helical secondary structure and the sequence FIGLLISAGKAIHDLIRRRH (Bachem Americas, Inc., Torrance, CA). The peptide has a relative molecular mass of 2286.8 Da and is more than 80% pure, measured by reverse phase high-perfomance liquid chromatography (HPLC). A 4.4 mM stock solution of the peptide was prepared in 50 mM tris-HCl and stored at 4 ºC until used.

5.3.2 Spore Preparation

B. anthracis Sterne 34F2 ($pXO1^+$ $pXO2^-$; referred to heareafter as "*B. anthracis* 34F2") was kindly provided by the Edgewood Chemical Biological Center, Edgewood, Maryland. *B. anthracis* 34F2 were grown in sporulation medium as described previously[26]. Sporulation medium consisting of 8 g of nutrient broth, 4 g of yeast extract, 0.001 g of $MnCl_2 \cdot 4H_2O$, 5 g of peptone, and 15 g of agar in 1 L of ultrapure water (Milli-Q water, Millipore Corp., Bedford, MA) was sterilized for 60 min and poured into Petri dishes.

Fresh cultures of *B. anthracis* 34F2 were obtained by adding 100 µL of spores from a glycerol stock solution into a flask with 25 mL of sterile nutrient broth (Himedia, Mumbai,

India). The flask was placed in a water bath at 37 ºC and agitated at 200 rpm for 20 hrs. This culture was used to inoculate plates of sporulation medium using aliquots of 50 µL solution. The plates were incubated at 37 ºC for 4 days to allow vegetative *B. anthracis* to form spores. Harvesting of the spores was done in autoclaved ultrapure water, and spores were collected by centrifugation at 5000 rpm for 20 min. The spores were washed eight times to remove partially sporulated cells and vegetative bacteria. Washed spores were stored at 4 ºC overnight and after 18-20 hrs, two additional washes were done to remove any remaining vegetative cells. Sporulation was verified through phase contrast microscopy and samples of prepared spores were considered ready when at least 99% of phase bright spores were observed under the microscope.

5.3.3 Exposure to Antimicrobial Peptide Chrysophsin-3 and Germination Treatments

To trigger germination of spores, *B. anthracis* at a concentration of 10^8 cells/mL was exposed to 50 mM L-alanine (Sigma-Aldrich, St. Louis, MO) and/or 5 mM inosine (Sigma-Aldrich) in 50 mM tris/HCl buffer (pH 8.0), and incubated for 2 hours at 37 ºC. To achieve outgrowth of spores into vegetative *B. anthracis*, a 1 mL sample of dormant spore solution was suspended in tryptic soy broth supplemented with 1% yeast extract, and grown for 6 hours at 37 ºC with rotation at 18 rpm. Germination was assessed through phase contrast microscopy. Untreated spores incubated in tris-HCl buffer for 2 hours were used as control. Germinated, sporulated (untreated), and vegetative *B. anthracis* were exposed to 0.22 mM of chrysophsin-3 for 1 hour at 37 ºC. After exposure to chrysophsin-3, bacteria were washed by centrifugation at 5000 rpm for 5 minutes and resuspended in ultrapure water to stop AMP treatment.

5.3.4 Viability of *B. anthracis* after Chrysophsin-3 Treatment

To determine the effects of chrysophsin-3 on spore viability, the treated bacteria solution was serially diluted and 100 µL of solution was inoculated onto tryptic soy agar plates and incubated at 37˚C for 18 hrs. The number of colony forming units (cfu) on the agar plates was counted and the experiment was done in triplicates. Control experiments with untreated spores on agar plates were also performed.

5.3.5 Atomic Force Microscopy

Changes in cellular spring constant and elastic modulus of the spores after treatment with germinants and/or chrysophsin-3 were investigated using AFM. Droplets of treated *B. anthracis* 34F2 (5 µL) were deposited onto freshly cleaved mica and dried for 18 hrs.

AFM experiments were carried out with a Dimension 3100 with a Nanoscope IIIa controller (Veeco Metrology, Santa Barbara, CA) operated in tapping mode in air to represent *B. anthracis* spores found in their natural environment. AFM measurements were taken at 30-35% relative humidity in air. A single rectangular cantilever with a conical silicon tip having a specified spring constant of 14 N/m and a resonant frequency of 315 kHz was used for all AFM measurements (Mikromasch, San Jose, CA). Samples were scanned at a rate of 1.0 Hz, and topographical images of treated and untreated *B. anthracis* were obtained. Once a spore was located, it was centered to ensure that force measurements were taken away from the edges. Forces were measured on five spores for each treatment, and ten force cycles were recorded per spore. All force cycles recorded per spore were taken at the same location of the cell to verify that no deformation of the surface was taking place. AFM images were taken before and after force measurements to ensure that no damage to the cell had occurred during force

measurements. The AFM tip was set to stay in contact with the sample for 1 ms before retracting. The velocity of the tip was set at 2 µm/s with a loading rate of 3 x 10^{-5} N/s. To calibrate the photodetector, force curves were made on freshly cleaved mica free of spores before any measurements were taken on cells. Data in ASCII format were exported to a spreadsheet and converted from deflection to force as previously described[26].

5.3.6 Spring Constant of *B. anthracis* 34F2

Cantilever sensitivity was used together with the cantilever spring constant (k_c) to convert raw AFM data into deflection (nm) vs. separation distance (nm) curves (Figure 23). When bacteria are probed with the AFM tip, the curvature approach profile represents the indentation of the tip into the spore coat, before the region of constant compliance is reached (linear response; Figure 23).

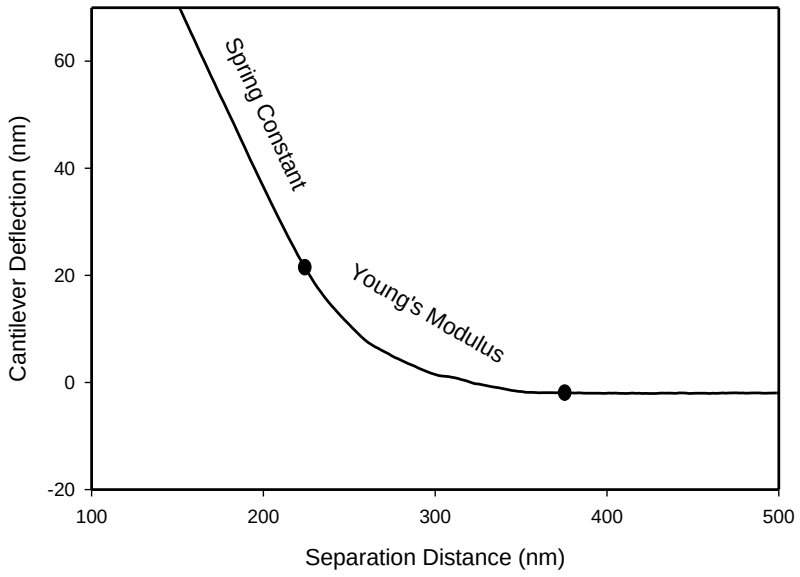

Figure 23. Representative AFM approach curve from a *B. anthracis* 34F2 cell. The linear region of the curve on the upper left corner represents the region of constant compliance, which was used to calculate the spring constant of the cell. The non-linear region between the two black dots denotes the indentation of the AFM tip into the cell and is used to calculate the Young's modulus of *B. anthracis*.

Once there is no further indentation of the spore coat by the AFM tip, the linear cantilever deflection-separation distance relation observed during the force cycle is due to the spore turgor pressure. The slope of the constant compliance region, which characterizes the rigidity of the whole spore, is then used to calculate the effective spore spring constant k_s by

$$k_s = \frac{k_c s}{1 - s} \tag{4}$$

where *s* is the slope of the constant compliance region (Figure 23)[30].

A total of 10 curves were analyzed per spore and the overall mean and standard deviation (SD) of the sample were calculated based on the k_s of 5 cells. Hence, data were collected on a total of 50 force curves per test condition. A MatLab script was written to analyze all raw data obtained with the AFM and calculate the spring constant of the spore for all treatments (MatLab Works Inc., Natick, MA).

5.3.7 Young's Modulus of *B. anthracis* 34F2

The deflection data obtained during force measurements were converted to loading force vs. indentation data following procedures described previously[26]. The tensile Young's modulus was obtained by applying the Hertz model of continuum mechanics of contact to the non-linear portion of the loading force – indentation depth data (Figure 23). The geometry of the AFM tip was taken into account and it was related to the AFM data by

$$F_{cone} = \frac{2}{\pi} tan\alpha \frac{E}{1 - \upsilon^2} \delta^2 \tag{5}$$

where α is the half-opening angle of the conical tip used, taken as 40º as specified by the manufacturer, *E* is the Young's modulus of the spore, ν is the Poisson ratio of the spore taken as

0.5[31], and δ is the indentation depth of the spore. A MatLab script was written to analyze all raw data obtained with the AFM and calculate the Young's modulus of the spore for all treatments (MatLab Works Inc., Natick, MA).

5.3.8 Limitations of Hertz Model

While other mathematical models that describe the elastic response of a substrate after applying pressure with an AFM tip are available, the Hertz model is a simple and classical way of describing at a very fundamental level the contact mechanics of an elastic half space (spore) by a rigid object (AFM tip). Several assumptions need to be met when applying the Hertz model: the sample being studied needs to be elastic, isotropic, homogeneous, and semi-infinate. While at the macroscopic level, spores may be considered homogeneous and isotropic, at a microscopic and nanomolecular level the surface of spores may be completely heterogeneous having physical properties that differ when measurements are made in different locations of the cell. The Johnson, Kendall, and Roberts (JKR) model, which is a modification of the Hertz theory, may be more appropriate when investigating the elastic properties of spores since accounts for the influence of surface energy. However, this model is more complex and difficult to use. The Hertz model, while not exact, can provide of a general idea of the properties of spores while they are undergoing the process of germination.

It is also important to keep in mind the the shape of the AFM probe may change with usage since prolonged use of the AFM tip may cause the probe to lose its sharpness. If that's the case, it is advisable to measure the radius of curvature of the AFM tip and determine if the Hertz models applies to the date. However, since we used a single brand new conical tip and the AFM was operating in tapping mode, the Hertz equation for a conical tip could be used.

5.3.9 Statistical Analysis

Elasticity, spring constant, and viability data were analyzed using the Kruskal-Wallis one-way analysis of variance (ANOVA) on ranks for repeated measurements. The null hypothesis tested was that there were no differences in the distribution of values between different groups. Tukey's test was used for comparisons between untreated spores and those treated with chrysophsin-3. A difference was considered significant if $P < 0.05$.

5.4 Results and Discussion

5.4.1 Spore Viability after Exposure to Chrysophsin-3

Exposure of *B. anthracis* 34F2 to 0.22 mM chrysophsin-3 resulted in a significant decrease in surviving spores (Table 3). Without any germinant, the peptide itself killed ~79% of the spores in their dormant state. Unlike chrysophsin-3, other AMPs, such as E4I subtilin and nisin, have been shown to promote germination of spores before killing[32, 33]. Similarly, nisin, an AMP isolated from *Lactococcus lactis*, does not inhibit germination and instead, germination is required for the peptide to cause disruption of membrane integrity[32]. Initiation of germination does not have to take place for chrysophsin-3 to act against *B. anthracis* spores.

Exposure of spores to chrysophsin-3 and germinants resulted in increased killing. Exposing *B. anthracis* 34F2 to 50 mM L-alanine or 5 mM inosine for 2 hours before exposure to chrysophsin-3 resulted in ~84% and ~82% killing of spores, respectively. Greater killing was observed when both germinants were used before exposure to the AMP. Over 99% of the spores were killed after exposure to chrysophsin-3 corresponding to a log-kill of ~2 (number of surviving spores was reduced by two-log). Killing of germinating spores by other AMPs have also been observed[32, 34-36]. The AMP licochalcone caused the release of calcium from spores and

the inhibition in spore growth[36]. Nisin also inhibited the growth of *B. anthracis* spores at low concentrations; however, germination was a necessary step for nisin to stop spore growth[32].

Table 3. Anti-sporal efficacy of chrysophsin-3 against *Bacillus anthracis* spores

Treatment[a]	Number of Surviving Spores (CFU/mL)	% Killed[b]	Log-Kill[c]
B. anthracis, no peptide or germinant	7.4×10^6	-	-
B. anthracis + chrysophsin	1.6×10^6	78.8	0.67
B. anthracis + Inosine	7.2×10^6		
B. anthracis + Inosine + chrysophsin	1.4×10^6	81.6	0.74
B. anthracis + L-alanine	8.2×10^6		-0.04
B. anthracis + L-alanine + chrysophsin	1.2×10^6	84.3	0.81
B. anthracis + L-alanine + Inosine	2.6×10^5		
B. anthracis + L-alanine + Inosine + chrysophsin	5.4×10^4	99.3	2.14
Vegetative *B. anthracis*	4.5×10^6		
Vegetative *B. anthracis* + chrysophsin	10	99.9	5.86

[a] Chrysophsin-3 concentration = 0.22 mM; L-alanine concentration = 50 mM; inosine concentration = 5 mM.

[b] Against control.

[c] Log-Kill = Log (number of original spores/number of surviving spores)

Not surprisingly, chrysophsin-3 had the most sporicidal effect against vegetative *B. anthracis* 34F2. The complete release of spore coats after outgrowth of the spore results in a vegetative bacterium with a susceptible thin cell membrane. In a previous study, we observed

that the surface of vegetative *B. anthracis* had comparable Young's modulus to that of *E. coli,* making the cell an easy target for eradication[26, 37]. Other AMPs have been effective in the killing or inactivating vegetative *Bacillus* sp. spores, such as surfactin and fengycin[34], retrocyclin and human neutrophil peptide-1[35], chrysophsin-1 and -2[22], subtilin[33], nisin[32], and licochalcone A[36].

5.4.2 Effects of Chrysophsin-3 on the Spring Constant of *B. anthracis* 34F2

B. anthracis in their dormant state are encased in layers of tough protein shells that protect the spores against environmental factors (Figure 24). By making use of AFM, it has been possible to understand the roles of spore coats and different proteins, and how these coats change as the spore is going through the process of germination[27, 28]. In a previous study, we characterized morphological changes that occur during the germination and killing of *B. atrophaeus* spores, a surrogate of *B. anthracis*[27]. AFM experiments allowed us to characterize changes in spore surface morphology, cell size, and surface roughness, as the spores were made to germinate with dodecylamine and L-alanine.

In the present study, AFM was used to quantify the spring constant of *B. anthracis* exposed to chrysophsin-3 in three states: sporulated, germinated, and as a vegetative cell. Spring constants of sporulated or germinated *B. anthracis* 34F2 did not change after exposure to chrysophsin-3 (Figure 4; $P>0.05$). The spring constant of untreated *B. anthracis* 34F2 remained the same after exposure to 0.22 mM chrysophsin-3 for 1 hour (6.03 ± 0.23 N/m and 6.03 ± 0.24 N/m; respectively). Germination of *B. anthracis* 34F2 with 50 mM L-alanine resulted in a slight decrease in cellular spring constant when compared to the sporulated cell (5.76 ± 0.22 N/m). However, this slight change in spring constant was not statistically different ($P>0.05$). Exposure of L-alanine-treated *B. anthracis* to chrysophsin-3 did not cause any changes in spring constant

and the values remained similar to the untreated L-alanine-germinated spore (5.73 ± 0.29 N/m). Use of 5 mM inosine as the germinating agent resulted in a lower spring constant (5.07 ± 0.54 N/m) and remained the same after exposure to the AMP (5.19 ± 0.25 N/m). Treatment of *B. anthracis* 34F2 with both germinants together resulted in a lower cellular spring constant and the value remained the same after additional exposure to the peptide (4.70 ± 0.49 N/m and 4.71 ± 0.51 N/m; respectively).

The values of spring constants of *Bacillus* spores found in this study are higher than those reported by other researchers[38]. The spring constant of *B. subtilis* has been reported to be ~0.4 N/m[38]. However, the cellular spring constant reported by Volle et al. is that of bacteria that were not in their sporulated form but in their vegetative form, since the cells were not devoid of nutrients[38]. The spring constant of the cantilever used in our study was > 40 times higher than the one used by Volle et al., which supports the high k_s values observed in our study. The cellular spring constants observed may be due to the thickness and molecular organization of spore coats. The sporulated form of *B. anthracis* has low water content, making the cell stiffer and increasing the spring constant value compared to a vegetative bacterium.

Not surprisingly, the lowest spring constant values were observed on fully germinated *B. anthracis*, which were vegetative cells. The spring constant of vegetative *B. anthracis* 34F2 was 4.51 ± 0.93 N/m (Figure 24). After exposure to the AMP, the spring constant of the cell increased significantly to 6.24 ± 0.25 N/m (P<0.05). Chrysophsin-3 seemed to only affect the stiffness of vegetative *B. anthracis*, and not that of the spores. This may have been due to the lack of spore coat proteins that would have slowed down or impeded the penetration of the AMP into the cell.

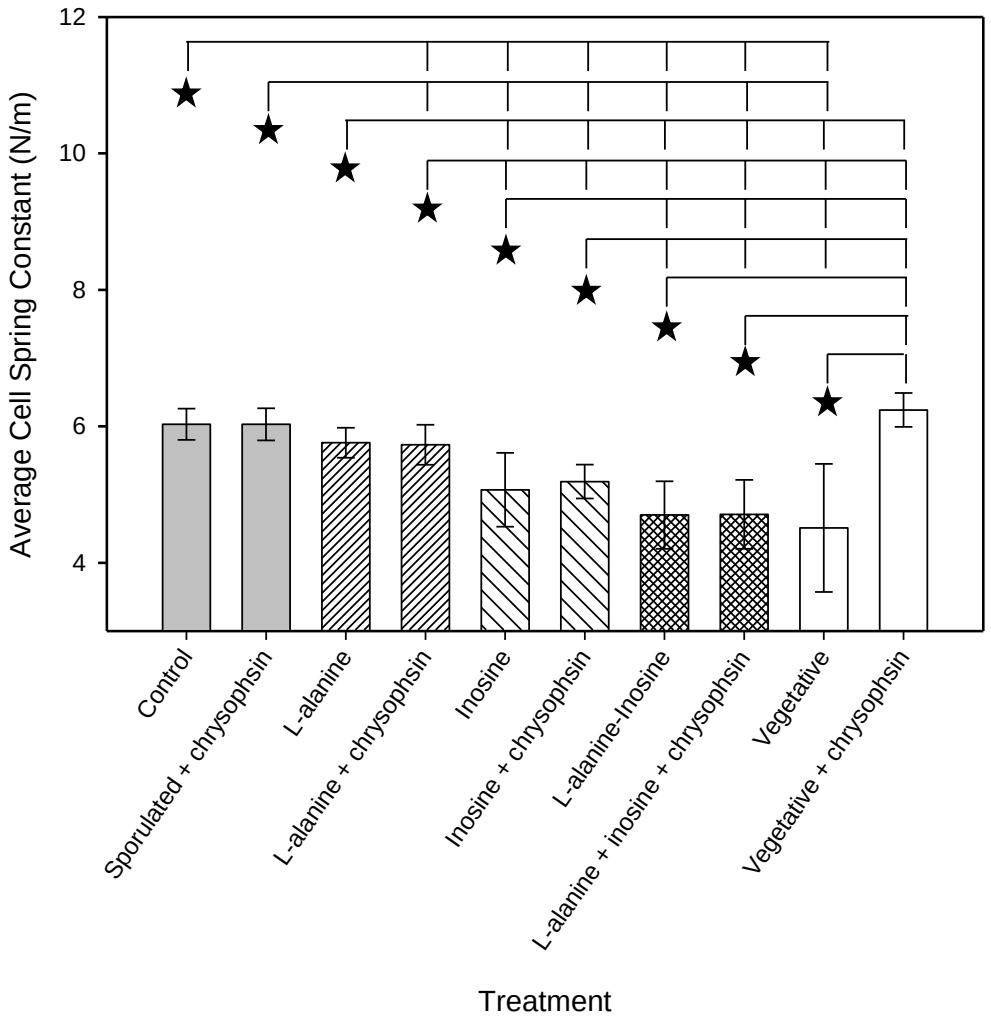

Figure 24. Average spring constant of *B. anthracis* 34F2 as a function of treatment. Spores were germinated with 50 mM L-alanine and/or 5 mM inosine for 2 hours at 37 ºC. After treatment with germinants, the spores were exposed to 0.22 mM of chrysophsin-3 for 1 hour at 37 ºC. Bars depict the average value of 50 force profiles per condition and standard deviation. The top line and star connect statistically distinct points (P<0.05) calculated by one way ANOVA on ranks. The star symbol indicates the condition that is being compared to other treatments.

Fernandes et al. observed that antimicrobial chitooligosaccharides (COS), a chitin byproduct derived from crustaceans and insects, are more effective against vegetative *B. cereus* than sporulated cells[39]. The slope of the constant compliance region of AFM curves taken on vegetative *B. cereus* changed significantly and became steeper after treatment with the antimicrobial compound, which indicates an increase in cellular stiffness. However, COS

treatment on *B. cereus* spores did not affect the AFM force profile of the spore and stiffness seemed to remain unchanged[39]. The penetration of chrysophsin-3 into vegetative *B. anthracis* may cause the loss of water content from the cell, which would result in an increase of the stiffness or spring constant of the cell.

5.4.3 Young's Modulus of *B. anthracis* 34F2 Spores and Germinated Cells after Exposure to Chrysophsin-3

After applying the Hertz model, we found that chrysophsin-3 did not have an effect on the Young's moduli of the spore surfaces in their dormant form or after germination had been initiated with L-alanine and inosine (Figure 25). The values of the elastic moduli of spores exposed to chrysophsin-3 were similar to those reported by us in a previous study where no AMPs were used[26]. The highest Young's modulus was obtained with the dormant spores treated with 0.22 mM chrysophsin-3 (233 ± 158 MPa; Figure 25).

The Young's modulus decreased significantly after exposure to germinants along with exposure to the peptide. L-alanine or inosine-treated *B. anthracis* 34F2 exposed to chrysophsin-3 had an elasticity of 53 ± 22 MPa and 70 ± 52 MPa; respectively. Treating *B. anthracis* 34F2 with both germinants together with the additional exposure to chrysophsin-3 resulted in a similar elastic modulus (45 ± 26 MPa). Comparison of chrysophsin-3-treated spores with untreated spores from our previous study[26] revealed that the Young's moduli were not statistically different from one other, regardless of whether AMP treatment was applied (Figure 25). Chrysophsin-3 does not affect the Young's moduli of the spores, and the decrease in Young's moduli observed in our previous study occur as a result of the degradation of spore coats that takes place during germination.

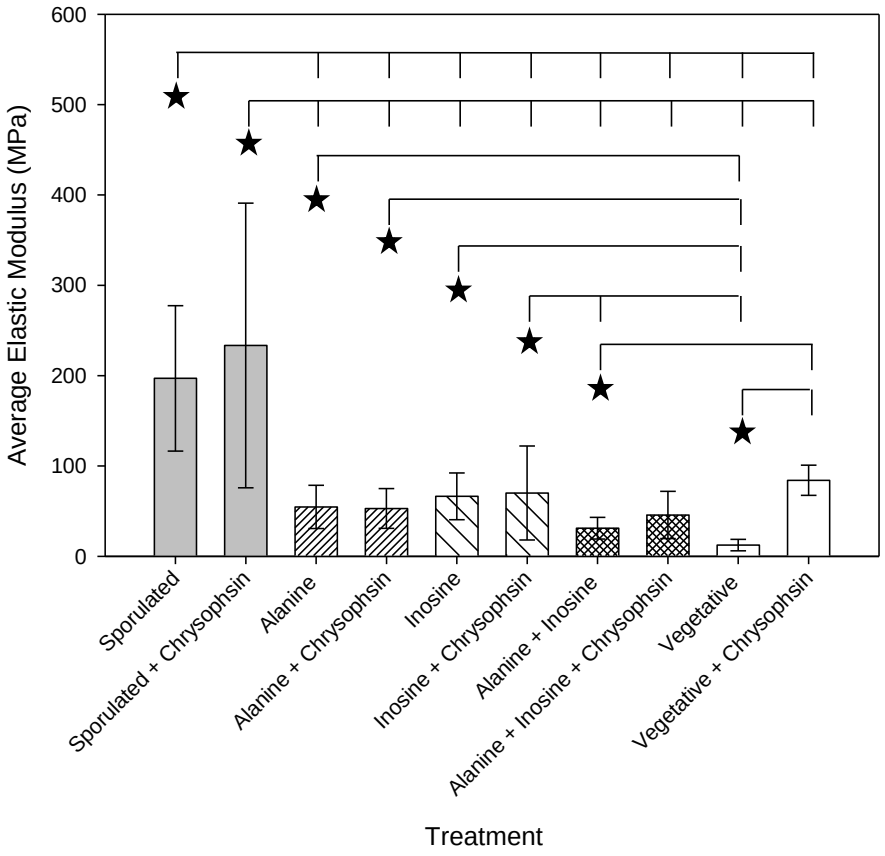

Figure 25. Average elastic modulus of *B. anthracis* spores as a function of treatment. Spores were first treated with 50 mM L-alanine and/or 5 mM inosine for 2 hours at 37 ºC. After treatment with germinants, 0.22 mM of chrysophsin-3 was introduced and spores were exposed to the AMP for an additional hour at 37 ºC. Bars depict the average value of 50 spores per condition and standard deviation. The top line and star connect statistically distinct points (P<0.05) calculated by Kruskal-Wallis one way ANOVA on ranks with Tukey's test to make pairwise comparisons. The star symbol indicates the condition that is being compared to other treatments.

The mechanisms of action of chrysophsin-3 against *B. anthracis* spores are not well understood. Based on our research, it is plausible that the Young's modulus of the spore is changing but at levels that are not detectable through AFM. Studies done in our laboratory have suggested that at low concentrations, chrysophsin-3 prefers insertion into a membrane over adsorption onto the surface[40]. In their study, insertion of the peptide into the membrane resulted in formation of pores and loss of mass from a lipid bilayer membrane[40]. Pore formation and mass

loss from the membrane results in the destabilization of the bacterial surface. AMPs such as magainin, alamethicin, and retrocyclins form pores in lipid membranes that have a diameter of <10 nm[20, 35]. Retrocyclin is a synthetic defensin peptide with a molecular mass of ~25 kDa that has been shown effective in the killing of vegetative *B. anthracis*[35]. Defensins, such as retrocyclins, form pores (water or ion permeable structures in the membrane) with diameters estimated at 25 Å[41]. Since the molecular mass of retrocyclins is ~12 times higher than that of chrysophsin-3 (~2.2 kDa), the pores formed by chrysophsin-3 may be of a much smaller diameter. The small diameter pores that may be formed by the peptide may be impossible to be detected by the AFM tip during the elasticity measurement, since the radius of curvature of the AFM tip used was > 10 nm (~8 times larger than the diameter of retrocyclin-formed pores). There have been a number of AFM studies that have reported the formation of pores by AMPs[42, 43]; however, these studies have only investigated the effects of AMPs on supported lipid bilayers instead of whole bacterial cells, or the diameter of the pores were > 10 nm, which would be larger than any pores formed by a small peptide, such as chrysophsin-3. Therefore, our results suggest that the Young's modulus of the *B. anthracis* spore would be similar for chrysophsin-3-treated and untreated spores, since the AFM tip would be too large to detect small pores formed by the AMP.

5.4.4 Elastic Modulus of Vegetative *B. anthracis* 34F2 after Exposure to Chrysophsin-3

The elastic modulus of vegetative *B. anthracis* exposed to chrysophsin-3 was also investigated (Figure 25). Untreated vegetative *B. anthracis* 34F2 had the lowest Young's modulus (12 ± 6 MPa), but increased significantly after exposure to 0.22 mM chrysophsin-3 (84 ±17 MPa; $P<0.001$). A significant difference in the indentation depth was also observed for

vegetative *B. anthracis* 34F2 since the value decreased from 246 ± 83 nm to 108 ± 14 nm after exposure to the AMP when the tip was traveling at a loading rate of 3 x 10^{-5} N/s (Figure 26; P<0.001). No other significant changes in indentation depths were observed between the germinant-treated spores and the chrysophsin-3-treated spores.

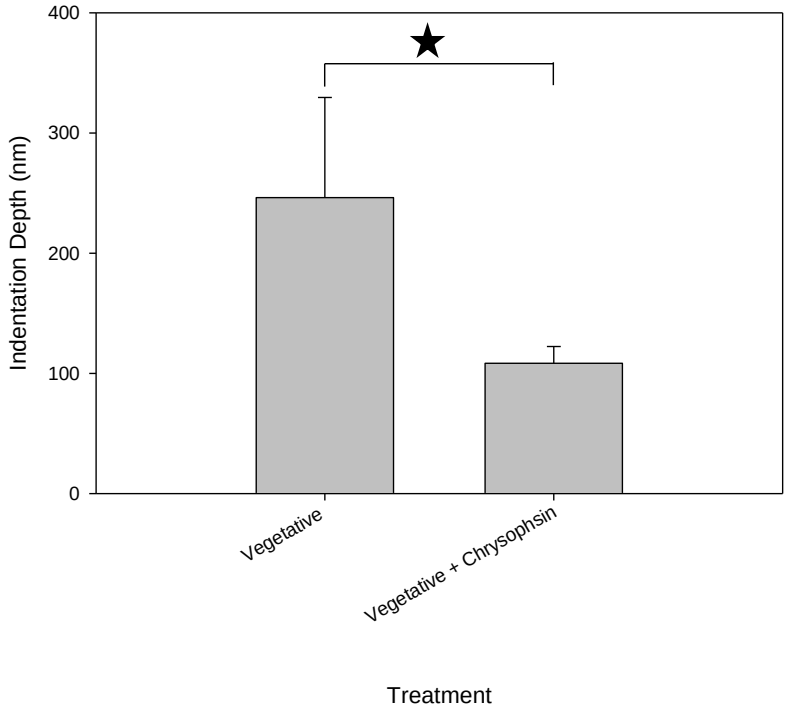

Figure 26: Average indentation depth of vegetative *B. anthracis* 34F2 after chrysophsin-3 treatment. Bars depict the average value of 50 spores per condition and standard deviation. The top line and star connect statistically distinct points (P<0.05)

The 0.22 mM concentration of chrysophsin-3 may have been high enough to cause changes in the Young's modulus of vegetative *B. anthracis* but too low to cause any changes in sporulated and germinated cells. The cell surface of vegetative *B. anthracis* is weaker and more susceptible to common disinfectants, since the 100 nm coat of proteins that protects the genetic material in spores is no longer present once the spore has germinated and outgrown into a fully virulent bacterium[5]. The cell membrane of *B. anthracis* 34F2 in their vegetative state is only composed of a thick peptidoglycan layer (murein sacculus) that protects the cells from

destructive osmotic changes[35]. This peptidoglycan layer contains multiple pores of 41Å in diameter that are capable of allowing passage to small molecules, such as retrocyclins[35]. Therefore, it is unlikely for vegetative *B. anthracis* to impede the passage of an even smaller molecule, such as chrysophsin-3, into the membrane. The passage of chrysophsin-3 into the membrane of vegetative *B. anthracis* may result in destabilization of the membrane due to the formation of multiple pores that will cause the loss of cellular content from *B. anthracis.* Lysis of vegetative bacteria and loss of water content would result in dehydration and hardening of the cell.

5.4.5 Morphological Changes of *B. anthracis* 34F2 after Chrysophsin-3 Treatment

Since the AMP only caused significant changes in the Young's modulus and spring constants of vegetative *B. anthracis,* the morphology of *B. anthracis* 34F2 cells was characterized using AFM (Figure 27). Untreated vegetative *B. anthracis* 34F2 had an elongated shape typical of vegetative bacteria and were found in chains of three or four cells. Vegetative *B. anthracis* cells varied in size and bacteria as long as 7 μm were observed (Figure 27A). Treatment of vegetative *B. anthracis* 34F2 with chrysophsin-3 resulted in lysis of the bacteria (Figure 27B). After an hour of treatment with the AMP, bacteria appeared to have lost cellular material and possibly water content, mostly around the edges, and were found with an irregular cell surface. Lysis of *B. anthracis* was observed and was characterized by what seemed like intracellular material being lost from the cells and cell debris that spread out around the edges of the cells and over the mica surface, as it has been previously observed in other AFM studies on *E. coli* lysis with sodium deoxycholate[44].

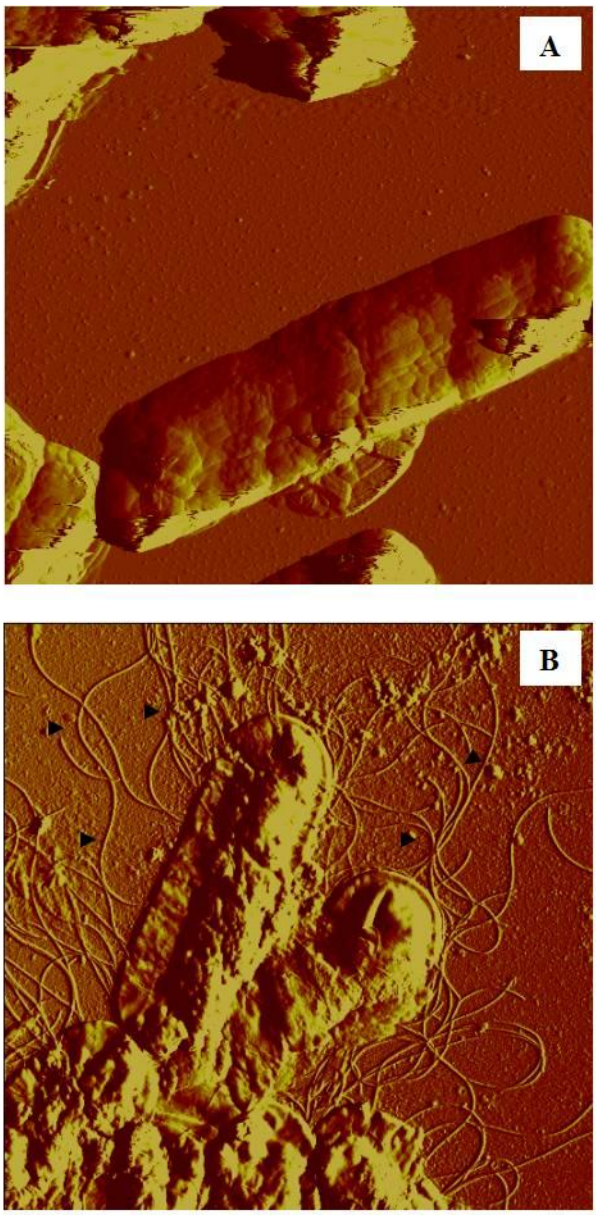

Figure 27. AFM amplitude images of *B. anthracis* Sterne before (A) and after (B) exposure to 0.22 mM chrysophsin-3 for 1 hour at 37 ºC. Imaging was done in tapping mode in air. Scan size: 10 µm x 10 µm.

While it is not completely clear how the AMP penetrates the spore coats, our results show that chrysophsin-3 may be a suitable candidate for the eradication of threatening spores, since germination, complete removal of spore coats, and expression of toxins are not required to allow passage of the peptide into the spore. The layers of proteins surrounding the spore coat of

Bacillus sp. (exosporium, spore coat, and the cortex) are composed of lipoproteins, hydrophobic ceratin, and peptidoglycan[34]. Huang et al. proposed that amphiphilic AMPs can bind with lipoprotein allowing a gradual internalization of the peptide into the spore[34]. Perhaps a similar mechanism of action takes place with chrysophsin-3.

5.5 Conclusions

Chrysophsin-3 may be a suitable candidate for the eradication of sporulated, germinated, and vegetative *B. anthracis* spores. The net positive charge of the peptide, along with its amphipathic properties, allows chrysophsin-3 to interact more strongly with microbial surfaces. While the mechanism of action of chrysophsin-3 against spores is not well understood, our study shows that the peptide is capable of penetrating the spore coat and killing *B. anthracis*. This killing may be due to the possible interaction of chrysophsin-3 with the lipoprotein found on spore coats, resulting in formation of pores with subsequent passage of the peptide. The interaction of chrysophsin-3 with spore coat proteins may cause a destabilization of the membrane, causing lysis of the cell due to loss of water content and other genetic material. This is the first study to conclusively demonstrate that AMPs have efficacy against *B. anthracis* in various states: sporulated, germinated and vegetative bacteria.

5.6 Acknowledgments

We would like to thank Prof. Nancy Burnham and Ms. Stephanie Marcott for helpful discussions regarding this project.

This work was supported in part by the National Science Foundation (CBET 0827229 and CBET 0922901) and the Defense Threat Reduction Agency (DTRA) Project BA07PRO102.

REFERENCES

1. Koch, R., The etiology of anthrax, based on the life history of *Bacillus anthracis*. *Beitr. Biol. Pflanz* **1876,** 2, 277-310.

2. Christopher, G. W.; Cieslak, T. J.; Pavlin, J. A.; Eitzen, E. M., Jr., Biological warfare. A historical perspective. *Jama* **1997,** 278, (5), 412-7.

3. Baweja, R. B.; Zaman, M. S.; Mattoo, A. R.; Sharma, K.; Tripathi, V.; Aggarwal, A.; Dubey, G. P.; Kurupati, R. K.; Ganguli, M.; Chaudhury, N. K.; Sen, S.; Das, T. K.; Gade, W. N.; Singh, Y., Properties of *Bacillus anthracis* spores prepared under various environmental conditions. *Arch Microbiol* **2008,** 189, (1), 71-9.

4. Ghosh, S.; Setlow, P., Isolation and characterization of superdormant spores of *Bacillus* species. *J Bacteriol* **2009,** 191, (6), 1787-97.

5. Henriques, A. O.; Moran, C. P., Jr., Structure and assembly of the bacterial endospore coat. *Methods* **2000,** 20, (1), 95-110.

6. Nagarajan, R.; Muller, W. S.; Ashley, R.; Mello, C. M. In *Decontamination Of Bacterial Spores by a Peptide-Mimic*, 25th Army Science Conference, Orlando, FL, December, 2006, 2006; Orlando, FL, 2006.

7. Atrih, A.; Foster, S. J., Bacterial endospores the ultimate survivors. *Int. Dairy J.* **2002,** 12, (2-3), 217-223.

8. Zaman, M. S.; Goyal, A.; Dubey, G. P.; Gupta, P. K.; Chandra, H.; Das, T. K.; Ganguli, M.; Singh, Y., Imaging and analysis of *Bacillus anthracis* spore germination. *Microsc Res Tech* **2005,** 66, (6), 307-11.

9. Carr, K. A.; Lybarger, S. R.; Anderson, E. C.; Janes, B. K.; Hanna, P. C., The role of *Bacillus anthracis* germinant receptors in germination and virulence. *Mol Microbiol* **2010,** 75, (2), 365-75.

10. Setlow, P., Spore germination. *Curr Opin Microbiol* **2003,** 6, (6), 550-6.

11. Jedrzejas, M. J.; Setlow, P., Comparison of the binuclear metalloenzymes diphosphoglycerate-independent phosphoglycerate mutase and alkaline phosphatase: their mechanism of catalysis via a phosphoserine intermediate. *Chem Rev* **2001,** 101, (3), 607-18.

12. Slieman, T. A.; Nicholson, W. L., Role of dipicolinic acid in survival of *Bacillus subtilis* spores exposed to artificial and solar UV radiation. *Appl Environ Microbiol* **2001,** 67, (3), 1274-9.

13. Indest, K. J.; Buchholz, W. G.; Faeder, J. R.; Setlow, P., Workshop report: modeling the molecular mechanism of bacterial spore germination and elucidating reasons for germination heterogeneity. *J Food Sci* **2009,** 74, (6), R73-8.

14. Bell, D. M.; Kozarsky, P. E.; Stephens, D. S., Clinical issues in the prophylaxis, diagnosis, and treatment of anthrax. *Emerg Infect Dis* **2002,** 8, (2), 222-5.

15. Dixon, T. C.; Meselson, M.; Guillemin, J.; Hanna, P. C., Anthrax. *N Engl J Med* **1999,** 341, (11), 815-26.

16. Goldenberg, A.; Shmueli, G.; Caruana, R. A.; Fienberg, S. E., Early statistical detection of anthrax outbreaks by tracking over-the-counter medication sales. *Proc Natl Acad Sci U S A* **2002,** 99, (8), 5237-40.

17. Pile, J. C.; Malone, J. D.; Eitzen, E. M.; Friedlander, A. M., Anthrax as a potential biological warfare agent. *Arch Intern Med* **1998,** 158, (5), 429-34.

18. Oncu, S.; Oncu, S.; Sakarya, S., Anthrax--an overview. *Med Sci Monit* **2003,** 9, (11), RA276-83.

19. Chen, Y.; Tenover, F. C.; Koehler, T. M., Beta-lactamase gene expression in a penicillin-resistant *Bacillus anthracis* strain. *Antimicrob Agents Chemother* **2004,** 48, (12), 4873-7.

20. Brogden, K. A.; Ackermann, M.; McCray, P. B., Jr.; Tack, B. F., Antimicrobial peptides in animals and their role in host defences. *Int J Antimicrob Agents* **2003,** 22, (5), 465-78.

21. Rajanbabu, V.; Chen, J. Y., Applications of antimicrobial peptides from fish and perspectives for the future. *Peptides* **2011,** 32, (2), 415-20.

22. Iijima, N.; Tanimoto, N.; Emoto, Y.; Morita, Y.; Uematsu, K.; Murakami, T.; Nakai, T., Purification and characterization of three isoforms of chrysophsin, a novel antimicrobial peptide in the gills of the red sea bream, *Chrysophrys major*. *Eur J Biochem* **2003,** 270, (4), 675-86.

23. Mason, A. J.; Bertani, P.; Moulay, G.; Marquette, A.; Perrone, B.; Drake, A. F.; Kichler, A.; Bechinger, B., Membrane interaction of chrysophsin-1, a histidine-rich antimicrobial peptide from red sea bream. *Biochemistry* **2007,** 46, (51), 15175-87.

24. Dûfrene, Y. F., Atomic force microscopy, a powerful tool in microbiology. *J Bacteriol* **2002,** 184, (19), 5205-13.

25. Dûfrene, Y. F., Nanoscale exploration of microbial surfaces using the atomic force microscope. *Future Microbiol* **2006,** 1, 387-96.

26. Pinzón-Arango, P. A.; Nagarajan, R.; Camesano, T. A., Effects of L-alanine and inosine germinants on the elasticity of *Bacillus anthracis* spores. *Langmuir* **2010,** 26, (9), 6535-41.

27. Pinzón-Arango, P. A.; Scholl, G.; Nagarajan, R.; Mello, C. M.; Camesano, T. A., Atomic force microscopy study of germination and killing of *Bacillus atrophaeus* spores. *J Mol Recognit* **2009,** 22, (5), 373-379.

28. Plomp, M.; Leighton, T. J.; Wheeler, K. E.; Hill, H. D.; Malkin, A. J., In vitro high-resolution structural dynamics of single germinating bacterial spores. *Proc Natl Acad Sci U S A* **2007,** 104, (23), 9644-9.

29. Plomp, M.; Leighton, T. J.; Wheeler, K. E.; Malkin, A. J., The high-resolution architecture and structural dynamics of *Bacillus* spores. *Biophys J* **2005a,** 88, (1), 603-8.

30. Arnoldi, M.; Fritz, M.; Bauerlein, E.; Radmacher, M.; Sackmann, E.; Boulbitch, A., Bacterial turgor pressure can be measured by atomic force microscopy. *Phys Rev E Stat Phys Plasmas Fluids Relat Interdiscip Topics* **2000,** 62, (1 Pt B), 1034-44.

31. Touhami, A.; Nysten, B.; Dûfrene, Y. F., Nanoscale mapping of the elasticity of microbial cells by atomic force microscopy. *Langmuir* **2003,** 19, (11), 4539-4543.

32. Gut, I. M.; Prouty, A. M.; Ballard, J. D.; van der Donk, W. A.; Blanke, S. R., Inhibition of *Bacillus anthracis* spore outgrowth by nisin. *Antimicrob Agents Chemother* **2008,** 52, (12), 4281-8.

33. Liu, W.; Hansen, J. N., The antimicrobial effect of a structural variant of subtilin against outgrowing *Bacillus cereus* T spores and vegetative cells occurs by different mechanisms. *Appl Environ Microbiol* **1993,** 59, (2), 648-51.

34. Huang, X.; Lu, Z.; Bie, X.; Lu, F.; Zhao, H.; Yang, S., Optimization of inactivation of endospores of *Bacillus cereus* by antimicrobial lipopeptides from *Bacillus subtilis* fmbj strains using a response surface method. *Appl Microbiol Biotechnol* **2007,** 74, (2), 454-61.

35. Wang, W.; Mulakala, C.; Ward, S. C.; Jung, G.; Luong, H.; Pham, D.; Waring, A. J.; Kaznessis, Y.; Lu, W.; Bradley, K. A.; Lehrer, R. I., Retrocyclins kill bacilli and germinating spores of *Bacillus anthracis* and inactivate anthrax lethal toxin. *J Biol Chem* **2006,** 281, (43), 32755-64.

36. Tsukiyama, R.; Katsura, H.; Tokuriki, N.; Kobayashi, M., Antibacterial activity of licochalcone A against spore-forming bacteria. *Antimicrob Agents Chemother* **2002,** 46, (5), 1226-30.

37. Abu-Lail, N. I.; Camesano, T. A., The effect of solvent polarity on the molecular surface properties and adhesion of *Escherichia coli*. *Colloids Surf B Biointerfaces* **2006,** 51, (1), 62-70.

38. Volle, C. B.; Ferguson, M. A.; Aidala, K. E.; Spain, E. M.; Nunez, M. E., Spring constants and adhesive properties of native bacterial biofilm cells measured by atomic force microscopy. *Colloids Surf B Biointerfaces* **2008,** 67, (1), 32-40.

39. Fernandes, J. C.; Eaton, P.; Gomes, A. M.; Pintado, M. E.; Xavier Malcata, F., Study of the antibacterial effects of chitosans on *Bacillus cereus* (and its spores) by atomic force microscopy imaging and nanoindentation. *Ultramicroscopy* **2009,** 109, (8), 854-60.

40. Wang, K.; Nagarajan, R.; Mello, C. M.; Camesano, T. A., Characterization of Supported Lipid Bilayer Disruption by Chrysophsin-3 using QCM-D. *J Phys Chem B* **In press**.

41. Ganz, T., Defensins: antimicrobial peptides of innate immunity. *Nat Rev Immunol* **2003,** 3, (9), 710-20.

42. Lam, K. L.; Ishitsuka, Y.; Cheng, Y.; Chien, K.; Waring, A. J.; Lehrer, R. I.; Lee, K. Y., Mechanism of supported membrane disruption by antimicrobial peptide protegrin-1. *J Phys Chem B* **2006,** 110, (42), 21282-6.

43. Meincken, M.; Holroyd, D. L.; Rautenbach, M., Atomic force microscopy study of the effect of antimicrobial peptides on the cell envelope of *Escherichia coli*. *Antimicrob Agents Chemother* **2005,** 49, (10), 4085-92.

44. Yoshimura, S. H.; Kim, J.; Takeyasu, K., On-substrate lysis treatment combined with scanning probe microscopy revealed chromosome structures in eukaryotes and prokaryotes. *J Electron Microsc (Tokyo)* **2003,** 52, (4), 415-23.

Chapter 6

Role of Ger operons in germination of *Bacillus anthracis* spores

6.1 Abstract

Germination of *Bacillus anthracis* is stimulated when receptors located in the inner membrane of spores are activated by amino acids and purine ribonucleoside germinants. The GerH and GerS germinant receptors play a role in germination inside macrophages, but their roles on germination of *B. anthracis* spores are not well understood. We investigated the role of the GerH and GerS receptor on germination of *B. anthracis* spores after exposure to 50 mM L-alanine and 5 mM inosine. The parental *B. anthracis* Sterne 34F2, which expresses all five receptors, mutant strains $gerH^+$ and $gerS^+$, which express only the GerH and GerS receptor, respectively, and the mutant ger_{null}, which lacks all five receptors, were incubated in the germinants for up to one hour at 37 ºC. Germination of spores was studied by the loss of optical density of spores in solution at 600 nm and changes in spore refractility through phase microscopy. The presence of the GerH receptor in *B. anthracis* was sufficient to elicit germination responses similar to the parental *B. anthracis* 34F2 strain. However, the $gerS^+$ strain failed to have a full germination response in L-alanine and inosine solutions. A weak but detectable germination response of the ger_{null} strain was observed suggesting that other mechanisms of germination may exist in *B. anthracis* spores. The results of this study provide information on the roles of individual receptors of *B. anthracis* spores, which may be used to develop anti-sporal compounds that target individual receptors that prevent germination of spores and development of anthrax infections.

6.2 Introduction

Bacillus anthracis is a Gram-positive bacterium that is capable of undergoing sporulation under conditions of nutrient deprivation[1]. During sporulation, the bacterium synthesizes polymer layers and protein coats that surround the spore's genetic material and inhibit the passage of

decontaminating agents into the spore core[2, 3]. *B. anthracis* spores do not divide, have no measurable metabolism, and are resistant to chemical and environmental factors including heat, radiation, desiccation, and common disenfectants[1]. Once the spores come into contact with nutrients, such as those found in a mammalian host, they can germinate and outgrow into the vegetative (virulent) state[4]. The rapid conversion from a spore into vegetative bacteria, allow the cells to multiply, release toxins into the host, and spread rapidly, resulting in an anthrax infection[1]. Due to its ability to remain viable in a sporulated state for years, along with its ability to regain metabolic activity in a very short time, *B. anthracis* spores have become a concern during bioterrorism attacks.

The current theory of spore inactivation assumes that germination must occur before spores can be killed by anti-sporal agents[3]. Germination of *B. anthracis* spores is triggered by nutrients such as amino acids and purine nucleosides that interact with germinant receptors located in the inner membrane of the spore[5]. During germination, the spore releases monovalent cations, Ca^{2+}, and dipicolinic adic (DPA), while water molecules enter and start hydrating the cell[6]. Water uptake causes swelling of the spore core and the activation of cortex lytic enzymes that hydrolyze the peptidoglycan cortex. Resumption of metabolism follows in the outgrowth phase and macromolecular synthesis converts the spore into a virulent vegetative bacterium[3].

The amino acid L-alanine triggers germination of several *Bacillus* species including *B. subtilis, B. cereus, B. anthracis,* and *B. atrophaeus*[7-9]. To trigger germination of *B. anthracis,* studies have observed that L-alanine-induced germination can only occur if the amino acid is present at very high concentrations (100 mM)[5]. Though physiological levels of L-alanine are subgerminant for *B. anthracis,* L-alanine can serve as a primary germinant with a separate amino acid or purine ribonucleoside functioning as cogerminant[5]. Inosine is a purine ribonucleoside that

is a potent germinant at low concentrations[10]. Inosine paired with a variety of L-isomer amino acids, such as L-alanine, induce a greater germination response in *B. anthracis* spores[5, 7].

Research has suggested that germination of spores is dependent upon the binding of germinants to germinant receptors located in the inner membrane of spores[11]. Activation of these receptors results in the initiation of complex processes where intracellular protease and extracellular hydrolases are activated to facilitate the conversion from spore to the vegetative form[12]. Five germinant receptors in *B. anthracis* have been found to play a role in triggering germination of spores. These receptors are encoded by the tricistronic operons *gerH, gerK, gerL, gerS* and *gerX*[11]. Only a few studies have investigated the role of germinant receptors on spore germination[5, 11, 13]. The gerS and gerH receptors have been shown to be necessary for spores to germinate in murine macrophages[11, 13]. *In vitro* studies showed that *B. anthracis* strains expressing only the *gerS* operon were capable of only germinating ~50% of the spores with L-alanine[11]. These results suggest that gerS and gerH may not be the only receptors necessary to initiate germination and other receptors may work in concert to achieve germination of spores.

As the infective particle for the initiation of an anthrax infection is the spore, it is important to identify the roles of germinant receptors that trigger the breakdown of spore dormancy. In the present study, we investigated the role of the gerH and gerS receptor on germination of *B. anthracis* Sterne by measuring the loss of optical density during the initiation of germination. In addition, we tested the role of these germinant receptors on spore susceptibility to surfactants, such as dodecylamine, which has been shown to have anti-sporal activities[14]. Our results were compared with germination measurements taken on a *B. anthracis* mutant that lacked all five germinant receptors. Our results suggest that multiple signals may be required to break dormancy in *B. anthracis.*

6.3 Materials and Methods

6.3.1 Bacterial Strains and Spore Preparation

Bacillus anthracis Sterne spores used in this study are listed in Table 4. The parental *B. anthracis* Sterne 34F2 strain was kindly provided by the Edgewood Chemical Biological Center, Edgewood, Maryland. The Sterne strain is a low virulence strain that lacks the extra chromosomal plasmid pXO2, responsible for the development of the bacterial capsule. However, it contains the pXO1 extra chromosomal plasmid, which is responsible for the expression of virulence factors[15]. The *B. anthracis* mutants $gerS^+$, $gerH^+$, and ger_{null} were kindly provided by Dr. Philip C. Hanna (University of Michigan Medical School, Ann Arbor, MI). The *B. anthracis* mutants were characterized by having one of the five triscistronic operons found in *B. anthracis* Sterne (*gerS, gerH, gerK, gerL,* and *gerX*). These mutants were created by performing allelic exchange sequentially, knocking out the appropriate *ger* allele[11]. For example, the $gerS^+$ strain retained the complete *gerS* operon but contained the deleted forms of the other four operons. The ger_{null} strain was constructed by knocking out all 5 *ger* alleles, resulting in a strain lacking all five germinant receptors encoded by the *ger* gene.

Strains were grown on plates of sporulation media as described previously[16]. Sporulation media consisting of 8 g nutrient broth, 4 g yeast extract, 0.001 g $MnCl_24H_2O$, 5 g of peptone and 15 g of agar in 1 L of ultrapure water (Milli-Q water, Millipore Corp. Bedford, MA) was maintained at a pH of 7.2 and sterilized. *B. anthracis* plated on sporulation media were incubated at 37 ºC for 4-5 days. Spores were collected by centrifugation at 5000 rpm for 20 minutes at 4 ºC and resuspended in ultrapure water. The cells were washed eight times to separate spores from partially sporulated cells. The washed spores were kept overnight at 4 ºC and washed again until

99% of sporulated cells (phase-bright spores) were observed through phase contrast microscopy (Nikon Eclipse E400, Tokyo, Japan).

Table 4. *Bacillus anthracis* strains used in this study

Strain	Mutant Name	Characteristics[a]	Reference
$34F_2$	-	Wild-type ($pXO1^+$, $PXO2^-$)	Pinzón-Arango et al. 2010
SL115	$gerH^+$	$34F_2$, Δ*gerK* Δ*gerL* Δ*gerS* Δ*gerX*	Carr et al. 2010
SL118	$gerS^+$	$34F_2$, Δ*gerH* Δ*gerK* Δ*gerL* Δ*gerX*	Carr et al. 2010
SL120	ger_{null}	$34F_2$, Δ*gerH* Δ*gerK* Δ*gerL* Δ*gerX* Δ*gerS*	Carr et al. 2010

[a] Mutant construction was achieved through markerless deletions of nearly the entire tricistronic germinant receptor operon (Carr et al., 2010)

6.3.2 Spore Germination Rates and Optical Density Measurements

Spore germination was monitored spectrophotometrically where the loss of light diffraction followed by the addition of germinants was reflected by a decrease in optical density (OD) at 600 nm. To trigger germination, spores were heat activated for 30 min at 65 ºC before resuspension in a germinating buffer consisting of 50 mM L-alanine and 5 mM inosine in 50 mM tris/HCl buffer (pH 8.0). To test for spontaneous germination of spores, *B. anthracis* strains were also exposed to 50 mM tris/HCl without germinants. Spore solutions were mixed at 18 rpm at 37 ºC and the optical density was monitored for 4 hrs. Spore germination was evaluated based on the decrease in OD_{600} at 37 ºC. The germination extent at each time point was expressed as a fraction of the actual OD divided by the OD at the beginning of germination (time 0 min). Relative OD values were plotted against time and germination rates were calculated as the slope of the linear portion following the lag phase of relative OD values over time. Every experiment was carried out in triplicates.

6.3.3 Phase Contrast Microscopy of Spore Suspensions

Germination of spores is associated with a loss of phase brightness or refractility caused by hydration of all internal structural compartments, resulting in a phase dark spore when observed under phase contrast microscopy[17]. Changes in phase or loss of light refraction of spores were evaluated by resuspending *B. anthracis* spores at a concentration of 10^9 spores/mL in a 50 mM L-alanine and 5 mM inosine solution in 50 mM tris/HCl. The solution was vortexed for 15 seconds to mix the germinants and spores and 5 µL of spore solution was transferred onto a glass microscope slide. The drop was covered with a 22 x 22 mm^2 coverslip and sealed with nail polish to avoid dehydration. The slides were imaged under phase-contrast microcopy (Nikon Eclipse E400, Tokyo, Japan). Groups of single spores that were attached to the underside of the cover slip were chosen for analysis. All spores were in a well defined local plane and immobilized. Images were taken every 10 minutes for one hour (SPOT 4.6 Advanced Software, Diganostic Instruments, MI). The camera was operated with manual gain and an exposure time of one second. Images were obtained at a magnification of 1000x under oil immersion. The percentages of dark-phase and bright-phase spores were determined for every strain at various time points.

6.3.4 Susceptibility of *B. anthracis* Spores to Dodecylamine

A solution of *B. anthracis* spores at 10^8 spores/mL was centrifuged and resuspended in 1 mM dodecylamine (DDA; Sigma-Aldrich, St. Louis, MO). Spores were incubated at 37 ºC for 60 minutes at 18 rpm. After treatment, the spores were washed by centrifugation for 10 minutes at 1000 rpm and resuspended in 50 mM tris/HCl. Spore solution was serially diluted and a 100 µL of solution was inoculated onto tryptic soy agar plates and incubated at 37˚C for 24 hrs. The

number of surviving *B. anthracis* or colony forming units (CFU) on the agar plates was determined. Untreated spores served as control.

6.3.5 Verification of *B. anthracis* Retention of Mutation after Germination Assays

The retention of mutation following germination assays was verified for *B. anthracis* ger_{null} through a protein chain reaction (PCR) method to ensure that the deletions of the Ger operons were permanent and no mutation had occurred during experiments. Diagnostic primers to test knockout genes in *B. anthracis* mutants were obtained from Eurofins mwg/operon (Huntsville, AL). The primers were 25 amino acids long (Table 5) and were reconstituted according to the manufacturer's specifications using ultrapure water.

Table 5. Sequence of diagnostic primers to test knockouts

	Knockout Primers	
Operon	**Sequence Primer 5'**	**Sequence Primer 3'**
gerH	GCATACGAGCTACATCAAGAAATGT	GAGTATTTGTCACAGGATGTCCGAA
gerK	TAAATATATATGATATAAAGCTGGA	GGCGATACAGAATGAATAGATTGAT
gerL	TCGGATCGACAAGTGGCAAAAGTAG	CGGCTTTATTCTAGCTGCGTTCATT
gerS	TGCTTCTTTCGCACGAGTAGAATTA	TTAATGTATGACCGTGAAGCGAAAT
gerX	CTGGAATCAAACTTGCAAAACAAAA	CCTGAACATTCAATGATTGTGAAAA

To extract DNA from spores, a fresh plate of the *B. anthracis* ger_{null} strain was prepared and left to incubate overnight. A small portion of a small colony was picked up from the plate and placed in a PCR tube with 20 µL of ultrapure water. The tube was vortexed for 10 seconds at

~13,000 rpm and incubated at 99 ºC for 10 minutes. After incubation, the lysed spores were kept on ice and 0.5 µL of solution was used as a template for PCR reactions.

In order to extend primers and amplify genes, a master mixture was prepared in a PCR tube consisting or 10 µL of 10X standard buffer, 10 µL of 2.5 mM DNTPs (free floating nucleotides), 1.5 µL of enzyme, 75 µL of ultrapure water, and 2.5 µL of template or lysed spores. The mixed solution was split in 5 different tubes, corresponding to 5 operons, and 0.5 µL of the reverse and forward primer of each operon (Table 5) was added to each tube. The tubes were placed in the PCR instrument for amplification of genes (DNA Engine Dyad Peltier Thermal Cycler, Bio-Rad Laboratories, Inc, Hercules, CA) and an annealing temperature of 46 ºC was set with a total of 35 cycles. The reaction was left running for ~2.5 hours. After completion of the extension of primers the samples were run using a 1% agarose gel.

6.4 Results

6.4.1 Germination Rates and Phase Contrast Microscopy of *B. anthracis*

B. anthracis 34F2 (spores containing all five germinant receptors) exhibited a strong germination response when exposed to a 50 mM L-alanine and 5 mM inosine mixture (Figure 28). Within 20 minutes of exposure to germinants, the optical density of the wild-type *B. anthracis* 34F2 strain decreased considerably by 30.5 ± 2.8% and the spores germinated at a rate of 1.135% OD loss/min. After an hour of exposure to the germinants, the optical density of *B. anthracis* 34F2 spores dropped ~40%. Surprisingly, the *gerH*$^{+}$ mutant exhibited a germination profile where there was a greater loss in optical density than the one observed with the wild-type strain. After 20 minutes of exposure to the alanine/inosine mixture, the average percent loss of optical density in the spore solution reached 40.2 ± 6.0%. Mutant spores of the *gerH*$^{+}$ genotype

germinated at a rate of 1.57% OD loss/min, which was significantly higher than the rate of germination of wild-type spores.

The *B. anthracis gerS*$^{+}$ strain exhibited some level of germination after exposure to L-alanine and inosine. After 20 minutes of exposure to germinants, the optical density of the *gerS*$^{+}$ strain decreased by 22.8 ± 2.9% and after an hour of exposure, the level of germination remained similar with only 27.1 ± 2.0% total loss in optical density. The *gerS*$^{+}$ strain germinated at a rate of 0.82% OD loss/min, which was significantly lower than the germination rate observed for the *B. anthracis* 34F2 strain ($P<0.05$). While the *B. anthracis* ger_{null} strain lacks all five germinant receptors, the mutant strain showed a level of germination that was similar to the *gerS*$^{+}$ strain (Figure 28). The mutant ger_{null} showed a decrease in optical density of 26.6 ± 1.9% in under 20 minutes of exposure to germinants. After an hour of being in the presence of L-alanine and inosine, the optical density of the spores had decreased by 36.9 ± 3.5% and the maximum germination rate that was observed was 0.88% OD loss/min.

Spores that were not exposed to germinants were phase bright and appeared to have a strong halo around the perimeter of the spore. After the addition on germinants, the process of germination took place almost instantly and delays in preparation of microscopy slides resulted in a few spores being phase dark at time 0 min (Figure 29). Addition of germinants resulted in the loss of refractility and phase brightness. After 60 minutes of exposure to L-alanine and inosine, more than half of the wild-type *B. anthracis* 34F2 spores had become phase dark. Phase dark germinating *B. anthracis* appeared to be swollen compared to the phase bright spores (Figure 29).

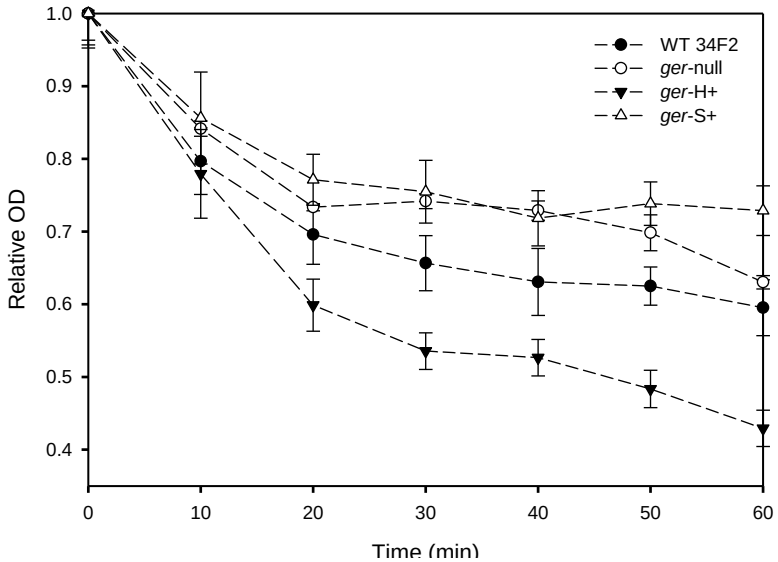

Figure 28. Germination kinetics for *B. anthracis* 34F2 and its mutants in 50 mM L-alanine and 5 mM inosine for 1 hour at 37 ºC. Relative OD measured at 600 nm. The mean of triplicate experiments with standard deviation is shown.

Similarly to the response in the germination kinetic studies, the *gerH*$^+$ strain mirrored the behavior of *B. anthracis* 34F2 in phase contrast microscopy experiments. The *gerH*$^+$ mutant had a comparable number of germinating spores (phase dark) after exposure to germinants when compared to the wild-type *B. anthracis* 34F2. After 60 minutes of exposure, ~56% of spores became phase dark, which was not significantly different from the number of phase dark *B. anthracis* 34F2 spores ($P > 0.05$). The *gerS*$^+$ and ger_{null} strains showed slower responses in phase dark conversion compared to the *B. anthracis* 34F2 and the *gerH*$^+$ strains. After an hour of exposure to L-alanine and inosine, only 30% of *gerS*$^+$ and 31% of ger_{null} spores became phase-dark.

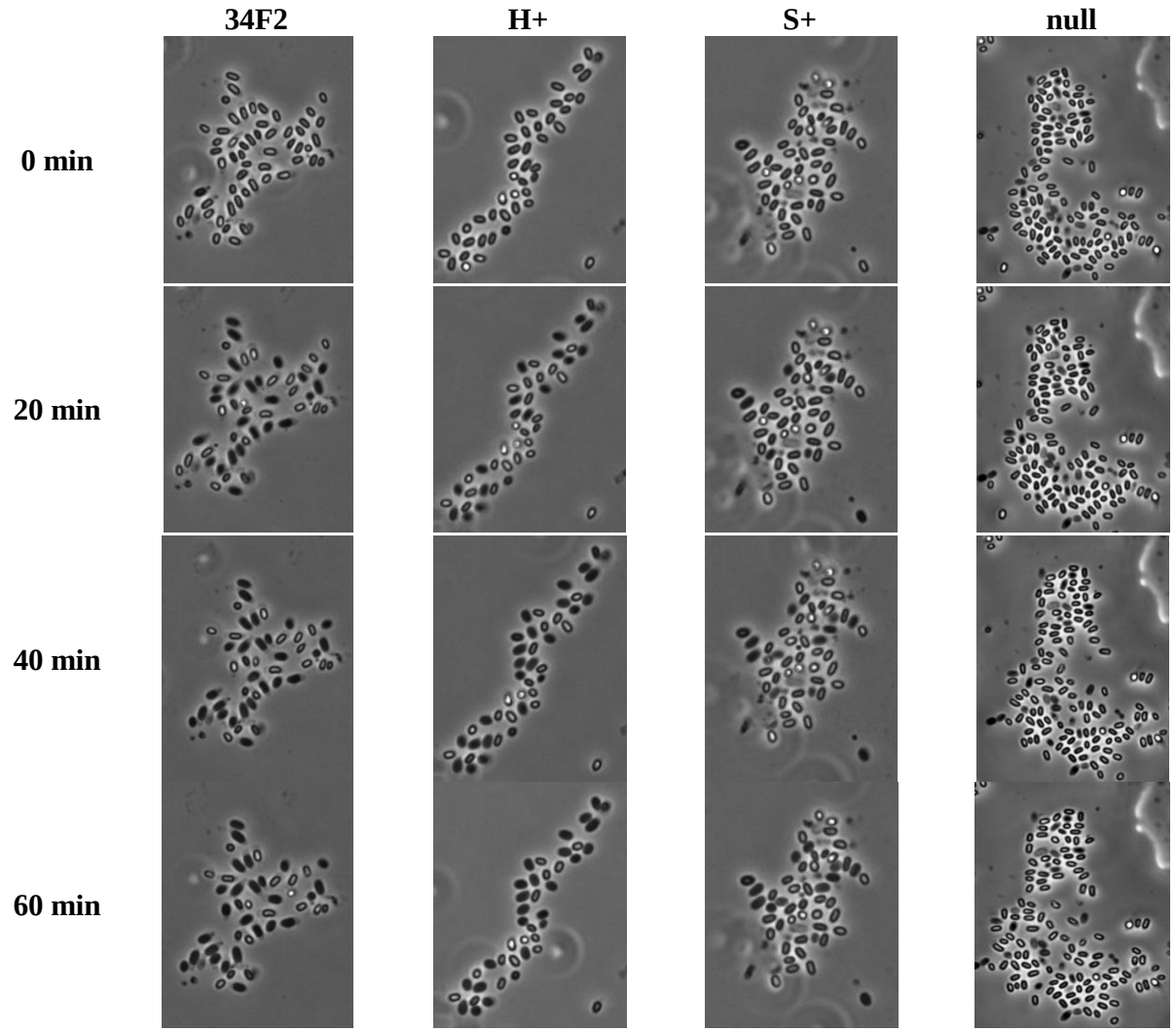

Figure 29. Time lapse phase contrast microscopy images of the response of *B. anthracis* Sterne 34F2 and its mutants to 50 mM L-alanine and 5 mM inosine. Magnification: 1000x.

6.4.2 Viability of *B. anthracis* after Exposure to Dodecylamine

Exposure of *B. anthracis* wild-type and mutant strains to 1 mM dodecylamine (DDA) resulted in a significant decrease in surviving spores (Table 6). While lower concentrations of DDA have been shown to induce germination of spores[14, 18], 1 mM DDA killed over 99% of spores, whether they had all or none of the germinant receptors.

Table 6. Number of *B. anthracis* spores surviving after treatment with 1 mM DDA (CFU/mL)

	***B. anthracis* 34F2**	***B. anthracis ger*H+**	***B. anthracis ger*S+**	***B. anthracis ger-null***
Untreated (CFU/mL)	1.26×10^7	8.15×10^6	2.02×10^7	9.75×10^6
Treated[b] (CFU/mL)	4.1×10^4	1.5×10^4	5×10^3	4.8×10^3
Percent Killed	99.67	99.8	99.9	99.9
Log-kill[a]	2.48	2.73	3.61	3.31

[a] Log-kill = Log(Number of original spores/Number of surviving spores)

[b] Spores treated with 1 mM DDA

A log-kill of 2.48 (a decrease of surviving spores by 2.48 log) was observed after treatment of the wild-type *B. anthracis* spores with 1 mM DDA. A similar response was observed with the $gerH^+$ strain since a 2.73 log-kill was achieved after exposure to the surfactant. A much more significant killing response was observed with the $gerS^+$ and the ger_{null} strains. Exposure of $gerS^+$ and ger_{null} mutants to 1 mM DDA resulted in a 3.61 and a 3.31 log-kill, respectively.

6.4.3 Retention of *B. anthracis* Genotype after Germination Experiments

After observing a significant germination response from the ger_{null} strain with exposure to L-alanine and inosine, the retention of the deletion of the Ger genes was verified through a PCR assay. A ~1.2 kb band was observed when checking for the presence of all five receptor operons, suggesting that the mutated *B. anthracis* strain retained the markerless deletion of nearly the entire five operons (Figure 30).

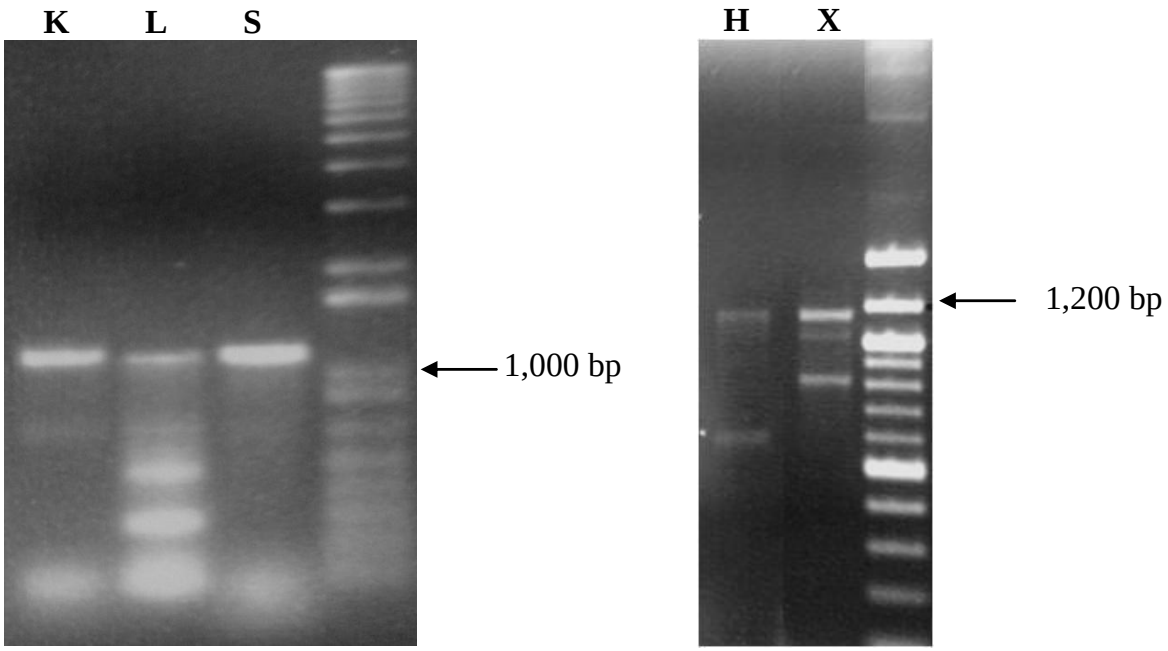

Figure 30. Verification of the ger_{null} genotype. PCR was performed using the primers listed on Table 2. Letters denote the germinant receptor being tested.

6.5 Discussion

6.5.1 Killing of *B. anthracis* Spores

While deactivation of spores is thought to be possible with initiation of germination, our previous study suggested that *B. anthracis* spores can be killed effectively if they are exposed to high concentrations of antimicrobial peptides[19]. Better killing activities were observed after germinated spores were exposed to the peptide; however, our research suggested that germination was not a necessary step to deactivate *B. anthracis* spores[19].

In this study we observed that all *B. anthracis* strains where susceptible to DDA since more than 99% of spores were killed in one hour. Previous research has observed spore killing with DDA[18]. *B. megaterium* spores exposed to 10^{-5} M DDA were killed after 3 minutes of incubation[20]. Over 99% of *B. atrophaeus* were killed in 5 minutes with 1 mM DDA[14]. In this study , we also observed that DDA killed *B. anthracis* mutants more effectively than the wild-

type *B. anthracis* 34F2. The *gerS*$^{+}$ strain was the most susceptible strain to the surfactant dodecylamine (Table 6). While no research has linked spore viability with germinant receptors, our study shows that spores that express only the GerS receptor are more susceptible to killing than spores expressing all five germinant receptors or than spores expressing the GerH receptor. Interactions between killing compounds and germinant receptors may take place. However, further research is needed to establish a role between spore viability and germinant receptors.

6.5.2 GerH Receptor on *B. anthracis*

Germination of *B. anthracis* spores requires that the germinants pass through the outer layers of the spore in order to interact with the receptor proteins of the GerA-like family in the inner membrane of *B. anthracis*. Differences found between the *B. anthracis* Sterne strain and the *gerH*$^{+}$ strain in germination assays establish the role of the GerH receptor in *B. anthracis* germination with commonly used germinants including L-alanine and inosine. Unlike other studies where the expression of the GerH receptor has been compromised, leaving the other four germinant receptors functional[21], the mutant strains used in this study contained only one receptor. Investigating the role of one germinant receptor at the time prevents us from misinterpreting germination data that may occur by two or more receptors acting in concert.

In previous studies, the *gerH*$^{+}$ strain exhibited wild-type colony forming efficiency and the germination profile mirrored the germination of wild-type spores when both strains were exposed to 0.5 mM L-alanine and 1 mM inosine[11]. In our experiments, we increased the concentration to 50 mM L-alanine and 5 mM inosine since studies have observed that maximum germination rates are reached at these concentrations[10]. The increase in germinant concentrations resulted in a germination response from the *gerH*$^{+}$ strain that initially mimicked the germination of *B. anthracis* 34F2. However, after 10 minutes of exposure to the germinants, the *gerH*$^{+}$ strain

germinated more rapidly than the parental Sterne 34F2 strain since there was a significantly higher percentage of OD loss within a specific incubation time (Figure 28). Carr et al. also reported a higher percentage of OD loss during germination of the *gerH*$^{+}$ strain compared to the parental strain expressing all receptors[11]. After 30 minutes of exposure to germinants, they observed that the germination or loss of OD of *gerH*$^{+}$ differed by 6% compared to the *B. anthracis* 34F2 strain. Our germination studies indicated that 30 minutes of incubation with a higher concentration of germinants resulted in a significant difference of 12% OD loss in the *gerH*$^{+}$ strain compared to the parental strain ($P<0.05$). This enhancement of germination response by the *gerH*$^{+}$ strain suggests that activation of the GerH receptor is highly dependent on the concentrations of inosine and L-alanine.

Previous research has shown that the GerH receptor is activated by purine-nucleosides accompanied by a variety of amino acids[21, 22]. Inosine alone is unable to germinate *B. anthracis* spores, but accompanied by L-alanine it acts as a potent cogerminant[21]. Therefore, it has been suggested that the GerH receptor is required for inosine-dependent responses and plays a major role in the amino acid and inosine dependent pathway-1[11, 12]. Other studies have also observed that L-alanine or inosine binding to receptors increase with increasing concentrations of the germinants[7]. Our results suggest that optimal activation of the GerH receptor is dependent on the cooperation between L-alanine and inosine molecules during binding. Our results suggest that as long as inosine and another germinant is present in the media, the presence of the GerH receptor alone may be sufficient to trigger a full germination response of spores, since the *gerH*$^{+}$ strain had a comparable response to the wild-type *B. anthracis* 34F2 spores.

6.5.3 GerS Receptor on *B. anthracis*

The *gerS*$^{+}$ strain exhibited some level of germination after exposure to L-alanine and inosine but at a much lower rate when compared to the germination of the wild-type *B. anthracis* 34F2 strain (Figure 28 and 29). The GerS receptor recognizes inosine and amino acids that are at least partially aromatic[5]. Activation of the GerS receptor is achieved by interactions with inosine and other amino acids including tryptophan, histidine, tyrosine, and proline[5]. Since the amino acid L-alanine is not an aromatic compound, it is not surprising to observe the low germination response of the *gerS*$^{+}$ strain to the germinants in our studies. In addition, germinant receptor proteins have been localized to the inner membrane of the spore at very low levels (approximately 24 – 40 receptors per spore)[23]. Having few receptors that are not fully activated because of their inability to react to L-alanine molecules would result in low germination levels. Since previous studies have shown that inosine alone is unable to trigger germination of *B. anthracis* spores[21], our results suggest that germination of spores may involve synergy between receptors of *B. anthracis* spores, and that the presence of more than one receptor is required to achieve wild-type germination levels. Complete germination of the *gerS*$^{+}$ strain may require the additional presence of other receptors, such as the GerH receptor, since this receptor recognizes L-alanine and the germination kinetics of the *gerH*$^{+}$ strain were similar to the germination of wild-type *B. anthracis* 34F2. Previous studies have observed that the presence of the GerS receptor is important but not sufficient for germination in the presence of a variety of germinants[11]. In the same study, the *gerS*$^{+}$ strain failed to cause a rapid onset of disease in mice after subcutaneous inoculation when compared to the wild-type strain, since the *gerS*$^{+}$ strain was highly attenuated with LD_{50} values about 30-fold greater than wild-type[11]. This suggests that the

gerS^{+} strain may have a lower response to germinants or more time may be required to achieve full germination of spores.

6.5.4 Germination of *B. antrhacis* ger_{null}

Our experiments revealed that germinant receptors were not the only means for *B. anthracis* spores to initiate germination after exposure to L-alanine and inosine. The ger_{null} strain, which lacks all five germinant receptors of the GerA-like family, exhibited germination that was comparable to the germination profile of the *gerS*$^{+}$ strain (Figure 28 and 29). Since our results with the ger_{null} strain differed from those reported by Carr et al.[11], our experiments were repeated in triplicate and at least two separate spore preparations were used. Our germination assays revealed that ger_{null} indeed exhibits low levels of germination when exposed to 50 mM L-alanine and 5 mM inosine. To verify the genotype of our ger_{null} strain, the retention of the deletion of the five Ger genes was verified through a PCR assay. Our PCR results revealed that the ger_{null} strain used for our germination assays lacked all Ger germinant receptors (Figure 30).

Previous research has suggested that variation in sporulation methods can change the properties of spores[24, 25]. Changes in sporulation medium composition affects the transcription of *ger* operons and germination responses in *B. subtilis* spores[26]. Changes in sporulation temperature of *B. cereus* spores, a close relative of *B. anthracis*, resulted in spores that were more resistant to the initiation of germination and inactivation by hydrostatic pressure[27]. Spores prepared in liquid were more susceptible that those prepared on plates[24]. Spore resistance to wet heat and hydrogen peroxide was altered by sporulation temperature[28]. The differences in our ger_{null} results and those observed by Carr et al., may be due to differences in spore preparation methods. Carr et al. prepared their spores using a liquid method[11], while we prepared our spores using a solid method in which *B. anthracis* are plated on nutritionally deprived media for 4 to 5

days. The germination response observed in the ger_{null} strain suggests that germination properties may be changed by making adjustments to sporulation methods. In addition, the concentration of germinants used in our study was higher than the concentration used by Carr et al. High concentrations of germinants may induce germination responses in *B. anthracis* strains that lack Ger receptors.

Previous studies have reported that spores of *Clostridium bifermentans* germinate in the presense of L-alanine, L-phenylalanine and L-lactate, without the presence of germinant receptors[29]. Germination of *B subtilis* that lacks all Ger receptors has been observed after exposure to peptidoglycan degradation products[30]. This suggests that the presence of Ger receptors may not be needed in *B. anthracis* with ideal concentrations of germinants or specific germinants.

Our results suggest that the Ger receptors may be needed to achieve full germination of spores but are not essential to initiate germination. In our studies, *B. anthracis* ger_{null} may have germinated with L-alanine and inosine due to a combination of i) changes of sporulation methods, which can affect spore properties and germination responses; ii) activation of non-Ger specific pathways after exposure to L-alanine and inosine; iii) differences in concentrations of L-alanine and inosine present in the media; and iv) activation of a non-receptor mediated pathway. However, further research is needed to understand any possible non-receptor mediated pathways that may play a role in germination of *B. anthracis.*

6.6 Conclusions

Knowledge of the roles of specific germinant receptors on *B. anthracis* allows further mechanistic studies of germination of spores and provides fundamental information for the

development of compounds useful for blocking the germination of spores responsible for anthrax infections. The goal of this study was to provide additional information of the germinant receptors GerH and GerS in *B. anthracis* and to characterize their involvement in germination with L-alanine and inosine acting as germinants. The GerH receptor in *B. anthracis* is sufficient to stimulate L-alanine and inosine germination responses in *B. anthracis* since germination profiles of our $gerH^+$ strain mirrored the germination of the parental strain *B. anthracis* 34F2. In addition, based on the lack of germination response by the $gerS^+$ strain, our studies suggest that the presence of more than one receptor may be needed to achieve wild-type-like germination responses if L-alanine is used as a germinant. The interaction of L-alanine and inosine with the Ger family of receptors may not be the only mechanism of germination in *B. anthracis* spores, since the ger_{null} strain germinated.

6.7 Acknowledgments

This work was supported in part by the National Science Foundation (CBET 0827229 and CBET 0922901) and the Defense Threat Reduction Agency (DTRA) Project BA07PRO102.

We would like to thank Charu Jain, Prachi Gupta and Harita Menon for their assistance in the PCR experiments.

REFERENCES

1. Dixon, T. C.; Meselson, M.; Guillemin, J.; Hanna, P. C., Anthrax. *N Engl J Med* **1999,** 341, (11), 815-26.

2. Henriques, A. O.; Moran, C. P., Jr., Structure and assembly of the bacterial endospore coat. *Methods* **2000,** 20, (1), 95-110.

3. Atrih, A.; Foster, S. J., Bacterial endospores the ultimate survivors. *Int. Dairy J.* **2002,** 12, (2-3), 217-223.

4. Setlow, P., Spore germination. *Curr Opin Microbiol* **2003,** 6, (6), 550-6.

5. Ireland, J. A.; Hanna, P. C., Amino acid- and purine ribonucleoside-induced germination of *Bacillus anthracis* ΔSterne endospores: *gerS* mediates responses to aromatic ring structures. *J Bacteriol* **2002,** 184, (5), 1296-303.

6. Jedrzejas, M. J.; Setlow, P., Comparison of the binuclear metalloenzymes diphosphoglycerate-independent phosphoglycerate mutase and alkaline phosphatase: their mechanism of catalysis via a phosphoserine intermediate. *Chem Rev* **2001,** 101, (3), 607-18.

7. Akoachere, M.; Squires, R. C.; Nour, A. M.; Angelov, L.; Brojatsch, J.; Abel-Santos, E., Identification of an in vivo inhibitor of *Bacillus anthracis* spore germination. *J Biol Chem* **2007,** 282, (16), 12112-8.

8. Gounina-Allouane, R.; Broussolle, V.; Carlin, F., Influence of the sporulation temperature on the impact of the nutrients inosine and l-alanine on *Bacillus cereus* spore germination. *Food Microbiol* **2008,** 25, (1), 202-6.

9. Titball, R. W.; Manchee, R. J., Factors affecting the germination of spores of *Bacillus anthracis*. *J Appl Bacteriol* **1987,** 62, (3), 269-73.

10. Clements, M. O.; Moir, A., Role of the gerI operon of *Bacillus cereus* 569 in the response of spores to germinants. *J Bacteriol* **1998,** 180, (24), 6729-35.

11. Carr, K. A.; Lybarger, S. R.; Anderson, E. C.; Janes, B. K.; Hanna, P. C., The role of *Bacillus anthracis* germinant receptors in germination and virulence. *Mol Microbiol* **2010,** 75, (2), 365-75.

12. Fisher, N.; Hanna, P., Characterization of *Bacillus anthracis* germinant receptors in vitro. *J Bacteriol* **2005,** 187, (23), 8055-62.

13. Ireland, J. A.; Hanna, P. C., Macrophage-enhanced germination of *Bacillus anthracis* endospores requires gerS. *Infect Immun* **2002,** 70, (10), 5870-2.

14. Pinzón-Arango, P. A.; Scholl, G.; Nagarajan, R.; Mello, C. M.; Camesano, T. A., Atomic force microscopy study of germination and killing of *Bacillus atrophaeus* spores. *J Mol Recognit* **2009,** 22, (5), 373-379.

15. Koehler, T. M., *Bacillus anthracis* physiology and genetics. *Mol Aspects Med* **2009,** 30, (6), 386-96.

16. Pinzón-Arango, P. A.; Nagarajan, R.; Camesano, T. A., Effects of L-alanine and inosine germinants on the elasticity of *Bacillus anthracis* spores. *Langmuir* **2010,** 26, (9), 6535-41.

17. Leuschner, R. G. K.; Ferdinando, D. P.; Lillford, P. J., Structural analysis of spores of *Bacillus subtilis* during germination and outgrowth. *Colloids Surf., B* **2003,** 19, 31-41.

18. Setlow, B.; Cowan, A. E.; Setlow, P., Germination of spores of *Bacillus subtilis* with dodecylamine. *J Appl Microbiol* **2003,** 95, (3), 637-48.

19. Pinzon-Arango, P. A.; Nagarajan, R.; Camesano, T. A., Changes in Mechanical Properties and Killing of Bacillus anthracis 34F2 After Exposure to the Antimicrobial Peptide Chrysophsin-3 **Submitted**.

20. Rode, L. J.; Foster, J. W., Germination of bacterial spores with alkyl primary amines. *J Bacteriol* **1961,** 81, 768-79.

21. Weiner, M. A.; Read, T. D.; Hanna, P. C., Identification and characterization of the gerH operon of Bacillus anthracis endospores: a differential role for purine nucleosides in germination. *J Bacteriol* **2003,** 185, (4), 1462-4.

22. Weiner, M. A.; Hanna, P. C., Macrophage-mediated germination of *Bacillus anthracis* endospores requires the gerH operon. *Infect Immun* **2003,** 71, (7), 3954-9.

23. Paidhungat, M.; Setlow, P., Localization of a germinant receptor protein (GerBA) to the inner membrane of *Bacillus subtilis* spores. *J Bacteriol* **2001,** 183, (13), 3982-90.

24. Rose, R.; Setlow, B.; Monroe, A.; Mallozzi, M.; Driks, A.; Setlow, P., Comparison of the properties of *Bacillus subtilis* spores made in liquid or on agar plates. *J Appl Microbiol* **2007,** 103, (3), 691-9.

25. Banerjee, D.; Markley, A. L.; Yano, T.; Ghosh, A.; Berget, P. B.; Minkley, E. G., Jr.; Khetan, S. K.; Collins, T. J., "Green" oxidation catalysis for rapid deactivation of bacterial spores. *Angew Chem Int Ed Engl* **2006,** 45, (24), 3974-7.

26. Hornstra, L. M.; de Vries, Y. P.; de Vos, W. M.; Abee, T., Influence of sporulation medium composition on transcription of ger operons and the germination response of spores of Bacillus cereus ATCC 14579. *Appl Environ Microbiol* **2006,** 72, (5), 3746-9.

27. Raso, J.; Gongora-Nieto, M. M.; Barbosa-Canovas, G. V.; Swanson, B. G., Influence of several environmental factors on the initiation of germination and inactivation of *Bacillus cereus* by high hydrostatic pressure. *Int J Food Microbiol* **1998,** 44, (1-2), 125-32.

28. Melly, E.; Genest, P. C.; Gilmore, M. E.; Little, S.; Popham, D. L.; Driks, A.; Setlow, P., Analysis of the properties of spores of *Bacillus subtilis* prepared at different temperatures. *J Appl Microbiol* **2002,** 92, (6), 1105-15.

29. Waites, W. M.; Wyatt, L. R., Germination of spores of Clostridium bifermentans by certain amino acids, lactate and pyruvate in the presence of sodium or potassium ions. *J Gen Microbiol* **1971,** 67, (2), 215-22.

30. Shah, I. M.; Laaberki, M. H.; Popham, D. L.; Dworkin, J., A eukaryotic-like Ser/Thr kinase signals bacteria to exit dormancy in response to peptidoglycan fragments. *Cell* **2008,** 135, (3), 486-96.

Chapter 7

Role of germinant receptors of *Bacillus anthracis* on invasion and cytokine response

7.1 Abstract

During the development of an anthrax infection, *Bacillus anthracis* spores are phagocytosed by macrophages and transported to regional lymph nodes where spores germinate and become virulent bacteria. The Ger-family of operons in *B. anthracis* is believed to be responsible for the germination of *B. anthracis* spores. However, the role of these receptors on virulence and innate immune responses of murine macrophages is poorly understood. We investigated the role of the GerH and GerS receptor on invasion of macrophages and virulence of *B. anthracis* spores. Macrophages were infected with the wild-type *B. anthracis* 34F2 strain, the $gerH^+$ and $gerS^+$strains, which only express GerH or GerS, respectively, and ger_{null} spores that do not express any germinant receptors. Germination and growth of *B. anthracis* inside macrophages and the ability of spore mutants to elicit a cytokine response from macrophages were determined. *B. anthracis* 34F2 and the $gerH^+$ strains interacted strongly with macrophages since these strains germinated and lysed macrophages with time post-infection. The $gerS^+$ and ger_{null} mutants were phagocytosed by macrophages but failed to germinate and lyse phagocytes. However, all strains elicited a strong cytokine response suggesting that cytokine expression is not only due to toxins being released by vegetative *B. anthracis*, as it was first thought, but also by macrophage-spore interactions. In this study, we provided evidence of the importance of *B. anthracis* germinant receptors on an acute cytokine response after infection of macrophages.

7.2 Introduction

Bacillus anthracis is a virulent bacterium that in the absence of nutrients is capable of forming spores, becoming extremely resistant to adverse environmental conditions[1]. While in their dormant state, spores continuously monitor their environment so they can germinate when

nutrients are available. Germination enables *B. anthracis* to proliferate, synthesize their virulence factors, and disseminate within the host[2].

During an anthrax infection, *B. anthracis* spores are phagocytosed by macrophages and transported to regional lymph nodes[3]. Following phagocytosis of spores, *B. anthracis* germinates, multiplies, and releases toxins within the phagocytes that result in lysis of the macrophage[1, 4, 5]. Consequentially, vegetative *B. anthracis* multiply within lymph nodes and gain entry into the blood-stream, resulting in development of severe septicemia[6]. The rapid progression of the disease and the difficulties in prompt diagnosis of anthrax infections, have made *B. anthracis* a bioweapon[7, 8].

Previous research has suggested that germination of *B. anthracis* spores is dependent upon the binding of nutrients to germinant receptors located in the inner membrane of spores[9]. A GerA-like family of germinant receptors has been found in *B. anthracis*, which are encoded by tricistronic operons containing three protein-coding genes (A, B, and C subunits)[10]. The *gerH, gerS, gerL, gerK,* and *gerX* operons play a role in *B. anthracis* germination and each operon or receptor responds differently to each germinant[11, 12]. For instance, the GerS receptor is activated by inosine and aromatic amino acids, but responds weakly to L-alanine[11, 12]. Five distinct germination pathways have been recognized where synergy between germinant receptors has been observed[10]. Some studies have shown that the *gerH* and *gerS* operons are necessary for spores to germinate inside murine macrophages[13, 14]. However, these studies investigated spore germination by measuring the amount of ^{45}Ca released from prelabeled spores after exposure to macrophages[13, 14]. To our knowledge, no studies have investigated how *B. anthracis* expressing one of these two receptors affect macrophage invasion by directly quantifying the number of

spores that are phagocytosed by macrophages, and quantifying differences in germination kinetics.

During germination, *B. anthracis* produce and synthesize two toxins that are encoded by the pXO1 plasmid of the bacterium, lethal toxin (LeTx) and edema toxin (EdTx)[6]. Expression of these two toxins results in the release of edema factor (EF) and lethal factor (LF) into the cytosol of macrophages causing the disruption of normal macrophage physiology and cell death[15]. The effects of *B. anthracis* spores and isolated EdTx and LeTx on virulence of macrophages have been investigated by measuring the expression of cytokines released by macrophages after exposure to spores and toxins[16, 17]. Sublytic levels of LeTx triggers the production of tumor necrosis factor alpha (TNF-α) and interleukin-1β (IL-1β)[3]. Macrophages infected with a *B. anthracis* strain that produced toxins but did not express a capsule, caused the expression of significant levels of TNF-α and IL-12, which play an important role in the activation of inflammatory pathways and cellular recruitment[16]. *B. anthracis* spores at a low multiplicity of infection (spore-macrophage ratio) elicited an early cytokine mRNA response in primary macrophages[18].While studies have observed that macrophages release cytokines after exposure to *B. anthracis*, other contradicting studies have suggested that LeTx inhibits cytokine responses to lipopolysaccharide (LPS)[17, 19]. Although there have been conflicting studies regarding the cytokine response elicited by *B. anthracis,* no study has investigated whether the expression of cytokines are affected by the presence of spore germinant receptors.

In the present study, we investigated the role of the germinant receptors GerH and GerS on the invasion of murine macrophages and cytokine expression. In addition, we test the ability of a mutant *B. anthracis* strain that lacks all Ger receptors to invade, and grow inside macrophages. Our results suggest that deletion of germinant receptors affects phagocytosis of *B.*

anthracis by murine macrophages and the expression of cell-signaling proteins that play an important role in immune responses and in anthrax pathogenesis.

7.3 Materials and Methods

7.3.1 *Bacillus anthracis* Strains and Spore Preparation

B. anthracis Sterne spores and mutants used in this study are listed in Table 7. The parental *B. anthracis* Sterne 34F2 strain was kindly provided by the Edgewood Chemical Biological Center, Edgewood, MD. The Sterne 34F2 strain is a low virulence *B. anthracis* spores that contains the pXO1 plasmid responsible for expression of toxins, but lacks the pXO2 plasmid, which is responsible for the development of the anti-phagocytic capsule[20]. Two distinct quadruple mutants, each containing only a single functional germinant receptor, $gerS^+$ and $gerH^+$, and a mutant lacking all five germinant receptors, ger_{null} were kindly provided by Dr. Philip C. Hanna (University of Michigan Medical School, Ann Arbor, MI). These mutants were created by performing allelic exchange sequentially, knocking out the appropriate Ger operon[11].

Table 7. *Bacillus anthracis* strains used in this study

Strain	Mutant Name	Characteristics[a]	Reference
$34F_2$	-	Wild-type ($pXO1^+$, $PXO2^-$)	Pinzón-Arango et al. (2010)
SL115	$gerH^+$	$34F_2$, Δ*gerK* Δ*gerL* Δ*gerS* Δ*gerX*	Carr et al. (2010)
SL118	$gerS^+$	$34F_2$, Δ*gerH* Δ*gerK* Δ*gerL* Δ*gerX*	Carr et al. (2010)
SL120	ger_{null}	$34F_2$, Δ*gerH* Δ*gerK* Δ*gerL* Δ*gerX* Δ*gerS*	Carr et al. (2010)

[a]Mutant construction was achieved through markerless deletions of nearly the entire tricistronic germinant receptor operon (Carr et al., 2010).

Spores were grown on agar plates containing sporulation media as previously described[21]. Sporulation media (8 g nutrient broth, 4 g yeast extract, 0.001 g $McCl_24H_2O$, 5 g peptone and 15

g of agar in 1 L of ultrapure water) was maintained at a pH of 7.2 and sterilized. *B. anthracis* spores were plated on sporulation media and left incubating at 37 ºC for 5 days. Spores were collected and washed by centrifugation at 5000 rpm for 20 minutes at 4 ºC and resuspended in ultrapure water. After each centrifugation step, the top of the pellet, consisting mainly of vegetative and partially sporulated cells, was discarded and the bottom layer resuspended. A total of 8 washes were performed and washed spores were kept in ultrapure water overnight at 4 ºC. Before use, spores were washed one more time or until 99% of sporulated (phase-bright spores) were observed through phase contrast microscopy (Nikon Eclipse E400, Tokyo, Japan). Before experiments, the spores were heat activated for 30 min at 65 ºC.

7.3.2 Growth of Murine Macrophages

A culture of murine macrophage-like cells RAW 264.7 was purchased (ATCC TIB-71, VA). Cells were recovered and kept in liquid nitrogen vapor phase according to manufacturer's instructions. Monolayers of macrophages were cultured in Dulbecco's modified Eagle medium (DMEM) supplemented with 10% fetal bovine serum (FBS). Tissue culture flasks were kept in a 5% CO_2 in air atmosphere incubator at 37 ºC for 6 – 7 days where the media was replaced every 48 hrs. Macrophages were detached by gentle scraping, washed by centrifugation at 1200 rpm for 6 min, resuspended in fresh DMEM and counted using a hemocytometer.

7.3.3 Infection of Murine Macrophages by *B. anthracis*

Murine macrophages were seeded at 10^6 cells/mL and allowed to attach to 24-well plates for 2 hrs prior to infection with spores. Monolayers of macrophages were infected with previously heat-activated *B. anthracis* spores at a multiplicity of infection of 1:10 (10 spores per macrophage) and were incubated for 30 min at 37 ºC. Gentamicin at a concentration of 10

μg/mL was added to remove extracellular *B. anthracis* and left incubating for an additional 30 min. After gentamicin treatment, monolayers were washed three times with Hanks balanced salt solution (Lonza, Walkersville, MD) and resuspended in fresh DMEM medium without antibiotics. For all experiments this was considered to be the zero time point post-infection.

7.3.4 Growth of *B. anthracis* within RAW 264.7 Macrophages

After infection of macrophages with *B. anthracis*, counts of extracellular colony forming units (CFU) were made by collecting the macrophage supernatants at 2, 4, 6, and 8 hrs post-infection. Supernatants were diluted, and 100 μL of supernatant solution was plated on trypsic soy agar. The agar plates were incubated for 24 hrs at 37 ºC and the number of *B. anthracis* colony forming units (CFU) was determined.

For intracellular measurements, macrophages were washed once with Hanks' balanced salt solution and lysed by incubation with 0.05% sodium deoxycolate solution for 15 min at 37 ºC. Lysate was serially diluted and a 100 μL of lysate solution was inoculated onto tryptic soy agar plates and incubated at 37 ºC for 24 hrs. CFU counts were determined with untreated macrophages serving as control.

7.3.5 Measurement of Cytokine Concentrations in Cell Culture Supernatants

Cytokine concentrations in cell culture supernatants were measured at 2, 5, and 8 hrs post-infection. Aliquots were stored at -70 ºC and thawed immediately prior to assay. Cytokine concentrations in culture supernatants were measured with a mouse cytokine antibody kit (Thermo Scientific, Rockford, IL) and a Perkin Elmer Victor3 multimode plate reader (Waltham, MA), according to the manufacturer's instructions. The limits of detection for each cytokine in this assay are as follows: IL-1β = 3 pg/mL, IL-6 = 7 pg/mL, and TNF-α = 9 pg/mL.

7.3.6 Statistical Analysis

Invasion and cytokine data was analyzed using a one-way analysis of Variance (ANOVA) for repeated measurements. The null hypothesis tested was that there were no differences in the distribution of values between different groups. A difference was considered significant if $P < 0.05$.

7.4 Results

7.4.1 Invasion and Growth of *B. anthracis* Spores in Murine Macrophages

The numbers of CFU inside macrophages and in culture supernatants were determined at various time points post-infection (Figure 31). Two hours post-infection, macrophages engulfed a significant number of *B. anthracis* 34F2 spores. Increasing times of incubation of macrophages post-infection resulted in a decrease of spores inside macrophages. This decrease in *B. anthracis* CFE lasted for at least 8 hrs post-infection. This suggests that either the macrophages were killing spores effectively, or the macrophages were being lysed by *B. anthracis* that had germinated and became virulent and vegetative bacteria. In culture supernatants, the number of CFU rapidly increased with time of incubation post-infection. The CFU count in culture supernatants increased exponentially by more than an order of magnitude, suggesting the complete germination and outgrowth of spores in the medium. Observation of macrophages under phase contrast revealed that the number of eukaryotic cells decreased with time and few numbers of macrophages were visible 8 hrs post-infection (data not shown).

B. anthracis mutants *gerS*$^+$, *gerH*$^+$ and *ger*$_{null}$ were also investigated for their ability to invade and grow inside macrophages. All three mutants were unable to invade macrophages at the same level as the wild type strain (Figure 31B). While the macrophages were still able to

engulf *B. anthracis* mutants, the concentration of mutant spores inside macrophages remained the same with prolonged incubation times post-infection. This suggests that the mutant strains were not germinating or killing macrophages the same way *B. anthracis* 34F2 did.

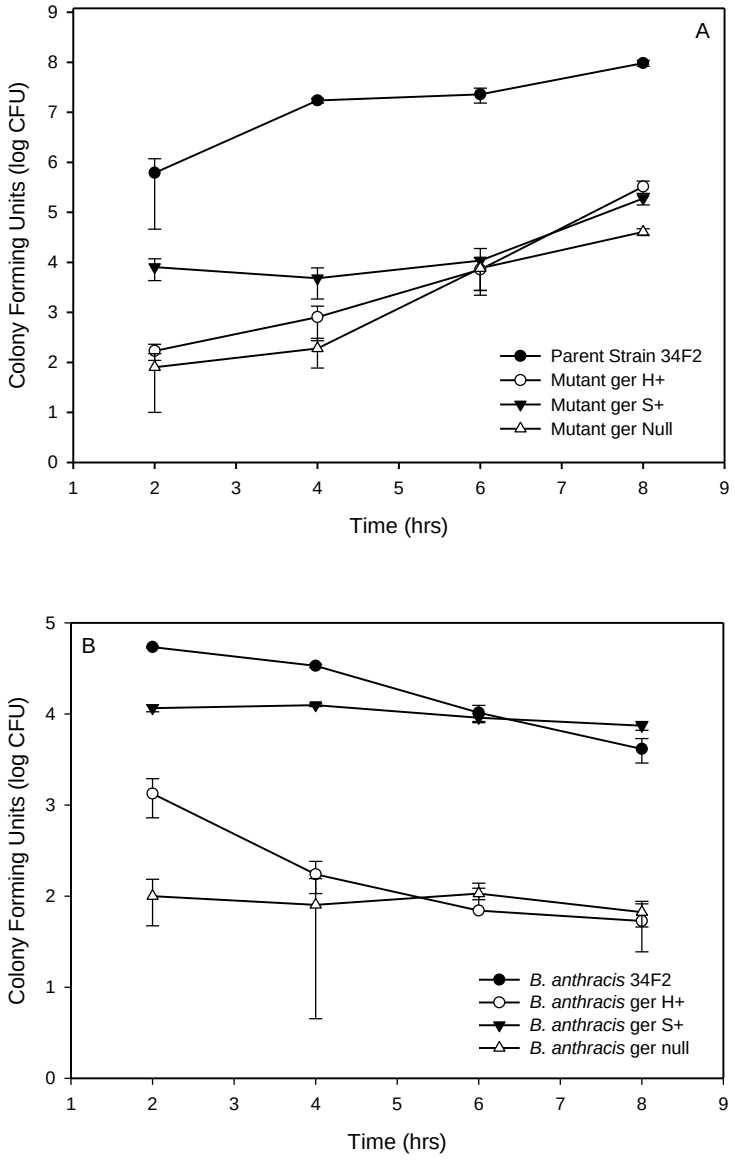

Figure 31. Growth of *B. anthracis* 34F2 and its Ger-mutants in murine macrophages. Macrophages were infected with *B. anthracis* spores at an MOI of 1:10, as described in the text. CFU were determined and are shown as a function of time post-infection. At each time point, the CFU number present in supernatants (A) and inside macrophages (B) were determined. The experiment was repeated three times. Each value corresponds to the average of three samples ± the standard deviation.

When investigating the germination and growth of *B. anthracis* mutants in culture supernatants, we found that there was no significant growth of *B. anthracis* $gerS^+$, $gerH^+$, or ger_{null} in the supernatants when compared to the wild type *B. anthracis* 34F2 strain. When examining just the mutant strains and comparing them against each other, we found that after 8 hours of incubation, the $gerH^+$ strain grew in the supernatants better than the $gerS^+$, and the $gerS^+$ strain grew better than the ger_{null} strain (Figure 31A). However, the germination and growth kinetics of these *B. anthracis* mutant strains was significantly lower than the germination of *B. anthracis* 34F2 strain ($P<0.05$).

7.4.2 Cytokine Response of *B. anthracis*-Infected Macrophages

We examined the concentrations of IL-1β, IL-6, and TNF-α in the supernatants from *B. anthracis*-infected murine macrophages at 2, 5, and 8 hours post-infection. After infection of macrophages with *B. anthracis* 34F2, a high concentration of IL-1β was detected at 5 hours of incubation post-infection, which was significantly higher than the concentrations found in the supernatants of untreated macrophages or in the supernatants of macrophages infected with the *B. anthracis* mutants (Figure 32A; $P<0.05$). Eight hrs post-infection, the concentration of IL-1β decreased for macrophages infected with the wild-type 34F2 spore, but increased for macrophages infected with the mutant strains.

Increasing concentrations of IL-6 with time post-infection were found when macrophages were infected with all *B. anthracis* strains (Figure 32B). Effects of *B. anthracis* infections on IL-6 concentrations levels were particularly emphasized for the $gerS^+$ and ger_{null} strains since the concentrations of this cytokine increased by an order of magnitude after 8 hours of infection. Infection of macrophages with *B. anthracis* $gerH^+$ resulted in a delay in the expression of IL-6 since it took 8 hrs of incubation post-infection to detect expression of the cytokine.

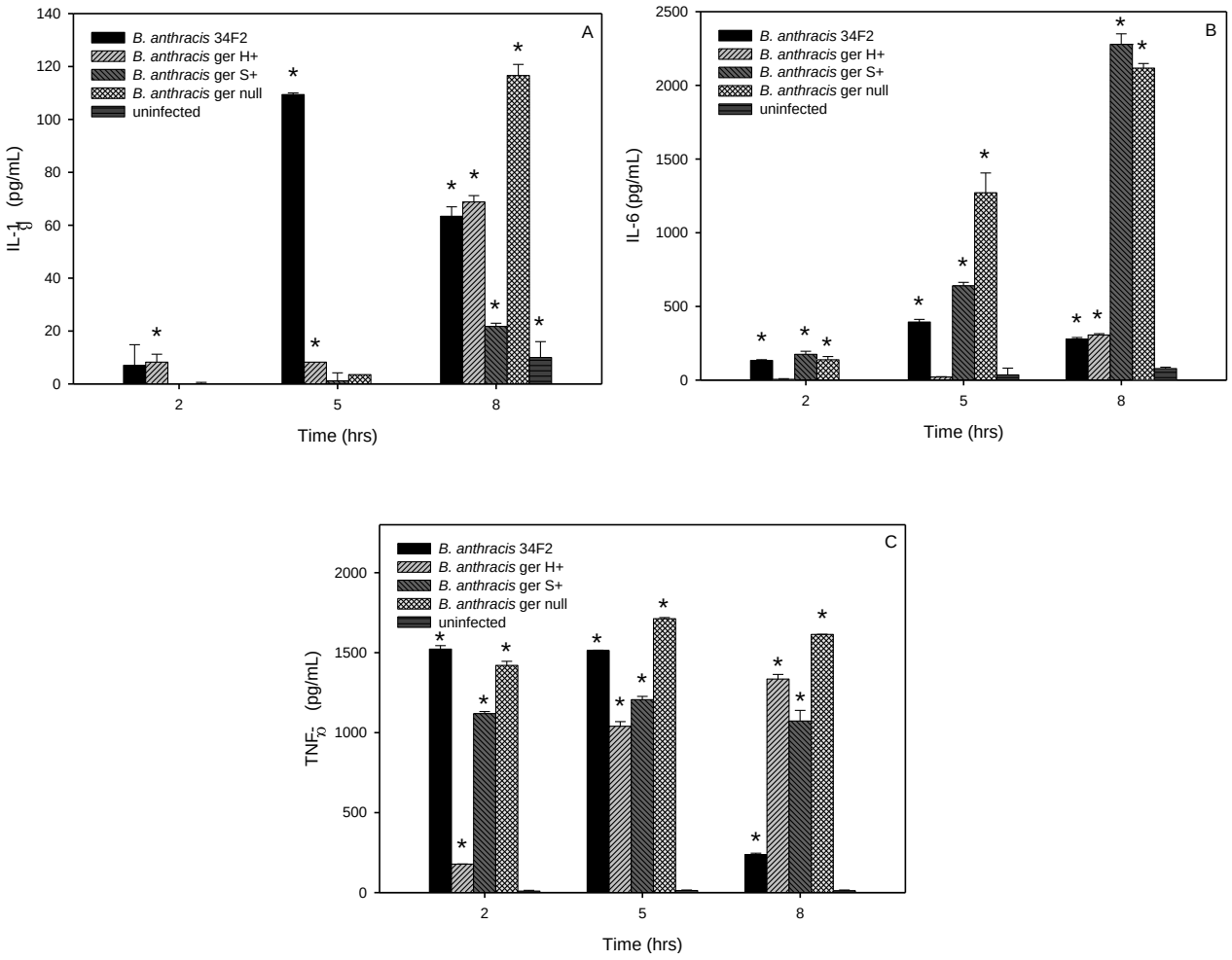

Figure 32. Release of cytokines by murine macrophages in response to infection by *B. anthracis* 34F2 and its Ger-mutants. Concentrations of IL-1β (A), IL-6 (B), and TNF-α (C) in supernatants collected as a function of time post-infection. Three experiments were performed, and the average concentration ± standard deviation is shown. Means were compared to those of uninfected control group. The star symbol indicates statistical significance when compared to untreated macrophages, $P<0.05$.

TNF-α was highly expressed at all times after infection with all strains of *B. anthracis* (Figure 32C). An increasing level of TNF-α with time was observed when the macrophages were infected with the *B. anthracis gerH*$^+$ strain. Concentrations of TNF-α in the culture supernatant were similar at all incubation times after infection with the *gerS*$^+$ and *ger*$_{null}$ strains. While high levels of TNF-α were detected in the supernatants of *B. anthracis* 34F2-infected macrophages

after 2 and 5 hours of incubation post-infection, the concentration of the cytokine decreased significantly after 8 hours of incubation.

7.5 Discussion

7.5.1 Germination and Growth of *B. anthracis* inside Macrophages

Murine macrophages readily engulfed *B. anthracis* 34F2 spores and the number of CFU inside macrophages decreased with time post-infection (Figure 31). This decrease in *B. anthracis* CFU with time has been observed by others[5, 16, 22]. Previous studies suggested that the drop of viable CFU was due to an initial killing of *B. anthracis* by macrophages following spore uptake[22]. In their study, Pickering et al. observed that following an initial killing of spores, the number of intracellular *B. anthracis* recovered, resulting in an increase of CFU with time. In our study, we did not see an increase in CFU count with time post-infection. Based on our results and Pickering's theory, the continuous decrease in the number of intracellular *B. anthracis* 34F2 suggested that the macrophages were digesting and killing spores and no recovery of *B. anthracis* was taking place.

Close observation of the number of *B. anthracis* 34F2 present in the supernatants of infected macrophages revealed that there was an inversely proportional increase of *B. anthracis* CFU with time post-infection (Figure 31A). If the macrophages were killing *B. anthracis* after spore uptake as it was first thought, we would not have observed a drastic increase of CFU counts in supernatants. Microscopy observation of the macrophages with time post-infection revealed that the number of macrophages attached to the surface of the 24-well plates decreased with time. Our microscopy observations and our decrease in intracellular CFU with time suggest that macrophages failed to kill *B. anthracis.* On the contrary, *B. anthracis* 34F2 spores

germinated and outgrew into vegetative bacteria that multiplied to high numbers and released toxins, which caused the lysis of macrophages and release of *B. anthracis* 34F2 into the media. Lysis of macrophages by *B. anthracis* has also been observed in other studies[16]. The lack of an exponential increase of CFU in macrophages observed in our studies suggests that lysed macrophages may release not only vegetative *B. anthracis*, but sporulated bacteria and *B. anthracis* that are undergoing the process of germination. The proposed sequence of events occurring during macrophage invasion by *B. anthracis* is summarized in Figure 33.

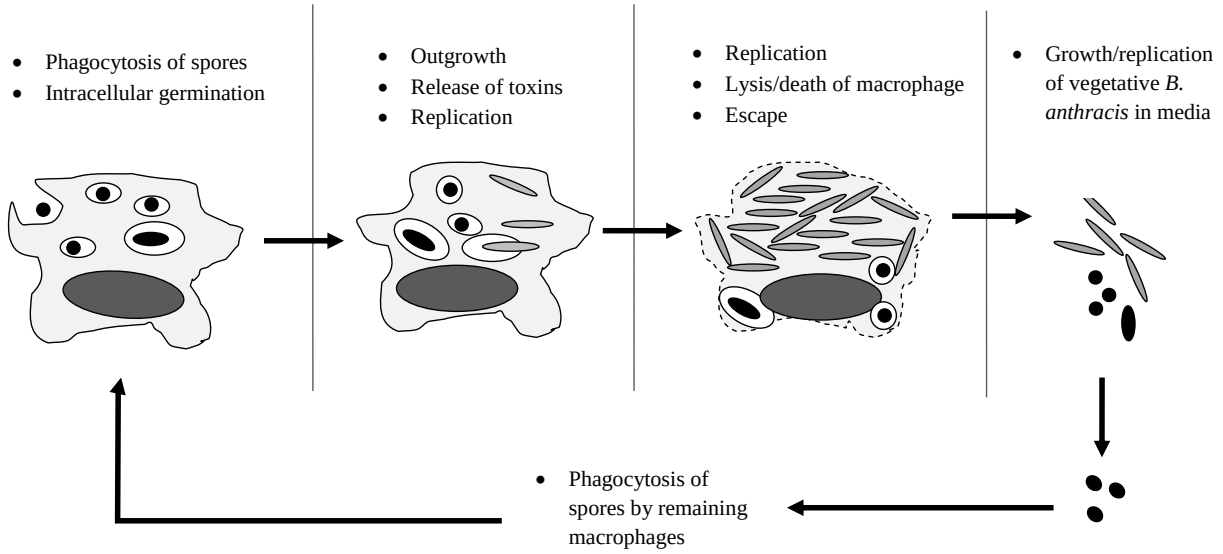

Figure 33. Proposed sequence of events occurring during *B. anthracis* infection of macrophages. *B. anthracis* was phagocytosed by macrophages where some spores germinated, outgrew, and became virulent due to the release of LeTx and EdTx into the cytosol of macrophages. After lysis of macrophages, vegetative *B. anthracis* remains in media replicating and sporulated *B. anthracis* is phagocytosed by remaining macrophages where the cycle starts again until all macrophages have been depleted.

The *ger* mutants of *B. anthracis* were phagocytosed but at lower numbers compared to the wild-type *B. anthracis* 34F2 (Figure 31). However, when comparing the mutant strains

among each other, macrophages engulfed significantly more *B. anthracis gerS*$^{+}$ than *gerH*$^{+}$ or *ger*$_{null}$ spores. Ireland and Hanna support our findings since they observed that the GerS receptor was required to enhanced macrophage-spore interactions[13]. The CFU count of *B. anthracis gerS*$^{+}$ inside macrophages remained the same with time post-infection. Our results suggest that phagocytosis of *B. anthracis gerS*$^{+}$ by macrophages takes place, but outgrowth and replication of vegetative bacteria do not. While Ireland and Hanna found that *B. anthracis* strains that had the GerS receptor were capable of initiating germination of spores inside macrophages[13], our results suggest that germination may be taking place but outgrowth of vegetative *B. anthracis* does not occur. In Ireland and Hanna's study, germination was measured by the release of ^{45}Ca from prelabeled spores after exposure to macrophages[13]. Release of ^{45}Ca from spores indicates that spores have initiated the irreversible process of germination; however, this technique does not test for outgrowth of germinating bacteria and release of spore coats.

The *B. anthracis gerH*$^{+}$ and *ger*$_{null}$ strains did not interact much with the macrophages and lower CFUs were found inside and outside of the macrophage at all times. There was a small decrease of *gerH*$^{+}$ CFU inside macrophages and a small increase in supernatants. This suggests that even though the spores are engulfed by macrophages in small quantities, the *gerH*$^{+}$ strain is capable of outgrowing into vegetative bacteria and toxins are released causing lysis of macrophages. In a previous study, we observed that the *gerH*$^{+}$ strain had similar germination kinetics when compared to the wild-type *B. anthracis* strain[23]. While the macrophage does not engulf a similar number of spores compared to the wild-type strain, their invasion and virulence properties are similar. Other studies have also found that the GerH operon is required for spore germination in macrophages[14].

Similarly to the *gerS*$^{+}$ strain, *B. anthracis* ger_{null} strain did not grow inside macrophages and comparable CFU counts were found at all times post-infection. However, low numbers of the ger_{null} strain were able to germinate and grow in macrophage supernatants (Figure 31A). The germination and growth of ger_{null} was nowhere near the behavior of wild-type spore, but it was significant. While it has been suggested that the deletion of Ger receptors from *B. anthracis* results in germination deficiency[11], we have observed that germination of ger_{null} can be initiated with high concentrations of L-alanine and inosine[23]. Germination of ger_{null} in supernatants may occur through activation of a non-receptor mediated pathway or a non-ger-specific pathway. However, more studies are needed to understand germination of *B. anthracis* in the absence of Ger receptors.

7.5.2 Effects of *B. anthracis* Germinant Receptors on Cytokine Response

When macrophages were infected with *B. anthracis* spores, cytokines were released as early as two hours after infection (Figure 32). We measured the levels of IL-1β, IL-6, and TNF-α because of their importance in stimulating different components of immune response, such as macrophages (IL-1β and TNF-α) and antibody formation (IL-6)[18]. Release of these cytokines in response to intracellular infection with *B. anthracis* spores has been observed by others[16, 18, 22]. Low levels of IL-1β were detected two hours post-infection with *B. anthracis* 34F2 and *B. anthracis gerH*$^{+}$ (Figure 32A). In a previous study we observed that the *gerH*$^{+}$ strain had similar germination kinetics when compared to the wild-type *B. anthracis* 34F2[23]. Therefore, it is not surprising to see that these two strains were the only ones that caused the release of IL-1β at 2 hours post-infection. With prolonged time post-infection, the release of IL-1β increased for the wild-type *B. anthracis* 34F2 strain by one order of magnitude and decreased by 8 hours. Based on our invasion results, the decrease in cytokine levels from 5 to 8 hours post-infection may be

due to a low number of macrophages available. It is also possible that with the lysis of macrophages, proteases and other compounds are released into the supernatants, which cause the degradation of the cytokine. A delayed IL-1β response was observed after infection with the *B. anthracis* mutants since a strong cytokine response was observed only at 8 hours post-infection. The delay in cytokine release may be due to a low or lack of a germination response by the mutant strains since they do not have all germinant receptors present. Recent studies have suggested that the release of cytokines is due to the production and release of LeTx after germination of spores in macrophages[3, 24]. In our previous study, we observed that *B. anthracis* germinant receptor mutants had a delayed response in germination compared to the wild-type strain[23]. Since our *B. anthracis* mutants take longer to germinate inside macrophages due to lack of germinant receptors, it is not surprising to observe a delay in cytokine response.

Interestingly, the *B. anthracis* ger_{null} strain released the most levels of IL-1β at 8 hours post-infection when compared to other strains. Since our invasion experiments suggested that the ger_{null} strain does not germinate and grow inside macrophages, the strong release of IL-1β observed at 8 hours post-infection suggests that release of cytokines is not only due to the release of lethal toxin from the vegetative *B. anthracis* but it may also be due to macrophage interactions with *B. anthracis* in their sporulated state. While in their dormant state *B. anthracis* spores do not synthesize and release toxins[22], our results suggest that expression of toxins may not be needed to elicit a macrophage response. Basu et al. observed that *B. anthracis* spores of the Sterne strain induced cytokine responses from macrophages in a dose-dependent manner and that this response was stronger than the response elicited by heat-killed bacilli[18].

The IL-6 response of macrophages to *B. anthracis* infection was similar to the IL-1β response (Figure 32B). However, the wild-type *B. anthracis* 34F2 strain induced a low cytokine

response at all times. Since *B. anthracis* 34F2 has all 5 germinant receptors present[11], the spore germinates faster than its ger-receptor mutants. The fast germination and outgrowth of *B. anthracis* 34F2 would result in a faster killing of macrophages and a low or blocked cytokine response. Not surprisingly, the $gerS^{+}$ and the ger_{null} strains had the highest IL-6 concentrations present in the supernatants obtained at 8 hours post-infection. From our previous study and from our invasion experiments, these two strains fail to germinate or germinate at a slower rate inside macrophages, causing a delay in the expression of IL-6.

A strong TNF-α response was observed at all times for all strains tested (Figure 32C). TNF-α is a potent pro-inflammatory cytokine that was released as early as 2 hours following infection of macrophages. There was a significant decrease of TNF-α production by *B. anthracis* 34F2-infected macrophages at 8 hours, which may be due to a decrease in the number of macrophages available at that time or by a degradation of the cytokine with compounds released after lysis of macrophages. It is also possible that the half-life of TNF-α may be short and degrade between 5 and 8 hours post infection. Similarly to the IL-6 response, high concentrations were observed after infection of macrophages with germinant mutants. Our results suggest that the release of TNF-β by macrophages may be a result of macrophages interacting with spores, and macrophages responding to the toxins release after germination and outgrowth of *B. anthracis.*

The expression of the cytokines tested in this study behaved differently among the three cytokines. There us a temporal sequence where TNF-α gets expressed before IL-6 and IL-1β. This temporal sequence suggests that cytokine response to *B. anthracis* spores likely requires the involvement of multiple signaling pathways that get activated at different times post-infection. The uncontrolled release of pro-inflammatory cytokines is believed to contribute to the

cardiovascular collapse during anthrax in a manner similar to endotoxin-mediated sepsis[25]. Based on the symptoms observed during an anthrax infection, inflammation of tissues and necrosis may be the result of an uncontrolled release of cytokines that results in cell death. Previous studies support this theory since mice that did not express TNF receptors and IL-1 receptors were less susceptible to *B. anthracis* infection than wild type mice[26]. It seems that not only LF and EF cause the release of cytokines, but the presence or absence of receptors also has an effect on cytokine response.

7.6 Conclusions

The results of this study suggest that there are at least two distinct interactions between *B. anthracis* and murine macrophages during an infection: 1) the macrophage-spore interaction that occurs during the first stage of infection where the disease would be established, and 2) the interaction of the macrophage with spores and bacilli toxins that cause the release of cytokines after an infection is established. The presence of germinant receptors in the inner membrane of *B. anthracis* affects the germination and outgrowth of spores inside macrophages but causes little effect on the levels of cytokines that are released during an infection. Our results suggest that not only LeTx and EdTx cause the release of cytokines, but the interaction of macrophages with sporulated *B. anthracis* is sufficient to induce a cytokine response since our ger_{null} strain caused a strong cytokine response.

7.7 Acknowledgments

This work was supported in part by the National Science Foundation (CBET 0827229 and CBET 0922901) and the Defense Threat Reduction Agency (DTRA) Project BA07PRO102.

We would like to thank Charu Jain and Shilpa Sathyanarayan for their assistance in the macrophage experiments and cytokine experiments.

REFERENCES

1. Dixon, T. C.; Meselson, M.; Guillemin, J.; Hanna, P. C., Anthrax. *N Engl J Med* **1999,** 341, (11), 815-26.

2. Glomski, I. J., *Bacillus anthracis* Dissemination through Hosts. In *Bacillus anthracis and Anthrax*, Bergman, N. H., Ed. John Wiley & Sons, Icn.: 2011.

3. Hanna, P. C.; Acosta, D.; Collier, R. J., On the role of macrophages in anthrax. *Proc Natl Acad Sci U S A* **1993,** 90, (21), 10198-201.

4. Guidi-Rontani, C., The alveolar macrophage: the Trojan horse of *Bacillus anthracis*. *Trends Microbiol* **2002,** 10, (9), 405-9.

5. Guidi-Rontani, C.; Weber-Levy, M.; Labruyere, E.; Mock, M., Germination of *Bacillus anthracis* spores within alveolar macrophages. *Mol Microbiol* **1999,** 31, (1), 9-17.

6. Pile, J. C.; Malone, J. D.; Eitzen, E. M.; Friedlander, A. M., Anthrax as a potential biological warfare agent. *Arch Intern Med* **1998,** 158, (5), 429-34.

7. Inglesby, T. V.; Henderson, D. A.; Bartlett, J. G.; Ascher, M. S.; Eitzen, E.; Friedlander, A. M.; Hauer, J.; McDade, J.; Osterholm, M. T.; O'Toole, T.; Parker, G.; Perl, T. M.; Russell, P. K.; Tonat, K., Anthrax as a biological weapon: medical and public health management. Working Group on Civilian Biodefense. *Jama* **1999,** 281, (18), 1735-45.

8. Jernigan, J. A.; Stephens, D. S.; Ashford, D. A.; Omenaca, C.; Topiel, M. S.; Galbraith, M.; Tapper, M.; Fisk, T. L.; Zaki, S.; Popovic, T.; Meyer, R. F.; Quinn, C. P.; Harper, S. A.; Fridkin, S. K.; Sejvar, J. J.; Shepard, C. W.; McConnell, M.; Guarner, J.; Shieh, W. J.; Malecki, J. M.; Gerberding, J. L.; Hughes, J. M.; Perkins, B. A., Bioterrorism-related inhalational anthrax: the first 10 cases reported in the United States. *Emerg Infect Dis* **2001,** 7, (6), 933-44.

9. Setlow, P., Spore germination. *Curr Opin Microbiol* **2003,** 6, (6), 550-6.

10. Ross, C.; Abel-Santos, E., The Ger receptor family from sporulating bacteria. *Curr Issues Mol Biol* **2010,** 12, (3), 147-58.

11. Carr, K. A.; Lybarger, S. R.; Anderson, E. C.; Janes, B. K.; Hanna, P. C., The role of *Bacillus anthracis* germinant receptors in germination and virulence. *Mol Microbiol* **2010,** 75, (2), 365-75.

12. Ireland, J. A.; Hanna, P. C., Amino acid- and purine ribonucleoside-induced germination of *Bacillus anthracis* ΔSterne endospores: *gerS* mediates responses to aromatic ring structures. *J Bacteriol* **2002,** 184, (5), 1296-303.

13. Ireland, J. A.; Hanna, P. C., Macrophage-enhanced germination of *Bacillus anthracis* endospores requires gerS. *Infect Immun* **2002,** 70, (10), 5870-2.

14. Weiner, M. A.; Hanna, P. C., Macrophage-mediated germination of *Bacillus anthracis* endospores requires the gerH operon. *Infect Immun* **2003,** 71, (7), 3954-9.

15. Golden, H. B.; Watson, L. E.; Lal, H.; Verma, S. K.; Foster, D. M.; Kuo, S. R.; Sharma, A.; Frankel, A.; Dostal, D. E., Anthrax toxin: pathologic effects on the cardiovascular system. *Front Biosci* **2009,** 14, 2335-57.

16. Pickering, A. K.; Merkel, T. J., Macrophages release tumor necrosis factor alpha and interleukin-12 in response to intracellular Bacillus anthracis spores. *Infect Immun* **2004,** 72, (5), 3069-72.

17. Erwin, J. L.; DaSilva, L. M.; Bavari, S.; Little, S. F.; Friedlander, A. M.; Chanh, T. C., Macrophage-derived cell lines do not express proinflammatory cytokines after exposure to *Bacillus anthracis* lethal toxin. *Infect Immun* **2001,** 69, (2), 1175-7.

18. Basu, S.; Kang, T. J.; Chen, W. H.; Fenton, M. J.; Baillie, L.; Hibbs, S.; Cross, A. S., Role of Bacillus anthracis spore structures in macrophage cytokine responses. *Infect Immun* **2007,** 75, (5), 2351-8.

19. Drysdale, M.; Olson, G.; Koehler, T. M.; Lipscomb, M. F.; Lyons, C. R., Murine innate immune response to virulent toxigenic and nontoxigenic *Bacillus anthracis* strains. *Infect Immun* **2007,** 75, (4), 1757-64.

20. Koehler, T. M., *Bacillus anthracis* physiology and genetics. *Mol Aspects Med* **2009,** 30, (6), 386-96.

21. Pinzón-Arango, P. A.; Nagarajan, R.; Camesano, T. A., Effects of L-alanine and inosine germinants on the elasticity of *Bacillus anthracis* spores. *Langmuir* **2010,** 26, (9), 6535-41.

22. Pickering, A. K.; Osorio, M.; Lee, G. M.; Grippe, V. K.; Bray, M.; Merkel, T. J., Cytokine response to infection with *Bacillus anthracis* spores. *Infect Immun* **2004,** 72, (11), 6382-9.

23. Pinzon-Arango, P. A.; Nagarajan, R.; Camesano, T. A., Role of *gerH* and *gerS* operons in germination of *Bacillus anthracis*. **In Preparation**.

24. Cordoba-Rodriguez, R.; Fang, H.; Lankford, C. S.; Frucht, D. M., Anthrax lethal toxin rapidly activates caspase-1/ICE and induces extracellular release of interleukin (IL)-1beta and IL-18. *J Biol Chem* **2004,** 279, (20), 20563-6.

25. Goldman, D. L.; Casadevall, A., Anthrax-associated shock. *Front Biosci* **2008,** 13, 4009-14.

26. Kalns, J.; Scruggs, J.; Millenbaugh, N.; Vivekananda, J.; Shealy, D.; Eggers, J.; Kiel, J., TNF receptor 1, IL-1 receptor, and iNOS genetic knockout mice are not protected from anthrax infection. *Biochem Biophys Res Commun* **2002,** 292, (1), 41-4.

Chapter 8

Thermodynamic model to predict macrophage-*Bacillus anthracis* spore interactions

8.1 Abstract

Phagocytosis of *Bacillus anthracis* spores by macrophages is the first step in the development of an anthrax infection. While several researchers have focused on the ability of spores to germinate and grow inside macrophages *in vitro*, no studies have investigated the mechanisms of spore adhesion to macrophages. Decontamination of *B. anthracis* spores could be significantly improved if the chemical basis of spore adherence was understood. A thermodynamic approach was used to calculate the Gibbs free energy of adhesion changes (ΔG_{adh}) for spore-macrophage interactions, based on measuring contact angles with three probe liquids. The role of germinant receptors on macrophage-spore interactions was also investigated. The wild-type *B. anthracis* 34F2, expressing all germinant receptors, mutant strains $gerH^+$ and $gerS^+$, expressing only the GerH and GerS receptor, respectively, and the mutant ger_{null}, lacking all germinant receptors were investigated. Strong adhesion energies were found with the ger_{null} strain suggesting that the interaction of this strain with macrophages is most favorable compared to other mutants. Low adhesion energies were observed with the wild-type 34F2 strain suggesting that adhesion between macrophages and *B. anthracis* 34F2 are less favorable. Germinant receptors on *B. anthracis* spores may play a role in macrophage-spore interactions. Phagocytosis of spores that adhere too strongly to macrophages may not occur, therefore inhibiting germination inside the macrophage. These results help form the mechanistic explanation of how macrophages engulf spores during the onset of an anthrax infection, and may lead to the development of anti-sporal compounds that prevent the germination of spores in macrophages.

8.2 Introduction

Before invasion of macrophages and germination of spores can occur, *B. anthracis* spores must adhere or bind to phagocytes to allow invasion[1]. The interaction of bacteria and biotic surfaces including macrophages is governed by long range forces such as steric and electrostatic forces, and by short range forces that include hydrophobicity, surface free energy, surface charge, and van der Waals interactions[2]. Furthermore, bacterial adhesion is also described by specific interactions, such as the binding of ligands on bacterial surfaces to receptors on eukaryotic cells, and by non-specific interactions or long range forces.

Many researchers have described bacterial adhesion in terms of surface free energy to predict I adhesion is favorable to a determined surface[3, 4]. Thermodynamic models such as the van Oss-Chaudhury-Good (VCG) approach, have been developed to account for the non-specific Lifshitz-van der Waals (LW) and acid/base (AB) interactions[5, 6]. Gibbs free energy of adhesion can be calculated based on the contact angle of several probe liquids on a given surface or a layer of bacterial cells[5]. While adhesion between *B. anthracis* and macrophages is receptor mediated, the long range forces governing spore adhesion to macrophages have not been well investigated. Studies have found that *B. anthracis* promotes interactions with macrophages due to the presence of a *Bacillus* collagen-like protein A (BclA) in the exosporium of spores, and an S-layer protein A (BslA) on the cell wall of vegetative *B. anthracis*[7, 8]. However, the presence of germinant receptors of *B. anthracis* and their role on the adhesion of spores to macrophages have not been studied. In this paper, we describe the adhesion of *B. anthracis* and its ger-mutants to macrophages using a thermodynamic model that predicts the favorability of adhesion based on the calculations of interfacial free energies from measuring contact angles on *B. anthracis* and macrophages, following the van Oss-Chaudhury-Good (VCG) approach[9, 10].

8.3 Materials and Methods

8.3.1 Contact Angle Measurements

B. anthracis spores at a concentration of 10^9 bacteria/mL and murine macrophages RAW 264.7 at a concentration of 10^6 cells/mL were deposited on 0.45 µm and 8 µm pore-size cellulose acetate filters (Millipore Corp.), respectively through vacuum filtration. The filters were left to dry for 75 min at room temperature in accordance to Liu et al.[3] Contact angles of droplets of ultrapure water (Millipore Corp., Bedford, MA), diiodomethane (99% pure, Sigma-Aldrich, St. Louis, MO), and formamide (99% pure, Sigma-Aldrich) were measured on monolayers of bacterial and cellular lawns using the sessile drop technique with a goniometer (Ramé-Hart, Netcong, NJ) at room temperature. Three replicate contact angles were taken per probe liquid per filter.

8.3.2 Interfacial Tensions and Gibbs Free Energy of Adhesion

Surface thermodynamic properties of *Bacillus* spores have been calculated using the van Oss-Chaudhury-Good (VCG) approach where the interfacial tensions of individual substrata are derived from the contact angles of three probe liquids[9, 12]. The total surface tension, γ, is the sum of the apolar or Lifshitz-van der Waals (LW) interactions and the acid-base (AB) interactions, expressed as

$$\gamma_{Total} = \gamma^{LW} + \gamma^{AB} \tag{6}$$

where the AB component of the surface tension equals

$$\gamma^{AB} = 2\sqrt{\gamma^{+}\gamma^{-}} \tag{7}$$

where γ^- and γ^+ are the electron-donating and electron-accepting surface free energy parameters, which determine the ability of the spores to exert acid-base interactions on a comparative scale with respect to a reference liquid probe[10].

The Young-Dupré equation can be used to relate the interfacial tensions between the liquid (L) and the solid (S), and the contact angle made by a drop of liquid deposited on a horizontal solid surface, given by

$$(1 + cos\theta)\,\gamma_L = 2\sqrt{\gamma_S^{LW}\gamma_L^{LW}} + 2\sqrt{\gamma_S^+\gamma_L^-} + 2\sqrt{\gamma_S^-\gamma_L^+} \quad (8)$$

Since the interfacial tension parameters of completely characterized liquids can be found in the literature[10, 13], the parameters of the solid surface can be calculated, as we have done in previous studies[3, 4].

If *B. anthracis* spores adhere to macrophages before phagocytosis takes place, then the Gibbs free energy of adhesion, ΔG_{adh}, can be calculated by

$$\Delta G_{adh} = \gamma_{S-mac} - \gamma_{S-L} - \gamma_{mac-L} \quad (9)$$

or

$$\Delta G_{adh} = \Delta G_{\mathrm{adh}}^{\mathrm{LW}} + \Delta G_{\mathrm{adh}}^{\mathrm{AB}} \quad (10)$$

where $\gamma_{S\text{-}mac}$ is the interfacial tension between spores and macrophages, $\gamma_{S\text{-}L}$ is the interfacial tension for spores and liquid media, $\gamma_{mac\text{-}L}$ is the interfacial tension for macrophages and liquid media and ΔG^{LW} and ΔG^{AB} are the LW and AB terms that contribute to the Gibbs free energy

change upon adhesion in aqueous media. The methods to calculate the interfacial free energy between 2 solids in a medium has been previously discussed[3, 4] and we have followed the same procedures to calculate the interfacial tensions and free energies of adhesion between *B. anthracis* spores and murine macrophages.

8.4 Results

8.4.1 Contact Angles and Surface Tensions

Contact angles were measured on lawns of cells that had reached equilibrium in their drying state[3, 10]. Allowing the lawns of cells to dry for 75 min resulted in the probing liquid to bind only to the surface of the cells. Using measured contact angles with water, diiodomethane, and formamide, allowed us to calculate the interfacial tension components of *B. anthracis* 34F2 and its mutants (Table 8). For *B. anthracis* spores, the water contact angles were lower for spores expressing all germinant receptors (44 ± 4º for *B. anthracis* 34F2) and were higher for the mutants *B. anthracis* $gerS^+$, $gerH^+$, and ger_{null} with contact angles of 66 ± 9º, 66 ± 4º, and 63 ± 5º, respectively. We did not observe a trend in the diiodomethane and formamide contact angles for any *B. anthacis* strains tested. For macrophages, the highest contact angle occurred when water was being used as the probe liquid (104 ± 1º), and contact angles were lower after the cells were probed with diiodomethane and formamide (75 ± 5º and 42 ± 2º, respectively).

The LW components of interfacial tensions for *B. anthracis* spores were lower for spores that contained all germinant receptors (*B. anthracis* 34F2), and increased with the partial deletion of germinant receptors (Table 8). The electron donating component, γ^-, of the interfacial tension of *B. anthracis* 34F2 was much greater than the electron donating component of the mutant strains. Our electron donating value for *B. anthracis* 34F2 of 44.5 mJ/m^2 is close to the *B.*

anthracis 34F2 value reported by Chen et al. of 42.5 mJ/m^2.[12] The electron accepting component, γ^+, remained low for all *B. anthracis* strains with the exception of the *gerH*$^+$ strain, which was significantly higher than the value for other spore strains (1.8 mJ/m^2). Since the electron donating component of the wild-type strain was much higher than the value of the mutant strains, this caused the value of the acid-base interfacial tension component, γ^{AB}, to be the highest value of all *B. anthracis* strains (11.9 mJ/m^2). Total surface tensions were calculated and the highest value was observed for *B. anthracis gerH*$^+$, which was caused by the high value observed for the electron accepting component.

Table 8. Contact angles and surface free energy components of *B. anthracis* and murine macrophages

Sample	Contact angle (°)[a]			Interfacial tension parameter value (mJ/m^2)[b]				
	θ_W	θ_D	θ_F	γ^{LW}	γ^-	γ^+	γ^{AB}	γ^{total}
B. ant 34F2	44 ± 4	47 ± 4	48 ± 9	27.0	44.5	0.8	11.9	38.9
B. ant ger S+	66 ± 9	41 ± 2	54 ± 8	32.9	16.9	0.4	5.3	38.3
B. ant ger H+	66 ± 4	36 ± 4	40 ± 2	36.6	10.4	1.8	8.7	45.2
B. ant ger-null	63 ± 5	46 ± 2	54 ± 3	29.9	21.5	0.6	7.0	36.9
Macrophages	104 ± 1	75 ± 5	42 ± 2	23.2	9.3	16.1	24.4	47.6

[a] θ_W, θ_D, θ_F; measured contact angles of water, diiodomethane, and formamide.

[b] γ^{LW}, Lifshitz-van der Waals component of interfacial tension; γ^-, γ^+, electron-donor and electron-acceptor components of interfacial tension; γ^{AB}, Lewis acid-base component of interfacial tension; γ^{total}, total surface tension found through the VCG approach.

A significantly high electron accepting component, γ^+, and significantly low electron donating component, γ^-, were observed for murine macrophages (16.1 mJ/m^2. and 9.3 mJ/m^2, respectively), that resulted in the acid-base interfacial tension component to be the highest in our

system with a value of 24.4 mJ/m^2. The total surface tension of macrophages was found to be the highest of all cells probed with a value of 47.6 mJ/m^2.

8.4.2 Interfacial Tensions and Gibbs Free Energy of Adhesion

The surface or interfacial tensions were also calculated for the three types of interfaces: spore-liquid, macrophage-liquid, and spore-macrophages (Table 9). The interaction of the wild-type *B. anthracis* 34F2 strain and water resulted in the only negative interfacial tension values among all the *B. anthracis* strains tested with a value of -13.4 mJ/m^2. *B. anthracis gerH*$^+$ had the highest interfacial tension between the spore and water with a value of 15.4 mJ/m^2, due to the high LW and AB values of the individual surface tension components. The new interfacial tension spore-macrophage was found to be negative for all *B. anthracis* strains except for the *gerH*$^+$ strain, which was slightly positive (0.6 mJ/m^2). The interfacial tension between macrophages and water was found to be low compared to the *B. anthracis* strains with a value of 4.1 mJ/m^2.

Gibbs free energy of adhesion calculations showed that *B. anthracis* 34F2 has the least negative ΔG_{adh} value (-13.4 mJ/m^2), indicating that adhesion would be least favorable between *B. anthracis* 34F2 strain and macrophages (Table 9). Deletion of germinant receptors resulted in mutant strains having a more negative Gibbs free energy of adhesion. After decoupling the ΔG_{adh} values into their individual AB and LW components, we found that the acid-base interactions decreased with the deletion of germinant receptors and these interactions were much greater compared to the Lifshitz-van de Waals interactions, suggesting that AB interactions controlled the overall Gibbs free energy of adhesion.

Table 9. Interfacial free energies and Gibbs free energy of adhesion

Sample	Interfacial free energy (mJ/m^2)			Gibbs free energy of adhesion (mJ/m^2)[a]		
	Spore-liquid	Macrophage-liquid	Spore-Macrophage	ΔG^{AB}	ΔG^{LW}	ΔG_{adh}
B. ant 34F2	-13.2	-	-22.4	-13.2	-0.2	-13.4
B. ant gerS$^+$	9.3	-	-6.3	-19.5	-0.4	-19.8
B. ant gerH$^+$	15.4	-	0.6	-18.5	-0.5	-18.9
B. ant ger_{null}	4.1	-	-9.9	-17.9	-0.3	-18.2
Macrophages	-	4.1	-	-	-	-

[a] ΔG^{AB}, Lewis acid-base component of the Gibbs free energy change; ΔG^{LW}, Lifshitz-van der Waals component of Gibbs free energy change; ΔG_{adh}, total Gibbs free energy of adhesion

8.5 Discussion

8.5.1 Thermodynamic Modeling and Favorability of Adhesion

Understanding the role that macrophages play in the initiation and propagation of a *B. anthracis* infection may be critical for understanding the mechanism by which the spore causes disease. While spore-macrophage adhesion is receptor mediated, the use of the van Oss-Chaudhury-Good (VCG) model allowed us to study the non-specific interactions of spore adhesion to macrophages by decoupling surface free energies into their fundamental components and understand their interactions in order to model the onset of an anthrax infection. Differences in contact angles were observed among the *B. anthracis* mutants (Table 8). The absence of some or all germinant receptors resulted in spore surfaces that were more hydrophobic than the wild-type *B. anthracis* 34F2. This change in hydrophobicity suggests that the coat and exosporium proteins, such as BclA, are not the only proteins that contribute to spore surface properties and that germinant receptors may play a role in spore-macrophage interactions.

To determine the contributions of germinant receptors on spore-macrophage interactions, the LW and AB components of interfacial tension were calculated (Table 8). All strains of *B. anthracis* were found to be monopolar since the electron donating component, γ^-, was approximately one order of magnitude greater than the electron accepting component γ^+. The *B. anthracis* strain that expressed only the GerH receptor had a much higher γ^+ value than other *B. anthracis* strains suggesting that *B. anthracis gerH*$^+$ has a greater ability to participate in electron acceptor interactions, such as hydrogen bonding. The high γ^+ caused the total interfacial tension of *B. anthracis gerH*$^+$ to be the highest among all the strains tested.

We also examined the interfacial free energies for the three types of interfaces: spore-liquid, macrophage-liquid, and spore-macrophage (Table 9). The interfacial free energy spore-water was found to be negative for the *B. anthracis* 34F2 strain but not for its mutants suggesting that the interaction between spores and macrophages was least favorable for the *B. anthracis* 34F2 strain compared to the *B. anthracis* mutants.

After estimating the relative strengths of acid-base and Lifshitz-van der Waals interactions we found that ΔG^{LW} did not change significantly among all the *B. anthracis* strains. Lifshitz-van der Waals interactions are a sum of non-polar interactions[9]. Since all *B. anthracis* strains and macrophages presented comparable γ^{LW} values, the ΔG^{LW} values were close to zero suggesting that non-polar interactions do not play a significant role in the adhesion of *B. anthracis* to macrophages. In the case of AB interactions differences were noted in the ΔG^{AB} contributions and the calculated values were more significant compared to their LW counterparts. Based on the thermodynamic modeling, the adhesion behavior of *B. anthracis* spores with macrophages is dominated by acid-base interactions, most likely due to hydrogen bonding. Similar results have been observed when investigating the adhesion between

Pseudomona aeruginosa and bovine serum albumin (BSA)[4] and the adhesion between *Escherichia coli* and uroepithelial cells[3].

Higher ΔG_{adh} values were observed with the wild-type *B. anthracis* 34F2 and the Gibbs free energy of adhesion became more negative with deletion of germinant receptors (Table 9). Prior work has suggested that adhesion of *B. anthracis* spores to cells or inert surfaces is due to the presence of the protein BclA on the surface of the exosporium[1, 14], or coat proteins[12]. Our Gibbs free energy of adhesion, ΔG_{adh}, values suggest that germinant receptors also play a role on adhesion of spores. Adhesion was increased in the mutants since the deletion of some or all germinant receptors caused *B. anthracis* spores to have a more favorable interaction with macrophages. If the adhesion energy is too strong, the spores may stick to the surface of the macrophage and phagocytosis may not occur. In a previous study, we observed that while ger_{null} and $gerS^{+}$ had the ability to germinate in L-alanine and inosine solutions[15], the mutated strains failed to germinate inside of macrophages but germinated outside in cell growth media[16]. Phagocytosis failure may be due to the spore adhering too strongly to the surface of macrophages. On the contrary, *B. anthracis* 34F2 germinated inside macrophages[16]. Since low adhesion energies were observed with the wild-type strain, these spores may come near the macrophage and be phagocytosed.

Even though *B. anthracis* ger_{null} responds weakly to germinants, as observed in our previous study[15], this study suggests that adhesion of *B. anthracis* to macrophages is affected by the presence of germinant receptors.

8.6 Conclusions

We have presented a quantitative explanation for the role of germinant receptors on macrophage-spore interactions through the use of a thermodynamic model. While the presence of germinant receptors has been linked to the ability of spores to germinate, our study provides evidence that Ger receptors also play a role on macrophage-*B. anthracis* interactions. Future work is needed to develop sporicidal compounds that inhibit this interaction.

8.7 Acknowledgments

This work was supported in part by the National Science Foundation (CBET 0827229 and CBET 0922901) and the Defense Threat Reduction Agency (DTRA) Project BA07PRO102.

REFERENCES

1. Glomski, I. J., *Bacillus anthracis* Dissemination through Hosts. In *Bacillus anthracis and Anthrax*, Bergman, N. H., Ed. John Wiley & Sons, Icn.: 2011.

2. Fang, H. H.; Chan, K. Y.; Xu, L. C., Quantification of bacterial adhesion forces using atomic force microscopy (AFM). *J Microbiol Methods* **2000,** 40, (1), 89-97.

3. Liu, Y.; Gallardo-Moreno, A. M.; Pinzon-Arango, P. A.; Reynolds, Y.; Rodriguez, G.; Camesano, T. A., Cranberry changes the physicochemical surface properties of *E. coli* and adhesion with uroepithelial cells. *Colloids Surf B Biointerfaces* **2008,** 65, (1), 35-42.

4. Atabek, A.; Liu, Y.; Pinzon-Arango, P. A.; Camesano, T. A., Importance of LPS structure on protein interactions with Pseudomonas aeruginosa. *Colloids Surf B Biointerfaces* **2008,** 67, (1), 115-21.

5. van Loosdrecht, M. C.; Lyklema, J.; Norde, W.; Schraa, G.; Zehnder, A. J., The role of bacterial cell wall hydrophobicity in adhesion. *Appl Environ Microbiol* **1987,** 53, (8), 1893-7.

6. Liu, Y.; Strauss, J.; Camesano, T. A., Thermodynamic Investigation of Staphylococcus epidermidis interactions with protein-coated substrata. *Langmuir* **2007,** 23, (13), 7134-42.

7. Cybulski, R. J., Jr.; Sanz, P.; Alem, F.; Stibitz, S.; Bull, R. L.; O'Brien, A. D., Four superoxide dismutases contribute to Bacillus anthracis virulence and provide spores with redundant protection from oxidative stress. *Infect Immun* **2009,** 77, (1), 274-85.

8. Mock, M.; Fouet, A., Anthrax. *Annu Rev Microbiol* **2001,** 55, 647-71.

9. van Oss, C. J.; Good, R. J.; Chaudhury, M. K., Additive and Nonadditive Surface Tension Components and the Interpretation of Contact Angles. *Langmuir* **1988,** 4, 884-891.

10. van der Mei, H. C.; Bos, R.; Busscher, H. J., A reference guide to microbial cell surface hydrophobicity based on contact angles. *Colloids Surf B Biointerfaces`* **1998,** 11, 213-221.

11. Pinzón-Arango, P. A.; Nagarajan, R.; Camesano, T. A., Effects of L-alanine and inosine germinants on the elasticity of *Bacillus anthracis* spores. *Langmuir* **2010,** 26, (9), 6535-41.

12. Chen, G.; Driks, A.; Tawfiq, K.; Mallozzi, M.; Patil, S., *Bacillus anthracis* and *Bacillus subtilis* spore surface properties and transport. *Colloids Surf B Biointerfaces* **2010,** 76, (2), 512-8.

13. Wu, W.; Giese, R. F.; van Oss, C. J., Evaluation of the Lifshitz-van de Waals/acid-base approach to determine surface tension components. *Langmuir* **1995,** 11, 379-382.

14. Bozue, J.; Moody, K. L.; Cote, C. K.; Stiles, B. G.; Friedlander, A. M.; Welkos, S. L.; Hale, M. L., Bacillus anthracis spores of the bclA mutant exhibit increased adherence to epithelial cells, fibroblasts, and endothelial cells but not to macrophages. *Infect Immun* **2007,** 75, (9), 4498-505.

15. Pinzon-Arango, P. A.; Nagarajan, R.; Camesano, T. A., Role of *gerH* and *gerS* operons in germination of *Bacillus anthracis*. **In Preparation**.

16. Pinzon-Arango, P. A.; Nagarajan, R.; Camesano, T. A., Role of germinant receptors of *Bacillus anthracis* on invasion and cytokine response. **In preparation**.

Chapter 9

Extra Experiments

The following are experiments that were done during the course of the past few years but have not been used for any publications

9.1 Release of Dipicolinic Acid from Spore's Core of B. anthracis after Exposure to L-alanine and/or Inosine

9.2 Materials and Methods

Germination of *B. anthracis* was monitored by determining the amount of dipicolinic acid (DPA) released from the core of the spore after exposure to L-alanine and/or inosine as a function of time. All chemicals were obtained from Sigma-Aldrich (St. Louis, MO) unless otherwise noted. DPA measurements on spores were performed as previously described.[1] A 50 µL solution of 4 mM terbium tri-chloride ($TbCl_3$) were placed in each well of a 96 well-plate, along with 100 µL of a solution of increasing concentrations of L-alanine (12.5 mM, 25 mM, 50 mM, and 100 mM) or increasing concentrations of inosine (1.25 mM, 2.5 mM, 5 mM, and 10 mM) or a mixture of both germinants (1.25 mM inosine + 12.5 mM L-alanine, 2.5 mM inosine + 25 mM L-alanine, 5 mM inosine + 50 mM L- alanine, and 10 mM inosine + 100 mM L-alanine) in 50 mM TRIS-HCl (pH= 8.0). The $TbCl_3$ and germinant solution was combined with 50 µL of *B. anthracis* spores at a concentration of 10^8 cells/mL. Terbium chloride reacts with DPA in spores and forms a chelate of terbium dipicolinate, $(Tb(DPA)_3)^{3-}$, which luminesces with UV excitation.[1] DPA release was quantitatively monitored by time-resolved fluorescence with a Gemini XPS Microplate Spectrofluorometer set at 37 °C. The microwell plate was read at various time intervals (up to 40 minutes), and the relative fluorescence units (RFU), which reflects the DPA release after exposure to germinants, were plotted against time.

9.3 Results

Our results show that L-alanine and inosine are strong germinants that induce the release of DPA from *B. anthracis* spores. L-alanine at concentrations of 50 and 100 mM are sufficient to start the germination process (Figure 34).

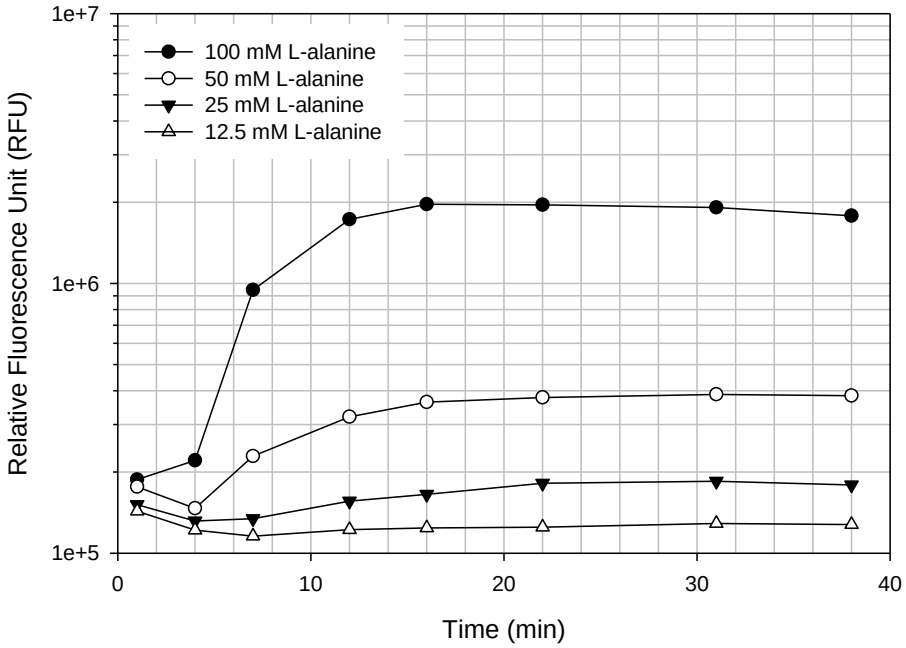

Figure 34. DPA release from the core of *B. anthracis* as a function of L-alanine concentration monitored by time-resolved fluorescence. Spectrofluorometer was set at 270 nm excitation wavelength, and fluorescence emission was collected at 546 nm, which corresponds to the optimal fluorescence spectra of the DPA-terbium complex.[1] The increase in fluorescence of the DPA-terbium complex was monitored over time in a microwell plate for up to 40 minutes. Experiment done in triplicates.

After 15 minutes of exposure to the germinant, the DPA released reached a limiting value. Low concentrations of L-alanine were not sufficient to cause the release of DPA from the spore core. Our results suggest that alanine concentrations not only affect the DPA release rate but also the amount of DPA released. This could be due to a smaller fraction of spores germinating at lower concentrations.

To allow for all the spore to germinate, we combined L-alanine with the germinant inosine (Figure 35).

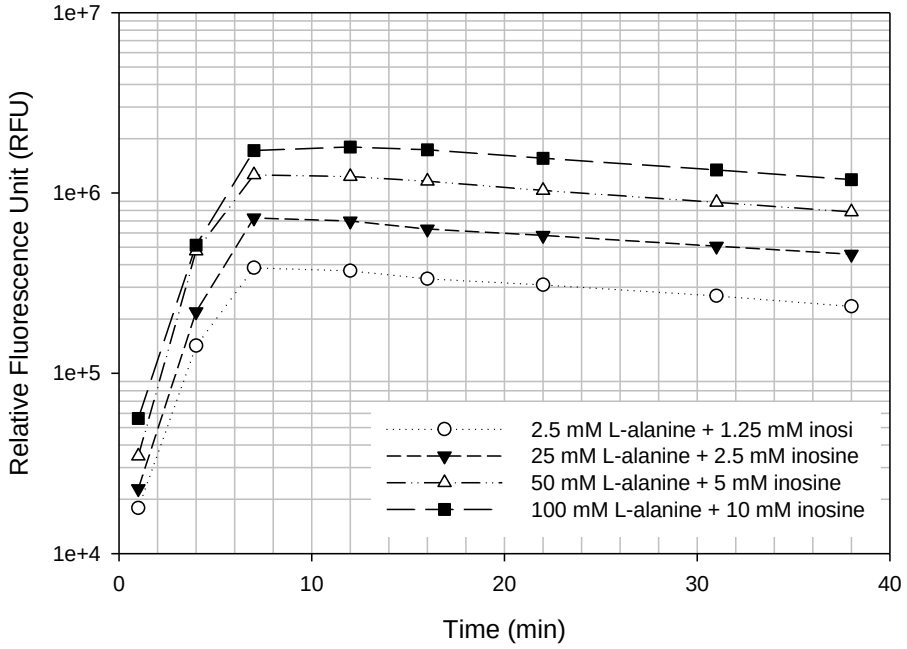

Figure 35. DPA release from the core of *B. anthracis* after exposure to a mixture of both germinants L-alanine and inosine at different concentrations. Spectrofluorometer was set at 270 nm excitation wavelength, and fluorescence emission was collected at 546 nm. The changes in fluorescence of the DPA-terbium complex was monitored over time in a microwell plate for up to 40 minutes. Experiment done in triplicates.

Our results showed that a higher amount of DPA was released from the spore after using both germinants, and little difference in RFU was observed low or high concentrations of germinants. Furthermore, the DPA release rate was similar among all concentrations tested and it was faster compared to the sample when L-alanine was used as the only germinant source. These results suggest that there may be a synergistic effect when both germinants are used; speeding up the germination of *B. anthracis* spore. Our results also showed that after 15 minutes of exposure to the germinant the RFU units started to decline, which could be due to sample bleaching.

1. Rosen, D. L.; Sharpless, C.; McGown, L. B., Bacterial Spore Detection and Determination by Use of Terbium Dipicolinate Photoluminescence. Anal. Chem. 1997, 69, (6), 1082-1085.

Chapter 10

Conclusions and Future Work

10.1 Conclusions

Recent terrorism events have shown that the microorganism responsible for anthrax infections, *Bacillus anthracis*, can be easily manipulated and can be used as a biological weapon[1]. These recent attacks have shown that there is a weakness in our defense programs and protection measures must be designed to understand the biology of the *B. anthracis* spore in order to design and develop anti-sporal compounds. *B. anthracis* spores are extremely resistant to chemical and environmental factors due to their ability to synthesize thick protein coats that prevent disinfectants from reaching genetic material[2]. The current theory of spore deactivation suggests that germination of spores is needed to kill *B. anthracis.* Germination of spores takes place after *B. anthracis* spores detect nutrients in the environment, where germinants bind to germinant receptors located in the inner membrane of the spore[3]. While germination of spores has been intensively studied through the use of AFM where changes in spore coats can be observed by obtaining high resolution images[4, 5], few studies have address the germination of spores through more quantitative assays.

With this in mind, the studies described in this thesis combine the remarkable capabilities of AFM together with other biological laboratory techniques to investigate the biological and physicochemical properties of *B. anthracis* spores during germination, virulence, and killing.

Investigations began using *Bacillus atrophaeus,* which is a close relative to *B. anthracis*. *B. atroaphaeus* was exposed to 1 mM DDA or 25 mM L-alanine for one hour. High resolution AFM images were obtained every 5 minutes and the root-mean-squared roughness of the spore surface was calculated. In this study, two different germination mechanisms where observed[6]. Germination with L-alanine causes the release of DPA from *B. atrophaeus* spores in less than 30 minutes. Roughness of spores do not change during germination suggesting that during the first

stages of germination, the spore coat remains intact and L-alanine causes internal restructuring of the spore. This effect may work its way to the outside of the spore after all internal changes have occurred. On the contrary, germination of *B. atrophaeus* with L-alanine resulted in an increase in roughness with time where the spore coats are degrading and breaking down one at the time. DDA starts acting from the outside of the spore and works its way in by causing the coat to rupture and form pores on the surface. Furthermore, during this investigation, we observed that over 99% of the spores get killed in less than 5 minutes after exposure to 1 mM DDA, suggesting that complete germination of spores is not needed to kill the spores[6].

In a second study, we used the AFM to measure changes in the mechanical properties of *B. anthracis* during germination with 50 mM L-alanine and 5mM inosine. We observed that sporulated *B. anthracis* had the highest elastic modulus and the lowest indentation depth by the AFM tip suggesting that the surface of *B. anthracis* is very hard compared to other bacterial species[7]. The elastic modulus decreased after exposure to the germinants and when *B. anthracis* were exposed to both germinants, the elastic modulus had decreased significantly. Lowest elastic moduli were observed with vegetative *B. anthracis* indicating that spore coats make the spore a hard microorganism incapable of being rupture through mechanical pressure of the AFM tip.

In another study, we investigated the ability of the antimicrobial peptide (AMP) chrysophsin-3 to change the mechanical properties of *B. anthracis* during germination and the roles of the AMP in spore killing. Sporulated, germinated, and vegetative *B. anthracis* were exposed to 0.22 mM chrysophsin-3 for one hour. Changes in elastic modulus were investigated and our results suggested that the AMP does not change the surface properties of sporulated of germinated *B. anthracis.* However, chrysophsin-3 had a significant effect in vegetative bacteria since the elastic modulus of vegetative *B. anthracis* increased after treatment with the AMP[8].

High resolutions AFM images suggest that chrysophsin-3 penetrated the cell wall of vegetative *B. anthracis* causing the lysis of the cell. Viability studies suggest that chrysophsin-3 was capable of killing *B. anthracis* spores; however, spore killing was more effective if germination of spores had commenced. This study suggests that chrysophsin-3 may be a suitable anti-sporal compound for the deactivation of *B. anthracis.*

In our fourth study, the role of germinant receptors in germination of *B. anthracis* was investigated. The wild-type *B. anthracis* 34F2 strain, which contains all germinant receptors, the *gerH*$^{+}$ and *gerS*$^{+}$ strain, which contain only the GerH or GerS receptor, and the *ger*$_{null}$ strain, which lacks all germinant receptors were investigated for their ability to germinated in 50 mM L-alanine and 5 mM inosine mixtures[9]. We found that the *gerH*$^{+}$ mutant had similar germination profiles compared to the wild-type strain and the *gerS*$^{+}$ was capable of initiating germination but at lower rates. Interestingly, the *ger*$_{null}$ mutant germinated similarly to the *gerS*$^{+}$ strain. While it has been suggested that *ger*$_{null}$ is incapable of germinating[10], our results suggests that this mutants strain can germinate if concentration of germinants are high in the media. Germination of the *B. anthracis* strain that lacked all germinant receptors suggests that germination may be happening through a receptor independent pathway or through a non-Ger specific receptor pathway. However, more research is needed to understand germination pathways of the *ger*$_{null}$ strain.

Our last study focused on the invasion and virulence of *B. anthracis* after macrophages had been infected with spores[11]. The wild-type strain was phagocytosed by macrophages and the spores were able to germinate inside the phagocytes. After germination, *B. anthracis* grew inside macrophages releasing toxins and causing the lysis of the cell. One the macrophage had been lysed, *B. anthracis* continued multiplying in the growth media or continued to infect other

macrophages. A similar trend was observed with the *gerH*$^{+}$ strain; however, lower numbers of spores where engulfed by macrophages. *B. anthracis gerS*$^{+}$ and *ger*$_{null}$ were engulfed by the spore. However, these two strains were not able to germinate inside macrophages or cause any lysis. In this study, we also investigated the ability of macrophages to induce cytokine responses after infection with *B. anthracis*. There was a dysregulation of IL-1β, IL-6, and TNF-α production after infection of macrophages. The mutant strains lacking 4 of 5 receptors induced a cytokine response at later times post-infection. Both sporulated and vegetative *B. anthracis* were able to elicit an immune response from macrophages.

Finally we make an attempt at understanding macrophage-spore interactions by using a thermodynamic approach that calculated the Gibbs free energy of adhesion, where the favorability of adhesion is investigated. We found that the wild-type *B. anthracis* strain has lower adhesion energies compared to the mutants. The highest adhesion energy was observed with the strain that lacks all germinant receptors. Through our thermodynamic model we could hypothesize that the *ger*$_{null}$ strain binds so strongly to the macrophage that it may be phagocytosed but germination does not occur. Or perhaps the strong adhesion prevents phagocytosis of the spore. This is the first study that attempts understanding macrophage-spore interactions through a mathematical model.

The results of this research can be summarized in Figure 36, where our results suggest that germination affects various spore surface properties, spore killing, virulence, macrophage response and cytokine release. We also showed that germination of spores can be modified by the presence or absence of germinant receptors and that other Ger-independent pathways may exist in *B. anthracis.*

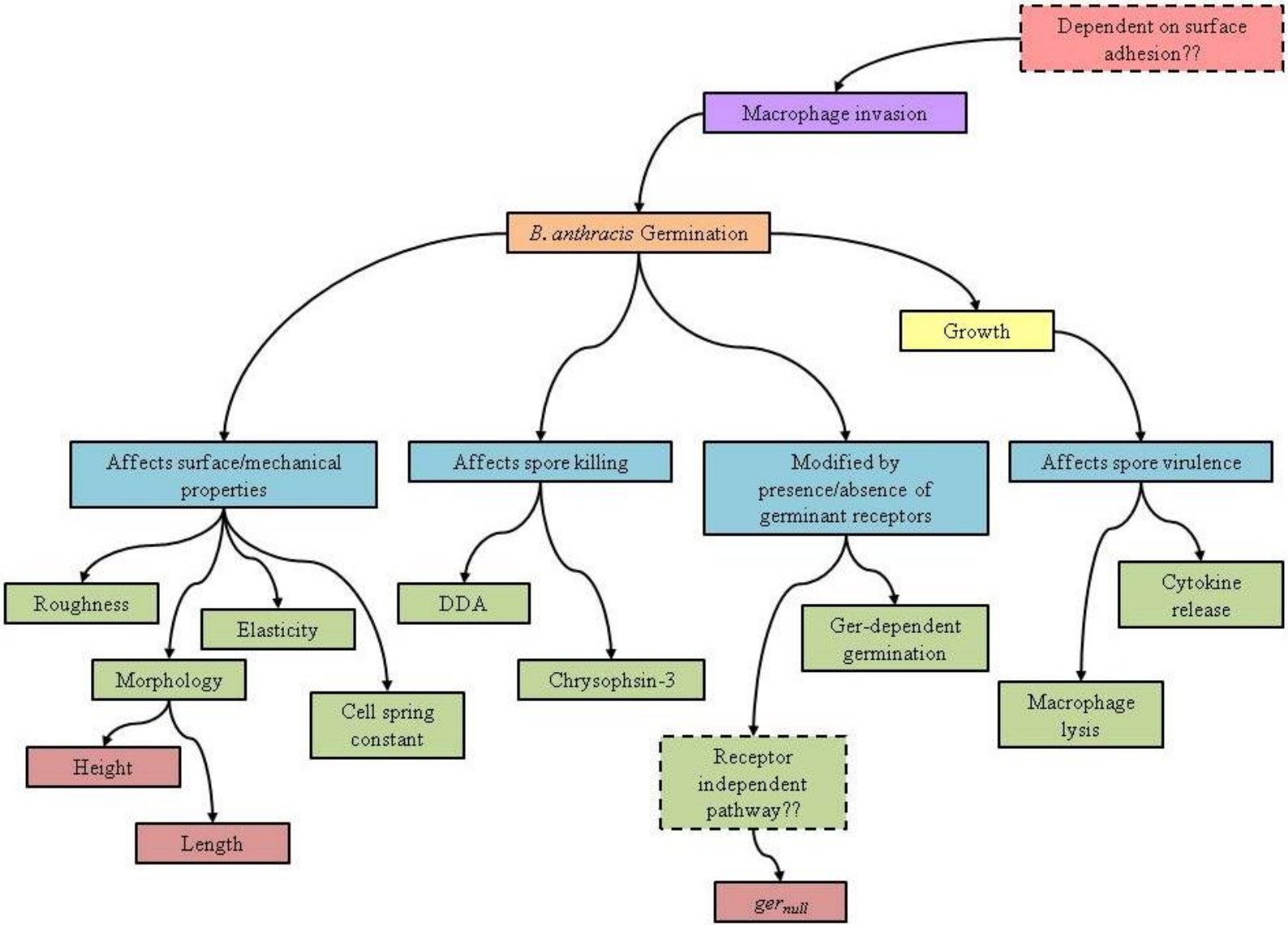

Figure 36. Germination of *B. anthracis* spores and its effects on spore surface, killing, and virulence.

10.2 Future Work

Future work will be beneficial to support the results of this thesis. First, investigation of the roles of the remaining three Ger receptors in germination of spores and virulence after macrophage infection can be beneficial in targeting specific receptors that inhibit the germination response and production of virulence factors when encountered by macrophages. *In vivo* experiments could help elucidate if activation of receptors is specific to the site of infection. If this is the case, different anti-sporal compounds that target different germinant receptors may be need to be developed.

An in-depth analysis of the adhesion or interaction that first takes place between spores and macrophages is crucial. Investigations are needed to determine what factors govern macrophage-spore interactions and if these interactions can be modified so the spore is engulfed by the macrophage but germination does not take place.

In addition, previous research has suggested that it is possible to change the properties of spores by changing the techniques employed for spore preparation[12]. Our protection measures must be designed to encompass the potential range of variability in these spore properties, engineering through changes in sporulation environments. At this time, we know little about how germinaton and virulence of spores depend on variation in the sporulation environment.

These are just a few directions that future work can take to improve our defense programs and prevent the use of *Bacillus anthracis* as a bioterrorism agent.

REFERENCES

1. Oncu, S.; Oncu, S.; Sakarya, S., Anthrax--an overview. *Med Sci Monit* **2003,** 9, (11), RA276-83.

2. Liu, H.; Bergman, N. H.; Thomason, B.; Shallom, S.; Hazen, A.; Crossno, J.; Rasko, D. A.; Ravel, J.; Read, T. D.; Peterson, S. N.; Yates, J., 3rd; Hanna, P. C., Formation and composition of the *Bacillus anthracis* endospore. *J Bacteriol* **2004,** 186, (1), 164-78.

3. Setlow, P., Spore germination. *Curr Opin Microbiol* **2003,** 6, (6), 550-6.

4. Zaman, M. S.; Goyal, A.; Dubey, G. P.; Gupta, P. K.; Chandra, H.; Das, T. K.; Ganguli, M.; Singh, Y., Imaging and analysis of *Bacillus anthracis* spore germination. *Microsc Res Tech* **2005,** 66, (6), 307-11.

5. Plomp, M.; Leighton, T. J.; Wheeler, K. E.; Hill, H. D.; Malkin, A. J., In vitro high-resolution structural dynamics of single germinating bacterial spores. *Proc Natl Acad Sci U S A* **2007,** 104, (23), 9644-9.

6. Pinzón-Arango, P. A.; Scholl, G.; Nagarajan, R.; Mello, C. M.; Camesano, T. A., Atomic force microscopy study of germination and killing of *Bacillus atrophaeus* spores. *J Mol Recognit* **2009,** 22, (5), 373-379.

7. Pinzón-Arango, P. A.; Nagarajan, R.; Camesano, T. A., Effects of L-alanine and inosine germinants on the elasticity of *Bacillus anthracis* spores. *Langmuir* **2010,** 26, (9), 6535-41.

8. Pinzon-Arango, P. A.; Nagarajan, R.; Camesano, T. A., Changes in Mechanical Properties and Killing of Bacillus anthracis 34F2 After Exposure to the Antimicrobial Peptide Chrysophsin-3 **Submitted**.

9. Pinzon-Arango, P. A.; Nagarajan, R.; Camesano, T. A., Role of *gerH* and *gerS* operons in germination of *Bacillus anthracis*. **In Preparation**.

10. Carr, K. A.; Lybarger, S. R.; Anderson, E. C.; Janes, B. K.; Hanna, P. C., The role of *Bacillus anthracis* germinant receptors in germination and virulence. *Mol Microbiol* **2010,** 75, (2), 365-75.

11. Pinzon-Arango, P. A.; Nagarajan, R.; Camesano, T. A., Role of germinant receptors of *Bacillus anthracis* on invasion and cytokine response. **In preparation**.

12. Baweja, R. B.; Zaman, M. S.; Mattoo, A. R.; Sharma, K.; Tripathi, V.; Aggarwal, A.; Dubey, G. P.; Kurupati, R. K.; Ganguli, M.; Chaudhury, N. K.; Sen, S.; Das, T. K.; Gade, W. N.; Singh, Y., Properties of *Bacillus anthracis* spores prepared under various environmental conditions. *Arch Microbiol* **2008,** 189, (1), 71-9.

Appendix 1: MatLab scripts to determine the Young's modulus of spores

A-1.1 MatLab script to convert raw data into force data

```
function [sep_points,force_appr,force_retr,kc,pathname,fname] =...
   force_convert(pathname,filename)

kc = 14;

% Define sensitivity of mica

Sensitivity = 34.67;

if nargin < 1
   [fname,pathname]=uigetfile;
end

% Open the data file for reading
fid = fopen([pathname, fname],'r');

% Read the header of the data file into memory.
i=1;
force_header(i,1)=cellstr(fgetl(fid));
 while ~strcmp(char(force_header(i,1)),'\*File list end');
     i=i+1;
     force_header(i,1)=cellstr(fgetl(fid));
 end

% Locate strings containing Sens. Deflection and Z scale.
SensDefl_force=char(getHeaderInfo( ...
   force_header,'\@Sens. Deflection: V',':','string'));
Zscale_force=char(getHeaderInfo( ...
   force_header,'\@4:Z scale: V [Sens. Deflection]',')','string'));
SensZscan_force=char(getHeaderInfo( ...
   force_header,'\@Sens. Zscan: V',':','string'));
ramp_force=char(getHeaderInfo( ...
   force_header,'\@4:Ramp size: V [Sens. Zscan]',')','string'));

% Since 2 deflection curves captured, need to separate out the appropriate
% Z scale conversion factor.
Zscale_force = Zscale_force(1,:);
ramp_force = ramp_force(1,:);

% Split SensDefl and Zscale strings into component parts, separated by
% spaces.
SensDefl_force=explode(SensDefl_force,' ');
```

```
Zscale_force=explode(Zscale_force,' ');
SensZscan_force = explode(SensZscan_force,' ');
ramp_force=explode(ramp_force,' ');

% Now convert the conversion factors from strings to numbers
SensDefl_force = str2double(SensDefl_force{3});
Zscale_force = str2double(Zscale_force{2});
SensZscan_force = str2double(SensZscan_force{3});
ramp_force = str2double(ramp_force{2});

Z_Cal_Factor = 0.99710;
ramp_size = round(SensZscan_force * ramp_force * Z_Cal_Factor);


j = length(force_header)+1;
fclose(fid);
raw_data = dlmread([pathname,fname],'\t',j,0);

% Determination of the configuration/location of the deflection data in the
% force curve file via user interface.
channel_button = questdlg(...
   'Please choose the channel used to capture the deflection data',...
   'Data Channel','Channel 1','Channel 2','Channel 2');

% Based on the configuration of the data (i.e., whether the deflection data
% were captured on the first or second channel of the AFM controller. This
% snippet of code is dedicated to Arzu.
if channel_button(1,9) == '1'
   curve_length = length(raw_data)/2;
   defl_appr = raw_data(1:curve_length);
   defl_retr = raw_data(curve_length+1:length(raw_data));
else
   curve_length = length(raw_data)/4;
   defl_appr = raw_data(2*curve_length+1:3*curve_length);
   defl_retr = raw_data(3*curve_length+1:4*curve_length);
end

for k = 1:curve_length;
   deflection_appr(k) = (Sensitivity*defl_appr(k)*Zscale_force)/65536;
   deflection_retr(k) = (Sensitivity*defl_retr(k)*Zscale_force)/65536;
end

for k = 1:curve_length;
   force_appr(k) = kc*deflection_appr(k);
   force_retr(k) = kc*deflection_retr(k);
end
```

```
% Define steps for separation axis.
for l = 1:curve_length
   sep_points(l) = l*(ramp_size/curve_length);
end
sep_points = sep_points';
force_appr=force_appr';
```

A-1.2 Script to find the indentation depth and Young's modulus

```
clear

[sep_points,force_appr,force_retr,kc,pathname,fname] = Hertz_convert;


% Define individual separation arrays for approach and retraction.
sep_appr = sep_points;


% Force data come in as row vectors, and are transposed into columns here.
force_appr = force_appr';

% Define an index array corresponding to the number of data points funny
% in the separation and force arrays.
i = (1:length(sep_points))';

% Plot the unmodified approach curve.
fig1 = figure;
plot(sep_appr,force_appr)

% Step 1: Define non-linear portion of the curve.
h = helpdlg('Draw one line parallel to the constant compliance region and another that is parallel
to the zero separation region');
uiwait(h);

% Turn on the data cursor to allow user to select points.
datacursormode on
dcm_obj = datacursormode(fig1);
set(dcm_obj,'DisplayStyle','window')

% Step 2: Constant compliance in the approach curve.
h = helpdlg('Click the two points in the constant compliance region ','Step 1');
uiwait(h);

% Record points for approach curve constant compliance.
```

```
w = waitforbuttonpress;
cc_appr(1,:)=struct2array(getCursorInfo(dcm_obj));
w = waitforbuttonpress;
cc_appr(2,:)=struct2array(getCursorInfo(dcm_obj));

% Step 2: Zero interaction in the approach curve.
h = helpdlg('Click the two points describing the zero interaction region for the approach
curve','Step 2');
uiwait(h);

% Record points for approach curve zero interaction.
w = waitforbuttonpress;
zi_appr(1,:)=struct2array(getCursorInfo(dcm_obj));
w = waitforbuttonpress;
zi_appr(2,:)=struct2array(getCursorInfo(dcm_obj));
close(fig1)

% Calculate the vertical offsets for each curve based on the average
% distance from the X-axis of the previously-defined zero interaction
% region.
%force_offset_appr = mean(force_appr(zi_appr(1,5):zi_appr(2,5)));
%force_offset_retr = mean(force_retr(zi_retr(1,5):zi_retr(2,5)));
force_offset_appr = mean(force_appr(zi_appr(1,4):zi_appr(2,4)));

% Shift both curves to the X-axis using the offsets calculated above.
for i = 1:length(force_appr)
   force_appr(i) = force_appr(i) - force_offset_appr;
end

% Sort separation data in ascending order.
sep_appr(:,1) = sort(sep_appr);

% Shift both curves to the Y-axis using the offsets calculated above.
for i = 1:length(force_appr)
   sep_appr(i) = sep_appr(i) - zi_appr(1,2);
end

plot(sep_appr,force_appr,'b');

% Step 1: Define non-linear portion of the curve.
h = helpdlg('Draw one line parallel to the constant compliance region and another that is parallel
to the zero separation region');
uiwait(h);

% Turn on the data cursor to allow user to select points.
datacursormode on
```

```
dcm_obj = datacursormode(fig1);
set(dcm_obj,'DisplayStyle','window')

% Choose two points to define non-linear region of the curve.
h = helpdlg('Choose the two points that define the non-linear region of the curve');
uiwait(h);

% Record points for non-linear region.
w = waitforbuttonpress;
non_lin(1,:)=struct2array(getCursorInfo(dcm_obj));
w = waitforbuttonpress;
non_lin(2,:)=struct2array(getCursorInfo(dcm_obj));
close(fig1);

% Export non-linear region data.
j1=non_lin(1,4);j2=non_lin(2,4);
sep_appr=sep_appr';force_appr=force_appr';
for j=j1:j2
   i=j-j1+1;
   x(i)=sep_appr(j);
   y(i)=force_appr(j);
end
Depth=x';Force=y';
Depth=abs(Depth);
plot(Depth,Force)

E=nlinfit(Depth,Force,@young,1);
ftheory=(2/pi)*tan(pi*40/180)*(E/(1-0.5^2)).*Depth.^2;
r=corrcoef(Force,ftheory);
r2=r.^2;
R2=r2(1,2);
plot(Depth,Force,'b',Depth,ftheory,'m')
legend('experiment','theory')
xlabel('Indentation depth (nm)');
ylabel('Force (nN)');
```

Appendix 2: MatLab script to determine cellular spring constants

A-2.1 MatLab script to convert raw data into deflection data

```
function [sep_points,deflection_appr, pathname,fname] =...
   Cell_spring_convert(pathname,filename)

% Define sensitivity of mica

Sensitivity = 34.67;

if nargin < 1
   [fname,pathname]=uigetfile;
end

% Open the data file for reading
fid = fopen([pathname, fname],'r');

% Read the header of the data file into memory.
i=1;
force_header(i,1)=cellstr(fgetl(fid));
 while ~strcmp(char(force_header(i,1)),'\*File list end');
     i=i+1;
     force_header(i,1)=cellstr(fgetl(fid));
 end

% Locate strings containing Sens. Deflection and Z scale.
SensDefl_force=char(getHeaderInfo( ...
   force_header,'\@Sens. Deflection: V',':','string'));
Zscale_force=char(getHeaderInfo( ...
   force_header,'\@4:Z scale: V [Sens. Deflection]',')','string'));
SensZscan_force=char(getHeaderInfo( ...
   force_header,'\@Sens. Zscan: V',':','string'));
ramp_force=char(getHeaderInfo( ...
   force_header,'\@4:Ramp size: V [Sens. Zscan]',')','string'));

% Since 2 deflection curves captured, need to separate out the appropriate
% Z scale conversion factor.
Zscale_force = Zscale_force(1,:);
ramp_force = ramp_force(1,:);

% Split SensDefl and Zscale strings into component parts, separated by
% spaces.
SensDefl_force=explode(SensDefl_force,' ');
Zscale_force=explode(Zscale_force,' ');
SensZscan_force = explode(SensZscan_force,' ');
```

```
ramp_force=explode(ramp_force,' ');

% Now convert the conversion factors from strings to numbers
SensDefl_force = str2double(SensDefl_force{3});
Zscale_force = str2double(Zscale_force{2});
SensZscan_force = str2double(SensZscan_force{3});
ramp_force = str2double(ramp_force{2});

Z_Cal_Factor = 0.99710;
ramp_size = round(SensZscan_force * ramp_force * Z_Cal_Factor);


j = length(force_header)+1;
fclose(fid);
raw_data = dlmread([pathname,fname],'\t',j,0);

% Determination of the configuration/location of the deflection data in the
% force curve file via user interface.
channel_button = questdlg(...
   'Please choose the channel used to capture the deflection data',...
   'Data Channel','Channel 1','Channel 2','Channel 2');

% Based on the configuration of the data (i.e., whether the deflection data
% were captured on the first or second channel of the AFM controller. This
% snippet of code is dedicated to Arzu.
if channel_button(1,9) == '1'
   curve_length = length(raw_data)/2;
   defl_appr = raw_data(1:curve_length);
   defl_retr = raw_data(curve_length+1:length(raw_data));
else
   curve_length = length(raw_data)/4;
   defl_appr = raw_data(2*curve_length+1:3*curve_length);
   defl_retr = raw_data(3*curve_length+1:4*curve_length);
end

for k = 1:curve_length;
   deflection_appr(k) = (Sensitivity*defl_appr(k)*Zscale_force)/65536;
   deflection_retr(k) = (Sensitivity*defl_retr(k)*Zscale_force)/65536;
end

% Define steps for separation axis.
for l = 1:curve_length
   sep_points(l) = l*(ramp_size/curve_length);
end
sep_points=sep_points';
deflection_appr=deflection_appr';
```

A-2.2 MatLab script to find cellular spring constant

```
[sep_points,deflection_appr,pathname,fname] = Cell_spring_convert;


kc=14;

% Define individual separation arrays for approach and retraction.
sep_appr = sep_points;


% Define an index array corresponding to the number of data points
% in the separation and force arrays.
i = (1:length(sep_points))';

% Plot the unmodified approach curve.
fig1 = figure;
plot(sep_appr,deflection_appr)

% Step 1: Define non-linear portion of the curve.
h = helpdlg('Draw one line parallel to the constant compliance region');
uiwait(h);

% Turn on the data cursor to allow user to select points.
datacursormode on
dcm_obj = datacursormode(fig1);
set(dcm_obj,'DisplayStyle','window')

% Step 2: Constant compliance in the approach curve.
h = helpdlg('Click the two points in the constant compliance region to find offset ','Step 1');
uiwait(h);

% Record points for approach curve constant compliance.
w = waitforbuttonpress;
cc_appr(1,:)=struct2array(getCursorInfo(dcm_obj));
w = waitforbuttonpress;
cc_appr(2,:)=struct2array(getCursorInfo(dcm_obj));

% Step 2: Zero interaction in the approach curve.
h = helpdlg('Click the two points describing the zero interaction region for the approach
curve','Step 2');
uiwait(h);

% Record points for approach curve zero interaction.
w = waitforbuttonpress;
zi_appr(1,:)=struct2array(getCursorInfo(dcm_obj));
```

```
w = waitforbuttonpress;
zi_appr(2,:)=struct2array(getCursorInfo(dcm_obj));
close(fig1)

% Calculate the vertical offsets for each curve based on the average
% distance from the X-axis of the previously-defined zero interaction
% region.
deflection_offset_appr = mean(deflection_appr(zi_appr(1,4):zi_appr(2,4)));

% Shift both curves to the X-axis using the offsets calculated above.
for i = 1:length(deflection_appr)
   deflection_appr(i) = deflection_appr(i) - deflection_offset_appr;
end

% Sort separation data in ascending order.
sep_appr(:,1) = sort(sep_appr);

% Shift both curves to the Y-axis using the offsets calculated above.
for i = 1:length(deflection_appr)
   sep_appr(i) = sep_appr(i) - zi_appr(1,2);
end

plot(sep_appr,deflection_appr,'b');

% Step 1: Define slope.
h = helpdlg('Draw one line parallel to the constant compliance region');
uiwait(h);

% Turn on the data cursor to allow user to select points.
datacursormode on
dcm_obj = datacursormode(fig1);
set(dcm_obj,'DisplayStyle','window')

% Step 2: define bacteria turgor pressure by selecting two points in the constant compliance
region.
h = helpdlg('Click the two points in the constant compliance region to find slope ','Step 1');
uiwait(h);

% Record points for approach curve constant compliance.
w = waitforbuttonpress;
slope_appr(1,:)=struct2array(getCursorInfo(dcm_obj));
w = waitforbuttonpress;
slope_appr(2,:)=struct2array(getCursorInfo(dcm_obj));
% Calculate the slope of the constant compliance region.
s=(slope_appr(1,3)-slope_appr(2,3))/(slope_appr(1,2)-slope_appr(2,2));
```

```
% Calculate Spring Constant of the Bacteria

kb=(kc*s)/(1-s);

close(fig1);
```

Appendix 3: Thermodynamic model to calculate interfacial free energy of adhesion

Interfacial free energy B. anthracis spores and murine macrophages

Known Parameters

$\gamma wLW := 21.6$ $\gamma wmin := 25.4$ $\gamma wplus := 25.4$

$\gamma dLW := 50.5$ $\gamma dmin := 0$ $\gamma dplus := 0.7$

$\gamma fLW := 38.7$ $\gamma fmin := 39.4$ $\gamma fplus := 2.3$

Finding the surface tension of water, diiodomethane and formamide

$\gamma wab := 2\left(\sqrt{\gamma wmin \cdot \gamma wplus}\right)$ $\gamma fab := 2\left(\sqrt{\gamma fmin \cdot \gamma fplus}\right)$

$\gamma wab = 50.8$ $\gamma fab = 19.039$

$\gamma w := \gamma wab + \gamma wLW$ $\gamma f := \gamma fab + \gamma fLW$

$\gamma w = 72.4$ $\gamma f = 57.739$

$\gamma dab := 2\left(\sqrt{\gamma dmin \cdot \gamma dplus}\right)$

$\gamma dab = 0$

$\gamma d := \gamma dab + \gamma dLW$

$\gamma d = 50.5$

Measured Contact Angles

$$\begin{pmatrix} \theta w \\ \theta d \\ \theta f \end{pmatrix} := \begin{pmatrix} 63.4 \\ 48.3 \\ 54.15 \end{pmatrix} \cdot \left(\frac{\pi}{180}\right)$$

$$\begin{pmatrix} \theta w \\ \theta d \\ \theta f \end{pmatrix} = \begin{pmatrix} 1.107 \\ 0.843 \\ 0.945 \end{pmatrix}$$

Calculated Lifshitz-van der Waals and electron donor and electron acceptor parameters

$$\begin{pmatrix} \gamma sLW \\ \gamma splus \\ \gamma smin \end{pmatrix} := \left[\left[2 \begin{pmatrix} \sqrt{\gamma wLW} & \sqrt{\gamma wmin} & \sqrt{\gamma wplus} \\ \sqrt{\gamma dLW} & \sqrt{\gamma dmin} & \sqrt{\gamma dplus} \\ \sqrt{\gamma fLW} & \sqrt{\gamma fmin} & \sqrt{\gamma fplus} \end{pmatrix} \right]^{-1} \cdot \begin{bmatrix} \gamma w \cdot (\cos(\theta w) + 1) \\ \gamma d \cdot (\cos(\theta d) + 1) \\ \gamma f \cdot (\cos(\theta f) + 1) \end{bmatrix} \right]^2$$

$$\begin{pmatrix} \gamma sLW \\ \gamma splus \\ \gamma smin \end{pmatrix} = \begin{pmatrix} 28.914 \\ 0.733 \\ 21.014 \end{pmatrix}$$

Calculation of the Acid-Base component of the surface tension

$$\gamma sAB := 2 \cdot \left(\sqrt{\gamma splus \cdot \gamma smin} \right)$$

$$\gamma sAB = 7.85$$

Total Surface Tension

$$\gamma s := \gamma sLW + \gamma sAB$$

$$\gamma s = 36.763$$

Interfacial Free Energy Calculations

Spore in water medium

$$\gamma s\_w := \left(\sqrt{\gamma sLW} - \sqrt{\gamma wLW} \right)^2 + 2 \left[\left(\sqrt{\gamma splus} - \sqrt{\gamma wplus} \right) \cdot \left(\sqrt{\gamma smin} - \sqrt{\gamma wmin} \right) \right]$$

$$\gamma s\_w = 4.346$$

Macrophage-spore interfacial tension

$$\gamma mac\_s := \left(\sqrt{23.159} - \sqrt{\gamma sLW} \right)^2 + 2 \left[\left(\sqrt{16.077} - \sqrt{\gamma splus} \right) \cdot \left(\sqrt{9.256} - \sqrt{\gamma smin} \right) \right]$$

$$\gamma mac\_s = -9.404$$

Appendix 4: Publications in support of this thesis

Special Issue

Received: 7 November 2008, Accepted: 14 January 2009, Published online in Wiley InterScience: 2009

(www.interscience.wiley.com) DOI:10.1002/jmr.945

Atomic force microscopy study of germination and killing of *Bacillus atrophaeus* spores†

Paola A. Pinzón-Arango[a], Geoffrey Scholl[b], Ramanathan Nagarajan[b], Charlene M. Mello[b] and Terri A. Camesano[a]*

Bacterial spores such as *Bacillus atrophaeus* are one of the most resistant life forms known and are extremely resistant to chemical and environmental factors in the dormant state. During germination, as bacterial spores progress towards the vegetative state, they become susceptible to anti-sporal agents. *B. atrophaeus* spores were exposed to the non-nutritive germinant dodecylamine (DDA), a cationic surfactant that can also be used as a killing agent, for up to 60 min, or to the nutrient germinant L-alanine. In kinetic studies, 99% of the spores were killed within 5 min of exposure to DDA. Atomic force microscopy (AFM) can be used as a sensitive tool to assess how the structure of the spore coat changes upon exposure to germinants or killing agents. Changes in cell height and roughness over time of exposure to DDA were examined using AFM. DDA caused the spore height to decrease by >50%, which may have been due to a partial breakdown of the spore coat. Treatment of *B. atrophaeus* with the nutrient germinant resulted in a decrease in height of spores after 2 h of incubation, from 0.7 ± 0.1 μm to 0.3 ± 0.2 μm. However, treatment with L-alanine did not change the surface roughness of the spores, indicating that the changes that occur during germination take place underneath the spore coat. We propose that exposure to DDA at high concentrations causes pores to form in the coat layer, killing *B. atrophaeus* without the need to fully germinate spores. Published 2009 by John Wiley & Sons, Ltd.

Keywords: RMS roughness; spore; L-alanine; dodecylamine

INTRODUCTION

Under nutrient deprivation, vegetative cells of *Bacillus* spp. and *Clostridium* spp. are able to undergo a restructuring and differentiation process known as sporulation (Atrih and Foster, 2002; Chada *et al.*, 2003; Giorno *et al.*, 2007). Bacterial spores are metabolically dormant and are the most resistant life forms known. Their inner cell membrane surrounds and protects the core of the spore, which contains its chromosome and other cellular contents. This membrane is protected from external environmental factors by a nearly 100 nm barrier consisting of a polymer layer and protein coat (Figure 1) (Henriques and Moran, 2000). Because of their unique structure and morphology, spores can overcome environmental and chemical factors such as radiation, desiccation, heat, changes in pH and exposure to toxic chemicals (Slieman and Nicholson, 2001; Setlow, 2003; Plomp *et al.*, 2007). Dormant spores are able to constantly monitor their surrounding environment so that when nutrients become available, they can return to a vegetative state, after passing through the stages of germination and outgrowth (Setlow, 2003). Because of their virulent pathogenic nature, *B. anthracis* and other spores are problematic since they can be used as biowarfare and bioterrorism agents causing severe and frequently lethal foodborne and airborne diseases, such as pulmonary anthrax (Atrih and Foster, 2002; Akoachere *et al.*, 2007).

The current theory of spore inactivation assumes that in most deactivation technologies germination must occur before spores can be killed by anti-sporal agents (Atrih and Foster, 2002), while some examples of spore killing, even in the absence of germination, also exist (Tennen *et al.*, 2000). Germination can be triggered in response to nutrients, such as amino acids, sugars and purine nucleosides, or by non-nutrient factors such as lysozyme, Ca^{2+}-DPA, cationic surfactants, high pressures or salts (Setlow, 2003). During the first phase of germination, the spore releases H^+, monovalent cations and Zn^{2+}, which causes an elevation of pH in the core (Jedrzejas and Setlow, 2001; Setlow, 2003). This is followed by the release of Ca^{2+} and pyridine-2 6-dicarboxylic acid (dipicolinic acid (DPA)), accounting for approximately10% of the spores dry weight (Setlow, 2003). As DPA is released, water molecules enter and hydrate the core, causing a loss of heat resistance (Slieman and Nicholson, 2001). During the second stage, further water uptake allows for hydrolysis of the spore cortex and swelling of the core and germ cell wall. After expansion of the core, metabolism begins and macromolecular synthesis converts the spore into a germinated cell, by breaking of the spore coat and final release of a vegetative cell (outgrowth) (Atrih and Foster, 2002).

* *Correspondence to: T. A. Camesano, Department of Chemical Engineering, Worcester Polytechnic Institute, Life Sciences and Bioengineering Center at Gateway Park, 100 Institute Rd., Worcester, MA 01609, USA.*
E-mail: terri@wpi.edu

a *P. A. Pinzón-Arango, T. A. Camesano*
Department of Chemical Engineering, Worcester Polytechnic Institute, Worcester MA 01609, USA

b *G. Scholl, R. Nagarajan, C. M. Mello*
Natick Soldier Research, Development and Engineering Center, Macromolecular Science Team, Natick, MA 01760, USA

† *This article is a US Government work and is in the public domain in the USA.*

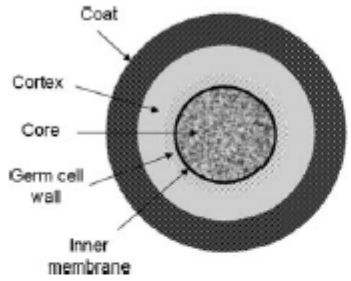

Figure 1. Schematic representation of *B. atrophaeus* spore structure. Common dimension of the different layers of spore structure are: Spore coat (60–100 nm), spore cortex (50–100 nm), germ cell wall (2–10 nm), inner membrane (3–4 nm) and spore core (0.7 to 1 μm).

Dodecylamine (DDA) is a cationic surfactant that has been used as a chemical agent to stimulate spore germination (Rode and Foster, 1961; Setlow *et al.*, 2003). Previous work with *B. subtilis* indicated that the mechanism by which DDA triggers germination is different from how other nutrients and non-nutrient factors, such as Ca^{2+}-DPA (Setlow *et al.*, 2003). Rather than binding to nutrient germinant receptors or to cortex lytic enzymes, DDA may act against and compromise the spore's inner membrane (Setlow *et al.*, 2003). *B. megaterium* spores exposed to 6×10^{-5} M DDA for more than 3 min could be killed as germination was taking place, suggesting that DDA both germinates and deactivates *B. megaterium* (Rode and Foster, 1961).

Traditional methods to study spore germination rely on bulk or indirect measurements. For example, spore germination is monitored by quantifying the amount of DPA released, through optical density measurements (Setlow *et al.*, 2003). Spore activity can also be monitored, such as assessment of the percentage of mammalian cells killed due to germination of spores (Akoachere *et al.*, 2007). One direct method to study spore germination is to use electron microscopy to examine how the morphology of the spores changes during germination (Zaman *et al.*, 2005). However, this technique has limitations since sample preparation dehydrates cells and can affect morphology, which would lead to misinterpretation of the images.

Atomic force microscopy (AFM) is a technique that can be used to examine individual spores with minimal sample preparation and it has been widely used to study epithelial cells, bacteria, viruses and fungi in their native conditions (Dufrene, 2002). Changes in morphology and ultrastructure of several *Bacillus* spp. before and after exposure to different nutrient germinants were studied using AFM, such as determining how mutations in particular coat proteins affect germination (Chada *et al.*, 2003). Most of these studies focused on a qualitative understanding of how the spore coat changes during germination and how these changes affect spore size (Plomp *et al.*, 2005b; Zaman *et al.*, 2005; Zolock *et al.*, 2006; Plomp *et al.*, 2007). To our knowledge, no study has assessed the morphological changes that spores undergo when treated with non-nutrient germinants, such as DDA, and how different treatments affect the roughness of the spore surface as it is being germinated.

In this study, AFM was used to quantify spore surface roughness as a function of incubation time in nutrient and non-nutrient germinants, and to measure changes in the heights of the spores, during the process of germination with DDA and L-alanine. Our results suggest that DDA kills *B. atrophaeus* spores before outgrowth occurs. Therefore, DDA may serve as a deactivation agent against a broad spectrum of normal and mutant *Bacillus* spp., since complete germination is not required in order for deactivation to occur.

MATERIALS AND METHODS

Bacterial strains and spore preparation

Bacillus atrophaeus, previously classified as *Bacillus subtilis* var. *niger*, *Bacillus niger*, or *Bacillus globigii* (Fritze and Pukall, 2001), is a Gram-positive, aerobic, spore-forming bacterium that has been widely used as a nonpathogenic surrogate for *B. anthracis* and as a biological indicator for decontamination and sterilization processes and environmental biotracers (Burke *et al.*, 2004; Plomp *et al.*, 2005b). *B. atrophaeus* NRRL B-4418 was purchased (American Tissue Culture Collection, ATCC 6455). *B. atrophaeus* cultures were grown on plates of sporulation media, consisting of 8 g nutrient broth, 4 g yeast extract, 0.001 g $MnCl_2.4H_2O$, 5 g peptone and 15 g agar in 1 L of ultrapure water (Milli-Q water, Millipore Corp., Bedford, MA) and maintained at a pH of 7.2.

Plates were incubated at 37°C for 4 days. Spores were collected by centrifugation at 5000 RPM for 20 min and resuspended in ultrapure water. The cells were washed eight times to separate the spores from vegetative and partially sporulated cells and stored at 4°C. The spores were allowed to remain in water overnight and then washed two more times to remove any remaining vegetative cells or semi-sporulated cells.

Kinetics studies of spore killing by DDA

A solution of *B. atrophaeus* at 10^7 spores/mL was centrifuged and resuspended in 1 mM DDA (Sigma-Aldrich, St. Louis, MO). Spores were incubated at 37°C for 0, 1, 5, 10, 20, 25, 30, 40, 50 and 60 min and kept in an ultrasonication bath (Bronson, 1510, 40 kHz, 130 W, Branson Ultrasonics Corp., Danbury, CT) to prevent settling. The action of DDA on the spores at the end of the incubation period was terminated by immersion of spore suspension into an ice bath.

To determine the effects of DDA on spore viability, the treated spore solution was serially diluted and aliquots of spore solution were inoculated onto sporulation agar plates and cultured in an incubator at 37°C. The number of surviving spores or colony forming units (cfu) that became vegetative cells on the agar plates was determined after 18 h.

Monitoring the germination of *B. atrophaeus* spores

Germination of *B. atrophaeus* was monitored by determining the amount of DPA released from the core of the spore, using time resolved fluorescence intensity measurements. A spore solution of approximately 10^7 cfu/mL was incubated at 37°C in the presence of L-alanine or DDA at various concentrations, for 0, 2, 10, 20, 30, 40, 50, 60 and 100 min. The spore solution was combined with a stock solution of terbium chloride ($TbCl_3$; Sigma-Aldrich, St. Louis, MO) to yield a 1 mM $TbCl_3$. Terbium chloride reacts with DPA and forms the chelate, terbium dipicolinate, $(Tb[DPA]_3)^{3-}$, which luminesces with UV excitation (Rosen *et al.*, 1997). After addition of $TbCl_3$ in a microtiter 96-well plate, 200 μL of spore solution were placed in each well and the

mixed system was excited at 270 nm. Photoluminescence excitation and emission spectra were measured from each sample with a Gemini XPS microplate Spectrofluorometer (Molecular Devices, now part of MDS Analytical Technologies Inc., Toronto, Canada).

Imaging of *B. atrophaeus* spores with AFM

AFM was used to study the morphological changes of *B. atrophaeus* spores after exposure to 1 mM DDA for 0, 1, 5, 15, 20, 25, 30, 40, 50 and 60 min, or after exposure to 25 mM L-alanine for 120 min. Droplets of treated *B. atrophaeus* spores (5 μL) were deposited directly onto freshly cleaved mica and allowed to air dry for imaging under ambient conditions.

Images were collected using an atomic force microscope (Digital Instruments Dimension 3100 with Nanoscope IIIa controller; Veeco Metrology; Santa Barbara, CA) that was operated in intermittent contact mode to minimize lateral forces on the sample during imaging. Rectangular cantilevers with conical silicon tips having force constants of approximately 40 N/m and resonance frequencies of approximately 300 kHz were used (Applied Nanostructures; Santa Clara, CA). Images were captured with scan areas of 0.5, 1, 5, 10 and 20 μm^2. Images of larger areas (10 and 20 μm^2) were acquired using hard tapping, where the proportional and integral gains were 1.2–1.5 and 0.8–1.0, respectively, and low amplitude setpoints. Smaller scanned areas (0.5, 1 and 5 μm^2) were probed using light tapping, where the proportional and integral gains were decreased to 0.5–0.8 and 0.2–0.4, respectively, and the amplitude setpoint was moderately increased to avoid missing important surface structures. All images were captured at a scan rate of 1 Hz and with a resolution of 512 × 512 points.

Off-line image analysis

AFM height and amplitude images were collected simultaneously. At least 10 images were obtained per time period and condition. Height images were used for quantitative analysis of the root-mean-squared roughness (R_{rms}), as well as height and length profiles of the spores. Amplitude images were used to obtain qualitative information. Height images were flattened using a zero order filter to remove the Z offset between scan lines before calculating R_{rms} values. The R_{rms} values were acquired on areas ranging from 0.05 to 0.5 μm^2.

Between 10 and 20 spores were analyzed per image and the calculated height and roughness values of the spores were analyzed using SigmaStat 2.03 statistical software. Statistical analysis was performed by one-way analysis of variance (ANOVA) for repeated measurements. Tukey's test was used for multiple comparisons among treatment groups, while Dunnett and Duncan's test was used for comparisons between treatment and control groups. A difference was considered significant if $p < 0.05$.

RESULTS

Anti-sporal activity of DDA against *B. atrophaeus*

Exposure of *B. atrophaeus* to 1 mM DDA resulted in a significant decrease in surviving spores with increasing exposure time to the anti-sporal agent (Figure 2). After 1 min of treatment with DDA, the number of cfu decreased from approximately 5×10^7 cfu to approximately 2×10^6 cfu, corresponding to 90% of the spores being killed. After 5 min of exposure, 99% of the spores had been killed and only 10^3 cfu remained after exposure to DDA for 60 min.

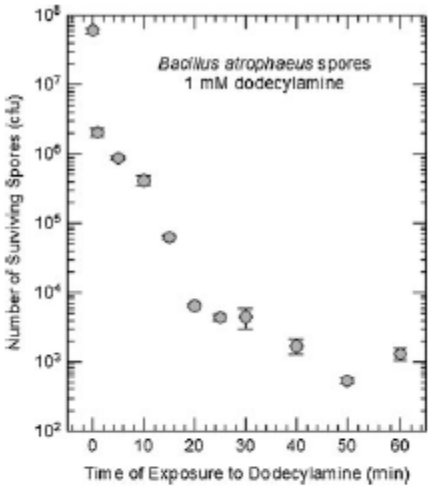

Figure 2. Kinetics of *B. atrophaeus* spore killing by DDA. Number of spore cfu as a function of time of exposure to 1 mM DDA. Error bars represent the standard deviation. Original spore inoculum was at 1×10^7 spores/mL.

Since germinated spores are more susceptible to anti-sporal agents, the germination of *B. atrophaeus* spores was monitored in terms of DPA release from the core. Exposure of *B. atrophaeus* to different concentration of L-alanine caused DPA to be released within 30 min (Figure 3A). The maximum concentration of DPA released from the core was obtained by exposing spores to a concentration of 25 mM L-alanine. Exposure of *B. atrophaeus* to various concentration of DDA resulted in a slower DPA release when compared to the effects of L-alanine. Total release of DPA took 100 min when bacteria were exposed to DDA (Figure 3B). The effect of DDA concentration on germination is complex and is affected by the self-assembly behaviour of DDA in solution (the critical concentration for aggregation is between 0.5 and 1 mM) and also by the promotion of clustering of spores with increasing DDA concentration.

B. atrophaeus size and surface morphology

The morphology of *B. atrophaeus* was characterized via AFM and images showed rodlet structures typically observed for these spores (Figure 4A). Drying of the *B. atrophaeus* on mica surfaces resulted in some clumping. Even when the spore concentration was decreased, spores always aggregated during the drying process on mica, thus it was difficult to observe isolated spores. Spore morphology changed after treatment with 1 mM DDA for 15 or 30 min (Figure 4B and 4C). Spores treated for 15 min appeared dehydrated and the images showed more creases or folds on the spore surface (Figure 4B). The spores treated with DDA for 30 min did not show as much evidence of dehydration,

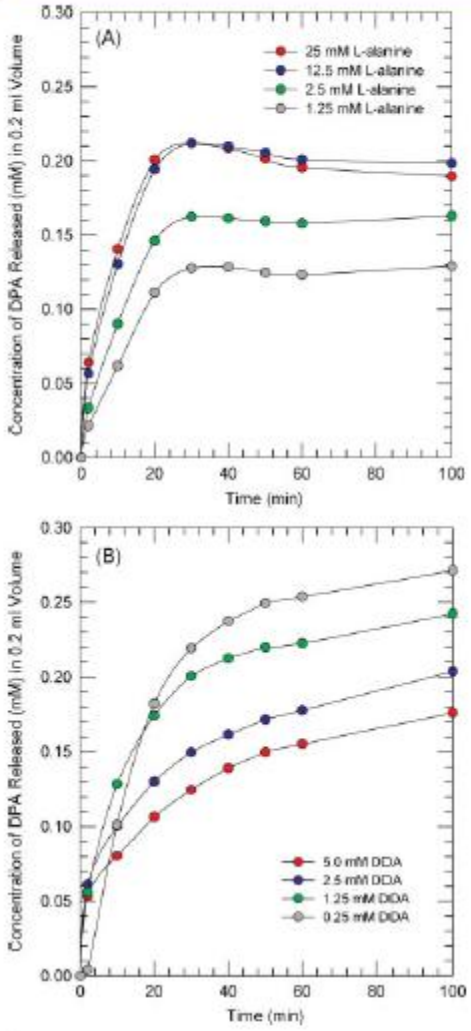

Figure 3. Germination of *B. atrophaeus* spores with various concentrations of (A) L-alanine or (B) DDA. The amount of DPA released from the core was measured by terbium enhanced fluorescence lifetime measurements. Original spore inoculum was at 1×10^7 spores/mL.

but we noticed that no rodlets were present on the surface, compared to the control case.

R_{rms} values were measured for *B. atrophaeus* exposed to DDA for several time points. Spores that were not treated with DDA had an average R_{rms} value of 25.0 ± 2.3 nm when areas of 500 nm^2 covering the surface of the spores were analyzed (Figure 5A). After treating the spores for 1 min with DDA, the average R_{rms} value increased to 28.2 ± 4.1 nm. The average roughness of the spores continued to increase with time, reaching a local maximum R_{rms} corresponding to 1 mM DDA

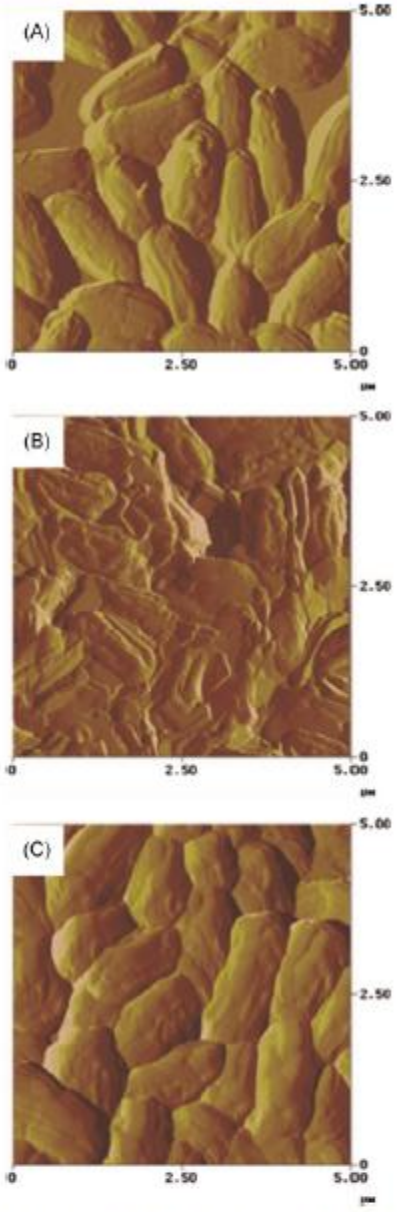

Figure 4. Representative amplitude AFM images of *B. atrophaeus* after exposure to 1 mM DDA for (A) 0 min, (B) 15 min and (C) 30 min. Images collected in intermittent contact mode.

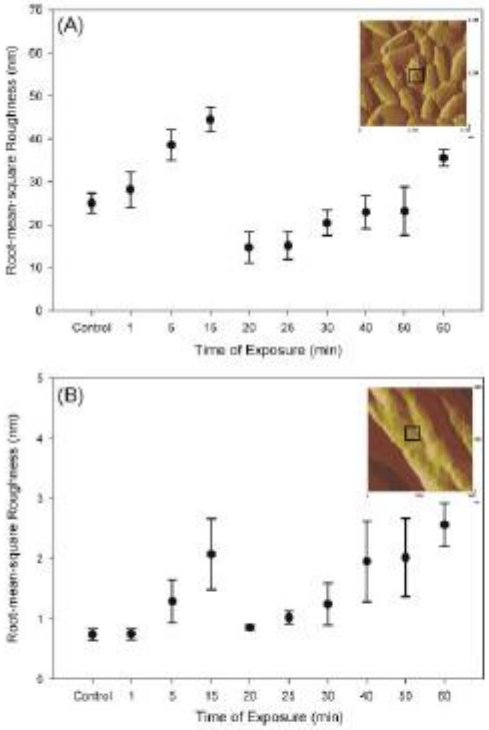

Figure 5. R_{rms} of *B. atrophaeus* as a function of exposure time to 1 mM DDA, for scan areas of (A) 5 μm^2 and (B) 0.5 μm^2. Data are expressed as the average R_{rms} with standard deviation. Inset AFM image represents how roughness analysis was carried out: for scan areas of 5 μm^2, a 500 nm^2 area box covering the surface of the spore was analyzed. For scan areas of 0.5 μm^2, the roughness within a 50 nm^2 area box of the spore surface was analyzed.

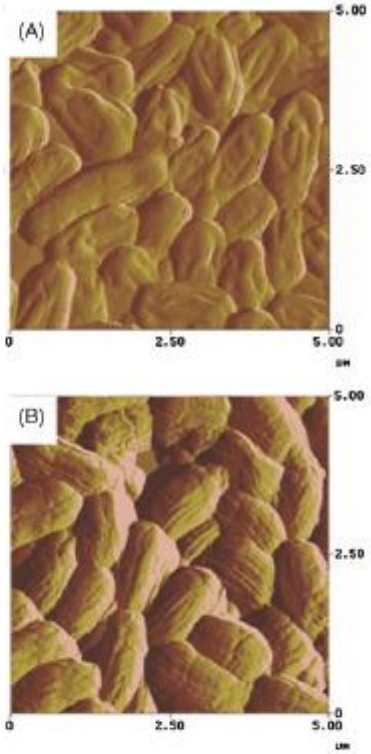

Figure 6. Representative amplitude AFM images of *B. atrophaeus* before and after exposure to L-alanine or DDA for (A) dead spores after 1 mM DDA treatment and (B) germinated spores after 25 mM L-alanine treatment. Images collected in intermittent contact mode.

treatment for 15 min, which was 44.5 ± 2.9 nm. At 20 min, R_{rms} decreased to an average of 14.7 ± 3.6 nm, but began to increase again after 25 min, and continued increasing until 60 min. Statistical analysis showed that R_{rms} values from times 5, 15, 20, 25, 30 and 60 min were significantly different when compared to the control group (untreated spores; $p < 0.001$).

Roughness values were also obtained using smaller scan areas of 50 nm^2 on a 0.5 μm^2 image. Sampled at a different scale, the roughness values decreased compared to the 5 μm^2 scanned image (Figure 5B). The roughness measured at this scale showed the same trend we observed for the larger scale, with roughness increasing until 15 min, then dropping and increasing again. Statistical analysis showed that the R_{rms} values at times 15, 40, 50 and 60 min were significantly different compared to the control group ($p < 0.001$).

Morphology changes were observed for spores exposed to L-alanine, as quantified by height measurements. Chemical treatments affected spore morphology (Figure 6A and 6B) and the height of spores decreased after treatment with DDA or L-alanine. After exposure to L-alanine, the height of the spores decreased from an average of 0.7 ± 0.1 μm to 0.3 ± 0.2 μm. Treatment with DDA resulted in a similar decrease of spore height, from an average of 0.7 ± 0.1 μm to 0.26 ± 0.1 μm. The differences in height were significant against the control group ($p < 0.05$). However, the roughness of the L-alanine treated spores did not increase (data not shown), in contrast with the spores exposed to DDA.

DISCUSSION

Previous studies have addressed the effects that nutrient and non-nutrient germinants have on *Bacillus* and *Clostridium* cells (Powell and Strange, 1953; Ando, 1980). Current theory suggests that germination of spores must occur before killing, since the peptidoglycan layer of vegetative cells is easier to penetrate than the thick multilayered structure of the spore coat (Figure 1). There are several studies that examined how nutrient and non-nutrient germinants affect spores (Rode and Foster, 1961; Barlass *et al.*, 2002; Akoachere *et al.*, 2007). While most studies focused on germination of spores using nutrients, such as L-alanine and inosine (Barlass *et al.*, 2002; Zaman *et al.*, 2005; Plompe *et al.*, 2007),

the use of non-nutrient germinants, such as DDA, have not been well studied. The mechanism of action of nutrient germinants such as L-alanine has been investigated and it is known that nutrient germinants bind to receptors located in the spore's inner membrane, which causes the opening of ion/DPA channels (Setlow, 2003). In this study, we exposed *B. atrophaeus* spores to the nutrient germinant L-alanine and to the non-nutrient germinant DDA. We propose the mechanism of action of DDA against bacterial spores and discuss how it is different from germination with L-alanine.

Germination mechanisms of *B. atrophaeus* after exposure to L-alanine

L-alanine has been widely used to study changes in morphology as well as biochemical alterations during germination (Rode and Foster, 1961; Barlass *et al.*, 2002). In *B. cereus* the major receptor for alanine germination was identified as GerL, from the GerA family at the inner membrane (Barlass *et al.*, 2002). Using L-alanine as the germinant, we observed that there is a rapid release of DPA and by 30 min all DPA was released (Figure 3A).

Treatment with L-alanine caused a >50% decrease in the height of the spores after 2 h of treatment, which is due in part to DPA release from the core. Prior work showed that the rapid release of DPA from the core due to L-alanine germination caused an estimated 32% loss of dry weight in bacterial spores (Rode and Foster, 1961). A flattening of *B. subtilis* spores and collapse around spore center was observed after exposure to L-alanine for 1 h, according to a previous optical microscopy study (Leuschner *et al.*, 2003). Although these spores were considered to be germinating, as observed qualitatively by the decrease in phase brightness, no swelling of the spore could be detected.

Although DPA release supports that germination began in our study with L-alanine, we did not observe outgrowth within the 2 h period, as no vegetative bacteria were observed in the AFM images. This may be because a longer time would be necessary to transform the spore to the vegetative state, which could vary within *Bacillus* spp. For instance, Zaman *et al.*, found *B. anthracis* became vegetative after treatment with L-alanine for 3 h (Zaman *et al.*, 2005) since the length of the spores increased from 0.8–0.9 to 3.4–3.8 μm. However, another study showed that approximately 30% of a *B. atrophaeus* population did not proceed to outgrowth after exposure to L-alanine for 3 to 7 h (Plomp *et al.*, 2007). The percentage of outgrowing cells was even lower in a different study where vegetative cells were only observed in a few cases, suggesting that L-alanine initiates the process of germination and metabolic activity but not the synthesis of macromolecules, such as cell wall peptidoglycan, for all the spore population (Leuschner *et al.*, 2003).

The roughness of L-alanine-treated spores was similar to the roughness of untreated spores, suggesting that the effects of L-alanine on the spore occur underneath the coat layer. This was confirmed by the AFM images, showing similar morphology for treated and control spores (Figures 4A and 6B). These findings suggest that during the first stages of germination, the spore coat remains intact and L-alanine causes internal restructuring of the spore. Since there is no degradation of the coat, this layer is a limiting barrier for outgrowing spores, which may explain why vegetative cells were not observed and why outgrowth did not occur consistently in previous studies. One recent study suggested that the spore coat has to crack laterally on one or both sides to allow the vegetative cell to expand (Leuschner *et al.*, 2003). L-alanine may start germination by changing the internal structure of the spore and this effect may work its way to the outside of the spore after all internal changes, such as DPA release and hydrolysis of the cortex, have occurred.

Germination mechanisms of *B. atrophaeus* after exposure to DDA

Although some studies have investigated the process of spore germination using a non-nutrient germinant, such as DDA (Rode and Foster, 1961; Setlow *et al.*, 2003; Paredes-Sabja *et al.*, 2008), the efficacy of this cationic surfactant as a sporicide has not been well studied. In the early 1960s, Rode and Foster reported that exposing *B. megaterium* spores to 10^{-5} M DDA for more than three min resulted in loss of heat resistance for 97% of the spore population and exposure to DDA for 10 min caused the killing of approximately 96% of the spores (Rode and Foster, 1961). In our studies, we have observed that approximately 95% of killed spores can be obtained under 1 min and 99% after 5 min if they are exposed to 1 mM DDA (Figure 2).

Even though spore killing occurs with exposure to 1 mM DDA, we studied the germination of spores by measuring the amount of DPA released from the core as a function of time (Figure 3B). Exposing spores to 1.25 mM DDA resulted in complete DPA release within 100 min. In a previous study, researchers using 1 mM DDA to germinate *B. subtilis* spores showed that it took approximately 3 h for the DPA to be released from the core (Setlow *et al.*, 2003). This difference in DPA release rate may be related to variability within the *Bacillus* spp., growth conditions, or treatment. For instance, Setlow *et al.* boiled spore cultures for 30 min to determine DPA release, while we did not (Setlow *et al.*, 2003).

The spore heights were significantly lower for DDA-treated spores, compared to untreated spores. We suggest that these height changes are due to decreased hydration of the core and a breakdown of the spore coat. A previous study showed that exposure of *Bacillus* spores to DDA results in a 45 to 55% loss of dry weight, which could have contributed to the reduced height of spores (Rode and Foster, 1961). In another study, it was observed that spores germinated with DDA did not rehydrate well and core water content in these spores was low, which prevented them from expanding normally (Setlow *et al.*, 2003). From our roughness analysis we also observed that the outer coat of the spore was affected by DDA treatments since there was an initial increase in roughness values. This increase in roughness indicates that the coat of the spore is rupturing and disintegrating. The inner and outer coat of spores can be up to 130 nm thick (Henriques and Moran, 2000), which could lead to a diameter decrease of 260 nm. When spore coat breakdown and loss of hydration simultaneously occurred, we observed a decrease in height and increase in roughness of the spores.

Based on our roughness, height and DPA release measurements, we considered a mechanism of action of DDA against bacterial spores. DDA does not interact with any receptors in the inner membrane of spores, as reported previously (Setlow *et al.*, 2003). From our roughness measurements we can state that DDA starts acting from the outside of the spore and works its way in by causing the coat to rupture and form pores on the surface. The drop in roughness observed after 15 min of treatment with DDA indicates that the outer coat layer was completely removed; leaving behind another smoother coat that will be subsequently

ruptured or disintegrated after prolonged treatment with DDA. With prolonged DDA treatment, the protective coat layers of the spore were compromised, decreasing the overall cell height. While most of the cells were killed within 1 min of exposure to DDA, this happened during the first stages of germination since there was a continuous release of DPA from the core. However, germination was interrupted and spores were killed without outgrowing. Using DDA as a germinant or sporicide may be a more effective mechanism to deactivate *B. atrophaeus* and perhaps other hazardous species such as *B. anthracis*, since DDA can act against spores that have not progressed to the fully vegetative state.

Acknowledgements

This work was supported in part by the National Science Foundation (CBET 0827229) and DTRA Project BA07PRO102.
We also thank Robert Stote for helpful discussions during the course of this research.

REFERENCES

Akoachere M, Squires RC, Nour AM, Angelov L, Brojatsch J, Abel-Santos E. 2007. Identification of an *in vivo* inhibitor of *Bacillus anthracis* spore germination. *J. Biol. Chem.* **282**(16): 12112–12118.
Ando Y. 1980. Mechanism of nitrite-induced germination of Clostridium perfringens spores. *J. Appl. Bacteriol.* **49**(3): 527–535.
Atrih A, Foster SJ. 2002. Bacterial endospores the ultimate survivors. *Int. Dairy J.* **12**(2–3): 217–223.
Barbass PJ, Houston CW, Clements MO, Moir A. 2002. Germination of *Bacillus cereus* spores in response to L-alanine and to inosine: the roles of gerL and gerQ operons. *Microbiology.* **148**(Pt 7): 2089–2095.
Burke SA, Wright JD, Robinson MK, Bronk BV, Warren RL. 2004. Detection of molecular diversity in *Bacillus atrophaeus* by amplified fragment length polymorphism analysis. *Appl. Environ. Microbiol.* **70**(5): 2786–2790.
Chada VG, Sanstad EA, Wang R, Driks A. 2003. Morphogenesis of *Bacillus* spore surfaces. *J. Bacteriol.* **185**(21): 6255–6261.
Dufrene YF. 2002. Atomic force microscopy, a powerful tool in microbiology. *J. Bacteriol.* **184**(19): 5205–5213.
Fritze D, Pukall R. 2001. Reclassification of bioindicator strains *Bacillus subtilis* DSM 675 and *Bacillus subtilis* DSM 2277 as *Bacillus atrophaeus*. *Int. J. Syst. Evol. Microbiol.* **51**(Pt 1): 35–37.
Giorno R, Bozue J, Cote C, Wenzel T, Moody KS, Mallozzi M, Ryan M, Wang R, Zielke R, Maddock JR, Friedlander A, Welkos S, Driks A. 2007. Morphogenesis of the *Bacillus anthracis* spore. *J. Bacteriol.* **189**(3): 691–705.
Henriques AO, Moran CP Jr. 2000. Structure and assembly of the bacterial endospore coat. *Methods.* **20**(1): 95–110.
Jedrzejas MJ, Setlow P. 2001. Comparison of the binuclear metalloenzymes diphosphoglycerate-independent phosphoglycerate mutase and alkaline phosphatase: Their mechanism of catalysis via a phosphoserine intermediate. *Chem. Rev.* **101**(3): 607–618.
Lauschner RGK, Ferdinando DP, Lillford PJ. 2003. Structural analysis of spores of *Bacillus subtilis* during germination and outgrowth. *Colloids Surf. B.* **19**: 31–41.
Paredes-Sabja D, Torres JA, Setlow P, Sarker MR. 2008. Clostridium perfringens spore germination: characterization of germinants and their receptors. *J. Bacteriol.* **190**(4): 1190–1201.
Plomp M, Leighton TJ, Wheeler KE, Hill HD, Malkin AJ. 2007. *In vitro* high-resolution structural dynamics of single germinating bacterial spores. *Proc. Natl. Acad. Sci. USA.* **104**(23): 9644–9649.
Plomp M, Leighton TJ, Wheeler KE, Malkin AJ. 2005a. The high-resolution architecture and structural dynamics of *Bacillus* spores. *Biophys. J.* **88**(1): 603–608.
Plomp M, Leighton TJ, Wheeler KE, Pitesky ME, Malkin AJ. 2005b. *Bacillus atrophaeus* outer spore coat assembly and ultrastructure. *Langmuir* **21**(23): 10710–10716.
Powell JF, Strange RE. 1953. Biochemical changes occurring during the germination of bacterial spores. *Biochem. J.* **54**(2): 205–209.
Rode LJ, Foster JW. 1961. Germination of bacterial spores with alkyl primary amines. *J. Bacteriol.* **81**: 768–779.
Rosen DL, Sharpless C, McGown. LB. 1997. Bacterial spore detection and determination by use of terbium dipicolinate photoluminescence. *Anal. Chem.* **69**(6): 1082–1085.
Setlow B, Cowan AE, Setlow P. 2003. Germination of spores of *Bacillus subtilis* with dodecylamine. *J. Appl. Microbiol.* **95**(3): 637–648.
Setlow P. 2003. Spore germination. *Curr. Opin. Microbiol.* **6**(6): 550–556.
Slieman TA, Nicholson WL. 2001. Role of dipicolinic acid in survival of *Bacillus subtilis* spores exposed to artificial and solar UV radiation. *Appl. Environ. Microbiol.* **67**(3): 1274–1279.
Tennen R, Setlow B, Davis KL, Loshon CA, Setlow P. 2000. Mechanisms of killing of spores of *Bacillus subtilis* by iodine, glutaraldehyde and nitrous acid. *J. Appl. Microbiol.* **89**(2): 330–338.
Zaman MS, Goyal A, Dubey GP, Gupta PK, Chandra H, Das TK, Ganguli M, Singh Y. 2005. Imaging and analysis of *Bacillus anthracis* spore germination. *Microsc. Res. Tech.* **66**(6): 307–311.
Zolock RA, Li G, Bleckmann C, Burggraf L, Fuller DC. 2006. Atomic force microscopy of *Bacillus* spore surface morphology. *Micron.* **37**(4): 363–369.

Langmuir
Article
pubs.acs.org/Langmuir

Effects of L-Alanine and Inosine Germinants on the Elasticity of *Bacillus anthracis* Spores

Paola A. Pinzón-Arango,[†] Ramanathan Nagarajan,[‡] and Terri A. Camesano*[,†]

[†]*Department of Chemical Engineering, Worcester Polytechnic Institute, Worcester, Massachusetts 01609, and* [‡]*U.S. Army Natick Soldier Research, Development & Engineering Center, Molecular Sciences and Engineering Team, Natick, Massachusetts 01760*

Received October 26, 2009. Revised Manuscript Received January 5, 2010

The surface of dormant *Bacillus anthracis* spores consists of a multilayer of protein coats and a thick peptidoglycan layer that allow the cells to resist chemical and environmental insults. During germination, the spore coat is degraded, making the spore susceptible to chemical inactivation by antisporal agents as well as to mechanical inactivation by high-pressure or mechanical abrasion processes. While chemical changes during germination, especially the release of the germination marker, dipicolinic acid (DPA), have been extensively studied, there is as yet no investigation of the corresponding changes in the mechanical properties of the spore. In this work, we use atomic force microscopy (AFM) to characterize the mechanical properties of the surface of *Bacillus anthracis* spores during germination. The Hertz model of continuum mechanics of contact was used to evaluate the Young's moduli of the spores before and after germination by applying the model to load−indentation curves. The highest modulus was observed for dormant spores, with average elasticity values of 197 ± 81 MPa. The elasticity decreased significantly after incubation of the spores with the germinants L-alanine or inosine (47.5 ± 41.7 and 35.4 ± 15.8 MPa, respectively). Exposure of *B. anthracis* spores to a mixture of both germinants resulted in a synergistic effect with even lower elasticity, with a Young's modulus of 23.5 ± 14.8 MPa. The elasticity of the vegetative *B. anthracis* cells was nearly 15 times lower than that of the dormant spores (12.4 ± 6.3 MPa vs 197.0 ± 80.5 MPa, respectively). Indeed from a mechanical strength point of view, the germinated spores were closer to the vegetative cells than to the dormant spores. Further, the decrease in the elasticity of the cells was accompanied by increasing AFM tip indentation depths on the cell surfaces. Indentation depths of up to 246.2 nm were observed for vegetative *B. anthracis* compared to 20.5 nm for the dormant spores. These results provide quantitative information on how the mechanical properties of the cell wall change during germination, which may explain how spores become susceptible to inactivation processes based on mechanical forces during germination and outgrowth. The study of spore elasticity may be a valuable tool in the design of improved antisporal treatments.

Introduction

Bacillus and *Clostridium* cells are some of the most resistant life forms known due to their ability to undergo the restructuring and differentiation process of sporulation under nutrient deprivation.[1] During this process, vegetative cells synthesize a series of polymer and protein layers that encase the cellular contents and genetic information in a ~100−200 nm barrier, which protects the cell from external environmental stressors.[2,3] Spores are metabolically dormant, but they maintain the ability to germinate and transform into vegetative cells once nutrients are available.[4,5] In their vegetative state, organisms such as *Bacillus anthracis* (*B. anthracis*) are highly virulent, and they are considered as potent biological threat agents since they cause critical or fatal airborne diseases, such as pulmonary anthrax.[6,7]

The first step of the process in which the spores return to a fully vegetative, pathogenic state is known as germination. Germination is usually initiated in response to availability of nutrients, such as amino acids and sugars, non-nutrient chemicals such as dodecylamine and dipicolinic acid (DPA), or by other factors such as high pressure and temperature.[5,8] Germination involves a series of steps where the release of monovalent cations, dipicolinic acid (DPA), calcium, and the intake of water molecules result in the loss of heat resistance and initiation of metabolic activity, converting the spore into a vegetative, fully virulent bacterium.[2,9]

The mechanism of germination triggered by nutrients involves the presence of spore-germination receptors on the surface or inner membrane of the spore, which stimulate the cell to germinate and to achieve vegetative growth.[10] L-Alanine is an amino acid that interacts with a receptor on the inner membrane of the spores[11] and is a well-studied molecule for the germination of several *Bacillus* species, such as *B. subtilis*, *B. cereus*, *B. anthracis*, and *B. atrophaeus*.[6,8,12] Inosine is a purine ribonucleoside that has been shown to be a strong germinant of *B. cereus* spores.[13] While either germinant, L-alanine or inosine, alone can cause the germination of *B. cereus*, for *B. anthacis* spores, a binary mixture of the germinants has been shown to be more effective.[10,11]

*Corresponding author: Ph 508 831 5380; Fax 508 831 5380; e-mail terric@wpi.edu.

(1) Atrih, A.; Foster, S. J. *Int. Dairy J.* **2002**, *12* (2−3), 217−223.
(2) Henriques, A. O.; Moran, C. P., Jr. *Methods* **2000**, *20* (1), 95−110.
(3) Pinzon-Arango, P. A.; Scholl, G.; Nagarajan, R.; Mello, C. M.; Camesano, T. A. *J. Mol. Recognit.* **2009**, *22* (5), 373−379.
(4) Setlow, B.; Cowan, A. E.; Setlow, P. *J. Appl. Microbiol.* **2003**, *95* (3), 637−48.
(5) Setlow, P. *Curr. Opin. Microbiol.* **2003**, *6* (6), 550−6.
(6) Akoachere, M.; Squires, R. C.; Nour, A. M.; Angelov, L.; Brojatsch, J.; Abel-Santos, E. *J. Biol. Chem.* **2007**, *282* (16), 12112−8.
(7) Drysdale, M.; Heninger, S.; Hutt, J.; Chen, Y.; Lyons, C. R.; Koehler, T. M. *EMBO J.* **2005**, *24* (1), 221−7.
(8) Gounina-Allouane, R.; Broussolle, V.; Carlin, F. *Food Microbiol.* **2008**, *25* (1), 202−6.
(9) Slieman, T. A.; Nicholson, W. L. *Appl. Environ. Microbiol.* **2001**, *67* (3), 1274−9.
(10) Barlass, P. J.; Houston, C. W.; Clements, M. O.; Moir, A. *Microbiology* **2002**, *148* (Pt. 7), 2089−95.
(11) Ireland, J. A.; Hanna, P. C. *J. Bacteriol.* **2002**, *184* (5), 1296−303.
(12) Tiball, R. W.; Manchee, R. J. *J. Appl. Bacteriol.* **1987**, *62* (3), 269−73.
(13) Clements, M. O.; Moir, A. *J. Bacteriol.* **1998**, *180* (24), 6729−35.

In contrast to the considerable attention paid to investigating the effects of nutrients on germination of spores, there are fewer studies in the literature on the effects of physical insults, such as pressure.[14,15] While it is widely known that the microbial cell wall has a structural role in maintaining the cellular shape and resisting turgor pressure,[16] changes in the mechanical properties of the cell wall during germination remains essentially unknown. *B. subtilis* spores exposed to 100 and 550 MPa resulted in the killing of < 25% and < 50% spores, respectively.[14] Treatment pressures at 550 MPa were able to induce the germination of spores without the need of activation of germinant receptors, as was confirmed by the number of viable colonies in Luria broth medium agar plates. However, spores treated at 100 MPa produced very few colonies on agar plates, suggesting that there may be a critical mechanical force necessary to initiate germination in the absence of nutrients.[14] Understanding the mechanical properties of *B. anthracis* spores, such as cell wall elasticity, may help us understand how germination affects the spore surface and ultimately how the cell resists chemical and physical insults.

Germination of spores is usually monitored by changes in optical densities that occur as DPA is released from the spore core after addition of germinants.[4] Electron microscopy (EM) has also been used to study changes in morphology of the spores during germination.[17] While EM explicitly demonstrates changes in cell structure, sample preparation necessitates dehydration and coating with a reflective material, which can cause artifacts.

Atomic force microscopy (AFM) is a technique that has proven practical for the physical characterization of individual spores, since it provides high-resolution imaging of the sample and the ability to obtain the adhesion forces present between the AFM probe and the cell surface under native conditions.[18] By studying the interaction of the AFM tip as it approaches or retracts from the spore surface, it is possible to study specific physical and chemical properties of the spore, such as elasticity, adhesion, and length of surface polymers. A few AFM studies available in the literature have addressed how nutrient germinants, such as L-alanine, affect the morphology of *Bacillus* species.[17,19−21] AFM has been used to obtain high-resolution images of the spore coat of *Bacillus* spores and understand how protein coat layers change during germination.[19,21]

Quantitative elasticity measurement with AFM is a new way to characterize how germinants affect the mechanical properties of the spore surface. Using the AFM probe as a nanoindentation tool, AFM deflection data can be converted into load vs indentation depth plots and analyzed using theoretical models that provide quantitative information on the elasticity of the sample (represented by the Young's modulus).[22] These models have been applied toward bacteria, such as *E. coli*, where it was suggested that the elasticity of the cells can change significantly depending on the solvent in which the cells are exposed.[23] The elasticity for *E. coli* in water was ~12.8 MPa, while the elasticity of the same bacterium in a more polar solvent, such as formamide, decreased to ~0.8 MPa.[23] The same technique has been applied with other types of cells, such as the yeast *Saccharomyces cerevisiae*, where the Young's modulus was ~0.6 MPa at the cell wall but ~6.1 MPa at the site of cellular division.[22] While these elasticity studies help characterize the physical properties of some bacterial strains, none of the cells studied possess the complex protein layers and coat structure that is common in sporulated *B. anthracis*.

Therefore, our objective was to use AFM to characterize how the nutrient germinants L-alanine and/or inosine affected the Young's modulus of *B. anthracis* spores. These results were compared with elasticity measurements on the dormant spores and also on the vegetative *B. anthracis* cells, these being the two limiting states of the spore subjected to germinants.

Experimental Section

Bacterial Strain and Preparation of Spores. *Bacillus anthracis* Sterne (referred to hereafter as "*B. anthracis*") was kindly provided by the U.S. Army Natick Soldier Research, Development & Engineering Center, Natick, MA. The Sterne strain is a low virulence strain that lacks the pXO2 extra chromosomal plasmid, which forms and develops the bacterial capsule; however, it contains the pXO1 extra chromosomal plasmid, which is responsible for the expression of virulent factors.[17]

Bacterial strains were grown in sporulation media as described previously.[3] A solution of sporulation media consisting of 8 g of nutrient broth, 4 g of yeast extract, 0.001 g of $MnCl_2 \cdot 4H_2O$, 5 g of peptone, and 15 g of agar in 1 L of ultrapure water (Milli-Q water, Millipore Corp., Bedford, MA) was maintained at a pH of 7.2 and sterilized for 60 min, followed by preparation in Petri dishes.

Fresh cultures of *B. anthracis* Sterne were obtained by adding 100 μL of spores from a glycerol stock solution into a flask with 25 mL of sterilized nutrient broth (Himedia, Mumbai, India). The flask was agitated at 200 rpm at 37 °C for ~20 h. This culture was used to inoculate plates of sporulation media using 50 μL aliquots, and the plates were incubated at 37 °C for 4 days to allow vegetative cells to sporulate. Harvesting of spores was done in autoclaved ultrapure water, and spores were collected by centrifugation at 5000 rpm for 20 min and resuspended in ultrapure water. The cells were washed eight times to separate spores from vegetative and partially sporulated cells since there is a significant difference in density between these two cell types.[24] The spores were stored overnight at 4 °C. After ~18 h, the cells were washed two more times to remove any remaining vegetative *B. anthracis* cells.

Spore Germination Assays and Atomic Force Microscopy (AFM). The surface elasticity of dormant and germinated spores and of vegetative cells of *B. anthracis* was investigated. To germinate the spores, *B. anthracis* were exposed to 50 mM L-alanine (Sigma-Aldrich, St. Louis, MO), 5 mM inosine (Sigma-Aldrich), or both germinants together, in 50 mM Tris/HCl buffer (pH 8.0), and incubated at 37 °C for 2 and 4 h. The final concentration of the spore solution was ~10^7 cells/mL. As a control condition, dormant *B. anthracis* spores were incubated for 4 h in 50 mM Tris/HCl buffer at 37 °C. To study the elasticity of vegetative *B. anthracis* cells, a 1 mL sample of dormant spore solution was suspended in tryptic soy broth (30 g/L, Sigma-Aldrich), supplemented with 1% yeast extract, and grown for 6 h at 37 °C with rotation at 18 rpm.

To test the effect of germinant concentration on the elasticity of the spores, additional experiments were carried out where *B. anthracis* spores were germinated with 25 mM L-alanine and/or 2.5 mM inosine for 2 h. The elasticity values obtained were

(14) Paidhungat, M.; Setlow, B.; Daniels, W. B.; Hoover, D.; Papafragkou, E.; Setlow, P. *Appl. Environ. Microbiol.* **2002**, *68* (6), 3172−5.
(15) Wuytack, E. Y.; Boven, S.; Michiels, C. W. *Appl. Environ. Microbiol.* **1998**, *64* (9), 3220−4.
(16) Vadillo-Rodriguez, V.; Beveridge, T. J.; Dutcher, J. R. *J. Bacteriol.* **2008**, *190* (12), 4225−32.
(17) Zaman, M. S.; Goyal, A.; Dubey, G. P.; Gupta, P. K.; Chandra, H.; Das, T. K.; Gangali, M.; Singh, Y. *Microsc. Res. Technol.* **2005**, *66* (6), 307−11.
(18) Dufrene, Y. F. *J. Bacteriol.* **2002**, *184* (19), 5205−13.
(19) Plomp, M.; Leighton, T. J.; Wheeler, K. E.; Hill, H. D.; Malkin, A. J. *Proc. Natl. Acad. Sci. U.S.A.* **2007**, *104* (23), 9644−9.
(20) Plomp, M.; Leighton, T. J.; Wheeler, K. E.; Malkin, A. J. *Biophys. J.* **2005**, *88* (1), 603−8.
(21) Plomp, M.; Leighton, T. J.; Wheeler, K. E.; Pitesky, M. E.; Malkin, A. J. *Langmuir* **2005**, *21* (23), 10710−6.
(22) Touhami, A.; Nysten, B.; Dufrene, Y. F. *Langmuir* **2003**, *19* (11), 4539−4543.
(23) Abu-Lail, N. I.; Camesano, T. A. *Colloids Surf., B* **2006**, *51* (1), 62−70.
(24) Tamir, H.; Gilvarg, C. *J. Biol. Chem.* **1966**, *241* (5), 1085−90.

compared with those obtained at higher concentrations of germinants (50 mM L-alanine and/or 5 mM inosine).

AFM was used to study changes in the elasticity of *B. anthracis* spores induced by exposure to different germinants. After incubation with L-alanine and/or inosine, the spore solution was centrifuged at 5000 rpm for 5 min and resuspended in ultrapure water to stop treatment. Droplets of treated *B. anthracis* spores (5 μL) were deposited onto freshly cleaved mica and dried for 18 h.

AFM experiments were carried out with a Dimension 3100 with Nanoscope IIIa controller (Veeco Metrology, Santa Barbara, CA) that was operated in tapping mode in air to represent conditions of airborne spores. *B. anthracis* are commonly found in soil at concentrations of up to 3000 spores per gram of soil.[25,26] Since germination can be affected by humidity,[27] AFM measurements were taken at 30−35% relative humidity in air. A single rectangular cantilever with a conical silicon tip having a spring constant of 14 N/m and a resonant frequency of 315 kHz was used (Mikromasch, San Jose, CA). Samples were scanned at a rate of 1 Hz, and once a spore was located, it was centered so that force measurements could be performed on the cell away from the edges. Forces were measured on five spores, and ten force cycles were recorded per spore for a total of 50 force curves obtained for each treatment. The ten force cycles obtained within each spore were taken at the same location of the cell (center of the spore away from edges) to ensure that no deformation of the surface was taking place. The force cycle was set so the tip stayed in contact with the sample for 1 ms before retracting and the tip would travel at 2 μm/s with a loading rate of 3×10^{-5} N/s during the force cycle. Data in ASCII format were exported to a spreadsheet and converted from deflection to force.

Elasticity of *B. anthracis* Spores Obtained from Force−Indentation Depth Curves. The conversion of cantilever deflection data to force data allows for the assessment of the elasticity of the surface of the spores in response to exposure to germinants. AFM data were converted to force−indentation depth curves following procedures described previously.[28−30] Briefly, the deflection of the cantilever, d, as it approaches and retracts from the surface is plotted as a function of tip−sample separation distance, z. Since there was some scanner hysteresis and drift in the detection system, we often observed that the deflection of the free cantilever was not equal to zero. To correct this, a deflection offset, d_0, was subtracted from all deflection values. This deflection offset was determined from the cantilever deflection−sample separation distance plot by calculating the average cantilever deflection when the AFM probe was far away from the sample surface. This was observed as a horizontal line, where no repulsive or attractive forces were experienced by the AFM tip. The cantilever deflection was converted to force or load (F) using Hooke's law

$$F = k_c(d - d_0) \tag{1}$$

where k_c is the spring constant.

Similar to the deflection offset, a separation distance offset, z_0, was defined. The value of this offset was the initial point where the tip makes contact with the sample surface or more specifically, when the deflection of the cantilever begins to increase from the horizontal line that represents the zero cantilever deflection (deflection offset). The distance offset was subtracted from all distance values.

Next, the force−indentation curves were created by taking into account the compliance of the sample surface. On a hard surface, such as mica, the slope of the compliance region of the cantilever deflection−separation distance curve is equal to 1, but this slope is expected to decrease for biological samples, such as bacteria.[22,23] The difference between the separation distance on a hard surface and the separation distance on the surface of the spore is the indentation depth of the sample, δ, and is defined by

$$\delta = (z - z_0) - (d - d_0) \tag{2}$$

From eqs 1 and 2, the cantilever deflection−separation distance curves were converted into load, F, versus indentation depth, δ. Force curves were made on freshly cleaved mica free of spores before any measurements were taken on cells in order to calibrate the sensitivity of the photodetector.

Young's Modulus of *B. anthracis*. The tensile elastic modulus or Young's modulus was obtained by applying the Hertz model of continuum mechanics of contact to the load−indentation depth data.[22,23] The Hertz model can be used for samples that are elastic, isotropic, homogeneous, and semi-infinite although it does not take into account tip−surface adhesion.[22,31] Since there were not significant adhesion forces observed during the force cycle, this model was applicable.

From Hertzian theory, the model describes the indentation (without permanent deformation) of an indenter (the silicon AFM probe) into an infinitely deformable elastic half-space (spore surface). The geometry of the indenter was taken into account, and it was related to the load−indentation depth curves by

$$F_{\text{cone}} = \frac{2}{\pi} \tan \alpha \frac{E}{1 - \nu^2} \delta^2 \tag{3}$$

where α is the half-opening angle of the conical tip used, taken as 40° as specified by the manufacturer, E is the Young's modulus or tensile elastic modulus of the spore, and ν is the Poisson ratio of the spore, taken as 0.5.[22]

A MatLab script was written to analyze all raw data obtained with the AFM and calculate the elastic modulus of the spores for all treatments (MatLab Works Inc., Natick, MA).

Statistical Analysis. Young's modulus and indentation depth values were analyzed using the Kruskal−Wallis one-way analysis of variance (ANOVA) on ranks for repeated measurements since the samples did not have equal variances. The null hypothesis tested was that there were no differences in the distribution of values between different groups. Tukey's test was used for multiple comparisons among treatment groups. A difference was considered significant if $P < 0.05$.

Results and Discussion

Rationale for Germination Conditions. Germination of *Bacillus* spores has been extensively studied over the past few decades. L-Alanine has been shown to influence the germination of spores of many *Bacillus* species.[6,8,12] For *Bacillus anthracis*, it has been shown that L-alanine is a strongly independent germinant at concentrations > 10 mM and that rapid germination responses are observed at high L-alanine concentrations (100 mM).[11] In the same study, it was observed that lower L-alanine concentrations could germinate *B. anthracis* spores as long as there was another germinant present, such as inosine.[11] L-Alanine at a concentration of 10 mM acting together with inosine at a concentration of 1 mM were able to germinate 73% of *B. anthracis* spores in less than 15 min.[11] In another study, optimal germination conditions for *B. anthracis* were observed when spores were exposed to

(25) Patra, G.; Vaissaire, J.; Weber-Levy, M.; Le Doujet, C.; Mock, M. *J. Clin. Microbiol.* **1998**, *36* (11), 3412−4.
(26) Ryu, C.; Lee, K.; Yoo, C.; Seong, W. K.; Oh, H. B. *Microbiol. Immunol.* **2003**, *47* (10), 693−9.
(27) Westphal, A. J.; Price, P. B.; Leighton, T. J.; Wheeler, K. E. *Proc. Natl. Acad. Sci. U.S.A.* **2003**, *100*, (6), 3461−6.
(28) Burnham, N. A.; Colton, R. J. *J. Vac. Sci. Technol. A* **1989**, *7* (4), 2906−13.
(29) Tomasetti, E.; Legras, R.; Nysten, B. *Nanotechnology* **1998**, *9* (4), 305−315.
(30) Weisenhorn, A. L.; Khorsandi, M.; Kasas, S.; Gotzos, V.; Butt, H.-J. *Nanotechnology* **1993**, *4* (2), 106−13.
(31) Mumkoshi, M.; Yoshida, N.; Ida, K.; Kumano, S.; Kobayashi, T.; Wada, H. *Auris, Nasus, Larynx* **2006**, *33* (2), 149−57.

15−150 mM L-alanine, and over 99% of the spore population had germinated within 24 h.[12] Clements and Moir observed that 50 mM L-alanine and 5 mM inosine were concentrations at which the germination rates were the maximum for *B. cereus*, which is a close genetic relative of *B. anthracis*.[13] In another study, inosine concentrations that ranged from 1 to 10 mM resulted in comparable germination processes as measured by the fall in optical density.[8] While inosine has been shown to be a weak germinant while acting alone compared to L-alanine, it has been suggested that inosine as a cogerminant is able to induce strong germination responses in *B. anthracis*. Germination with L-alanine as the sole germinant has been shown to involve a single receptor while inosine as a sole germinant has been shown to require the interaction of two different receptors in *B. cereus*.[10] On the basis of these findings, and knowing that germinants at high enough concentrations resulted in optimal germination responses, we chose high concentrations of L-alanine and inosine for our elasticity studies. To assess whether germinant concentration had an effect on elasticity, AFM experiments were also carried out on spores that were exposed to different concentrations of L-alanine and/or inosine.

Elasticity of *B. anthracis* after Exposure to Germinants. Cantilever deflection vs tip−sample separation curves were converted to load vs indentation depth plots to quantify the elasticity of *B. anthracis* spores after exposure to L-alanine and/or inosine (Figure 1A). A distinct nonlinear region of the curve was observed for all samples, which allowed for the detection of deflection and separation distance offsets. Once these offsets were defined, the plot was converted to loading force vs indentation depth (Figure 1B). When we probed a hard surface, such as mica, the nonlinear region of the curve was absent, so the deflection and separation offsets were defined as the point where a sudden jump to contact was observed in the approach curve.[22] The Young's modulus of the spores was obtained by fitting the nonlinear portion of the loading force vs indentation depth curves to the Hertz model. A quasi-quadratic relation was observed between the loading force and the indentation depth (Figure 1B), which was predicted by the model for a conical AFM probe. There was a good agreement between the Hertz model and the experimental data obtained, which suggests that this model can be used for the measurement of elasticity of cells with harder surfaces such as *Bacillus* and *Clostridium* species. Furthermore, for all treatments, no adhesion forces were observed during approach or retraction of the AFM tip, allowing for the analysis of the data using the Hertz model. The lack of adhesive interactions during AFM force cycles has been associated with the crystalline nature of the surface of microorganisms, such as the one present in *Lactobacilli*.[32] A crystalline cell surface protein, S-layer, has been observed in the structure of *Bacillus* species,[33] which may consist of compactly folded proteins that prevent the AFM tip from experiencing adhesion during force measurements.

The slope of the load vs indentation depth curve was higher when taking AFM measurements on the dormant *B. anthracis* spores that were not exposed to any germinants or yeast extract and decreased significantly after incubation with either L-alanine or inosine (Figure 2). Based on the shape of the loading force vs indentation depth curve, fewer data points were available to fit the Hertz model for the cells that showed harder surfaces (dormant, untreated spores), since the nonlinear portion of the curve that describes the indentation of the AFM probe into the untreated

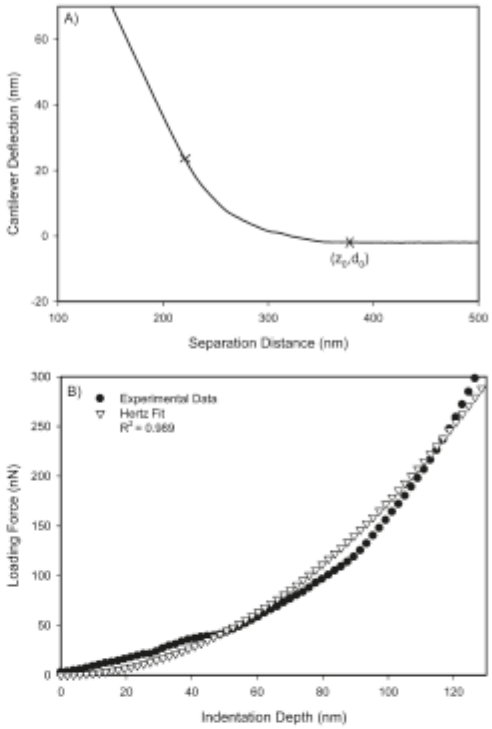

Figure 1. (A) Representative AFM approach curve obtained when a silicon AFM tip approaches and indents a *B. anthracis* Sterne spore. The deflection offset d_0 and the offset in the separation distance z_0 used to calibrate the deflection vs distance plot are shown. The nonlinear portion of the curve is depicted within the two X marks. (B) Loading force−indentation depth curve corresponding to the deflection−distance curve in (A). The open triangles correspond to the best fit obtained after applying the Hertz model to the nonlinear portion of the approach curves (eq 3).

B. anthracis cell was significantly smaller. This may be due to the multiple protein layers that surround the cell, making the spore surface harder than the cell wall of vegetative bacteria.

Treatment of spores with TSB supplemented with yeast extract resulted in vegetative cells with weaker surfaces since very low loads were required to substantially indent the sample with the AFM tip. The slope of the load vs indentation depth curve for the vegetative *B. anthracis* resulting from the TSB and yeast extract treatment was the lowest of all conditions (Figure 2). Since untreated *B. anthracis* spores are covered by multiple layers of protein coats, higher loading forces were required to cause indentation of the spore. This suggests that the protein coat layers of dormant spores strengthen the surface and resist applied pressure, such as the one created by the AFM probe during force cycles. Similar changes in the slope of the load vs indentation plot have been observed for other microorganisms, such as *S. cerevisiae*.[22] During the division of *S. cerevisiae*, a scar is formed on the cell wall where the bud emerges, resulting in a steeper slope in the AFM data, which suggests strengthening of the surface and higher loading forces being required to indent the cell with an AFM probe.

(32) Schaer-Zammaretti, P.; Ubbink, J. *Ultramicroscopy* **2003**, *97* (1−4), 199−208.
(33) Kotiranta, A.; Haapasalo, M.; Kari, K.; Kerosuo, E.; Olsen, I.; Sorsa, T.; Meurman, J. H.; Lounatmaa, K. *Infect. Immun.* **1998**, *66* (10), 4895−902.

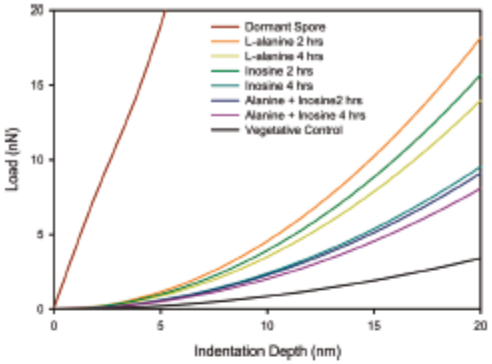

Figure 2. Representative load vs indentation depth curves of *B. anthracis* Sterne before and after incubation with 50 mM L-alanine and/or 5 mM inosine or tryptic soy broth supplemented with 1% yeast extract (vegetative control). Each line is the average of 50 approach curves measured between *B. anthracis* Sterne and a silicon AFM probe.

The effects of pressure on the germination of spores have been previously studied.[14,15,26] Exposure of spores to high pressure can initiate the process of germination.[14] Exposure of *Bacillus* spores to pressures of 550 MPa resulted in initiation of germination without the involvement of any germinant receptors.[14] However, treatment at lower pressures (100 MPa) did not initiate germination, unless one of the spore's germinant receptors was activated by nutrients. Since the pressure applied by the AFM tip to the spores was much lower than 100 MPa, a pressure-induced germination of untreated spores probably did not occur in our study.

The highest Young's moduli were obtained with dormant spores that were not exposed to germinants or yeast extract (197.02 ± 80.48 MPa; Figure 3). The high elasticity value may be due to the thickness of the inner and outer coats of the sporulated cells, which can be up to 130 nm.[2] This thickness may result in a hardening of the spore surface, protecting it from environmental insults. Young's moduli of *B. anthracis* spores decreased significantly after incubation for 4 h with L-alanine, inosine, or both germinants (47.54 ± 41.79, 35.41 ± 15.88, and 23.50 ± 14.87 MPa, respectively; $P < 0.05$). Incubation of *B. anthracis* with both germinants resulted in >90% of the spores having an elastic modulus lower than 50 MPa. There was no statistically significant difference between the Young's modulus of spores treated with L-alanine for 2 or 4 h; in the case of inosine, the elasticity decreased from 66.42 ± 25.90 MPa after 2 h of incubation to 35.41 ± 15.88 MPa after 4 h of incubation ($P > 0.05$). The rather large standard deviation values obtained for all conditions suggest that there may be heterogeneity of the distribution of proteins on the spore surface, especially in the dormant spores. The germination of spores using only inosine as the triggering molecule has been shown to require the interaction of the germinant with two different receptors in *B. cereus* spores, GerI and GerQ, since the activation of only one of them does not provide sufficient activation of the spore to carry on with the germination process.[10] *B. cereus* is a close relative of *B. anthracis*, and the *gerQ* and *gerI* operons are also present in *B. anthracis* and recognize inosine as a germinant.[34] Based on our

(34) Baillie, L.; Hibbs, S.; Tsai, P.; Cao, G. L.; Rosen, G. M. *FEMS Microbiol. Lett.* **2005**, *245* (1), 33–8.

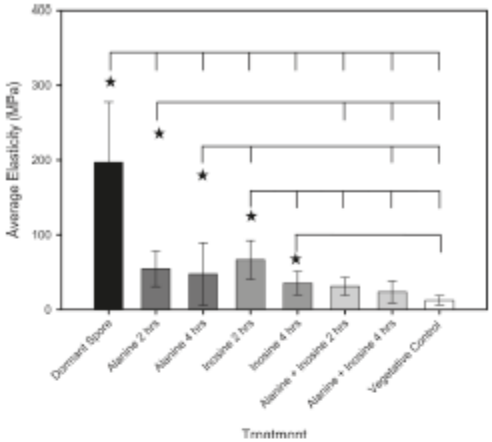

Figure 3. Elasticity of *B. anthracis* Sterne spores as a function of treatment. Spores germinated with 50 mM L-alanine and/or 5 mM inosine for 2 or 4 h. Bars depict the average elasticity of 50 spores per condition. Error bars show the standard deviation. The top lines connect statistically distinct points ($P < 0.05$) calculated by Kruskal–Wallis one-way ANOVA on ranks with Tukey's test to make pairwise comparisons The star symbol indicates the condition that is being compared to other treatments.

results, germination with inosine may require longer exposure time of the cells to the ribonucleoside to allow for the interaction with both receptors. Our investigation also suggests that while other studies have shown that inosine acting alone is a weak germinant for *B. anthracis* spores as measured by the rate of optical density change, it does display a stronger impact on the mechanical properties of the cells since the surface elasticity decreases significantly compared to the dormant spore.

The elasticity values of *B. anthracis* incubated with both germinants were significantly lower compared to the spores incubated with each of the individual nutrients ($P < 0.05$). It has been suggested in the literature that *B. anthracis* may not germinate in the presence of inosine alone but may require coupling with another germinant, such as an amino acid.[6,11] Ireland and Hanna showed that high concentrations of inosine (up to 50 mM) did not trigger a germination response from *B. anthracis* even when incubated for up to 16 h.[11] In the same study, it was concluded that L-alanine is a strong germinant only at high concentrations (>10 mM), but the presence of a second cogerminant, such as inosine, will result in a stronger germination response.[11] Our results suggest that a weakening of the spore surface is taking place after incubation of *B. anthracis* with L-alanine and inosine, since the elasticity values decreased significantly ($P < 0.05$). The use of two germinants may not only weaken the surface of the spore but speed up the degradation of the spore coat and the peptidoglycan cortex that protects the spore core, which would change the mechanical properties of the cell.

Spores treated with lower concentrations of L-alanine and/or inosine (25 and/or 2.5 mM, respectively) did not show significantly different Young's moduli when compared to the values obtained with higher concentrations of L-alanine and/or inosine (50 and/or 5 mM, respectively; Table 1). Clements and Moir have shown that comparable germination rates of *Bacillus* spores were achieved over inosine concentrations ranging from 1 to 30 mM and over L-alanine concentrations ranging from 10 to 100 mM.[13]

Table 1. Effects of Germinant Concentration on Young's Modulus and Indentation Depths of *Bacillus anthracis*

germinant concentration	average Young's modulus (MPa)	*P* value[a,b]	average indentation depth (nm)	*P* value[a,c]
25 mM L-alanine	55.7 ± 31.9	0.846	137.7 ± 31.6	0.612
50 mM L-alanine	54.7 ± 23.9		135.0 ± 41.6	
2.5 mM inosine	69.5 ± 16.6	0.608	121.8 ± 19.7	0.458
5 mM inosine	66.4 ± 25.9		117.8 ± 25.1	
25 mM L-alanine + 2.5 mM inosine	32.3 ± 14.2	0.669	224.7 ± 35.1	0.123
50 mM L-alanine + 5 mM inosine	31.15 ± 11.9		223.9 ± 82.1	

[a]Comparisons of Young's modulus and indentation depth data between germinant concentrations were done using one-way analysis of variance (ANOVA) for repeated measurements. Tukey's test was used for multiple comparisons among treatment groups. A difference was considered significant if $P < 0.05$. [b]*P* value obtained when comparing average Young's moduli. [c]*P* value obtained when comparing average indentation depths.

In another study, spore germination was measured by studying the decrease of optical density of spore suspensions after addition of germinants, and it was determined that inosine concentrations of 1 or 10 mM and L-alanine concentrations of 10 or 100 mM caused the same decrease of optical density of spore suspensions.[8] Based on these studies, the concentrations of L-alanine and inosine chosen for our elasticity experiments fall within the range where optimal spore germination rates occur. In this study we observe surface elasticity values for *B. anthracis* that are unaffected by the change in germinant concentration when the spores are exposed to high concentrations of L-alanine (25 and 50 mM) or inosine (2.5 and 5 mM). Similarly, mixtures of both germinants at concentrations of 50 mM L-alanine and 5 mM inosine or 25 mM L-alanine and 2.5 mM inosine yielded comparable Young's moduli. These results suggest that once the spores have been exposed to high enough concentrations of the germinants, the changes in elasticity will be the same independent of the amount of L-alanine and/or inosine in the spore suspension. The elasticity of vegetative *B. anthracis* showed the lowest Young's modulus with an average of 12.39 ± 6.32 MPa, and the values were significantly different when compared to other treatments ($P < 0.05$), except when the cells were treated with L-alanine and inosine for 4 h ($P > 0.05$). This elasticity value is close to the elastic modulus of other vegetative bacteria. For *E. coli*, a Young's modulus of ~12.8 MPa was estimated.[23] Once a spore has completely germinated, there is an outgrowth process leading to the vegetative cell where the spore coat is lost, leaving the cell with a membrane that is much thinner and allows for the transport of nutrients and release of waste products.[5,35] The degradation of the spore coat resulted in a cell that could be more easily indented by the AFM probe, as was observed on vegetative bacteria (Figure 4).

Indentation Depths of *B. anthracis* as a Function of Treatment. Indentation depths were significantly lower for the untreated spores than for those treated with L-alanine, inosine, or TSB supplemented with yeast extract ($P < 0.05$). For the dormant spores (untreated spores), the depth indented by the AFM probe was 20.45 ± 14.88 nm. However, this indentation depth increased significantly after incubation of germinants for 2 or 4 h. Higher indentation depth values were observed for spores treated with L-alanine compared to inosine. For the germinant-treated spores, the highest indentation depths were observed for spores treated with both L-alanine and inosine for 2 h (223.97 ± 82.14 nm) or with incubation of the cells in L-alanine for 4 h (225.37 ± 98.65 nm). Lower concentrations of L-alanine and/or inosine (2.5 and 2.5 mM, respectively) showed similar indentation depth values, suggesting that there is no appreciable effect of germinant concentration on surface elasticity and indentation depth, once an optimal germination condition has been achieved

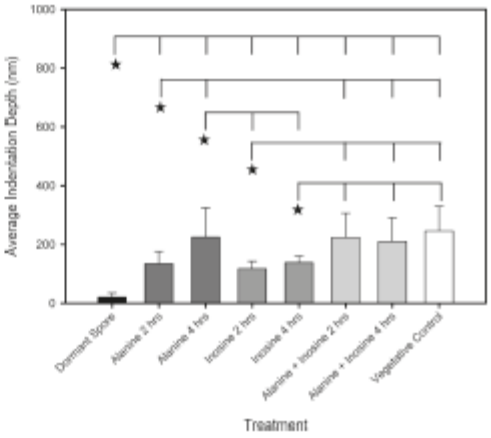

Figure 4. Average indentation depths of *B. anthracis* Sterne spores probed with a silicon AFM tip as a function of treatment. Spores germinated with 50 mM L-alanine and/or 5 mM inosine for 2 or 4 h. Error bars show the standard deviation of 50 measurements obtained for each condition. The top lines connect statistically distinct points ($P < 0.05$) calculated by Kruskal–Wallis one-way ANOVA on ranks. The star symbol indicates the condition that is being compared to other treatments.

(Table 1). The incubation of *B. anthracis* spores in TSB supplemented with yeast extract resulted in the highest indentation depths (246.23 ± 84.31 nm). Our results suggest that the surface of dormant (untreated) *B. anthracis* spore is harder and therefore higher loading forces are required to indent the cell. Once germination is initiated, there is a degradation of the spore coat that allows the spore to outgrow and become a vegetative cell.[5] Vegetative *B. anthracis* need to have a much thinner cell wall with more flexibility to allow the release of waste products as well as toxins during infection and invasion of macrophages.[5,35] Because of the more flexible and thinner surface, the AFM probe can indent the vegetative cell more than the sporulated cell. Analogous changes in the elasticity have been observed for *S. cerevisiae* at the location where the bud emerges during cell division.[22] When the cell undergoes cellular division, a chitin ring of polysaccharide of (β1−4)-linked *N*-acetylglucosamine forms to strengthen the bud scar, marking the division site.[22] The proteins that form this chitin ring are highly glycosylated peptides that are 50−95 wt % carbohydrate, which makes chitin fibers insoluble, causing stiffening of the bud scar.[36] Because of the rigidity of the chitin ring, the

(35) Leuschner, R. G. K.; Ferdinando, D. P.; Lillford, P. J. *Colloids Surf., B* **2003**, *29*, 31−41.

(36) Alsteens, D.; Dupres, V.; Mc Evoy, K.; Wildling, L.; Gruber, H. J.; Dufrene, Y. F. *Nanotechnology* **2008**, *19* (38), 384005/1−384005/9.

portion of the cell that had the bud scar had higher Young's modulus values and lower indentation depths made by the AFM probe compared to the rest of the cell surface. In another study, the spring constant of the *S. cerevisiae* cell body and the bud scar were determined from the slope of the linear portion of the force−distance curve, and the bud scar displayed higher cell spring constant due to the increased chitin content of the area.[37]

Conclusions

The rigidity of the spore coat of dormant *B. anthracis* cells is severely compromised by exposure to germinants or nutrients, such as TSB and yeast extract. During germination, the spores start losing their coat, making the cell's surface more flexible, lowering the surface elasticity, and allowing the AFM probe to indent the surface more during the force cycle. Vegetative *B. anthracis* showed the weakest cell surface with elasticity values that were 15 times lower than sporulated cells. This decrease in elasticity accompanied by a decrease in the thickness of the spore coat, which we previously observed,[3] would explain why vegetative cells are sensitive to sporicidal compounds. Based on our findings, the study of elasticity of spores may be a valuable tool to predict how to weaken spores, thus making them more susceptible to spore inactivation processes based on mechanical forces, such as the high-pressure, high-temperature inactivation method practiced in the food industry. Indeed, on the basis of our results, we anticipate that the decrease in the elasticity of the spores caused by germinators such as L-alanine, inosine, dodecylamine, etc., either alone or in mixtures, would make spore inactivation possible at lower pressures compared to that in the absence of such germinators. It may also be possible to reduce the small population of "difficult to kill" or "superdormant" spores that often survive the current high-pressure inactivation methods by the use of germinants in the high-pressure spore inactivation process.

Acknowledgment. This work was supported in part by the National Science Foundation (CBET 0827229) and the Defence Threat Reduction Agency (DTRA) Project BA07PRO102.

We also thank Ms. Angela Tao for her assistance in the development of the MatLab script used for elasticity measurements, Mr. Robert Stote and Ms. Stephanie Marcott of NSRDEC for help with spore preparation, and Prof. Nancy Burnham for helpful discussions.

(37) Pelling, A. E.; Sehati, S.; Gralla, E. B.; Valentine, J. S.; Gimzewski, J. K. *Science* **2004**, *305* (5687), 1147−50.